

C. Rainieri

Operational Modal Analysis for Seismic Protection of Structures



University of Naples "Federico II"

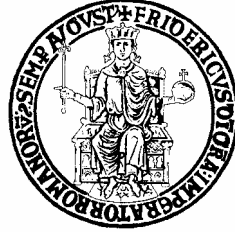
## Operational Modal Analysis for Seismic Protection of Structures

*Carlo Rainieri*



Engineering of Materials and Structures  
PhD Programme

UNIVERSITY OF NAPLES “FEDERICO II”



*Operational Modal Analysis  
for Seismic Protection  
of Structures*

DISSERTATION SUBMITTED  
FOR THE DEGREE OF  
DOCTOR OF PHILOSOPHY  
IN  
ENGINEERING OF MATERIALS AND STRUCTURES

by

CARLO RAINIERI

SUPERVISORS

PROF. G. FABBROCINO  
PROF. E. COSENZA

COORDINATOR

PROF. D. ACIERNO

December 2008



*The ultimate measure of a man is not where he stands  
in moments of comfort and convenience, but where he stands  
at times of challenge and controversy (Martin Luther King)*

-

This thesis is dedicated to who has made me a man



# ACKNOWLEDGEMENTS

*There are those that look at things  
the way they are, and ask why?  
I dream of things that never  
were, and ask why not?*

(R.F. Kennedy quoting G.B. Shaw)

Several things changed since I started this adventure... I faced several challenges... The world changed... But I had some steady references...

I would like to express my gratitude to Prof. Fabbrocino, for his guidance, his understanding and his continuous support: his wide scientific knowledge and his character have given a fundamental contribution to my (scientific and human) growth.

I wish to express my gratitude also to Prof. Cosenza: every time I met him, I had the chance to improve myself and my work from his experience and kind suggestions.

Special thanks to Prof. Verderame for his contribution to the present research, for his valuable advices and for his sincere friendship.

Special thanks also to my parents, Luigi and Carmelina, and to my brother, Jammy: they have taught me that only those who dare to fail greatly can ever achieve greatly.

This thesis is also the result of Annalisa's love: she has always supported me during times of challenge and controversy by reminding me that "great spirits have always encountered violent opposition from mediocre minds".

Finally, I would like to thank my colleagues and, above all, friends at StreGa Lab (University of Molise): Prof. Filippo Santucci de Magistris, Antonio Di Carluccio, Carmine Laorenza and Mariella Mancini, and all my friends at DIST (University of Naples).

# CONTENTS

LIST OF FIGURES	Pag.	VII
LIST OF TABLES	Pag.	XII
ABSTRACT	Pag.	XVI
CHAPTER 1		
§ 1.1 INTRODUCTION	Pag.	1
§ 1.1.1 Why (Operational) Modal Analysis for seismic protection of structures?	Pag.	1
§ 1.1.2 Experimental vs. Operational Modal Analysis	Pag.	4
§ 1.2 APPLICATIONS OF OMA AND OPEN ISSUES	Pag.	7
§ 1.3 THESIS OUTLINE	Pag.	13
CHAPTER 2		
§ 2.1 OPERATIONAL MODAL ANALYSIS: FUNDAMENTALS	Pag.	21
§ 2.2 STRUCTURAL DYNAMIC MODELS IN TIME AND FREQUENCY DOMAIN	Pag.	24
§ 2.2.1 Basic concepts	Pag.	24
§ 2.2.2 State-space models	Pag.	29
§ 2.2.3 Stochastic state-space models	Pag.	35
§ 2.2.4 ARMA models	Pag.	42
§ 2.2.5 A unified approach to modal identification	Pag.	48

## CONTENTS

---

§ 2.3 CHARACTERIZATION OF OUTPUT-ONLY TECHNIQUES	Pag.	54
§ 2.4 OMA IN FREQUENCY DOMAIN	Pag.	60
§ 2.4.1 The peak-picking method	Pag.	60
§ 2.4.2 The (Enhanced) Frequency Domain Decomposition	Pag.	64
§ 2.4.3 Frequency domain parametric procedures	Pag.	70
§ 2.5 OMA IN TIME DOMAIN	Pag.	72
§ 2.5.1 NExT-type procedures	Pag.	72
§ 2.5.2 AR- and ARMA-type procedures: Instrumental Variable and Prediction Error Method	Pag.	76
§ 2.5.3 Covariance-Driven Stochastic Subspace Identification	Pag.	80
§ 2.5.4 Data-Driven Stochastic Subspace Identification	Pag.	87
§ 2.6 SPECIAL METHODS	Pag.	99
§ 2.7 REMARKS	Pag.	104
CHAPTER 3		
§ 3.1 INTRODUCTION	Pag.	109
§ 3.2 THE MEASUREMENT CHAIN	Pag.	110
§ 3.2.1 Motion transducers	Pag.	110
§ 3.2.2 Data acquisition hardware: choice of measurement system	Pag.	116
§ 3.2.3 Data acquisition hardware: characteristics	Pag.	122
§ 3.3 DATA PROCESSING SOFTWARE AND PROGRAMMABLE HARDWARE: CUSTOMIZED SOLUTIONS FOR OMA	Pag.	125
§ 3.4 AN INTEGRATED OMA SYSTEM	Pag.	130
§ 3.4.1 Hardware selection	Pag.	130
§ 3.4.2 Software implementation: conceiving and organization	Pag.	133
§ 3.4.3 Data acquisition	Pag.	134
§ 3.4.4 Data pre-treatment	Pag.	138
§ 3.4.5 Data processing	Pag.	140
§ 3.4.6 Software validation	Pag.	145

---

---

**CHAPTER 4**

<b>§ 4.1 INTRODUCTION</b>	Pag.	149
<b>§ 4.2 DAMPING MECHANISMS</b>	Pag.	151
<b>§ 4.3 EXPERIMENTAL DAMPING ESTIMATION</b>	Pag.	159
<b>§ 4.4 DAMPING DATABASES AND EMPIRICAL PREDICTIONS</b>	Pag.	162
<b>§ 4.5 DAMPING ESTIMATION BY EFDD AND SSI: MAIN ISSUES</b>	Pag.	166
<b>§ 4.6 BUILDING A DATABASE OF MODAL PROPERTIES</b>	Pag.	169
<b>§ 4.7 REMARKS</b>	Pag.	170

**CHAPTER 5**

<b>§ 5.1 INTRODUCTION</b>	Pag.	173
<b>§ 5.2 THE MASONRY STAR VAULT (LECCE)</b>	Pag.	177
§ 5.2.1 Research background and motivations	Pag.	177
§ 5.2.2 The star vault: increasing the first level of knowledge	Pag.	183
<b>§ 5.3 THE TOWER OF THE NATIONS (NAPLES)</b>	Pag.	196
§ 5.3.1 Research motivations	Pag.	196
§ 5.3.2 The Tower of the Nations	Pag.	198
§ 5.3.3 Test program	Pag.	204
§ 5.3.4 Dynamic tests: setup	Pag.	205
§ 5.3.5 Experimental results	Pag.	208
§ 5.3.6 The Finite Element model	Pag.	212
§ 5.3.7 Model refinement	Pag.	219
§ 5.3.8 Other OMA tests	Pag.	230
<b>§ 5.4 THE SCHOOL OF ENGINEERING MAIN BUILDING (NAPLES)</b>	Pag.	233
<b>§ 5.5 "S. MARIA DEL CARMINE" BELL TOWER (NAPLES)</b>	Pag.	240
<b>§ 5.6 REMARKS</b>	Pag.	244

## CONTENTS

---

### CHAPTER 6

§ 6.1 INTRODUCTION	Pag.	245
§ 6.2 SHM: STATE-OF-THE-ART AND OPEN ISSUES	Pag.	248
§ 6.3 THE SCHOOL OF ENGINEERING MAIN BUILDING SHM SYSTEM	Pag.	255
§ 6.4 AUTOMATED MODAL PARAMETER IDENTIFICATION: LITERATURE REVIEW	Pag.	263
§ 6.5 FULLY AUTOMATED OMA: LEONIDA	Pag.	269
§ 6.5.1 The algorithm background	Pag.	269
§ 6.5.2 Implementation	Pag.	273
§ 6.5.3 Applications	Pag.	280
§ 6.6 AUTOMATED MODAL TRACKING: AFDD-T	Pag.	286
§ 6.6.1 Algorithm	Pag.	286
§ 6.6.2 Numerical validation	Pag.	290
§ 6.6.3 Implementation	Pag.	296
§ 6.7 AUTOMATED OMA FOR SHM: LEONIDA + AFDD-T	Pag.	298
§ 6.7.1 Leonida applied to the School of Engineering Main Building data	Pag.	298
§ 6.7.2 Integration of automated modal identification and tracking	Pag.	302
§ 6.8 REMARKS	Pag.	306
CHAPTER 7		
§ 7.1 CONCLUSIONS	Pag.	307
§ 7.2 FUTURE RESEARCH	Pag.	309
APPENDIX A	Pag.	311
APPENDIX B	Pag.	317
REFERENCES	Pag.	325
PUBLICATIONS	Pag.	357

## LIST OF FIGURES

<b>Figure 1.1.</b> Thesis outline	Pag. 20
<b>Figure 3.1.</b> Typical frequency response for Force Balance accelerometers	Pag. 113
<b>Figure 3.2.</b> Grounded (a) and floating (b) signal sources ( <a href="http://zone.ni.com/devzone">http://zone.ni.com/devzone</a> )	Pag. 117
<b>Figure 3.3.</b> LabView Front Panel	Pag. 126
<b>Figure 3.4.</b> LabView Block Diagram	Pag. 127
<b>Figure 3.5.</b> The Measurement and Automation eXplorer	Pag. 128
<b>Figure 3.6.</b> Connection to MySQL Database	Pag. 135
<b>Figure 3.7.</b> Data acquisition software	Pag. 136
<b>Figure 3.8.</b> EFDD flowchart	Pag. 141
<b>Figure 3.9.</b> SSI flowchart	Pag. 142
<b>Figure 3.10.</b> “Peak selection” subVI	Pag. 143
<b>Figure 4.1.</b> Decay curve for viscous damping	Pag. 153
<b>Figure 4.2.</b> Hysteresis loop	Pag. 154

## LIST OF FIGURES

---

<b>Figure 4.3.</b> Decay curve for friction damping	Pag. 155
<b>Figure 4.4.</b> Model for total damping vs. amplitude level	Pag. 158
<b>Figure 5.1.</b> Methodological path for interventions on historical constructions	Pag. 175
<b>Figure 5.2.</b> “Convento dei Carmelitani scalzi”: cadastral view (a); view from Libertini street (b)	Pag. 179
<b>Figure 5.3.</b> 3D definition of the star vault	Pag. 184
<b>Figure 5.4.</b> AC cut-off frequency response of the data acquisition modules	Pag. 186
<b>Figure 5.5.</b> Test setups: setup A (a) and setup B (b)	Pag. 189
<b>Figure 5.6.</b> CrossMAC matrices (DD-SSI vs. Cov-SSI): setup A (a) and setup B (b)	Pag. 193
<b>Figure 5.7.</b> Identified mode shapes: mode 1 (a) and mode 2 (b)	Pag. 193
<b>Figure 5.8.</b> AutoMAC matrices: setup A (a) and setup B (b)	Pag. 194
<b>Figure 5.9.</b> Complexity plots (Setup A): mode 1 (a) and mode 2 (b)	Pag. 194
<b>Figure 5.10.</b> Complexity plots (Setup B): mode 1 (a) and mode 2 (b)	Pag. 195
<b>Figure 5.11.</b> The Tower of the Nations: under construction (left), at completion (right)	Pag. 199
<b>Figure 5.12.</b> Carpentries: the first floor and the basement (a), the second floor (b), the third floor (c), the fourth floor (d), the fifth floor (e), the tenth floor (f)	Pag. 200
<b>Figure 5.13.</b> Transversal (left) and longitudinal (right) section	Pag. 201

---

## LIST OF FIGURES

---

<b>Figure 5.14.</b> Views from survey: r.c. diagonals and tuff walls (a), false ceiling linked to the floors (b)	Pag. 203
<b>Figure 5.15.</b> Views from survey: column reinforcement (a), foundation geometry (b), tested smooth rebars (c)	Pag. 204
<b>Figure 5.16.</b> Test layout	Pag. 206
<b>Figure 5.17.</b> Singular Value plots	Pag. 208
<b>Figure 5.18.</b> AutoMAC matrix	Pag. 209
<b>Figure 5.19.</b> Complexity plots	Pag. 210
<b>Figure 5.20.</b> CrossMAC matrices: Cov-SSI vs. EFDD (a), DD-SSI vs. EFDD (b)	Pag. 211
<b>Figure 5.21.</b> Construction of the FE model (from the 1st to the 4th level)	Pag. 213
<b>Figure 5.22.</b> FE model without (left) and with (right) basement	Pag. 214
<b>Figure 5.23.</b> Sensitivity of natural frequencies to elastic modulus changes (Floor = Shell – With basement)	Pag. 218
<b>Figure 5.24.</b> MAC matrix for the refined FE model	Pag. 229
<b>Figure 5.25.</b> Influence of the number of block rows on natural frequency and damping ratio estimates (mode 1 – RC3 – Cov-SSI)	Pag. 237
<b>Figure 5.26.</b> Influence of the number of block rows on natural frequency and damping ratio estimates (mode 2 – RC3 – Cov-SSI)	Pag. 238



## LIST OF FIGURES

---

<b>Figure 5.27.</b> Influence of the number of block rows on natural frequency and damping ratio estimates (mode 3 – RC3 – Cov-SSI)	Pag. 239
<b>Figure 5.28.</b> School of Engineering: CrossMAC EFDD – DD-SSI (a), CrossMAC EFDD – Cov-SSI (b)	Pag. 240
<b>Figure 5.29.</b> S. Maria del Carmine bell tower – courtesy of Ceroni F.	Pag. 241
<b>Figure 5.30.</b> S. Maria del Carmine bell tower: Singular Value plots (EFDD)	Pag. 243
<b>Figure 6.1.</b> The School of Engineering Main Building	Pag. 256
<b>Figure 6.2.</b> SHM system architecture: (a) Monitored constructions, (b) local server, (c) data transmission, (d) satellite communication and seismic network, (e) master server	Pag. 258
<b>Figure 6.3.</b> The remote database	Pag. 260
<b>Figure 6.4.</b> Roof sensors	Pag. 262
<b>Figure 6.5.</b> Averaged MAC vs. frequency plot	Pag. 274
<b>Figure 6.6.</b> Averaged MAC vs. step number: (a) noise, (b) mode bandwidth	Pag. 275
<b>Figure 6.7.</b> The algorithm for automated modal parameter identification	Pag. 277
<b>Figure 6.8.</b> Leonida software: state machine architecture and start-up phase	Pag. 278
<b>Figure 6.9.</b> Leonida software: data sources	Pag. 279

## LIST OF FIGURES

---

<b>Figure 6.10.</b> The Tower of the Nations: averaged MAC vs. frequency plot for TdN1 (a) and TdN2 (b) record	Pag. 281
<b>Figure 6.11.</b> The Tower of the Nations: Identified bandwidths (TdN2) for mode I (a), II (b), III (c) and IV (d)	Pag. 282
<b>Figure 6.12.</b> AFDD-T: algorithm for automated modal tracking	Pag. 286
<b>Figure 6.13.</b> MAC vs. frequency plot (a) and dispersion of values due to noise (b)	Pag. 288
<b>Figure 6.14.</b> Effect of number of sensors: poor spatial definition (a); improved spatial definition (b)	Pag. 289
<b>Figure 6.15.</b> AFDD-T sensitivity analyses: simulated data, shear type frame	Pag. 291
<b>Figure 6.16.</b> AFDD-T sensitivity analyses: simulated data, 3D frame (stiffness change)	Pag. 293
<b>Figure 6.17.</b> AFDD-T sensitivity analyses: simulated data, 3D frame (moment release)	Pag. 294
<b>Figure 6.18.</b> Mode bandwidth limit according to visual inspection of the first Singular Value plot	Pag. 295
<b>Figure 6.19.</b> AFDD-T: software interface	Pag. 297
<b>Figure 6.20.</b> School of Engineering Main Building: plots of monitoring results (summer 2008)	Pag. 304

## LIST OF TABLES

<b>Table 3.1.</b> Simulated identification (EFDD)	Pag. 146
<b>Table 3.2.</b> Simulated identification (Cov-SSI)	Pag. 147
<b>Table 3.3.</b> Simulated identification (DD-SSI)	Pag. 147
<b>Table 5.1.</b> Masonry properties	Pag. 188
<b>Table 5.2.</b> Star vault: results of modal identification (EFDD)	Pag. 191
<b>Table 5.3.</b> Star vault: results of modal identification (Cov-SSI)	Pag. 191
<b>Table 5.4.</b> Star vault: results of modal identification (DD-SSI)	Pag. 192
<b>Table 5.5.</b> Results of identification (EFDD)	Pag. 209
<b>Table 5.6.</b> Identified natural frequencies: comparison from different methods	Pag. 211
<b>Table 5.7.</b> Participating mass ratios (Floors = Shell – With basement)	Pag. 222
<b>Table 5.8.</b> Participating mass ratios (Floors = Diaphragm – With basement)	Pag. 222
<b>Table 5.9.</b> Participating mass ratios (Floors = Shell – Without basement)	Pag. 223

## LIST OF TABLES

---

<b>Table 5.10.</b> Participating mass ratios (Floors = Diaphragm – Without basement)	Pag. 223
<b>Table 5.11.</b> Optimization results (minimization of cumulative error on six modes)	Pag. 224
<b>Table 5.12.</b> Optimization results (minimization of cumulative error on six modes and maximum scatter lower than 5% for the single mode)	Pag. 225
<b>Table 5.13.</b> Optimization results (minimization of cumulative error on the first three modes)	Pag. 226
<b>Table 5.14.</b> Optimization results (weighted)	Pag. 227
<b>Table 5.15.</b> Mode shape correlation	Pag. 228
<b>Table 5.16.</b> Tower of the Nations: results of modal identification (EFDD)	Pag. 231
<b>Table 5.17.</b> Tower of the Nations: results of modal identification (Cov-SSI)	Pag. 232
<b>Table 5.18.</b> Tower of the Nations: results of modal identification (DD-SSI)	Pag. 232
<b>Table 5.19.</b> School of Engineering: results of modal identification (EFDD)	Pag. 234
<b>Table 5.20.</b> School of Engineering: results of modal identification (Cov-SSI)	Pag. 235
<b>Table 5.21.</b> School of Engineering: results of modal identification (DD-SSI)	Pag. 236
<b>Table 5.22.</b> S. Maria del Carmine bell tower: results of identification (EFDD)	Pag. 242

## LIST OF TABLES

---

<b>Table 5.23.</b> S. Maria del Carmine bell tower: results of identification (Cov-SSI)	Pag. 242
<b>Table 5.24.</b> S. Maria del Carmine bell tower: results of identification (DD-SSI)	Pag. 243
<b>Table 6.1.</b> Worldwide SHM systems	Pag. 253
<b>Table 6.2.</b> The Tower of the Nations: summary	Pag. 280
<b>Table 6.3.</b> The Tower of the Nations: results of automated modal identification	Pag. 283
<b>Table 6.4.</b> The star vault: summary	Pag. 284
<b>Table 6.5.</b> The star vault: results of automated modal identification	Pag. 284
<b>Table 6.6.</b> S. Maria del Carmine bell tower: summary	Pag. 285
<b>Table 6.7.</b> S. Maria del Carmine bell tower: results of automated modal identification	Pag. 285
<b>Table 6.8.</b> AFDD-T validation: simulated data, shear type frame	Pag. 290
<b>Table 6.9.</b> AFDD-T validation: simulated data, 3D frame	Pag. 292
<b>Table 6.10.</b> The School of Engineering Main Building: summary	Pag. 299
<b>Table 6.11.</b> The School of Engineering Main Building monitoring results: observed values of natural frequencies	Pag. 299
<b>Table 6.12.</b> School of Engineering Main Building: results of automated modal identification	Pag. 300

## LIST OF TABLES

---

<b>Table 6.13.</b> The School of Engineering Main Building: automated identification of mode bandwidth	Pag. 300
<b>Table 6.14.</b> School of Engineering Main Building: synthesis of monitoring results (summer 2008)	Pag. 303
<b>Table B.1.</b> Building-like structures: steel – earthquake	Pag. 317
<b>Table B.2.</b> Building-like structures: r.c. – earthquake	Pag. 317
<b>Table B.3.</b> Building-like structures: masonry – operational conditions	Pag. 318
<b>Table B.4.</b> Building-like structures: steel – operational conditions	Pag. 319
<b>Table B.5.</b> Building-like structures: steel – operational conditions	Pag. 320
<b>Table B.6.</b> Building-like structures: r.c. – operational conditions	Pag. 321
<b>Table B.7.</b> Bridges: steel–concrete composite – operational conditions	Pag. 322
<b>Table B.8.</b> Bridges: steel (cable stayed) – operational conditions	Pag. 322
<b>Table B.9.</b> Bridges: r.c. – operational conditions	Pag. 323
<b>Table B.10.</b> Bridges: r.c. (cable stayed) – operational conditions	Pag. 324

## ABSTRACT

This thesis focuses on output-only modal identification tests and on the opportunities they provide in the field of seismic protection of structures.

The problem of a good measurement process, in order to obtain high quality data and reliable results, is investigated. Reliability of estimates is assessed above all towards the problem of damping estimation, due to the fundamental role it plays in determining the structural response to dynamic loads, such as earthquakes.

Specific attention is focused on the relationship between experimental tests and numerical modelling, and on the opportunities given by model updating procedures in the field of earthquake engineering.

Finally, an algorithm for fully automated modal parameter identification and tracking is described, pointing out the importance of Operational Modal Analysis in the field of Structural Health Monitoring.

---

# 1

## Thesis Outline

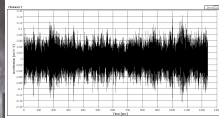
---

*«Why Output-Only Modal Analysis  
is a Desiderable Tool  
for a Wide Range of Practical Applications»*

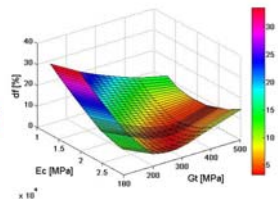
*Rune Brincker, Carlos E. Ventura, Palle Andersen*



?



$f, \xi, \psi$







# CHAPTER 1

## 1.1 INTRODUCTION

### 1.1.1 Why (Operational) Modal Analysis for seismic protection of structures?

In the last decades, new and powerful numerical methods for static and dynamic analysis and design of civil structures have been developed: the Finite Element (FE) method, in particular, and the fast progress in computer technology have provided the structural designer excellent analysis instruments, able to accurately simulate the structural behaviour. However, development of new high-performance materials and the increasing complexity of designed structures led engineers to ask for appropriate experimental tools in order to identify the most relevant structural properties, thus obtaining reliable data to support calibration and validation of numerical models.

Dynamic properties computed by FE analysis can differ from the actual dynamic properties of the structure for several reasons: first of all, FE analysis is based on a discretization of reality, and the displacement fields are approximated by predefined shape functions within each element;

## 1.1 INTRODUCTION

---

moreover, some simplified modelling assumption such as mass lumping or rigid diaphragm can cause scatter with respect to the actual behaviour. Damping is another source of uncertainty. Finally, the actual geometry of the structure can be somewhat different from that one used for the FE model.

Ageing and structural deterioration are also crucial issues in structural design and maintenance: effective structural health monitoring systems are, therefore, necessary and regular identification of modal parameters plays a relevant role in this field.

For such reasons, during the last thirty years, civil engineers began to take advantage of a number of techniques developed in the system identification and experimental modal analysis field: they firstly referred to electrical engineering but progressively spread to several other fields such as automotive, aerospace and civil engineering. Such techniques allowed the experimental identification of dynamic properties of structures by applying input-output modal identification procedures.

Traditional Experimental Modal Analysis (EMA), however, suffers some limitations, such as:

- Need of an artificial excitation in order to measure Frequency Response Functions (FRF) or Impulse Response Functions (IRF): in some cases, such as large civil structures, it is very difficult or even impossible to provide adequate excitation, so that background loading like wind or traffic is small if compared to the response from the artificial loading;

even in the case where this is possible, problems may arise due to non-linearities introduced by exciting the structure to a higher response level. Moreover, artificial loading is usually expensive and affected by the risk of damaging the structure;

- Operational conditions often different from those ones applied in the tests, since traditional EMA is carried out in the lab environment;
- Simulated boundary conditions, since tests are usually carried in the lab environment on components instead of complete systems.

As a consequence, since early 1990's increasing attention has been paid by the civil engineering community to Operational Modal Analysis (OMA) with applications on several structures (buildings, bridges, off-shore platforms, etc.).

OMA is based on measurements affecting only the response of the structure in operational conditions and subject to ambient (or natural) excitation in order to extract modal characteristics: for this reason, it is called also ambient, or natural-excitation, or output-only modal analysis.

OMA is very attractive due to a number of advantages with respect to traditional EMA:

- first of all, testing is fast and cheap to conduct;
- no excitation equipments are needed, neither boundary condition simulation;

## 1.1 INTRODUCTION

---

- it does not interfere with the normal use of the structure;
- it allows identification of modal parameters which are representative of the whole system in its actual operational conditions;
- operational modal identification by output-only measurements can be used also for vibration-based structural health monitoring and damage detection of structures.

Typical drawbacks are, instead, related to the availability of output data only for parameter identification, so that just unscaled mode shapes can be obtained, and to a signal-to-noise ratio in measured data much lower than in the case of controlled tests in lab environment: thus, very sensitive equipment and careful data analysis are needed.

### 1.1.2 Experimental vs. Operational Modal Analysis

Even if most of Operational Modal Analysis techniques are derived from traditional EMA procedures, the main difference is related to the basic formulation of input: in fact, EMA procedures are developed in a deterministic framework while OMA methods are based on random response, that is to say on a stochastic approach. Thus, many OMA techniques can be seen as the stochastic counterpart of the deterministic methods used in classical EMA, even if new hybrid deterministic-stochastic techniques are appearing (Van Overschee & De Moor 1994, Fassois 2001).

In Operational Modal Analysis input is assumed to be a Gaussian white noise, characterized by a flat spectrum in frequency domain: so, all modes are assumed to be equally excited in the frequency range of interest and extracted by appropriate procedures. However, this assumption has some drawbacks: modal participation factors cannot be computed and a reliable extraction of modal parameters can be difficult in presence of spurious harmonics close to a natural frequency.

The assumption on the nature of input has another consequence, which is related to the classification of methods.

In both cases of OMA and EMA, techniques can be categorized in frequency domain or time domain methods depending on the domain in which they operate.

Another common distinction is between global and local methods and between SDOF and MDOF methods (Heylen et al. 2002). However, while EMA techniques can be classified also according to the number of inputs and outputs (Single Input Single Output, Single Input Multiple Output, Multiple Input Single Output, Multiple Input Multiple Output), the identification algorithms for OMA are always MIMO-type, because of the above mentioned definition for the input. If assumptions about the input are not fulfilled, like in the case of free decay data used for operational modal identification, multiple sets of initial conditions are needed in order to handle closely spaced or even repeated modes, since multi-output measurements with respect to a single set of initial conditions are equivalent to SIMO, but not MIMO, systems (Zhang 2004).

## 1.1 INTRODUCTION

---

Notwithstanding these differences, modal analysis is always based on the following three steps:

- planning and execution of tests (proper location of sensors and, eventually, of actuators; selection of data acquisition parameters; eventual application of external excitation);
- data processing and identification of modal parameters (filtering, decimation, windowing; extraction of modal parameters);
- validation of the modal model.

Once the modal model has been found, it can be used for different purposes:

- Troubleshooting, if the identified vibrational properties are used to find out the cause of problems often encountered in real life such as excessive noise or vibrations;
- Model updating, if the experimental modal properties are used to enhance a FE model of the structure in order to make it more adherent to the actual behaviour of the structure itself; this is particularly useful in presence of historical or heritage structures characterized by complex structural systems and by uncertain material properties;
- Structural modification and sensitivity analysis, in order to evaluate the effect of changes on the dynamics without actually modifying the structure;

- Structural health monitoring and damage detection, by comparing modal parameters from the current state of a structure with the modal parameters at a reference state in order to obtain indications about presence, location and severity of damage on the structure;
- Performance evaluation, if modal parameters and mode shapes are used to assess the dynamic performance of a system;
- Force identification, starting from measurements of the structural response only.

### 1.2 APPLICATIONS OF OMA AND OPEN ISSUES

Operational Modal Analysis is the base for a number of applications: in particular, it is currently used in vibration-based structural health monitoring systems for performance evaluation or damage detection purposes, within force reconstruction methods and for model updating applications.

Assessment of the short-term impact due to natural hazards, such as earthquakes, and of the long-term deterioration process, due, for example, to age and fatigue, requires a continuous monitoring of structural performance and health state. Vibration-based structural health monitoring is an effective methodology for such an assessment. It is based on the relation between damage and changes in structural properties, such as mass, damping and stiffness. In general, damage detection algorithms



## 1.2 APPLICATIONS OF OMA AND OPEN ISSUES

---

can be classified in modal-based and non-modal-based: the first ones starts from the results of modal analysis, while the others are mainly related to the changes in structural response expressed, as an example, in terms of interstorey drift. Modal analysis is an effective tool for monitoring of the dynamic characteristics of structures since it allows identification of modal frequencies, damping ratios, mode shapes and their derivatives.

Some methods for modal-based damage detection and monitoring are herein briefly reviewed: more details can be found in the extensive literature available in this field (Doebling et al. 1996, Sohn et al. 2003, Farrar et al. 2007).

A first approach is based on the observation that changes in structural properties have consequences on natural frequencies. However, their relatively low sensitivity to damage requires high levels of damage and high accuracy of measurements in order to obtain reliable results. Moreover, since modal frequencies are global quantities, they cannot, in general, provide spatial informations about damage. Only higher mode natural frequencies can express local changes, but it is quite difficult to excite such modes in case of civil structures (Doebling et al. 1996, Farrar & Doebling 1999). On the other hand, significant changes in modal frequencies could not imply presence of damage, because of the effects of some environmental factors such as temperature changes. A variation of about 5% seems to be necessary to detect damage with confidence.

Application of changes in natural frequencies within vibration-based damage detection and monitoring can be found in a number of papers

(Doebling et al. 1996, Cawley & Adams 1979, Hearn & Testa 1991, Messina et al. 1992).

Another modal indicator for damage is based on mode shape changes. A number of applications are reported in the literature (Doebling et al. 1996 Kim et al. 1992): they use different approaches but the most popular ones are based on some indexes such as MAC (Allemang & Brown 1982) or COMAC (Lieven & Ewins 1988). Mode shape changes seem to be good indicators of damage: they can give informations also about location and can be employed also without a prior FE model. The main drawback is related to a quite high sensitivity to noise. An alternative could be the use of mode shape curvatures (Pandey et al. 1991).

A particular class of damage detection methods is based on the use of the flexibility matrix. Damage is identified by comparing the flexibility matrices of the structure in the undamaged and damaged states. Thanks to the inverse relation to the square of modal frequencies, these techniques are very sensitive to changes in the lower order modes.

Damage detection algorithms based on changes in modal damping ratios are less developed since influence of damage on damping in structures is not well-established, like the sources of damping. Other uncertainties are related to the way of modeling damping: even if the actual mechanism of dissipation in structures is closer to the hysteretic damping than to the viscous damping, the latter model is widely used thanks to its efficiency and reliability (Büyüköztürk & Yu 2003). Mass-proportional damping, stiffness-proportional damping and Rayleigh damping are further

## 1.2 APPLICATIONS OF OMA AND OPEN ISSUES

---

possible options for the behaviour of damping. Reliable analysis results can be obtained only with an appropriate choice of damping type: velocity-dependent viscous damping is currently extensively applied mainly because of its mathematical convenience.

As a general concept, damage should increase damping in structures. However, currently there are not available methods for accurate extraction of damping and for identification of its type or source, thus it is rarely used for vibration-based monitoring applications.

Another important application of system identification, which is in some way related to the issues of monitoring and damage prognosis, is force reconstruction: in fact, knowledge of loads acting on structures gives opportunities in the field of structural health assessment and of estimation of the remaining life-time. In a lot of practical applications it is impossible to measure forces resulting, as an example, from wind or traffic directly. Therefore, they can be determined only indirectly from dynamic measurements. A comprehensive discussion about time domain load reconstruction methods can be found in Klinkov & Fritzen (Klinkov & Fritzen 2007), while a frequency domain approach can be found in Aenlle et al. (Aenlle et al. 2007). All these methods require system identification as a first step for load estimation. Each technique has some advantages and suffers some drawbacks: advantages are mainly related to the possibility of some of them to be used on-line; the main drawbacks are, instead, related to ill-conditioning of the inverse problem (but it can be overcome by regularization techniques or by transformation of a ill-posed

problem into a well-posed one), to a certain degree of sensitivity to measurement noise and, in some cases, to the adoption of complex measurement setups.

The last main application of results of modal analysis concerns model updating. The extracted modal parameters, in fact, can be used to validate or enhance numerical models. In fact, FE models are usually affected by errors and uncertainties: some of them cannot be easily removed, being related to some intrinsic limitations of numerical methods or to modelling hypotheses and approximations. However, if a quite accurate model is available and there is some a-priori knowledge about characteristics of the structure or materials, it is possible to carry out sensitivity analyses on the remaining uncertain parameters in order to identify the values associated to the “best model”, that is to say a model able to reproduce experimental results within a certain degree of accuracy. Usual applications of FE model updating aim at identify material properties or boundary conditions. Anyway, in general a small set of parameters can be updated at a time.

Several techniques for model updating exist, including manual tuning of the update parameters. The updated model can be used for damage detection purposes (De Roeck 2005, Link et al. 2008) or for evaluation of short-term impact of natural hazardous events (earthquakes) or of manmade activities (rehabilitation, retrofitting).

Several applications of FE model updating are reported in the literature: the main progress in this field is related to uncertainty treatment by the use of probabilistic methods, in order to take into account variability in

## 1.2 APPLICATIONS OF OMA AND OPEN ISSUES

---

material properties or in geometrical parameters, of interval approaches, in order to judge about model admissibility of uncertain systems (Gabriele et al. 2007), and of fuzzy techniques, in order to take into account the lack of knowledge in parameters and initial or boundary conditions, deficiencies in modelling (related to idealization, simplification or errors in the modeling procedure) and subjectivity in implementation (Hanss 2005).

Even if Operational Modal Analysis concerns a lot of practical applications, there are still some open issues. The first one is related to structures excited by stochastic signals contaminated by spurious harmonics, due, for example, to rotating parts. The main drawbacks concerning the presence of deterministic signals superimposed to the stochastic part are the following:

- Potential mistakes in identification of modes (harmonics can be erroneously identified as structural modes);
- Potential bias in mode estimation, affecting natural frequency, damping and/or mode shape, in particular if the spurious harmonic is very close to the structural mode;
- Need of a high dynamic range to extract weak modes in presence of such harmonics.

Some techniques are currently available to identify deterministic signals and to reduce their influence on modal parameter estimation (Jacobsen et al. 2007) but further improvements are needed to threat this problem with confidence.

As said before, a limit of Operational Modal Analysis techniques is related to the lack of knowledge about the input, which allows only estimation of un-scaled mode shapes. However, some techniques have been recently developed in order to estimate the scaling factor: one of them is based on a mass change strategy (Aenlle et al. 2005) which allows identification of scaling factors through identification of the modal parameters of the unmodified structure and of the same structure after a mass modification. However, the added mass must cause a minimum frequency shift: thus, accuracy of modal parameter identification is crucial. Further improvements are still needed to enhance the accuracy of the method.

The last issue is related to the automation of modal parameter identification techniques, in order to fit the needs of fully automated structural health monitoring systems; however, a significant progress has been achieved in recent years, thanks to the development of a number of modal identification and tracking procedures which do not need any user intervention (Verboven et al. 2002, Verboven et al. 2003, Brincker et al. 2007, Deraemaeker et al. 2008, Rainieri et al. 2007a, Rainieri et al. 2008a). Only for tracking algorithms a preliminary identification of modal parameters is required.

### 1.3 THESIS OUTLINE

In the present thesis, Operational Modal Analysis techniques and their applications for seismic protection of structures are investigated. The

### 1.3 THESIS OUTLINE

---

reliability and high versatility of such techniques, which do not require knowledge about the excitation that causes structural vibrations, is demonstrated by applying them to a number of different case studies.

The thesis is basically organized in two parts. In the first part, the theoretical background of Operational Modal Analysis is reviewed and several methods are described, trying to point out similarities and differences among them. The common mathematical background underlying most of these techniques is described in order to define advantages and limitations of the different techniques and to choose some of them for implementation and application to actual measurements. Implementation and validation of some Operational Modal Analysis procedures is extensively described before applying them to actual records. Since measurement corrupted by noise are often a problem for a reliable identification process, some criteria for hardware selection and test execution are described, aiming at obtain high quality data. In order to keep bias error in modal parameter estimation as low as possible, some criteria for data processing, deriving from an extensive literature review and from personal experience, are reported. Damping estimation is very sensitive to such errors and this circumstance justifies also the large scatter encountered in the literature. Since the structural response to dynamic loads is strongly influenced by damping, a deeper knowledge about it is crucial; thus, the main damping mechanisms are reviewed and a collection of data from the literature is reported as a reference. Influence of data processing technique on damping estimates is also investigated.

In the second part of the thesis, some case studies are reported, pointing out the role of Operational Modal Analysis techniques for seismic protection of structures. In particular, the relationship between experimental tests and numerical modelling is described by mean of two case studies: in the first one, the role of FE modelling for proper definition of test setups is highlighted; in the second one, instead, the use of experimental data for model refinement is described, pointing out how this procedure can be driven by the requirements of seismic analyses. Some other case studies are also described because of their role for implementation and validation of fully automated output-only modal identification and tracking procedures. The role played by OMA and, in particular, by fully automated algorithms for modal identification in the field of Structural Health Monitoring (SHM) is extensively described, together with the basic concepts of SHM and its application for seismic protection of structures.

A more detailed chapter-by-chapter overview of this thesis is given in the following (see also Figure 1.1):

### *Chapter 1*

The research work is introduced by defining the subject, pointing out the own contributions and clarifying the organization of the text;



### 1.3 THESIS OUTLINE

---

#### *Chapter 2*

An extensive literature review of Operational Modal Analysis procedures is carried out, describing their theoretical background and pointing out similarities and differences, advantages and limitations. OMA techniques have been classified according to their characteristics and some of them have been extensively described in view of their implementation into a software.

#### *Chapter 3*

The problem of the correct choice of measurement hardware in presence of weak vibrations, such as in ambient vibration tests, is addressed, trying to define some criteria for selection. Data acquisition and validation are two preliminary phases of primary importance in order to obtain high quality data or to judge them: thus, such phases are described before the main data processing procedures. Then, implementation of selected OMA procedures into a software package is described: well-known and widely spread OMA techniques, working both in time and frequency domain, have been selected for implementation. Before applying them to actual measurements, a validation process, based on simulated data obtained from Finite Element models, has been carried out and the main results are presented.

### *Chapter 4*

Due to the high level of uncertainty characterizing structural damping, the main damping mechanisms are reviewed, together with the main factors influencing its values. The main problems related to its reliable estimation are described and some suggestions to obtain correct estimates are given. A database of natural frequencies and damping ratios for different kinds of structures is also reported and used as a reference: in fact, it is instructive to compare damping estimates from tests with those ones measured on similar structures, so that obvious errors or anomalies can be detected.

### *Chapter 5*

Application of OMA to some case studies is described. Results of modal identification tests carried out on a masonry star vault, in order to ultimately characterize the seismic vulnerability of the structure itself, are described: the role of Finite Element modelling, for a proper definition of test setups, and of dynamic tests and monitoring, for structural assessment and improvement of the level of knowledge about the structure, have been investigated.

The role played by OMA in the field of structural and seismic vulnerability assessment of historical constructions is further described by its application to the Tower of the Nations: in such a case, the results of modal tests are used for a model refinement. Requirements of seismic analyses have guided the process to the definition of an updated model.

### 1.3 THESIS OUTLINE

---

The results of modal tests on these and some other structures are summarized at the end of this chapter and used in the next one to validate an automated modal identification procedure.

#### *Chapter 6*

The basic concepts and targets of Structural Health Monitoring, the main techniques and the hardware solutions are reviewed. Implementation of a SHM system at the School of Engineering Main Building in Naples is described. The role played by OMA for the assessment of the health state of structures is summarized. An attempt to overcome the traditional limitations of OMA procedures related to the need of an extensive user interaction is described. An extensive literature review about automation of OMA methods has been carried out, pointing out advantages and limitations of the different procedures. A new algorithm is then described and applied to the case studies reported in the previous chapter. Moreover, a faster modal tracking procedure, based on the results of the fully automated algorithm and allowing a continuous near real-time evaluation of the modal parameters and, therefore, of the health state of the monitored structure, is discussed. Effective integration of the proposed automated modal parameter identification and tracking procedures within the SHM system of the School of Engineering Main Building in Naples is described, and the main results are shown.

### *Chapter 7*

Conclusions of the present research work are summarized. Moreover, open issues and suggestions for future research in the field of vibration-based structural health monitoring are given.

### 1.3 THESIS OUTLINE

---

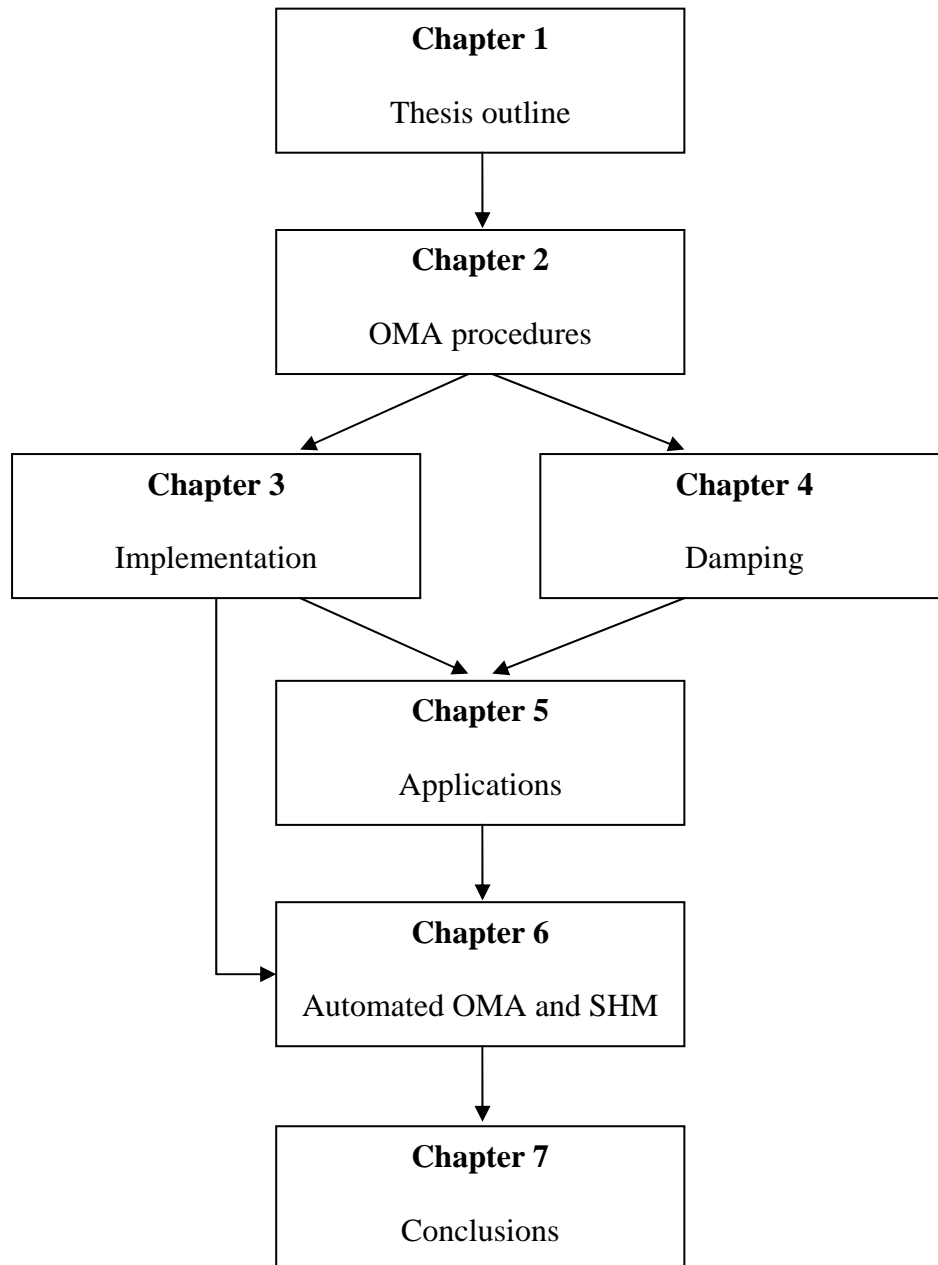


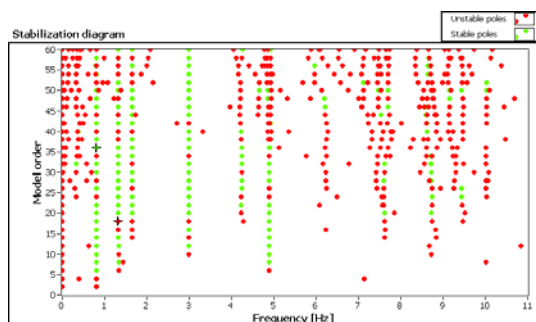
**Figure 1.1.** Thesis outline

# 2

## OMA Techniques

*«As far as the laws of mathematics refer to reality,  
they are not certain, and as far as they are certain,  
they do not refer to reality»*

*Albert Einstein*

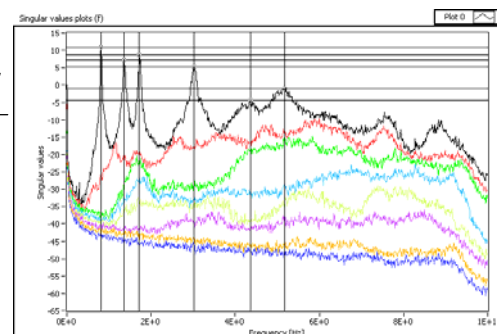


$$\{\dot{x}(t)\} = [A_c] \{x(t)\} + [B_c] \{u(t)\}$$

$$\{y(t)\} = [C_c] \{x(t)\} + [D_c] \{u(t)\}$$

$$[G_{yy}(\omega)] = \sum_{k \in \text{Sub}(\omega)} \frac{d_k \{\phi\}_k \{\phi\}_k^T}{j\omega - \lambda_k} + \frac{d_k^* \{\phi\}_k^* \{\phi\}_k^{*T}}{j\omega - \lambda_k^*}$$

$$[\hat{G}_{yy}(j\omega_i)] = [U]_i [S]_i [U]_i^H$$





## CHAPTER 2

### 2.1 OPERATIONAL MODAL ANALYSIS: FUNDAMENTALS

The expression Operational Modal Analysis is usually used to mean a large class of output-only modal identification procedures, that is to say techniques able to identify a modal model by response testing only. Such techniques are based on natural excitation, that is to say environmental vibrations (for civil structures) or vibrations in operational conditions (mechanic and aerospace systems). Several successful applications are reported in the literature. In the civil engineering field, Operational Modal Analysis has been applied to bridges (Brownjohn 1988, Gentile 2005, Benedettini et al. 2005, Gentile 2007, Cantieni 2005), buildings (Ventura & Turek 2005, Brownjohn 2005, Tamura et al. 2005), historical structures (Gentile 2005, Ramos et al. 2007), offshore platforms (Brincker et al. 1995), wind turbines (Ibsen & Liingaard 2005), dams (Baptista et al. 2005), stadia (Reynolds et al., 2005). Applications to ships (Rosenow et al. 2007), car bodies (Brincker et al. 2000a), trucks (Peeters et al. 2007), engines (Møller et al. 2000) and rotating machinery are, instead, directly related to the



## 2.1 OPERATIONAL MODAL ANALYSIS: FUNDAMENTALS

---

mechanical engineering field. In aerospace engineering, examples of output-only tests concern modal identification of aircrafts and shuttles by mean of in-flight tests (Marulo et al. 2005), and studies about flutter phenomena (Klepka & Uhl 2008).

Operational Modal Analysis techniques are based on the following assumptions:

- Linearity: the response of the system to a certain combination of inputs is equal to the same combination of the corresponding outputs;
- Stationarity: the dynamic characteristics of the structure do not change over time, that is to say, coefficients of differential equations describing the problem are constant with respect to time;
- Observability: test setup must be defined in order to be able to measure the dynamic characteristics of interest (nodal point must be avoided in order to detect a certain mode).

Moreover, being input unknown, it is assumed to be a stationary zero mean Gaussian white noise: this assumption implies that input is characterized by a flat spectrum in the frequency range of interest and, therefore, it gives a broadband excitation, so that all modes are excited. As a consequence, the output spectrum contains full information about the structure, since all modes are equally excited. From a mathematical point of view, signals are completely described by their correlation functions or by their counterpart in the frequency domain, the auto and cross power

spectra. It is worth noticing, however, that input actually has a spectral distribution of its own which is not necessarily flat: thus, modes are weighted by the spectral distribution of the input force and the response shows informations originating not only from structural modes but also from the excitation signal. Actual modes, therefore, must be selected among informations not related to physical modes, such as those ones due to input forces, measurement noise and harmonic vibrations created by rotating parts.

The assumption about stationarity of input and structural system is fundamental in the field of Operational Modal Analysis: however, these techniques seem to be robust also in presence of time varying inputs, leading to a reliable estimation of modal parameters. Application of Operational Modal Analysis techniques to time varying systems, instead, must be avoided.

In the next sections, after a short review about models of vibrating structures, classification of OMA methods according to different features will be discussed and the basic theory underlying the different methods will be reported.

## 2.2 STRUCTURAL DYNAMIC MODELS IN TIME AND FREQUENCY DOMAIN

### 2.2.1 Basic concepts

The dynamic behaviour of a structure can be represented either by a set of differential equations in the time domain, or by a set of algebraic equations in the frequency domain. Equations of motion are traditionally expressed in time domain, thus obtaining, for a general Multi-Degree-Of-Freedom (MDOF) system, the following set of linear, second order differential equations expressed in matrix form:

$$[M]\{\ddot{x}(t)\} + [C]\{\dot{x}(t)\} + [K]\{x(t)\} = \{f(t)\} \quad (2.1)$$

where  $\{\ddot{x}(t)\}$ ,  $\{\dot{x}(t)\}$  and  $\{x(t)\}$  are the acceleration, velocity and displacement vector respectively, while  $[M]$ ,  $[C]$  and  $[K]$  denote the mass, damping and stiffness matrices;  $\{f(t)\}$  is the forcing vector. This matrix equation is written for a linear, time invariant ( $[M]$ ,  $[C]$  and  $[K]$  are constant), observable system with viscous or proportional damping (see Chapter 4 for more details about damping models and related implications). In particular, it describes the dynamics between  $n$  discrete degrees of freedom (DOFs) of the structure and it is usually defined by using finite element modelling in order to obtain the mass and stiffness matrices. It is worth noticing that this kind of representation requires a

large number of DOFs (some order of magnitude larger than the number of DOFs required for an accurate experimental model) in order to adequately describe the dynamic behaviour of the structure. Equations of motion, which are coupled in this formulation, can be decoupled under the above mentioned assumptions by solving an eigenproblem: as a result, the solution can be obtained by superposition of eigensolutions. This is a standard formulation of the dynamic problem reported in several structural dynamics and modal analysis books (Chopra 2001, Ewins 1984, Heylen et al. 2002, Maia et al. 1997).

The matrix differential equation (2.1) becomes a set of linear algebraic equations by making use of the Fourier transform or of the Laplace transform, and of their properties (the interested reader can refer to classical signal processing books, or to Heylen et al. 2002); in particular, by Fourier transforming the equation of motion, one obtains:

$$-\omega^2 [M] \{X(\omega)\} + j\omega [C] \{X(\omega)\} + [K] \{X(\omega)\} = \{F(\omega)\} \quad (2.2)$$

where  $\{X(\omega)\}$  and  $\{F(\omega)\}$  are the Fourier transforms of  $\{x(t)\}$  and  $\{f(t)\}$ , respectively, and  $j = \sqrt{-1}$ .

It is worth noticing that time and frequency domain are two ways of representing the same problem: thus, the solutions of the dynamic problem are the same even if the mathematical expressions look like quite different. This concept can be easily understood by looking at the

## 2.2 STRUCTURAL DYNAMIC MODELS IN TIME AND FREQUENCY DOMAIN

---

solutions of the equations of motion due to a unit impulse, thus obtaining the so-called Impulse Response Function (IRF) in time domain:

$$[h(t)] = \sum_{r=1}^N \left[ [A]_r e^{\lambda_r t} + [A]_r^* e^{\lambda_r^* t} \right] \quad (2.3)$$

and its counterpart in frequency domain, the Frequency Response Function (FRF):

$$[H(\omega)] = \sum_{r=1}^N \left[ \frac{[A]_r}{j\omega - \lambda_r} + \frac{[A]_r^*}{j\omega - \lambda_r^*} \right] \quad (2.4)$$

being  $[A]_r$  the residue matrix,  $N$  the number of modes and  $\lambda_r$  the  $r$ -th eigenvalue;  $*$  denotes complex conjugate. IRF and FRF can be expressed also in terms of eigenvalues and left and right eigenvectors as follows:

$$[h(t)] = [\psi] e^{\lambda t} [L] \quad (2.5)$$

$$[H(\omega)] = [\psi] \left[ \frac{1}{j\omega - \lambda} \right] [L] \quad (2.6)$$

still pointing out that they are merely transform pairs and carry exactly the same informations. Similar expressions can be obtained by applying the Laplace transform<sup>1</sup>.

A linear time-invariant system can be, therefore, represented also through its FRF (or its transform, the IRF): in fact, by recalling that the FRF can be expressed also as the ratio between the Fourier transform of the output over the Fourier transform of the input, equation (2.2) becomes:

$$[Z(\omega)]\{X(\omega)\} = \{F(\omega)\} \quad (2.7)$$

with:

$$[Z(\omega)] = -\omega^2[M] + j\omega[C] + [K] \quad (2.8)$$

Thus, the FRF is:

$$[H(\omega)] = [Z(\omega)]^{-1} \quad (2.9)$$

---

<sup>1</sup> The Fourier and Laplace transforms are closely related. In general, the Fourier transform is important in the measurement process while the Laplace transform is often used in modal parameter estimation or data reduction process from a theoretical point of view. The solution of the equations of motion due to a unit impulse is the transfer function if the problem is solved in the Laplace domain: it is closely related to the FRF, being the FRF a transfer function evaluated along the imaginary axis. Numerical implementations of such transforms are the Fast Fourier Transform (FFT) and the z-transform, used in place of the Fourier transform and the Laplace transform respectively.

## 2.2 STRUCTURAL DYNAMIC MODELS IN TIME AND FREQUENCY DOMAIN

---

and, even if it is computed directly from the output and the input measurements, it carries all the informations about the inertial, elastic and energy dissipating properties of the structure.

By focusing on the structure of the FRF matrix it is possible to identify some other useful characteristics for modal analysis. First of all, the partial fraction expansion (2.4) of the FRF matrix shows that each mode gives a contribution to the response of the system at any frequency: therefore, ideally speaking it is impossible to excite only one mode of a structure by mean of a single frequency sine wave (Richardson & Schwarz 2003). However, near a resonance this summation can be approximated by the term related to the corresponding mode: SDOF identification methods are based on this assumption, as it will be discussed in the next sections. Moreover, from (2.4) it is evident that every element of the FRF matrix has the same denominator: since the poles of the system are related to denominator terms and since the poles are directly related to the modal frequency and damping of a mode, they can be estimated from any FRF or from multiple FRFs measured on the same structure, thus allowing classification of modal analysis techniques as local or global. Informations about mode shapes, instead, are held in the modal residue matrix, which is a complex valued matrix basically given by an outer product of the mode shape vector with itself (Heylen et al. 2002):

$$[A]_r = Q_r \{\psi\}_r \{\psi\}_r^T \quad (2.10)$$

being  $Q_r$  a constant, while the superscript  $^T$  means transpose.

Being IRF and FRF a transform pair, like the FRFs each IRF is a summation of contributions due to each mode. In particular, equation (2.3) can be rewritten as a sum of damped sinusoids:

$$[h(t)] = \sum_{r=1}^N [|A|_r e^{-\sigma_r t} \sin(\omega_{dr} t + \alpha_r)] \quad (2.11)$$

where  $|A|_r$  is the matrix of residue magnitudes and  $\alpha_r$  the matrix of residue phases. Equation (2.11) clarifies the role that each modal parameter plays in an IRF: in fact, the damping factor  $\sigma_r$ , given by the product of the undamped natural frequency  $\omega_{nr}$  and of damping ratio  $\xi_r$ , defines the exponential decay envelope for each mode; the damped natural frequency  $\omega_{dr}$ :

$$\omega_{dr} = \omega_{nr} \sqrt{1 - \xi_r^2} \quad (2.12)$$

defines the sinusoidal frequency for each mode; the residue defines the amplitude of response of each mode.

### 2.2.2 State-space models

State space-models are used to convert the second order problem, stated by the differential equation of motion (2.1) in matrix form, into two first



## 2.2 STRUCTURAL DYNAMIC MODELS IN TIME AND FREQUENCY DOMAIN

---

order problems, defined by the so-called “state equation” and “observation equation”.

The state equation can be obtained by the second order equation of motion by some mathematical manipulations. For clarity reasons, notations in equation (2.1) are changed as follows:

$$[M]\{\ddot{q}(t)\} + [C]\{\dot{q}(t)\} + [K]\{q(t)\} = \{f(t)\} = [\bar{B}]\{u(t)\} \quad (2.13)$$

where  $\{\ddot{q}(t)\}$ ,  $\{\dot{q}(t)\}$  and  $\{q(t)\}$  are the acceleration, velocity and displacement vector respectively. The forcing vector  $\{f(t)\}$  is factorized into the matrix  $[\bar{B}]$ , which defines the location of inputs, and into the vector  $\{u(t)\}$ , describing inputs in time. By defining the “state vector”  $\{x(t)\}$ :

$$\{x(t)\} = \begin{Bmatrix} \dot{q}(t) \\ q(t) \end{Bmatrix} \quad (2.14)$$

from (2.13) the following equation can be obtained:

$$\{\ddot{q}(t)\} + [M]^{-1}[C]\{\dot{q}(t)\} + [M]^{-1}[K]\{q(t)\} = [M]^{-1}\{f(t)\} = [M]^{-1}[\bar{B}]\{u(t)\} \quad (2.15)$$

and therefore, by combining (2.14) and (2.15) and adding the identity  $[M]\{\dot{q}(t)\} = [M]\{\dot{q}(t)\}$ :

$$\{\dot{x}(t)\} = \begin{bmatrix} -[M]^{-1}[C] & -[M]^{-1}[K] \\ [I] & [0] \end{bmatrix} \{x(t)\} + \begin{bmatrix} [M]^{-1}[\bar{B}] \\ [0] \end{bmatrix} \{u(t)\} \quad (2.16)$$

By defining the “state matrix”  $[A_c]$  and the “input influence matrix”  $[B_c]$  as follows:

$$[A_c] = \begin{bmatrix} -[M]^{-1}[C] & -[M]^{-1}[K] \\ [I] & [0] \end{bmatrix} \quad (2.17)$$

$$[B_c] = \begin{bmatrix} [M]^{-1}[\bar{B}] \\ [0] \end{bmatrix} \quad (2.18)$$

the state equation is given by:

$$\{\dot{x}(t)\} = [A_c] \{x(t)\} + [B_c] \{u(t)\} \quad (2.19)$$

where the subscript  $c$  denotes continuous time.

Before deriving the observation equation, it is worth emphasizing that a real structure is characterized by an infinite number of DOFs which becomes a finite but large number in finite element models, where lumped systems are considered. However, in a practical vibration test, this number decreases from hundreds and hundreds to a few dozens or even less: thus,

## 2.2 STRUCTURAL DYNAMIC MODELS IN TIME AND FREQUENCY DOMAIN

---

by assuming that measurements are taken at  $l$  locations and that the sensors are either accelerometers, velocimeters and displacement transducers in the most general case, the observation equation can be written as:

$$\{y(t)\} = [C_a]\{\ddot{q}(t)\} + [C_v]\{\dot{q}(t)\} + [C_d]\{q(t)\} \quad (2.20)$$

where  $\{y(t)\}$  is the vector of the outputs,  $[C_a]$ ,  $[C_v]$  and  $[C_d]$  are the output location matrices for acceleration, velocity and displacement respectively. Combining equations (2.20) and (2.13) the following equation is obtained:

$$\begin{aligned} \{y(t)\} = & \left( -[C_a][M]^{-1}[C] + [C_v] \right) \{\dot{q}(t)\} + \\ & + \left( -[C_a][M]^{-1}[K] + [C_d] \right) \{q(t)\} + \left( [C_a][M]^{-1}[\bar{B}] \right) \{u(t)\} \end{aligned} \quad (2.21)$$

and using the definition of state vector:

$$\{y(t)\} = [C_c]\{x(t)\} + [D_c]\{u(t)\} \quad (2.22)$$

where  $[C_c]$  is the “output influence matrix” and  $[D_c]$  is the “direct transmission” matrix, whose expressions are:

$$\begin{aligned}
[C_c] &= [C_v] - [C_a][M]^{-1}[C] \quad [C_d] - [C_a][M]^{-1}[K], \\
[D_c] &= [C_a][M]^{-1}[\bar{B}]
\end{aligned}
\tag{2.23}$$

The direct transmission matrix disappears if no accelerometers are used for output measurements. The physical sense of this matrix is related to the circumstance that a step change in the force  $\{u(t)\}$  causes a step change in the acceleration response  $\{y(t)\}$ .

By combining equations (2.19) and (2.22), the classical continuous-time state-space model is obtained:

$$\begin{aligned}
\{\dot{x}(t)\} &= [A_c]\{x(t)\} + [B_c]\{u(t)\} \\
\{y(t)\} &= [C_c]\{x(t)\} + [D_c]\{u(t)\}
\end{aligned}
\tag{2.24}$$

An important characteristic of this model is the existence of an infinite number of equivalent state-space representations for a given system: each one is referred to as a realization. Since every system has an infinite number of realizations, all we can hope to do experimentally is to establish one of these realizations. Multiplicity of realizations can be easily shown by considering the following “similarity transformation”:

$$\{x(t)\} = [T]\{z(t)\} \quad (2.25)$$

where  $[T]$  is an arbitrary non-singular square matrix. Substitution of (2.25) in (2.24) yields:

$$\{\dot{z}(t)\} = [T]^{-1}[A_c][T]\{z(t)\} + [T]^{-1}[B_c]\{u(t)\} \quad (2.26)$$

$$\{y(t)\} = [C_c][T]\{z(t)\} + [D_c]\{u(t)\}$$

It is evident that the matrices  $[T]^{-1}[A_c][T]$ ,  $[T]^{-1}[B_c]$ ,  $[C_c][T]$  and  $[D_c]$  describe the same relationship as the matrices  $[A_c]$ ,  $[B_c]$ ,  $[C_c]$  and  $[D_c]$ . However, it is worth noticing that, since the state matrices of any two realizations are related by a similarity transformation, the eigenvalues (related to the modal properties of the system) are preserved.

Since experimental tests yield measurements taken at discrete time instants while equations (2.24) are expressed in continuous time, the state space model must be converted to discrete time. By choosing a certain fixed sampling period  $\Delta t$ , the continuous-time equations can be discretized and solved at all discrete time instants  $t = k\Delta t$ ,  $k \in N$ . A certain behaviour of the time-dependent variables between two samples have to be assumed to this aim: for example, the Zero Order Hold (ZOH) assumption states that the input is piecewise constant over the sampling

period. Under this assumption the continuous-time state-space model (2.24) can be converted to the discrete-time state-space model:

$$\begin{aligned}\{x_{k+1}\} &= [A]\{x_k\} + [B]\{u_k\} \\ \{y_k\} &= [C]\{x_k\} + [D]\{u_k\}\end{aligned}\tag{2.27}$$

where  $\{x_k\} = \{x(k\Delta t)\}$  is the discrete-time state vector yielding the sampled displacements and velocities,  $\{u_k\}$  and  $\{y_k\}$  are the sampled input and output,  $[A]$  is the discrete state matrix,  $[B]$  is the discrete input matrix,  $[C]$  is the discrete output matrix and  $[D]$  is the direct transmission matrix. These last two matrices are not influenced by the ZOH sampling. Mathematical derivation of equations (2.27) and of relations between continuous-time and discrete-time matrices is beyond the scope of this thesis: the interested reader can refer to (Juang 1994).

### 2.2.3 Stochastic state-space models

The model given by (2.27) is a deterministic model, that is to say the system is driven only by a deterministic input: however, stochastic components must be necessarily included in order to describe actual measurement data. If stochastic components are included in the model, the following “discrete-time combined deterministic-stochastic state-space model” is obtained:

$$\begin{aligned}\{x_{k+1}\} &= [A]\{x_k\} + [B]\{u_k\} + \{w_k\} \\ \{y_k\} &= [C]\{x_k\} + [D]\{u_k\} + \{v_k\}\end{aligned}\tag{2.28}$$

where  $\{w_k\}$  is the “process noise” due to disturbances and model inaccuracies, while  $\{v_k\}$  is the “measurement noise” due to sensor inaccuracy. These vector signals are both unmeasurable: they are assumed to be zero mean Gaussian white noise processes with covariance matrices given by:

$$E\left[\begin{pmatrix} \{w_p\} \\ \{v_p\} \end{pmatrix} \begin{pmatrix} \{w_q^T\} & \{v_q^T\} \end{pmatrix}\right] = \begin{pmatrix} [Q] & [S] \\ [S]^T & [R] \end{pmatrix} \delta_{pq}\tag{2.29}$$

where  $E$  is the expected value operator,  $\delta_{pq}$  is the Kronecker delta (if  $p=q$  then  $\delta_{pq} = 1$ , otherwise  $\delta_{pq} = 0$ ),  $p$  and  $q$  are two arbitrary time instants.

More details about combined deterministic-stochastic systems can be found in (Van Overschee & De Moor 1996): in this section, instead, attention is focused on purely stochastic systems in compliance with the Operational Modal Analysis framework concerning structures excited by some unmeasurable inputs. Due to the lack of information about the input  $\{u_k\}$ , it is implicitly modelled by the noise terms  $\{w_k\}$  and  $\{v_k\}$ , thus obtaining the following “discrete-time stochastic state-space model”:

$$\begin{aligned}\{x_{k+1}\} &= [A]\{x_k\} + \{w_k\} \\ \{y_k\} &= [C]\{x_k\} + \{v_k\}\end{aligned}\tag{2.30}$$

The white noise assumption about  $\{w_k\}$  and  $\{v_k\}$  cannot be omitted for the proof of this class of identification methods (see also Van Overschee & De Moor 1996). If this assumption is violated, that is to say the input include white noise and some additional dominant frequency components, such components will appear as poles of the state matrix  $[A]$  and cannot be separated from the eigenfrequencies of the system.

Stochastic state-space models are characterized also by some other properties than those ones affecting  $\{w_k\}$  and  $\{v_k\}$ . First of all, the stochastic process is assumed to be stationary with zero mean:

$$E[\{x_k\}\{x_k\}^T] = [\Sigma], \quad E[\{x_k\}] = \{0\}\tag{2.31}$$

where the state covariance matrix  $[\Sigma]$  is independent of the time instant  $k$ . Moreover, since  $\{w_k\}$  and  $\{v_k\}$  have zero mean and are independent of the actual state, the following relations are obtained:

$$E[\{x_k\}\{w_k\}^T] = [0], \quad E[\{x_k\}\{v_k\}^T] = [0]\tag{2.32}$$

The output covariance matrices are, instead, defined as:



$$[R_i] = E[\{y_{k+i}\}\{y_k\}^T] \quad (2.33)$$

From stationarity, the assumptions about the noise terms and these last properties, the following relations can be obtained:

$$[\Sigma] = [A][\Sigma][A]^T + [Q], [R_0] = [C][\Sigma][C]^T + [R] \quad (2.34)$$

$$[G] = [A][\Sigma][C]^T + [S], [R_i] = [C][A]^{i-1}[G]$$

The last property, in particular, is the most important: in fact, it states that the output covariance sequence can be estimated from measurement data. As a consequence, by decomposing the estimated output covariance sequence according to (2.34), the state-space matrices can be obtained and the modal identification problem is solved.

When dealing with discrete-time stochastic state-space models, where the input is implicitly modelled by disturbance, that is to say process noise and measurement noise, an alternative model, the so-called “forward innovation model” can be obtained by applying the steady-state Kalman filter to the stochastic state-space model given by equation (2.30). In order to describe this model, some concepts about Kalman filter are reported, together with definitions of “state prediction error” and “innovation”.

Let us suppose for a moment that the system matrices of the state-space system are known; moreover, given a time instant  $k$ , let us suppose that all previous measurements  $[Y^{k-1}]$  from  $t_0$  to  $t_{k-1}$  are known:

$$[Y^{k-1}] = [\{y_0\}, \{y_1\}, \dots, \{y_{k-1}\}]^T \quad (2.35)$$

The state prediction error:

$$\{\varepsilon(t_k)\} = \{x(t_k)\} - \{\hat{x}(t_k | t_{k-1})\} \quad (2.36)$$

represents the part of  $\{x_k\}$  which cannot be predicted by the one-step-ahead predictor of the state vector:

$$\{\hat{x}(t_k | t_{k-1})\} = E[\{x(t_k)\} | [Y^{k-1}]] \quad (2.37)$$

which is defined as the conditional mean of  $\{x_k\}$  given all previous measurements.

The innovation:

$$\{e(t_k)\} = \{y(t_k)\} - \{\hat{y}(t_k | t_{k-1})\} \quad (2.38)$$

## 2.2 STRUCTURAL DYNAMIC MODELS IN TIME AND FREQUENCY DOMAIN

---

represents, instead, the part of the measured response  $\{y_k\}$  which cannot be predicted by the one-step-ahead predictor defined by the following conditional mean:

$$\{\hat{y}(t_k | t_{k-1})\} = E[\{y(t_k)\} | Y^{k-1}] \quad (2.39)$$

Since  $\{y_k\}$  is assumed zero mean and Gaussian distributed,  $\{e_k\}$  is a zero-mean Gaussian white noise process.

The optimal state estimation can be obtained by the Kalman filter. The Kalman filter is standard in control theory: for more details or for mathematical derivations, the interested reader can refer to the literature (Juang 1994, Brown 1983); here just some basic concepts are reported.

Let us suppose that the state-space model matrices and the measurements  $\{y\}$  are known: the optimal (in the sense that the state prediction error is as small as possible) estimate  $\{\hat{x}_k\}$  for the state  $\{x_k\}$  can be obtained by applying the Kalman filter. In order to obtain the Kalman gain matrix, the state prediction error covariance matrix  $[P_k]$  has to be obtained as a solution of the algebraic Ricatti equation (Juang 1994); then, the Kalman gain matrix and the state estimate can be computed. It is worth noticing that, at start-up, the prediction of the state and, therefore, the state prediction error covariance are not steady. Thus, the Kalman filter experiences a transient phase: the non-steady-state Kalman filter state estimates  $\{\hat{x}_k\}$  are obtained by a recursive process. However, the estimates

often reach a steady value very quickly: it is possible, therefore, to compute the constant value  $[P]$  of the error covariance which satisfies the steady-state algebraic Ricatti equation and then the steady-state Kalman filter gain matrix  $[K]$  (which is a constant matrix, too).

Theoretically, the Kalman filter is very attractive because of the closed-form solution (given by the Ricatti equation) for its gain matrix: however, the Kalman filter requires informations about the system matrices, including the covariances of the process and measurement noises. Even if the measurement noise can be quantified by a large number of repeated tests on the sensors, the process noise due to modelling errors and system uncertainties is very difficult to quantify in practice. In practical applications, therefore, the Kalman sequence  $\{\hat{x}_k\}$  is estimated directly from experimental data without estimating the covariance of the process and measurement noises and solving the Ricatti equation (see, for example, Van Overschee & De Moor, 1996).

Even if in system identification the Kalman filter is unknown, the stochastic state-space model (2.30) can be expressed in terms of the steady-state Kalman filter and of the innovation, thus obtaining the following forward innovation model:

$$\begin{aligned}\{\hat{x}_{k+1}\} &= [A]\{\hat{x}_k\} + [K]\{e_k\} \\ \{y_k\} &= [C]\{\hat{x}_k\} + \{e_k\}\end{aligned}\tag{2.40}$$

### 2.2.4 ARMA models

Under the usual assumption of linear time-invariant behaviour of the dynamic system, when it is excited by ambient excitation the dynamic equation of motion can be written as follows:

$$[M]\{\ddot{x}(t)\} + [C]\{\dot{x}(t)\} + [K]\{x(t)\} = \{w(t)\}, \quad \{w(t)\} \in NID([0], [W])\tag{2.41}$$

that is to say the ambient vibration is modelled by mean of a continuous-time Gaussian white noise  $\{w(t)\}$  with zero mean and intensity described by the matrix  $[W]$ . In Andersen (Andersen 1997) and Andersen et al. (Andersen et al. 1996) it is shown how this system can be represented in terms of a discrete-time Auto-Regressive Moving Average Vector (ARMAV<sup>2</sup>) model and its application for extraction of modal parameters of civil structures is reported.

In order to explain how modal parameters can be extracted from an ARMA model, a continuous-time system is assumed to be observed at

---

<sup>2</sup> The model is said to be an ARMA vector model to point out its multivariate character.

discrete time instants  $k$  with a sampling interval  $\Delta t$ . A covariance equivalence technique (Bartlett 1946, Pandit & Wu 1984) is used for discretization: in fact, being the input on the structure not available (measurable), the equivalent discrete-time system can be obtained only by requiring that the covariance function of the system response for a Gaussian white noise input is coincident at all discrete time lags with that one of the continuous-time system: this implies that the first and second order moments of the response of the continuous-time system must be equal to the first and second order moments of the response of the discretized model at all discrete time instants. By assuming that such response is Gaussian distributed, the covariance equivalent model is the most accurate approximated model, being it exact at all discrete time lags. In Andersen et al. (Andersen et al. 1996) this approach has been generalized to multivariate second order systems. It is worth emphasizing that the dynamic behaviour of the system is determined by the ambient vibration (the Gaussian white noise  $\{w(t)\}$ ) but the system is also affected by disturbances (process and measurement noise), and they must be taken into account by the equivalent discrete-time model. If disturbances are taken into account, the covariance equivalent ARMA model is an ARMAV( $n_\alpha, n_\gamma$ ) model expressed by the following polynomial form:

$$\{y_k\} + [\alpha_1]\{y_{k-1}\} + \dots + [\alpha_{n_\alpha}]\{y_{k-n_\alpha}\} = \{e_k\} + [\gamma_1]\{e_{k-1}\} + \dots + [\gamma_{n_\gamma}]\{e_{k-n_\gamma}\} \quad (2.42)$$

---

## 2.2 STRUCTURAL DYNAMIC MODELS IN TIME AND FREQUENCY DOMAIN

---

where  $\{y_k\}$  is the output vector and  $\{e_k\}$  is a white noise sequence vector (the innovation). The left-hand side is the Auto-Regressive (AR) part, while the right-hand side is the Moving Average (MA) part. The matrices  $[\alpha_i]$  are the AR matrix parameters, while the matrices  $[\gamma_i]$  are the MA matrix parameters;  $n_\alpha$  and  $n_\gamma$  are the AR and MA order of the model respectively, and, for the considered covariance equivalent model, they are equal to the same value  $p$ : this particular model is referred to as an ARMAV ( $p, p$ ) model. All coefficient matrices of the polynomials have dimension  $l \times l$ , being  $l$  the number of observed responses. The innovation is a zero mean Gaussian white noise with a second-order moment described by the covariance matrix  $[\Lambda]$ . This ARMAV model can be equivalently represented by a stochastic state-space system of the form (Andersen & Brincker 1999):

$$\begin{aligned}\{x(t_{k+1})\} &= [A]\{x(t_k)\} + [B]\{e(t_k)\} \\ \{y(t_k)\} &= [C]\{x(t_k)\} + \{e(t_k)\}\end{aligned}\tag{2.43}$$

where  $\{x(t_k)\}$  is a  $pl \times 1$  dimensional state vector. In fact, in Andersen (Andersen 1997) it is shown that, given a minimal realization of order  $n$  of a state-space system, an equivalent ARMA model can be obtained apart from the actual realization: in particular, if the state-space dimension  $n$  of the stochastic state-space system divided by the number  $l$  of outputs is an

integer value  $p$ , the state-space system can be equivalently represented by the ARMAV( $p, p$ ) model. On the contrary, in order to convert an ARMA model to a state-space representation, it is necessary to choose a realization: a realization which can be easily constructed from the auto-regressive and moving average matrices and which is well-conditioned, in order to be numerically efficient when implemented into a system identification software, must be adopted. In Andersen (Andersen 1997) it is suggested to use the so-called observability canonical state-space realization given by:

$$\begin{aligned}
 [A] &= \begin{bmatrix} [0] & [I] & [0] & \dots & [0] \\ [0] & [0] & [I] & \dots & [0] \\ \dots & \dots & \dots & \dots & \dots \\ [0] & [0] & [0] & \dots & [I] \\ -[\alpha_p] & -[\alpha_{p-1}] & -[\alpha_{p-2}] & \dots & -[\alpha_1] \end{bmatrix} \\
 [B] &= \begin{bmatrix} [I] & [0] & [0] & \dots & [0] \\ [\alpha_1] & [I] & [0] & \dots & [0] \\ \dots & \dots & \dots & \dots & \dots \\ [\alpha_{p-2}] & [\alpha_{p-3}] & [\alpha_{p-4}] & \dots & [0] \\ [\alpha_{p-1}] & [\alpha_{p-2}] & [\alpha_{p-3}] & \dots & [I] \end{bmatrix} \parallel \begin{bmatrix} [\gamma_1] - [\alpha_1] \\ [\gamma_2] - [\alpha_2] \\ \dots \\ [\gamma_{p-1}] - [\alpha_{p-1}] \\ [\gamma_p] - [\alpha_p] \end{bmatrix} \quad (2.44)
 \end{aligned}$$

$$[C] = [[I] \quad [0] \quad [0] \quad \dots \quad [0]]$$

which yields the following relation between the auto-regressive system matrices and the state-space matrices:



$$\begin{bmatrix} [\alpha_p] & [\alpha_{p-1}] & \dots & [\alpha_1] \end{bmatrix} \begin{bmatrix} [O_p] \end{bmatrix} = -[C][A]^p \quad (2.45)$$

where:

$$\begin{bmatrix} [O_p] \end{bmatrix} = \begin{bmatrix} [C] \\ [C][A] \\ \dots \\ [C][A]^{p-1} \end{bmatrix} \quad (2.46)$$

is the so-called observability matrix.

The state matrix  $[A]$ , when expressed in the form (2.44), is also known as the companion matrix for the auto-regressive matrix polynomial. The modal parameters can then be extracted by modal decomposing the companion matrix as:

$$[A] = [\psi][\mu][\psi]^{-1}, \quad [\mu] = \begin{bmatrix} \ddots & & \\ & \mu_i & \\ & & \ddots \end{bmatrix} \quad (2.47)$$

The modal decomposition is described by the pl eigenvectors, which are the columns of  $[\psi]$ , and by the pl eigenvalues  $\mu_i$ . The eigenvectors  $\{\psi_i\}$  are made by the mode shapes  $\{\phi_i\}$  and the eigenvalues  $\mu_i$ :

$$[\psi] = \begin{bmatrix} \{\phi_1\} & \dots & \dots & \{\phi_{pl}\} \\ \mu_1 \{\phi_1\} & \dots & \dots & \mu_{pl} \{\phi_{pl}\} \\ \dots & \dots & \dots & \dots \\ \mu_1^{p-1} \{\phi_1\} & \dots & \dots & \mu_{pl}^{p-1} \{\phi_{pl}\} \end{bmatrix} \quad (2.48)$$

The mode shapes, natural eigenfrequencies and damping ratios of the continuous-time system can therefore be extracted starting by the following relations:

$$\{\phi_i\} = [C] \{\psi_i\}, \quad (\mu_i, \mu_i^*) = e^{\left(-2\pi f_i \xi_i \pm j 2\pi f_i \sqrt{1-\xi_i^2}\right) \Delta t} \quad (2.49)$$

where  $i=1, \dots, pl/2$ , if the modes are underdamped and, thus, appear in complex conjugate pairs.

As a result, a  $p^{\text{th}}$  order ARMA model is a good representation of a vibrating structure. Since modal properties of the structure are obtained by the eigenvalue decomposition of the companion matrix, holding the AR coefficient matrices, some authors (Pandit 1991, De Roeck et al. 1995) have demonstrated the possibility to use an AR model for modal parameter estimation. However, a  $p^{\text{th}}$  order AR model is not an equivalent representation of such a structure. The use of an AR model, instead of an ARMA one, can be justified if the AR model order goes to infinity, but, under this assumption, lots of spurious poles are introduced and they have to be separated from the true system poles.

### 2.2.5 A unified approach to modal identification

A number of modal identification techniques, both input-output methods or output-only methods (which can be considered as a particular case of the first ones, where input is not measured but its spectrum is assumed to be constant in the frequency range of interest), has been derived according to the theoretical expressions of FRF or IRF. Different physically based models and different mathematical manipulations produced a number of different methods over the time. However, Allemang & Brown (Allemang & Brown 1998) have shown that these apparently unrelated procedures can be treated according to a unified matrix polynomial approach. Such an approach is here briefly reviewed because it is useful to highlight the common ideas underlying NExT-type procedures, Auto Regressive (AR) and Auto Regressive Moving Average (ARMA) models and stochastic state-space models, whose correlation is stronger than it appears at a first insight.

This unified approach has been originally developed for input-output methods but its extension to the output-only case is immediate.

The original approach starts from the polynomial model historically used for the frequency response function:

$$H_{pq}(\omega) = \frac{X_p(\omega)}{F_q(\omega)} = \frac{\beta_n(j\omega)^n + \beta_{n-1}(j\omega)^{n-1} + \dots + \beta_1(j\omega)^1 + \beta_0(j\omega)^0}{\alpha_m(j\omega)^m + \alpha_{m-1}(j\omega)^{m-1} + \dots + \alpha_1(j\omega)^1 + \alpha_0(j\omega)^0} \quad (2.50)$$

which can be rewritten as:

$$H_{pq}(\omega) = \frac{X_p(\omega)}{F_q(\omega)} = \frac{\sum_{k=0}^n \beta_k (j\omega)^k}{\sum_{h=0}^m \alpha_h (j\omega)^h} \quad (2.51)$$

Further manipulations yield the following linear equation in the unknown  $\alpha$  and  $\beta$  terms:

$$\sum_{h=0}^m \alpha_h (j\omega)^h X_p(\omega) = \sum_{k=0}^n \beta_k (j\omega)^k F_q(\omega) \quad (2.52)$$

or, in matrix form:

$$\sum_{h=0}^m [\alpha_h] (j\omega)^h \{X(\omega)\} = \sum_{k=0}^n [\beta_k] (j\omega)^k \{F(\omega)\} \quad (2.53)$$

and, in terms of frequency response functions:

$$\sum_{h=0}^m [\alpha_h] (j\omega)^h [H(\omega)] = \sum_{k=0}^n [\beta_k] (j\omega)^k \quad (2.54)$$

A similar expression is derived in time domain where, in terms of sampled data, the time domain matrix polynomial results from a set of finite difference equations (Allemang & Brown, 1998):

## 2.2 STRUCTURAL DYNAMIC MODELS IN TIME AND FREQUENCY DOMAIN

---

$$\sum_{h=0}^m [\alpha_k] \{x(t_{i+k})\} = \sum_{k=0}^n [\beta_k] \{f(t_{i+k})\} \quad (2.55)$$

This model corresponds to an ARMA(m, n) model. It is also worth noticing that, if the discussion is limited to the use of free decay or impulse response function data, the time domain equations can be simplified by observing that the forcing function can be assumed to be zero for all time instants greater than zero. Thus, the  $[\beta_k]$  coefficients can be eliminated:

$$\sum_{h=0}^m [\alpha_h] [h(t_{i+k})] = 0 \quad (2.56)$$

and the number of roots that will be found is given by the order of polynomial times the number of measurement points, like in classical ARMA models.

By comparing (2.53) and (2.55), the unified matrix polynomial approach (UMPA) proposed by the Authors recognizes that both the time and frequency domain models lead to functionally similar matrix polynomial models: thus, they proposed the UMPA terminology in order to describe both domains, since the ARMA terminology is traditionally related to the time domain.

Obviously, even if in this thesis and in the original paper by Allemang & Brown the same nomenclature for the coefficient matrices has been used in both time and frequency domain formulations in order to point out similarities, such matrices are not the same. Moreover, the roots of the matrix characteristic equations derived according to these two statements of the problem, the time domain one and the frequency domain one, are already expressed in frequency domain in the second case, while they are expressed in the  $z$  domain when the problem is formulated in the time domain and must be converted to the frequency domain according to the following relations:

$$z_r = e^{\lambda_r \Delta t}, \quad \lambda_r = \sigma_r + j\omega_r, \quad \sigma_r = \text{Re}[\ln z_r / \Delta t], \quad \omega_r = \text{Im}[\ln z_r / \Delta t] \quad (2.57)$$

The development of UMPA allowed the Authors to gather a number of input-output time domain and frequency domain algorithms in a unified framework: in particular they considered the Least Square Complex Exponential (LSCE) method, the Ibrahim Time Domain (ITD) method, the Polyreference Time Domain (PTD), which includes LSCE and ITD as special cases, the Eigensystem Realization Algorithm (ERA), the Rational Fraction Polynomial (RFP) and the Polyreference Frequency Domain (PFD), thus pointing out the relations among modal identification algorithms apart from their mathematical formulation (time domain, frequency domain, state-space, AR, ARMA).

## 2.2 STRUCTURAL DYNAMIC MODELS IN TIME AND FREQUENCY DOMAIN

---

Extension of this formulation to the output-only case is immediate if correlation functions or random decrement (Asmussen 1997) are used to generate free decays, like in the Natural Excitation Techniques (NExT). Proof that auto and cross-correlation functions of responses to white noise can be handled as impulse response functions, so that standard input-output time domain algorithms such as LSCE, ITD or PTD (which is called Instrumental Variable method after substituting impulse responses by output correlations) can be used for modal identification, is reported in Appendix A. In this thesis, for historical reasons, the LSCE method and the ITD method are discussed in the framework of NExT procedures, while the Instrumental Variable (IV) method is described in the section about ARMA models. However, since the underlying relation between all these techniques has been already clarified, it should not be surprising if all these methods are not grouped all together within the single comprehensive class of covariance driven methods.

The link between ARMA models and state-space models is again well explained in Andersen (Andersen 1997) and some aspects have been discussed in the previous section: one of the main differences between these two models is related to the fact that, in state-space representation, the internal structure of a system is described, while ARMA models only describe the input-output behaviour of the system; for this reason, a state-space model is also referred to as an internal representation of a system, while the ARMA model as an external representation of it. The relation

between these two classes of models has been recently further analyzed by Lardiès (Lardiès 2008).

The Prediction Error Method is a typical technique of modal parameter identification by mean of an ARMA model: it is a data-driven method, since estimation of modal parameters is carried out directly from the raw data. Notwithstanding the strong relationship between ARMA and state-space models, in this thesis data-driven methods such as PEM and Stochastic Subspace Identification will be treated separately in order to point out the main differences, which are mainly related to the role played by noise.

As a final remark, in this section the relationships between parametric methods have been discussed in the light of the unified matrix polynomial approach. Non-parametric methods can be seen as zero order models where only the spatial information related to sensor position is used and data are processed at a single frequency line at a time.

In the next sections, some characteristics of modal identification techniques historically used to classify them will be reviewed; data reduction techniques and strategies for model order determination will be also summarized: the last ones, in particular, are common to a number of parametric procedures; finally, a basic review of modal identification techniques will be reported, with a larger discussion only about the techniques effectively used in this work.



### 2.3 CHARACTERIZATION OF OUTPUT-ONLY TECHNIQUES

Even if most of OMA techniques are derived from traditional EMA procedures, they are developed in a stochastic framework, due to the assumptions about input. Such assumptions have some consequences: first of all, modal participation factors cannot be computed being the input unknown; moreover, due to the assumptions on input, OMA techniques are always of multiple input type: thus, classification according to the number of inputs, like in classical EMA, is senseless.

Some classification concepts, already introduced in the previous sections, are better systematized here.

Modal identification methods can be first of all classified according to the domain for implementation. Parameter estimation methods directly based on time histories of the output signals are referred to as time domain methods. Methods based on Fourier transform of signals are, instead, referred to as frequency domain methods. Even if this distinction may look artificial, since it is always possible to transform signals from one domain to the other, there are some differences in terms of practical applications. Time domain methods are, in fact, usually better conditioned than the frequency domain counterpart. This is mainly related to the effect of the powers of frequencies in frequency domain equations. Moreover, time domain methods are usually more suitable for handling noisy data, and they avoid most signal processing errors (for example, leakage) if

applied directly to raw time domain data. On the other hand, in noisy measurement conditions, averaging is easier and more efficient in frequency domain. The last distinction affects the possibility to take into account the effects of out-of-band modes: when this effect is important, frequency domain methods have to be preferred since they can approximate it.

A second distinction is between parametric and non-parametric methods; if a model is fitted to data, the technique is said parametric. These procedures are more complex and computational demanding with respect to non-parametric ones, but they usually show better performance with respect to the faster and easier non-parametric techniques which, however, give a first insight into the identification problem.

By recalling that the system dynamic response is given by the superposition of its modal responses, Single Degree Of Freedom (SDOF) and Multiple Degree Of Freedom (MDOF) methods can be identified. If in a certain frequency band only one mode is assumed to be important, the parameters of this mode can be determined separately, leading to the so-called SDOF methods. Even if these methods are very fast and characterized by a low computational burden, the SDOF assumption is a reasonable approximation only if the modes of the system are well decoupled. MDOF methods are, therefore, necessary when dealing with close coupled modes or even coincident modes.

Modal frequencies and damping ratios are independent of the output location and can be estimated on a local basis, that is to say by considering

## 2.3 CHARACTERIZATION OF OUTPUT-ONLY TECHNIQUES

---

a single response at a time. In this case, the process may lead to a different estimate of the same parameter each time and, as a result, a set of local estimates is obtained. If the identification process is, instead, carried out on all responses at the same time, a global estimate for the modal parameters is obtained.

In the class of parametric models, a further distinction is between low order and high order models. A low order model is used for those cases where the spatial information is complete. In other words, the number of physical coordinates is greater than the number of measurable eigenvalues. A high order model is, instead, usually adopted when the system is undersampled in the spatial domain.

One-stage methods can be distinguished from two-stage ones: in the first case, natural frequencies, damping ratios and mode shapes are estimated at the same time; in the second case, instead, natural frequencies and damping ratios are estimated at the first step, and then mode shapes are extracted according to the identified modal frequencies and damping ratios.

The last distinction is among covariance-driven and data-driven methods: in the second case modal analysis is carried out directly on the raw data, while in the first case correlation functions are estimated from the measured responses before carrying out modal identification.

When dealing with modal identification, it often happens that a large amount of data must be processed: however, in such data a certain degree of redundancy or overdetermination is present. A reduction of the amount

of data to be processed can be obtained in different ways: it could be sometimes necessary in order to keep computational time within reasonable values. Filtering and decimation are usually used to reject unnecessary informations or to limit the frequency band under investigation. Reference channels (Peeters 2000) can be, instead, adopted in order to keep computational time low by reducing data redundancy: however, reference channel must be properly selected to avoid that some modes could be lost together with redundant informations. The problem of missing modes when using reference channels can take place, in particular, in presence of repeated roots and a too small number of reference channels, or in the case of local modes, which do not appear in the reference channels.

Different strategies are adopted by the various methods to deal with noisy measurements. In frequency domain methods, based on computation of auto and cross power spectra, an averaging process is used to reduce noise effects. Some time domain techniques, instead, basically use SVD to reject noise while some other methods, such as ARMA models, try to model also the noise: a higher model order, however, is required to fit noise, and lots of additional poles appear as a consequence.

Determination of the correct model order for a model is a fundamental task for parametric methods. The model order is related to the number of modes as follows:

### 2.3 CHARACTERIZATION OF OUTPUT-ONLY TECHNIQUES

---

$$n = 2n_2 \quad (2.58)$$

where  $n$  is the model order and  $n_2$  the number of modes. However,  $n_2$  is an unknown quantity in the modal identification process. The expected number of modes can be determined based on a physical insight or counted as twice the number of peaks in response spectra. A more accurate estimation can be obtained by looking at the SVD of the Power Spectral Density (PSD) matrix, which takes into account mode multiplicity. More formal procedures start by estimating models of different orders, which are then compared according to a predefined criterion (for example, the Akaike's Final Prediction Error, or the Minimum Description Length criterion; see Ljung 1999) including a penalty for model complexity in order to avoid overfit. However, in modal analysis the obtained modal parameters are more important than a good model as such: by tracking modal frequencies, damping ratios and mode shapes for increasing model orders, the physical modal parameters stabilize as the correct model order is found. In particular, for well-excited modes, the modal parameters stabilize at a very low model order; poorly excited modes, instead, do not stabilize until a high model order is reached. Nevertheless, non-physical poles do not stabilize at all during this process and can be separated from the actual modal parameters. This job can be done by constructing the so-called stabilization diagram (Heylen et al. 2002): the poles corresponding to a certain model order are

compared with those ones of a one-order lower model. If the eigenfrequency, the damping ratio and the related mode shape differences are within preset limits, the pole is labelled as a stable one. An example of stability requirement is:

$$\begin{aligned} \frac{(f^{(p)} - f^{(p+1)})}{f^{(p)}} \cdot 100 &< 1\% \\ \frac{(\xi^{(p)} - \xi^{(p+1)})}{\xi^{(p)}} \cdot 100 &< 5\% \\ [1 - MAC(\{\psi^{(p)}\}, \{\psi^{(p+1)}\})] \cdot 100 &< 2\% \end{aligned} \quad (2.59)$$

with a limit of 1% for eigenfrequencies, 2% for mode shapes and 5% for damping ratios.

The Modal Assurance Criterion (MAC) is a measure of the correlation between two modal vectors and is given by:

$$MAC(\{\psi^{(p)}\}, \{\psi^{(p+1)}\}) = \frac{|\{\psi^{(p)}\} \{\psi^{(p+1)}\}^H|^2}{(\{\psi^{(p)}\} \{\psi^{(p)}\}^H) (\{\psi^{(p+1)}\} \{\psi^{(p+1)}\}^H)} \quad (2.60)$$

By definition, the MAC is a number between 0 and 1.

In order to judge the quality of a model for a certain model order, spectra can be synthesized and compared with those ones obtained by applying

## 2.3 CHARACTERIZATION OF OUTPUT-ONLY TECHNIQUES

---

Fast Fourier Transform (FFT) to the original data: this comparison allows to verify if modes have been missed and, therefore, can be used as a measure of the overall success of the modal parameter estimation procedure. It is worth noticing, however, that a poor comparison can be due to several reasons: an incorrect model order is just one of the possibilities

## 2.4 OMA IN FREQUENCY DOMAIN

### 2.4.1 The Peak-Picking method

The most undemanding method for modal parameter estimation from output-only data is the Basic Frequency Domain (BFD) technique (Bendat & Piersol 1993), also called the Peak-Picking method. It is widely used and a practical implementation was made by Felber (Felber 1993). The name of the method is related to the fact that natural frequencies are determined as the peaks of the Power Spectral Density plots, obtained by converting the measured data to the frequency domain by the Discrete Fourier Transform (DFT).

The BFD technique is a SDOF method for OMA: in fact, it is based on the assumption that, around a resonance, only one mode is dominant. When it happens, taking into account the expression (2.4) for the FRF and that the input spectrum is assumed to be constant, the output spectrum matrix, which can be expressed as follows:

$$[G_{yy}(\omega)] = \sum_{k=1}^n \sum_{s=1}^n \left[ \frac{[R_k]}{j\omega - \lambda_k} + \frac{[R_k^*]}{j\omega - \lambda_k^*} \right] [C] \left[ \frac{[R_s]}{j\omega - \lambda_s} + \frac{[R_s^*]}{j\omega - \lambda_s^*} \right]^H \quad (2.61)$$

can be approximated by considering only the contribution of the dominant mode, for example the  $r^{\text{th}}$  mode, as:

$$[G_{yy}(\omega)] \approx \frac{[R_r]}{j\omega - \lambda_r} + \frac{[R_r]^*}{j\omega - \lambda_r^*} \quad (2.62)$$

where the residues are related to the mode shape. It means that, at resonance, each column of the spectrum matrix can be considered as an estimate of the corresponding mode shape, up to a scaling factor being the input unknown. In order to obtain such mode shape, however, the column of the spectrum matrix (and, therefore, the reference sensor) must be chosen so that it carries information about that mode: equivalently, the reference sensor cannot be a sensor placed at a node of the mode shape. As a consequence, a good choice for the reference sensor allows the computation of only the spectra between all sensors and the reference instead of the full spectrum matrix.

Identification of actual natural frequencies can be carried out by looking not only at peaks of the spectra but also by inspecting the so-called coherence function between two channels, defined as:



## 2.4 OMA IN FREQUENCY DOMAIN

---

$$\gamma_{rs}^2(f) = \frac{|G_{rs}(f)|^2}{G_{rr}(f)G_{ss}(f)} \quad (2.63)$$

and assuming values between 0 and 1;  $G_{rs}(f)$  is the value of the cross-spectrum between channels  $r$  and  $s$  at the frequency  $f$ , while  $G_{rr}(f)$  and  $G_{ss}(f)$  are the values of the auto-spectra of channel  $r$  and channel  $s$ , respectively, at the same frequency. If  $f$  is a resonant frequency, the coherence function is close to one because of the high signal-to-noise ratio at that frequency: this characteristic is helpful for a correct identification of eigenfrequencies. Moreover, the coherence function can be useful also for the identification of the nature of a mode. If, for example, there are two close bending modes, the first one in the  $x$  direction and the second one in the  $y$  direction, and a torsional mode, the coherence function for the torsional mode gives a value close to one if the two channels are in the same direction but also if a channel is in the  $x$  direction and the other in the  $y$  direction. Bending modes, instead, show low values of coherence if it is computed between a channel in the  $x$  direction and the other in the  $y$  direction. By combining informations from spectra and coherence functions is therefore possible to identify even close modes. However, the success of the identification process heavily depends on the geometry of the structure and the skill of the analyst.

The BFD allows the evaluation of natural frequencies and mode shapes: about damping ratios, in Bendat (Bendat & Piersol 1993) it is suggested to

use the half-power bandwidth method to estimate it. In Peeters (Peeters 2000), however, it is shown that this estimate is not accurate.

As said before, this method is very simple and not demanding from a computational point of view: however, it suffers some drawbacks due to the SDOF assumption. The BFD technique works well when damping is low and modes are well-separated: if these conditions are violated it may lead to erroneous results. In fact, the method identifies the so-called operational deflection shapes (which are a combination of all mode shapes: they are a good approximation of actual mode shapes only if one mode is dominant at the considered frequency) instead of actual mode shapes: in case of closely-spaced modes, this shape is the superposition of multiple modes.

Another important drawback is that the selection of eigenfrequencies can become a subjective task if the spectrum peaks are not very clear. Moreover, eigenfrequencies are estimated on a local basis (local estimate) by looking at single spectra. The last drawback is the need of a fine frequency resolution in order to obtain a good estimation of the natural frequency.

The BFD method has been implemented as a part of a modal identification software, which will be discussed in the next chapter.

### 2.4.2. The (Enhanced) Frequency Domain Decomposition

The main drawbacks of the BFD method have been overcome by the introduction of the Frequency Domain Decomposition (FDD) technique (Brincker et al. 2000b): this method was originally applied to FRFs and was known as Complex Mode Indicator Function (CMIF) in order to point out its ability to detect multiple roots and, therefore, the possibility to count the number of modes present in the measurement data. The method has been then better systematized by Brincker and applied to response spectrum data. It is an extension of the BFD technique: in fact, it is possible to recognize that the relationship between the input  $x(t)$  and the output  $y(t)$  can be written in the form (Bendat & Piersol 1986):

$$[G_{yy}(\omega)] = [H(\omega)]^* [G_{xx}(\omega)] [H(\omega)]^T \quad (2.64)$$

where  $[G_{xx}(\omega)]$  is the  $r \times r$  input PSD matrix,  $r$  is the number of inputs,  $[G_{yy}(\omega)]$  is the  $l \times l$  output PSD matrix,  $l$  is the number of outputs,  $[H(\omega)]$  is the  $l \times r$  FRF matrix, and the superscripts  $*$  and  $T$  denote complex conjugate and transpose respectively. The FRF matrix can be expressed in a typical partial fraction form in terms of poles,  $\lambda_k$ , and residues,  $[R_k]$ :

$$[H(\omega)] = \frac{[Y(\omega)]}{[X(\omega)]} = \sum_{k=1}^n \frac{[R_k]}{j\omega - \lambda_k} + \frac{[R_k]^*}{j\omega - \lambda_k^*} \quad (2.65)$$

with:

$$\lambda_k = -\sigma_k + j\omega_{dk} \quad (2.66)$$

being  $n$  the number of modes,  $\lambda_k$  the pole of the  $k^{\text{th}}$  mode,  $\sigma_k$  the modal damping (decay constant) and  $\omega_{dk}$  the damped natural frequency of the  $k^{\text{th}}$  mode.  $[R_k]$  is the residue, and it is given by:

$$[R_k] = \{\phi\}_k \{\gamma\}_k^T \quad (2.67)$$

where  $\{\phi\}_k$  is the mode shape vector and  $\{\gamma\}_k$  is the modal participation vector.

Therefore, combining equations (2.64) and (2.65) and assuming that input is random both in time and space and has a zero mean white noise distribution (that is to say, its PSD matrix is a constant:  $[G_{xx}(\omega)] = [C]$ ), the output PSD matrix can be written as:

$$[G_{yy}(\omega)] = \sum_{k=1}^n \sum_{s=1}^n \left[ \frac{[R_k]}{j\omega - \lambda_k} + \frac{[R_k^*]}{j\omega - \lambda_k^*} \right] [C] \left[ \frac{[R_s]}{j\omega - \lambda_s} + \frac{[R_s^*]}{j\omega - \lambda_s^*} \right]^H \quad (2.68)$$

Using the Heaviside partial fraction theorem for polynomial expansions, the following expression can be obtained:

## 2.4 OMA IN FREQUENCY DOMAIN

---

$$[G_{yy}(\omega)] = \sum_{k=1}^n \frac{[A_k]}{j\omega - \lambda_k} + \frac{[A_k]^*}{j\omega - \lambda_k^*} + \frac{[B_k]}{-j\omega - \lambda_k} + \frac{[B_k]^*}{-j\omega - \lambda_k^*} \quad (2.69)$$

This is the pole-residue form of the output PSD matrix.  $[A_k]$  is the  $k^{\text{th}}$  residue matrix of the output PSD; it is a  $l \times l$  hermitian matrix given by:

$$[A_k] = [R_k] \mathbb{I} C \left( \sum_{s=1}^n \frac{[R_s^H]}{-\lambda_k - \lambda_s^*} + \frac{[R_s^T]}{-\lambda_k - \lambda_s} \right) \quad (2.70)$$

If only the  $k^{\text{th}}$  mode is considered, it gives the following contribution:

$$[A_k] = \frac{[R_k] \mathbb{I} C [R_k]^H}{2\sigma_k} \quad (2.71)$$

This term can become dominating if the damping is light, thus obtaining a residue which is proportional to the mode shape vector as follows:

$$[A_k] \propto [R_k] \mathbb{I} C [R_k]^H = \{\phi\}_k \{\gamma\}_k^T [C] \{\gamma\}_k \{\phi\}_k^T = d_k \{\phi\}_k \{\phi\}_k^T \quad (2.72)$$

where  $d_k$  is a scaling factor for the  $k^{\text{th}}$  mode.

Considering a lightly damped system and that the contribution of the modes at a particular frequency is limited to a finite number (usually one

or two), then the response spectral density matrix can be written in the following final form:

$$[G_{yy}(\omega)] = \sum_{k \in Sub(\omega)} \frac{d_k \{\phi\}_k \{\phi\}_k^T}{j\omega - \lambda_k} + \frac{d_k^* \{\phi\}_k^* \{\phi\}_k^{*T}}{j\omega - \lambda_k^*} \quad (2.73)$$

where  $k \in Sub(\omega)$  is the set of modes that contribute at the considered frequency. The singular value decomposition of the output PSD matrix known at discrete frequencies  $\omega = \omega_i$  yields:

$$\left[ \hat{G}_{yy}(j\omega_i) \right] = [U]_i [S]_i [U]_i^H \quad (2.74)$$

where the matrix  $[U]_i$  is a unitary matrix holding the singular vector  $\{u_{ij}\}$  and  $[S]_i$  is a diagonal matrix holding the scalar singular values  $s_{ij}$ . Near a peak corresponding to the  $k^{th}$  mode in the spectrum, this mode will be dominant: if only the  $k^{th}$  mode is dominant, there will be only one term in equation (2.73) and the PSD matrix approximates to a rank one matrix as:

$$\left[ \hat{G}_{yy}(j\omega_i) \right] = s_i \{u_{i1}\} \{u_{i1}\}^H \quad \omega_i \rightarrow \omega_k \quad (2.75)$$

In such a case, the first singular vector  $\{u_{i1}\}$  is an estimate of the mode shape:

## 2.4 OMA IN FREQUENCY DOMAIN

---

$$\{\hat{\phi}\} = \{u_{il}\} \quad (2.76)$$

and the corresponding singular value belongs to the auto power spectral density function of the corresponding SDOF system. In case of repeated modes, the PSD matrix rank is equal to the number of multiplicity of the modes.

The auto power spectral density function of the corresponding SDOF system is identified around the peak of the singular value plot by comparing the mode shape estimate  $\{\hat{\phi}\}$  with the singular vectors associated to the frequency lines around the peak: every line characterized by a singular vector which gives a MAC value with  $\{\hat{\phi}\}$  higher than a user-defined MAC Rejection Level belongs to the SDOF PSD function.

This equivalent SDOF PSD function is used, when applying the Enhanced Frequency Domain Decomposition (EFDD) algorithm, to obtain an estimate of the natural frequency which is independent of the frequency resolution of the spectra computed by the FFT algorithm, and an estimate of damping. In fact, the SDOF PSD function is transferred back to time domain through inverse FFT, thus obtaining an approximated correlation function of the equivalent SDOF system. From the free decay function of the SDOF system, the damping ratio can be calculated by the logarithmic decrement technique. A similar procedure is adopted in order to extract natural frequencies, carrying out a linear regression on the zero crossing times of the equivalent SDOF system correlation function and, in

principle, taking into account the relation between damped and undamped natural frequency.

The SVD of the PSD matrix, which is the core of the FDD algorithm, allows to overcome the typical drawbacks of the BFD technique. The SVD, in fact, is a standard linear algebra tool for estimating the rank of a matrix (the number of non-zero singular values is the rank): its application in this context allows to solve the problem of mode multiplicity. In this case, every singular vector corresponding to a non-zero singular value yields a mode shape estimate, if the mode shapes are orthogonal each other. However, this is not always true: in such a case, the first singular vector is still a good estimate of a mode shape, but this is not true for the other.

In the third generation of FDD, the so-called (Zhang et al. 2005a) Frequency-Spatial Domain Decomposition (FSDD), a spatial filtering<sup>3</sup> procedure has been applied to enhance the estimation of modal frequencies and damping ratios. The FSDD makes use of the mode shapes estimates computed via SVD of the output PSD matrix to enhance PSDs. The use of the estimated mode shapes as weighting vectors gives, as a result, an enhanced PSD which can be approximated as a SDOF system:

---

<sup>3</sup> The spatial filtering procedure, also known as coherent averaging, is a method for data condensation based on a dot product of the data with a weighting vector: informations in the data which are not coherent with the weighting vectors are averaged out of the data. Typical spatial filtering procedures are based on the use of data coming from sensors located in a local area of the system in order to enhance local modes, or on the use of estimates of mode shapes as weighting functions to enhance particular modes. The spatial filtering belongs to the class of the so-called condensation algorithms: other important condensation algorithms are Least Squares (one of the most popular procedures for computing a pseudo-inverse solution to an over-specified system) and transformations (SVD is one of the most popular).



## 2.4 OMA IN FREQUENCY DOMAIN

---

therefore, a SDOF curve fitter can be adopted to estimate the natural frequency and the damping ratio of the considered mode.

The EFDD algorithm has been also implemented as a part of the modal identification software which will be discussed in the next chapter.

### 2.4.3. Frequency domain parametric procedures

About frequency domain parametric procedures, the frequency domain Maximum Likelihood (ML) approach, originally intended for application to frequency response functions, has been recently extended for the extraction of modal parameters using spectra obtained from output-only data (Hermans et al. 1998).

Maximum likelihood estimators were originally developed to deal with noisy measurements: the ML identification is an optimization-based method that estimates the modal parameters of a model by minimizing an error norm (more details about the use of ML estimator to identify parametric frequency domain models can be found in Shoukens & Pintelon 1991, Pintelon et al. 1994): as a result, non-linear equations in the unknown parameters are obtained and they have to be solved by adopting an iterative procedure, with the related problems of not guaranteed convergence, local minima, sensitivity to the initial values and high computational burden.

A least-square complex frequency domain (LSCF) method has been also introduced to find initial values for the iterative ML frequency domain

method (Guillaume et al. 1998): however, it has been then found that it gives a quite accurate estimation of modal parameters with lower computational effort and, thus, can be used as a modal identification technique. The most important advantage of the LSCF estimator is that very clear stabilization diagrams are obtained. The main drawback of this method is, instead, related to its inability to deal with closely spaced poles which are shown as a single pole; moreover, the stabilization diagram can be constructed using only pole informations (eigenfrequencies and damping ratios), since mode shapes are not available at a first step: it is, therefore, an example of two-step method.

The problem of separation of closely-spaced poles has been recently overcome by the introduction of a polyreference version of the LSCF method, the so-called PolyMAX (Guillaume et al. 2003, Peeters & Van der Auweraer 2005, Peeters et al. 2004). Like the original LSCF method, it is a two-step method (identification of mode shapes must be preceded by identification of modal frequencies and damping ratios) which leads to very clear and, thus, easy-to-interpret stabilization diagrams. This implies a potential automation of the method and the possibility to apply it to particular estimation cases such as high order or highly damped systems with large modal overlap.

For a comprehensive treatment of these parametric frequency domain methods the reader can refer to several publications available in the literature (Hermans et al. 1998, Guillaume et al. 1998, Pintelon & Schoukens 2001, Guillaume et al. 1996, Parloo 2003, Cauberghe 2004).

## 2.5 OMA IN TIME DOMAIN

### 2.5.1 NExT-type procedures

These techniques have been initially developed in the deterministic framework of traditional input-output modal analysis. In their original formulation, they worked on the IRF of the system determined through tests. In the case of natural excitation and modal identification from output-only measurements, correlation functions of the random response of the structure under natural excitation are used. In fact, it is possible to show that the correlation function can be expressed as a summation of decaying sinusoids, each one characterized by a damped natural frequency, damping ratio and mode shape coefficient identical to those ones of the corresponding structural mode (Appendix A). Correlation functions can therefore be used as IRF for the estimation of modal parameters. When it happens, this procedure is also referred to as NExT (Natural Excitation Technique).

The three main algorithms belonging to this class are:

- The Polyreference Least Square Complex Exponential (LSCE) method,
- The Multiple Reference Ibrahim Time Domain (MRITD) method,
- The Eigensystem Realization Algorithm (Juang & Pappa 1984).

It is beyond the scope of this thesis to give an extensive explanation of these algorithms; just the main concepts of the first two methods are

herein discussed. The Eigensystem Realization Algorithm will be discussed apart since it relies upon the system realization theory. Because of its similarities with subspace-based methods, it will be described next in the framework of subspace approaches.

It is worth emphasizing again that, even if these algorithms have been originally obtained as separate methods, a common mathematical derivation can be obtained by applying the UMPA approach proposed by Allemang & Brown (Allemang & Brown 1998): however, for historical reasons, these techniques are reviewed according to their original formulation. Moreover, it is worth noticing that the first two techniques are the results of improvements carried out over the years by several authors with respect to their original formulations, basically in order to deal with close or repeated roots: such resulting techniques are now applied in the OMA framework. Further improvements have been recently obtained in order to deal with spurious harmonics (Mohanty 2005).

The main idea underlying the Polyreference LSCE is that the generic correlation function can be written as follows:

$$R_{ij}(k \cdot \Delta t) = \sum_{r=1}^{n_2} e^{\mu_r k \Delta t} C_{rj} + \sum_{r=1}^{n_2} e^{\mu_r^* k \Delta t} C_{rj}^* \quad (2.77)$$

where  $\mu_r$  is the system pole related to natural frequency and damping of the  $r^{\text{th}}$  mode,  $C_{rj}$  is a constant associated with the  $r^{\text{th}}$  mode for the  $j^{\text{th}}$

## 2.5 OMA IN TIME DOMAIN

---

response signal,  $n_2$  is the number of modes,  $\Delta t$  is the sampling time step and the superscript  $*$  denotes the complex conjugate. Since  $\mu_r$  appears in complex conjugate forms, there exists a polynomial of order  $2n_2$  (known as Prony's equation) of which  $e^{\mu_r \Delta t}$  are roots. In order to find the coefficients  $\{\beta\}$  of this polynomial, the Prony's equation is written for  $2n_2$  times, starting at subsequent time samples, thus obtaining a linear system of equations which can be written in matrix form. By repeating this procedure for all available auto and cross-correlation functions, and stacking the resulting matrix equations (taking into account that the unknown coefficients  $\{\beta\}$  are global quantities related to the modal parameters and as such they must be the same for all different correlation functions), a single system of equations is obtained and it can be solved in a least square sense using pseudoinverse techniques for the unknown coefficients  $\{\beta\}$ . Once these are known, the system poles can be computed by solving a generalized eigenvalue problem.

The Polyreference LSCE is a two step method: thus, a second step is needed to extract the mode shapes using the identified modal frequencies and damping ratios. This can be done, for example, by fitting the correlation functions (Hermans & Van der Auweraer 1997).

More details about the Polyreference LSCE method can be found in (Brown et al. 1979, Vold et al. 1982).

The Multiple Reference Ibrahim Time Domain method basically starts from arranging correlation functions in two Hankel matrices<sup>4</sup>,  $[H_0]$  and  $[H_1]$ , shifted in time by one time interval. A recurrence matrix  $[A]$  is then computed by solving the following equation:

$$[A][H_0] = [H_1] \quad (2.78)$$

in a least square sense by applying pseudoinverse, thus obtaining:

$$[A] = [H_1][H_0]^+ \quad (2.79)$$

where the superscript  $+$  denote pseudoinverse. By computing the eigenvalues of this matrix, the poles of the system, and therefore modal frequencies and damping ratios, can be extracted. The eigenvectors are, instead, residues from which mode shapes can be determined. The Ibrahim Time Domain is a low order method: as a consequence, said  $l$  the number of responses, no more than  $l$  modes can be identified; if, instead,  $l$  is larger than the number of modes to be detected, there will be also some computational modes.

More details about the MRITD method can be found in (Ibrahim & Mikulcik 1977, Fukuzono 1986).

---

<sup>4</sup> A Hankel matrix is a matrix that is constant along its anti-diagonals.

## 2.5 OMA IN TIME DOMAIN

---

### 2.5.2 AR- and ARMA-type procedures: Instrumental Variable and Prediction Error Method

The Instrumental Variable (IV) method is herein discussed in order to point out its correspondence with the Polyreference LSCE method. Even if it is shown here by following its original formulation in the framework of ARMA models, its final equations correspond to those ones of the Polyreference LSCE method, thus proving again how different algorithms can be traced back to a common mathematical background as discussed earlier.

In section 2.2.4 it has been shown that a vibrating structure can be represented by an ARMA model: however, due to the MA terms, a highly non-linear optimization problem must be solved in order to extract modal parameters. The main idea of the IV method is to formulate a linear problem related to the identification of the AR parameters, but by keeping an ARMA model as underlying model structure. Besides, it has already been shown that modal parameters rely only upon the AR part of the model.

Let us consider an ARMA(p, p) model and l outputs so that the product  $p \times l$  is larger than the actual order n of the system and all system poles are included in the model:

$$\{y_k\} + [\alpha_1]\{y_{k-1}\} + \dots + [\alpha_p]\{y_{k-p}\} = \{e_k\} + [\gamma_1]\{e_{k-1}\} + \dots + [\gamma_p]\{e_{k-p}\} \quad (2.80)$$

Such a model is adequate for modal parameter estimation if, by fitting it to the measured data  $\{y_k\}$ , it is able to extract the maximum information from the data, leaving residuals  $\{e_k\}$  uncorrelated with past data:

$$\forall i > 0 \quad E[\{e_k\}\{y_{k-i}\}^T] = E[\{e_k\}]E[\{y_{k-i}\}^T] = [0] \quad (2.81)$$

where the second equality follows from the zero-mean property of the noise sequence. Taking into account that  $\{e_{k-p}\}$  is the oldest term in the MA part, the post-multiplication of both sides of equation (2.80) by  $\{y_{k-p-i}\}^T$  (for  $i > 0$ ) yields (by taking expectation and recalling equation (2.81)):

$$\begin{aligned} \forall i > 0 \quad & E[\{y_k\}\{y_{k-p-i}\}^T] + [\alpha_1]E[\{y_{k-1}\}\{y_{k-p-i}\}^T] + \\ & + \dots + [\alpha_p]E[\{y_{k-p}\}\{y_{k-p-i}\}^T] = [0] \end{aligned} \quad (2.82)$$

From stationarity it follows:

$$\forall i > 0 \quad E[\{y_k\}\{y_{k-i}\}^T] = E[\{y_{k+i}\}\{y_k\}^T] = [R_i] \quad (2.83)$$

thus, equation (2.82) can be written as:

$$\forall i > 0 \quad [R_{p+i}] + [\alpha_1][R_{p+i-1}] + \dots + [\alpha_p][R_i] = [0] \quad (2.84)$$



## 2.5 OMA IN TIME DOMAIN

---

or:

$$\forall i > 0 \quad [\alpha_1][R_{p+i-1}] + \dots [\alpha_p][R_i] = -[R_{p+i}] \quad (2.85)$$

which is exactly the same equation the Polyreference LSCE method is based on. By replacing the output covariances by their estimates:

$$[\hat{R}_i] = \frac{1}{N} \sum_{k=0}^{N-1} \{y_{k+1}\} \{y_k\}^T \quad (2.86)$$

and writing equation (2.85) for all available time lags  $i$ , the AR parameters  $[\alpha_1], \dots, [\alpha_p]$  can be estimated by solving the resulting over-determined set of equations in a least square sense. Natural frequencies, damping ratios and mode shapes are finally obtained from the eigenvalue decomposition of the companion matrix of the AR coefficients, as described in section 2.2.4.

The Prediction Error Method (PEM) is, instead, an ARMA model-based data-driven method. A detailed description of the method can be found in Ljung (Ljung 1999) while a comprehensive description of its application for estimation of modal parameters of civil engineering structures is reported in Andersen (Andersen 1997), where it is shown that the ARMA model (2.80) is a good representation of a linear, time-invariant structure vibrating under unknown input forces which can be modelled as a zero-mean Gaussian white noise process. The AR coefficients models the

dynamics of the combined system (structural modes plus noise modes), while the MA parameters ensures that the statistical description of the data is optimal. As shown in section 2.2.4, the model order  $p$  depends on the number of modes as well as on the dimension of the measurement vector.

The ARMAV model is fitted to the measured time signals by minimizing the prediction error:

$$\{\varepsilon(t_k, \{\theta\})\} = \{y(t_k)\} - \{\hat{y}(t_k | t_{k-1}, \{\theta\})\} \quad (2.87)$$

given by the difference between the measured time signals and the predicted output of the ARMAV model;  $\{\theta\}$  is the vector of model parameters. The criterion function to be minimized is (Ljung 1999):

$$V = \det \left( \frac{1}{N} \sum_{k=1}^N \{\varepsilon(t_k, \{\theta\})\} \{\varepsilon(t_k, \{\theta\})\}^T \right) \quad (2.88)$$

If the prediction errors are Gaussian white noise, it can be shown that this criterion function corresponds to a maximum likelihood: in such a case, therefore, the criterion provides the maximum accuracy (Söderström & Stoica 1989).

The prediction error can be minimized only by a non-linear optimization procedure: since in practical applications a large number of parameters have to be estimated, this can result in problem with computational time,

## 2.5 OMA IN TIME DOMAIN

---

computer memory and convergence. In (Brincker & Andersen 1999a) an optimization scheme able to reduce the set of parameters to be estimated is proposed: basically, it carries out a translation of the ARMA model in state-space form, defines a reduced optimization set of parameters in modal domain and then goes back to the ARMA domain to perform optimization according to PEM. However, it seems that in presence of good quality data, this optimization scheme does not improve significantly the modal parameter estimates with respect to the stochastic state-space model (Brincker & Andersen 1999b).

### 2.5.3 Covariance-Driven Stochastic Subspace Identification

The Covariance-driven Stochastic Subspace Identification (Cov-SSI) can be considered an SVD-enhanced IV method (Peeters 2000): the role played by SVD is basically related to noise rejection. The Cov-SSI method addresses the so-called stochastic realization problem, that is to say the problem of identifying a stochastic state-space model from output-only data. The algorithm is briefly outlined here. Being a covariance-driven method, output correlations must be computed as a first step:

$$[\hat{R}_i] = \frac{1}{N-i} [Y(1:N-i)][Y(i:N)]^T \quad (2.89)$$

where  $[Y(1:N-i)]$  is the data matrix with the last  $i$  points removed, while  $[Y(i:N)]$  is the data matrix with the first  $i$  points removed;  $N$  is the

number of available data points.  $\left[\widehat{R}_i\right]$  denotes that it is an estimate of the true correlation matrix at time lag  $i$  based on a finite number of data: however, it is an unbiased estimate.

Correlation matrices are then gathered into a block Toeplitz<sup>5</sup> matrix:

$$\left[T_{l|i}\right] = \begin{bmatrix} \left[\widehat{R}_i\right] & \left[\widehat{R}_{i-1}\right] & \dots & \left[\widehat{R}_1\right] \\ \left[\widehat{R}_{i+1}\right] & \left[\widehat{R}_i\right] & \dots & \left[\widehat{R}_2\right] \\ \dots & \dots & \dots & \dots \\ \left[\widehat{R}_{2i-1}\right] & \left[\widehat{R}_{2i-2}\right] & \dots & \left[\widehat{R}_i\right] \end{bmatrix} \quad (2.90)$$

Each correlation matrix has dimensions  $l \times l$ , being  $l$  the number of outputs: thus, the block Toeplitz matrix has dimensions  $li \times li$ . If the system is of order  $n$ , in order to identify it the following condition must be fulfilled:

$$li \geq n \quad (2.91)$$

The actual order of the system is obviously unknown but it can be estimated by looking at the peaks of the PSDs or by inspecting the SVD of the PSD matrix (see section 2.3). After having estimated the order of the system, being the number of output a constant of the identification problem, the value of  $i$  can be chosen: it is basically a user-choice based on a physically insight of the problem.

---

<sup>5</sup> A Toeplitz matrix is a matrix where each diagonal consists of the repetition of the same element.

## 2.5 OMA IN TIME DOMAIN

---

Applying the factorization property (2.34) to the block Toeplitz matrix:

$$\begin{aligned}
 [T_{li}] &= \begin{bmatrix} [\hat{R}_i] & [\hat{R}_{i-1}] & \dots & [\hat{R}_1] \\ [\hat{R}_{i+1}] & [\hat{R}_i] & \dots & [\hat{R}_2] \\ \dots & \dots & \dots & \dots \\ [\hat{R}_{2i-1}] & [\hat{R}_{2i-2}] & \dots & [\hat{R}_i] \end{bmatrix} = \\
 &= \begin{bmatrix} [C] \\ [C][A] \\ \dots \\ [C][A]^{i-1} \end{bmatrix} \begin{bmatrix} [A]^{i-1}[G] & \dots & [A][G] & [G] \end{bmatrix} = [O_i][\Gamma_i]
 \end{aligned} \tag{2.92}$$

the observability matrix  $[O_i]$  and the reversed controllability matrix  $[\Gamma_i]$  are obtained; definitions of such matrices immediately follow from equation (2.92):  $[O_i]$  and  $[\Gamma_i]$  have dimensions  $li \times n$  and  $n \times li$ , respectively. If condition (2.91) is fulfilled and the system is observable and controllable, the rank of the block Toeplitz matrix equals  $n$ , being it a product of a matrix with  $n$  columns and a matrix with  $n$  rows. The rank of the block Toeplitz matrix can be determined by applying SVD as follows:

$$[T_{li}] = [U][S][V]^T = \begin{bmatrix} [U_1] & [U_2] \end{bmatrix} \begin{bmatrix} [S_1] & [0] \\ [0] & [0] \end{bmatrix} \begin{bmatrix} [V_1]^T \\ [V_2]^T \end{bmatrix} \tag{2.93}$$

The rank of the matrix is given by the number of non-zero singular values. By omitting the zero singular values and the corresponding singular vectors, the following matrices are obtained: the  $li \times n$  matrix  $[U_1]$ , the

$n \times li$  matrix  $[V_1]^T$  and the  $n \times n$  matrix  $[S_1]$  which is a diagonal matrix holding the positive singular values in descending order. By comparing equations (2.92) and (2.93), the matrices  $[O_i]$  and  $[\Gamma_i]$  can be computed by splitting the SVD in two parts:

$$[O_i] = [U_1][S_1]^{1/2}[T] \quad (2.94)$$

$$[\Gamma_i] = [T]^{-1}[S_1]^{1/2}[V_1]^T \quad (2.95)$$

where  $[T]$  is a non-singular matrix which plays the role of a similarity transformation applied to the state-space model; since the choice of  $[T]$  simply determines one of the infinite equivalent realization of the state-space model, it can be set as:

$$[T] = [I] \quad (2.96)$$

From definitions (2.92) of the observability and controllability matrices, the output matrix  $[C]$  and the next state-output covariance matrix  $[G]$  can be easily obtained as the first  $l$  rows of  $[O_i]$  and the last  $l$  columns of  $[\Gamma_i]$  respectively.

In order to compute the state transition matrix  $[A]$ , the shifted block Toeplitz matrix has to be computed:

$$[T_{2|i+1}] = \begin{bmatrix} [\hat{R}_{i+1}] & [\hat{R}_i] & \dots & [\hat{R}_2] \\ [\hat{R}_{i+2}] & [\hat{R}_{i+1}] & \dots & [\hat{R}_3] \\ \dots & \dots & \dots & \dots \\ [\hat{R}_{2i}] & [\hat{R}_{2i-1}] & \dots & [\hat{R}_{i+1}] \end{bmatrix} = [O_i][A][\Gamma_i] \quad (2.97)$$

which can be decomposed as shown in equation (2.97). The state matrix  $[A]$  can be computed by introducing equations (2.94) and (2.95) into (2.97) and solving for  $[A]$ :

$$[A] = [O_i]^+ [T_{2|i+1}] [\Gamma_i]^+ = [S_1]^{-1/2} [U_1]^T [T_{2|i+1}] [V_1] [S_1]^{-1/2} \quad (2.98)$$

being  $[U]$  and  $[V]$  orthonormal matrices ( $[U]^T [U] = [U][U]^T = [I]$  and  $[V]^T [V] = [V][V]^T = [I]$ ).

The identification problem is now theoretically solved. The modal parameters can be obtained from the two matrices  $[A]$  and  $[C]$ . The eigenvalue decomposition of  $[A]$  yields:

$$[A] = [\psi][M_d][\psi]^{-1} \quad (2.99)$$

where  $[M_d]$  holds the discrete poles. Because of the relation between the state matrix in continuous time (denoted by the subscript c) and discrete time (denoted by the subscript d):

$$[A] = e^{[A_c]\Delta t} \quad (2.100)$$

the eigenvalues of  $[A_c]$ :

$$(\mu_{c_q}, \mu_{c_q}^*) = -\xi_q \omega_q \pm j \omega_q \sqrt{1 - \xi_q^2} \quad (2.101)$$

can be computed as:

$$\mu_{c_q} = \frac{\ln(\mu_{d_q})}{\Delta t} \quad (2.102)$$

Natural frequencies are, then, obtained from the complex modules of the continuous-time poles as:

$$f_q = \frac{|\mu_{c_q}|}{2\pi} \quad (2.103)$$

while damping ratios are given by:

$$\xi_q = \frac{\text{Re}(\mu_{c_q})}{|\mu_{c_q}|} \quad (2.104)$$



## 2.5 OMA IN TIME DOMAIN

---

Mode shapes are, instead, obtained from the eigenvectors of the state matrix  $[A]$  and the output matrix  $[C]$  as:

$$[\phi] = [C][\psi] \quad (2.105)$$

It is worth emphasizing that, since the number of data points is finite, the output covariances are estimates of the actual ones: as a consequence, since they are the basis of this method, also the identified matrices  $[A]$ ,  $[C]$ ,  $[G]$  and  $[R_0]$  ( $[R_0] = [C][A]^{-1}[G]$  is simply the zero-lag output covariance matrix) have to be considered as estimates. Moreover, even if the order  $n$  of the system can theoretically be obtained by inspecting the number of non-zero singular values of the block Toeplitz matrix  $[T_{|i|}]$ , since it is also an estimate, it is affected by some kinds of noise leading to singular values all different from zero. As already mentioned in section 2.2.3, typical noise sources are modelling inaccuracies (for example, the system that generated the data cannot be modelled exactly as a stochastic state-space model), measurement noise (due to sensors and measurement hardware), computational noise (due to the finite precision of computers), the finite number of data points (leading to estimates of output covariances: as a consequence, the factorization property (2.34) does not hold exactly and the rank of  $[T_{|i|}]$  will not be exactly  $n$ ). A rule of thumb suggests to look at the gap between two successive singular values: the singular value where the maximum gap occurs yields the model order.

However, this criterion cannot be applied slavishly since actual structures often show no clear gaps. In order to find the modal properties of the system, therefore, it is better to construct a stabilization diagram. Then, it is possible to compare the identified model with recorded data by comparing, for example, the synthesized spectra with those ones directly estimated from recorded data by applying the Welch's (or periodogram) method, or the correlogram method (see also Bendat & Piersol 1986). The spectrum of a stochastic state-space model can be expressed as follows in terms of z-transform (see also Peeters 2000, Ljung 1999):

$$[S_y(z)] = [C](z[I] - [A])^{-1}[G] + [R_0] + [G]^T(z^{-1}[I] - [A]^T)^{-1}[C]^T \Big|_{z=e^{j\omega\Delta t}} \quad (2.106)$$

The Cov-SSI method herein described is equivalent to the Eigensystem Realization Algorithm when it is applied to the output covariances and, as such, it can be considered also as a NexT-type procedure. Cov-SSI has been also implemented as a part of the modal identification software which will be discussed in the next chapter.

#### 2.5.4 Data-Driven Stochastic Subspace Identification

In the last decade increasing attention has been paid by the scientific community to subspace identification (Ljung 1999, Van Overschee & De Moor 1996). The first data-driven subspace identification algorithms can be found in Van Overschee & De Moor (Van Overschee & De Moor 1991,

## 2.5 OMA IN TIME DOMAIN

---

Van Overschee & De Moor 1993), while a comprehensive overview of data-driven subspace identification (in the deterministic, stochastic and combined deterministic-stochastic frameworks) can be found in the book by Van Overschee and De Moor (Van Overschee & De Moor 1996).

The data-driven stochastic subspace identification (DD-SSI) algorithm starts from a block Hankel matrix constructed directly from measurement data. It has  $2i$  block rows and  $j$  columns (for the statistical prove of the method, it is assumed that  $j \rightarrow \infty$ , thus  $j$  must be rather large): the value of  $i$  is determined as in the case of Cov-SSI. Said  $l$  the number of outputs, the block Hankel matrix has dimension  $2li \times j$  and can be partitioned into the two submatrices of the past and future outputs as follows:

$$[H_{0|2i-1}] = \frac{1}{\sqrt{j}} \begin{bmatrix} [y_0] & [y_1] & \dots & [y_{j-1}] \\ [y_1] & [y_2] & \dots & [y_j] \\ \dots & \dots & \dots & \dots \\ [y_{i-1}] & [y_i] & \dots & [y_{i+j-2}] \\ [y_i] & [y_{i+1}] & \dots & [y_{i+j-1}] \\ [y_{i+1}] & [y_{i+2}] & \dots & [y_{i+j}] \\ \dots & \dots & \dots & \dots \\ [y_{2i-1}] & [y_{2i}] & \dots & [y_{2i+j-2}] \end{bmatrix} = \begin{bmatrix} [Y_{0|i-1}] \\ [Y_{i|2i-1}] \end{bmatrix} = \begin{bmatrix} [Y_p] \\ [Y_f] \end{bmatrix} \quad (2.107)$$

These two submatrices have dimensions  $li \times j$ . It is worth noticing that output data are scaled by the factor  $1/\sqrt{j}$ , in order to be consistent with

the definition of covariance<sup>6</sup>. In practical applications, the number of columns  $j$  is taken equal to  $N - 2i + 1$ , which implies that all given data samples are used. Another division is obtained by adding one block row to the past outputs and omitting the first block row of the future outputs:

$$[H_{0|2i-1}] = \begin{bmatrix} [Y_{0|i-1}] \\ [Y_{i|i}] \\ [Y_{i+1|2i-1}] \end{bmatrix} = \begin{bmatrix} [Y_{0|i}] \\ [Y_{i+1|2i-1}] \end{bmatrix} = \begin{bmatrix} [Y_p^+] \\ [Y_f^-] \end{bmatrix} \quad (2.108)$$

where, in this case, the superscript  $+$  denotes addition of one block row instead of pseudo-inverse.

The DD-SSI algorithm is based on the projection of the row space of the future outputs onto the row space of the past outputs. The definition of this projection (more details about projections can be found in Van Overschee & De Moor 1996) is:

$$[P_i] = [Y_f] / [Y_p] = [Y_f [Y_p]^T] ([Y_p [Y_p]^T])^+ [Y_p] \quad (2.109)$$

From this definition it is clear that projections and covariances are closely related, being  $[Y_f [Y_p]^T]$  and  $[Y_p [Y_p]^T]$  block Toeplitz matrices containing covariances between the outputs.

---

<sup>6</sup> For  $j \rightarrow \infty$  and assuming ergodicity, the block Toeplitz matrix of covariances can be computed from the block Hankel matrix of output data:  $[T_{1|i}] = [Y_f [Y_p]^T]$ .

## 2.5 OMA IN TIME DOMAIN

---

In order to compute the projection (2.109), a QR factorization of the block Hankel matrix of outputs is adopted:

$$\begin{array}{c}
 \begin{array}{ccc}
 & li & l & l(i-1) & j \\
 & \leftrightarrow & \leftrightarrow & \leftrightarrow & \leftrightarrow \\
 \begin{bmatrix} H_{0|2i-1} \end{bmatrix} = & \begin{array}{c} li \\ l \\ l(i-1) \end{array} & \begin{array}{c} \updownarrow \\ \updownarrow \\ \updownarrow \end{array} & \begin{array}{ccc} \begin{bmatrix} R_{11} \end{bmatrix} & \begin{bmatrix} 0 \end{bmatrix} & \begin{bmatrix} 0 \end{bmatrix} \\ \begin{bmatrix} R_{21} \end{bmatrix} & \begin{bmatrix} R_{22} \end{bmatrix} & \begin{bmatrix} 0 \end{bmatrix} \\ \begin{bmatrix} R_{31} \end{bmatrix} & \begin{bmatrix} R_{32} \end{bmatrix} & \begin{bmatrix} R_{33} \end{bmatrix} \end{array} & \begin{array}{c} \begin{bmatrix} Q_1 \end{bmatrix}^T \\ \begin{bmatrix} Q_2 \end{bmatrix}^T \\ \begin{bmatrix} Q_3 \end{bmatrix}^T \end{array}
 \end{array}
 \end{array} \quad (2.110)$$

The Hankel matrix is, therefore, expressed as the product of a orthonormal matrix  $[Q]$  ( $[Q]^T [Q] = [Q][Q]^T = [I]$ ) and a lower triangular matrix  $[R]$ . It is possible to show that the RQ factorization yields the following expression for the projections of future row spaces onto past row spaces:

$$[P_i] = \begin{bmatrix} R_{21} \\ R_{31} \end{bmatrix} [Q_1]^T \quad (2.111)$$

$$[P_{i-1}] = [Y_f^-] / [Y_p^+] = \begin{bmatrix} R_{31} & R_{32} \end{bmatrix} \begin{bmatrix} Q_1 \\ Q_2 \end{bmatrix}^T \quad (2.112)$$

Moreover, the output sequence  $[Y_{i|i}]$  in equation (2.108) can be expressed as:

$$\begin{bmatrix} Y_{i|i} \end{bmatrix} = \begin{bmatrix} R_{21} & R_{22} \end{bmatrix} \begin{bmatrix} Q_1^T \\ Q_2^T \end{bmatrix} \quad (2.113)$$

The main theorem of stochastic subspace identification (Van Overschee & De Moor 1996) states that the projection matrix  $[P_i]$  can be factorized as the product of the observability matrix  $[O_i]$  and the Kalman filter state sequence  $[\hat{X}_i]$ :

$$[P_i] = [O_i][\hat{X}_i] = \begin{bmatrix} [C] \\ [C][A] \\ \dots \\ [C][A]^{i-1} \end{bmatrix} \begin{bmatrix} \{\hat{x}_i\} & \{\hat{x}_{i+1}\} & \dots & \{x_{i+j-1}\} \end{bmatrix} \quad (2.114)$$

Since the projection matrix is the product of a matrix with  $n$  columns and a matrix with  $n$  rows, its rank equals  $n$  if the condition expressed by (2.91) is fulfilled. The rank of this matrix can be estimated by applying SVD; after omitting the zero singular values and the corresponding singular vectors, the projection matrix can be rewritten as:

$$[P_i] = [U_i][S_i][V_i]^T \quad (2.115)$$

The observability matrix and the Kalman filter state sequence are then obtained by splitting the SVD in two parts:

## 2.5 OMA IN TIME DOMAIN

---

$$[O_i] = [U_i][S_i]^{1/2}[T] \quad (2.116)$$

$$[\hat{X}_i] = [O_i]^+ [P_i] \quad (2.117)$$

where the superscript  $+$  here denotes pseudo-inverse.

Up to now the order  $n$  of the system (obtained as the number of non-zero singular values of the projection matrix  $[P_i]$ ), the observability matrix  $[O_i]$  and the Kalman filter state sequence  $[\hat{X}_i]$  have been estimated. In order to solve the identification problem, the matrices  $[A]$ ,  $[C]$ ,  $[G]$  and  $[R_0]$  have to be computed, too. It can be proved that the projection between past and future outputs when the shifted Hankel matrix (2.108) is considered yields:

$$[P_{i-1}] = [Y_f^-] / [Y_p^+] = [O_{i-1}][\hat{X}_{i+1}] \quad (2.118)$$

where the observability matrix  $[O_{i-1}]$  can be directly obtained from  $[O_i]$  by deleting the last  $l$  rows. Thus, combining equations (2.112) and (2.118), the state sequence  $[\hat{X}_{i+1}]$  can be computed as:

$$[\hat{X}_{i+1}] = [O_{i-1}]^+ [P_{i-1}] \quad (2.119)$$

where the superscript  $+$  here denotes pseudo-inverse.

The state matrix and the output matrix can be now derived in different ways. In Van Overschee & De Moor (Van Overschee & De Moor 1996) three algorithms are suggested: the first one is based on the states, the second one on the shifted structure of the observability matrix while the third one leads to positive real sequences. The problem of positive realness affects the output covariance sequence  $[R_i]$  when it is computed from the matrices  $[A]$ ,  $[C]$ ,  $[G]$  and  $[R_0]$  (see equations (2.34)): if this sequence is not a positive real sequence, the spectrum matrix obtained from this sequence is not positive definite for all frequencies  $\omega$ . Since only if a matrix is positive definite all its diagonal entries are positive (Golub & Van Loan, 1996), in practice it may happen that the synthesized power spectra become negative at certain frequencies but this has, of course, no physical meaning. The third algorithm proposed by Van Overschee & De Moor (Van Overschee & De Moor 1996), however, does not lead to an asymptotically unbiased estimate of the estimated covariance sequence, unless the number  $i$  of block rows in the Hankel matrices goes to infinity. Here only the first two algorithms (which do not guarantee the positive realness of the estimated covariance sequences) are reviewed, since they have been implemented as a part of the modal identification software which will be discussed in the next chapter. It is worth noticing that also the Cov-SSI method does not guarantee the positive realness of the identified covariance sequence.



## 2.5 OMA IN TIME DOMAIN

---

After having identified the Kalman filter state sequences  $[\hat{X}_i]$  and  $[\hat{X}_{i+1}]$  from the output data, the system matrices can be recovered from the following over-determined set of linear equations, obtained by stacking the state-space models for time instants  $i$  to  $i + j - 1$ :

$$\begin{bmatrix} [\hat{X}_{i+1}] \\ [Y_{i:i}] \end{bmatrix} = \begin{bmatrix} [A] \\ [C] \end{bmatrix} [\hat{X}_i] + \begin{bmatrix} [\rho_w] \\ [\rho_v] \end{bmatrix} \quad (2.120)$$

Since the Kalman filter residuals  $[\rho_w]$  and  $[\rho_v]$  are uncorrelated with the states  $[\hat{X}_i]$  (see also section 2.2.3, equations (2.32)), this set of equations can be solved in a least square sense (since the least square residuals are orthogonal and, thus, uncorrelated with the regressors  $[\hat{X}_i]$ ). In Van Overschee & De Moor (Van Overschee & De Moor 1993) it is shown that the least square solution provides an asymptotically unbiased estimate of  $[A]$  and  $[C]$  as:

$$\begin{bmatrix} [A] \\ [C] \end{bmatrix} = \begin{bmatrix} [\hat{X}_{i+1}] \\ [Y_{i:i}] \end{bmatrix} [\hat{X}_i]^+ \quad (2.121)$$

It should be noted that, because of equations (2.113), (2.117) and (2.119), all right-hand-side quantities of equation (2.121) can be expressed in terms of the QR factors. Because of their orthonormality, the Q factors cancel out in this equation: thus, it is unnecessary to compute the orthonormal matrix

$[Q]$ . Moreover, a significant data reduction is achieved by replacing the Hankel matrix by its  $[R]$  factor.

When the second algorithm is considered, the state matrix  $[A]$  can be estimated in different ways: two of them are herein reviewed.

After having computed the matrix  $[\bar{O}_i]$  by deleting the first  $l$  rows of  $[O_i]$ , the least square solution for  $[A]$  is given by:

$$[A] = [O_{i-1}]^+ [\bar{O}_i] \quad (2.122)$$

where the superscript  $+$  here denotes pseudo-inverse.

The second approach is, instead, based on the SVD of the concatenated matrix  $\begin{bmatrix} [\bar{O}_i] \\ -[O_{i-1}] \end{bmatrix}$ :

$$\begin{bmatrix} [\bar{O}_i] \\ -[O_{i-1}] \end{bmatrix} = [U][S][V]^T \quad (2.123)$$

By partitioning the matrix  $[V]$  as:

$$[V] = \begin{matrix} & \begin{matrix} n & n \end{matrix} \\ \begin{matrix} n \\ n \end{matrix} & \begin{matrix} \updownarrow & \updownarrow \\ \begin{bmatrix} [V_{11}] & [V_{12}] \\ [V_{21}] & [V_{22}] \end{bmatrix} \end{matrix} \end{matrix} \quad (2.124)$$

it is possible to compute the total least square solution as:

## 2.5 OMA IN TIME DOMAIN

---

$$[A] = [V_{22}] [V_{12}]^{-1} \quad (2.125)$$

According to the second algorithm, the matrix  $[C]$  is directly obtained from the first  $l$  rows of  $[O_i]$ .

From the matrices  $[A]$  and  $[C]$ , the modal properties of the system can be extracted as outlined in the previous section (equations from (2.99) to (2.105)).

In order to compute the spectrum matrix of the model, the matrices  $[G]$  and  $[R_0]$  have to be determined. The autocorrelation of  $[Y_{i|i}]$  immediately yields  $[R_0]$ :

$$[R_0] = \Phi([Y_{i|i}], [Y_{i|i}]) \quad (2.126)$$

where  $\Phi$  denotes covariance.

The matrix  $[G]$  is, instead, obtained as the last  $l$  columns of  $[\Gamma_i]$ , where:

$$[\Gamma_i] = [O_i]^+ \Phi([Y_f], [Y_p]) \quad (2.127)$$

with the usual meaning of notations. The spectrum matrix of the model can now be computed according to equation (2.106).

It is worth emphasizing that, due to the finite data length, the identified state-space model (and therefore the matrices  $[A]$ ,  $[C]$ ,  $[G]$  and  $[R_0]$ ) is just

an estimate of the true model that generated the data. Like in the Cov-SSI method, when looking for the model order  $n$ , the singular values of the projection matrix must be inspected: due to noise, none of these singular values will be exactly zero and the order will be determined by looking at the gap between two subsequent singular values. Alternatively, the problem of order determination can be solved by constructing a stabilization diagram.

Several variants of SSI exist, characterized by different weights applied to data matrices ( $[T_{l|i}]$  for Cov-SSI,  $[P_i]$  for DD-SSI) before SVD. The weighting determines the state-space basis in which the model will be identified (for more details, Van Overschee & De Moor 1996). Herein the so-called Unweighted Principal Component (UPC) variant of the method has been discussed, since the weights are identity matrices (this is the variant implemented into the modal identification software). Another variant is the so-called Canonical Variate Analysis (CVA), according to which the singular values can be interpreted as the cosines of the principal angles between two subspaces (Van Overschee & De Moor 1996): the row space of the future outputs  $[Y_f]$  and the row space of the past outputs  $[Y_p]$ . If this approach is applied to Cov-SSI, the weighting of the covariance Toeplitz matrix before the application of SVD is given by (Akaike 1974):

$$([Y_f \mathbf{I} Y_f]^T)^{-1/2} [T_{l|i}] ([Y_p \mathbf{I} Y_p]^T)^{-1/2} \quad (2.128)$$

## 2.5 OMA IN TIME DOMAIN

---

If, instead, CVA is applied to DD-SSI, the weighting of the projection matrix before SVD is given by (Van Overschee & De Moor 1996):

$$\left( \begin{bmatrix} Y_f & Y_f \end{bmatrix}^T \right)^{-1/2} [P_i] \quad (2.129)$$

The last variant is the Principal Component (PC): it has also equivalent implementations for Cov-SSI and DD-SSI. As a rule of thumb, the UPC should be used in presence of modes of equal strength and of a good signal-to-noise ratio in the data: a low value for the maximum model order used for construction of the stabilization diagram can be used in this case. The CVA should be, instead, used in presence of modes characterized by widely different strength and when dealing with noisy data: a high value for the maximum model order used for construction of the stabilization diagram is required in this case. The PC variant seems to be a compromise between UPC and CVA. Even if these three methods have different physical explanation, a number of computer simulations and practical applications have demonstrated that there are no significant accuracy differences among them in output-only modal identification applications (Zhang et al. 2005b).

In comparison with Cov-SSI, DD-SSI seems to be less efficient in terms of computational time (Peeters, 2000): however, the main advantages of DD-SSI with respect to Cov-SSI are the direct use of stochastic response data, without estimation of covariances as first stage, and the robustness in presence of coloured noise (Zhang et al. 2005b).

## 2.6 SPECIAL METHODS

Beside the above described methods, which can be considered as classical, some new approaches for OMA are appearing in the literature. Some of them can be, in a way, classified within the traditional classes of time domain or frequency domain methods; some others, instead, works in different domains and should be mentioned apart.

One of these methods for modal identification in output-only conditions is based on the use of transmissibility functions. Transmissibility functions are a kind of FRF which, however, is not obtained from conjugate variables (motion response vs. force input) but from like variables (for example, two motion records). Since the mathematical structure is that one of FRFs, this approach can be in a way classified as a frequency domain one.

FRFs are widely used functions in the field of experimental modal analysis: nevertheless, transmissibility functions have recently made their appearance in the field of OMA (Devriendt & Guillaume 2007). The main difference with respect to FRFs is that transmissibility functions can be measured without knowledge about the excitation forces: even if they are estimated in the same way as FRFs, transmissibility functions are actually the ratio between the response  $X_i$  and a reference response signal  $X_j$ , instead of an excitation signal as in the case of FRFs:

## 2.6 SPECIAL METHODS

---

$$T_{ij}(\omega) = \frac{X_i(\omega)}{X_j(\omega)} \quad (2.130)$$

Like FRFs, transmissibility functions are complex valued quantities characterized by a magnitude and a phase at each frequency. Even if they can be computed in several ways, the  $H_1$  estimator<sup>7</sup> is usually adopted (Devriendt et al. 2008):

$$T_{ij}(\omega) = \frac{S_{X_i X_j}(\omega)}{S_{X_j X_j}(\omega)} \quad (2.131)$$

Since the reference output is present in all transmissibility functions, it must be properly chosen, in a way that it carries the maximum amount of information about structural modes.

It can be easily shown, by recalling the relation between FRFs and Fourier transforms of input and output and the structure (2.4), that the system poles disappear when computing the ratio between two responses, namely transmissibility: as a consequence, in transmissibility measurements each resonance is represented by a flat zone instead of a peak. However, the most important property of transmissibility functions is that they approach a constant value when converging to a system pole:

---

<sup>7</sup> When the  $H_1$  estimator is used, FRF is computed as the ratio of the cross-spectrum to the input auto-spectrum

---

$$\lim_{\omega \rightarrow \omega_n} T_{ij}(\omega) = \frac{\phi_{in}}{\phi_{jn}} \quad (2.132)$$

and, in particular, such value is directly related to mode shape components at measurement points  $i$  and  $j$ . Moreover, since the limit (2.132) is independent of the input, transmissibility functions relating the same responses but obtained from two tests characterized by different loading conditions cross each other exactly at resonances and, therefore, their difference is zero. By considering the inverse of such a difference, a function characterized by poles equal to the system poles is again obtained based on transmissibility measurements. By applying a frequency domain estimator (Pintelon et al. 1994, Peeters et al. 2004), natural frequencies and damping ratios of the system under test can be obtained. Based on the results of this first step, mode shapes can then be obtained from transmissibility functions. In the original approach, therefore, it can be considered as a two step method: however, it has been recently enhanced in order to get all modal parameters in a single step.

One of the main advantages of the use of transmissibility functions for OMA with respect to more traditional approaches is related to the fact that they do not depend on the nature of the forces and this circumstance reduces the risk of wrongly identifying the modal parameters in presence of non-white excitations (Devriendt et al. 2008).



## 2.6 SPECIAL METHODS

---

In time domain, instead, new procedures for OMA are based on Blind Source Separation (BSS) techniques: as a general concept, BSS techniques aim at recover the unobservable inputs of a system, the so-called sources ( $s_i$ ), from the measured outputs ( $x_i$ ) basically without knowledge about the mixing system. By assuming that such a system is linear and time invariant, the relation between the source signals and their mixtures is expressed by the following matrix equation:

$$\{x(t)\} = [A]\{s(t)\} + \{\sigma(t)\} \quad (2.133)$$

where  $[A]$  is referred to as the mixing matrix, while  $\{\sigma(t)\}$  is the noise vector corrupting the data. This equation is very similar to the modal expansion of the response of a dynamic system:

$$\{x(t)\} = [\Phi]\{q(t)\} \quad (2.134)$$

where  $[\Phi]$  is the mode shape matrix and  $\{q(t)\}$  is the vector of modal coordinates. By comparing equations (2.133) and (2.134), a one-to-one relationship between  $[\Phi]$  and  $[A]$  can be observed; moreover, the modal coordinates can be interpreted as virtual sources. An in-depth discussion about this class of techniques is beyond the scope of this thesis: more details about BSS techniques and their applicability for output-only modal analysis can be found in (Kerschen et al. 2007, Poncelet et al. 2007, Belouchrani et al. 1997). It is just worth emphasizing that, among BSS

techniques, a very promising one in the field of OMA seems to be the so-called Second Order Blind Identification (SOBI): it is a kind of two step method where, however, mode shapes are identified at the first step while natural frequencies and damping ratios are recovered from the second step. More details about SOBI can be found in (Poncelet et al. 2007, Belouchrani et al. 1997, Poncelet et al. 2008).

Other special and recently developed procedures for OMA are based on cepstral analysis and wavelet transform. A cepstrum is defined as the IFT of a logarithmic spectrum. Examples of application of cepstral techniques in the field of OMA, also in combination with BSS techniques, can be found in (Hanson et al. 2007a, Hanson et al. 2007b, Chia 2007, Randall 2008). The main advantages are related to a weaker assumption about the input with respect to that one of white noise, and to the possibility to recover scaled mode shapes if a minimum of information is provided (Randall 2008).

The wavelet transform is, instead, defined from a basic wavelet, the so-called mother wavelet  $\psi$ , which is an analyzing function located in both time and frequency. From the mother wavelet a set of analyzing functions can be obtained simply by scaling (parameter  $a$ ) and translation (parameter  $b$ ). The wavelet transform of a signal  $s$  is thus defined as:

$$W_s(a,b) = \frac{1}{\sqrt{a}} \int_{-\infty}^{+\infty} s(t) \psi^* \left( \frac{t-b}{a} \right) dt \quad (2.135)$$

## 2.6 SPECIAL METHODS

---

where the superscript  $*$  denotes complex conjugation. In order to interpret the wavelet transform in terms of time-frequency analysis, a relation between the scale parameter  $a$  and the frequency  $f$  has to be established. Several applications of wavelet transform in the field of OMA are reported (Ruzzene et al. 1997, Lardiès 1997, Staszewski 1997, Gouttebroze & Lardiès 2001), yielding to accurate estimations of natural frequencies and damping ratios. Moreover, a wavelet-based output-only modal analysis procedure for extraction also of mode shapes has been recently proposed (Han et al. 2005). The main advantage of wavelet transforms is related to the possibility to process non-stationary signals (for example, transient signals): for this reason, they are also widely applied within vibration-based damage detection procedures.

## 2.7 REMARKS

Far from being a comprehensive description of Operational Modal Analysis techniques, the mathematical framework and some output-only modal identification procedure have been analyzed in detail, trying to put in evidence the main steps of the selected algorithms in view of their software implementation. Some other techniques, not directly concerning the work described in this thesis, have been shortly reviewed; also some new methods based on less standard approaches, such as transmissibility, BSS, wavelet transform and cepstral techniques, have been reported.

For classical time domain methods, the main characteristics and the relationships existing among them have been analyzed by focusing attention on the ARMA model mathematical background and its relation with stochastic state-space models. This approach allowed to point out advantages and disadvantages of these methods: the final result was the selection of some of these algorithms for implementation in a modal identification software. The reasons of the choice are here briefly outlined. NExT-type procedures, even if developed since a long time and widely applied to civil engineering structures, suffer some limitations. When they appeared, they represented a significant enhancement in output-only modal analysis with respect to the classical Peak Picking technique, since improved the accuracy of data analysis, in particular in presence of close modes, and allowed the extraction of actual mode shapes instead of operating deflection shapes. Notwithstanding their historical relevance, they suffer some disadvantages with respect to the other time domain methods. The Polyreference LSCE, for example, is a two step procedure which allows estimation of mode shapes, only after having identified modal frequencies and damping ratios, by curve fitting techniques: as a result, poor estimates of mode shapes are obtained in comparison with other algorithms (for example, stochastic realization based or subspace based procedures). The ITD method, instead, suffers the lack of noise truncating mechanisms, thus leading to several spurious poles; moreover, high order modes require filtering procedures to be extracted (Fujino & Siringoringo 2007): a repeated application of the procedure to the same

## 2.7 REMARKS

---

dataset have to be carried out, thus resulting in a time consuming identification process.

ARMA models aim at model the dynamics of both the structural system and the noise: since also noise is modelled, lots of additional spurious poles, not related to the dynamics of the system under test, appear. As a consequence, selection of system poles may become difficult and the presence of noise can affect the modal parameter estimates. For example, the lack of a noise truncating mechanism in the IV method is reflected in less accurate mode shape estimates with respect to subspace methods; moreover, higher order models are required to obtain good modal parameter estimates (Peeters 2000). On the other hand, the presence of a lot of additional poles for fitting the noise makes the stabilization diagram less clear. When PEM is considered, the advantage of a optimal statistical description of data due to the presence of the MA matrix polynomial is paid by the need to solve a highly non-linear optimization problem, which is time consuming, computational demanding and may suffer for convergence. Since its application does not improve too much modal parameter estimates (Brincker & Andersen 1999b), it is possible to use subspace methods by taking advantage of a reduced computational time and no convergence problems.

Subspace methods are based on the use of SVD to reject noise, thus requiring lower order models to estimate modal parameters from measured data. Moreover, since the identification problem is solved just by mean of linear algebra tools, no non-linear optimization problems have

to be solved, thus resulting in a lower computational burden. In presence of noise, weighting matrices can be applied to improve the performance of the estimators.

Both Cov-SSI and DD-SSI seem to behave equally well in terms of modal parameter estimation performance; however, DD-SSI can be also implemented in a way that positive realness of covariance sequence is ensured.

By taking into account the performance of the different time domain algorithms, it is obvious the choice of subspace methods for implementation in a modal identification software. However, implementation of non-parametric frequency domain OMA procedures is also necessary because they give a first insight into the identification problem, thus allowing a better choice of parameters in subspace algorithms. Moreover, they are less computational demanding with respect to subspace methods and give, under some more restrictive assumptions for the Peak Picking technique, less restrictive ones for the EFDD, reasonable estimates of the modal parameters. A comparison of the estimates among time and frequency domain methods is also useful for a successful identification process.

## 2.7 REMARKS

---

---

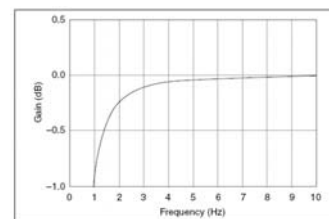
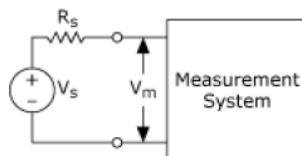
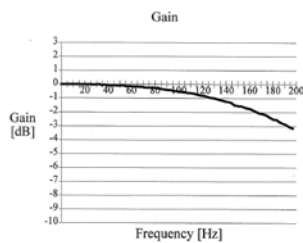
# 3

## The Measurement Chain

---

*«Everything should be made  
as simple as possible,  
but not simpler»*

*Albert Einstein*







## CHAPTER 3

### 3.1 INTRODUCTION

A good identification process in output-only conditions (that means weak ambient vibrations in the case of civil engineering structures) cannot leave out of consideration high quality measurements. Thus, a proper selection and good knowledge of equipment and measurement instruments has the same importance of theoretical knowledge of experimental modal analysis procedures.

The main components of a modal analysis test are the device under test (DUT), namely the structure to be investigated, a number of motion transducers, a data acquisition device and a data processing system for extraction of modal informations from recorded data.

In this chapter, the hardware component (sensors, data acquisition hardware) characteristics and some practical issues are described in some details, in order to define the parameters to look at for a proper choice of the hardware to be used for ambient vibration tests, and to identify, deal with and hopefully solve noise problems. Moreover, some data pre-treatment procedures are discussed: in fact, a detailed data analysis

### 3.1 INTRODUCTION

---

should be always preceded by a data qualification step, in order to be aware of non-stationary characteristics of the signal or of the presence of spurious harmonics (even if this is still an open issue in operational modal analysis). Moreover, a careful inspection of acquired signals can reveal anomalies and errors which should be removed, if possible, or suggest the repetition of the test, in the worst case. Obviously, in the case of fully automated monitoring systems, where data are acquired and analyzed in real or near-real time, this qualification step is not feasible; in case of off-line analyses, instead, it should never be omitted.

Finally, some basic aspects related to the implementation of a data acquisition software for programmable hardware management, of data pre-treatment procedures and of some OMA procedures described in the previous chapter will be reviewed, thus showing how an entirely home-made data acquisition and processing system for OMA can be obtained.

## 3.2 THE MEASUREMENT CHAIN

### 3.2.1 Motion transducers

The most used sensors for ambient vibration tests are accelerometers, even if in recent years a number of geophone-based applications is appearing in the literature (Brincker et al. 2005, Schmidt 2007). Geophones are robust high performance sensors, in particular with respect to sensor self noise, but they are characterized by poor performance for low frequency values, even if there are some proposals for digital correction of the output signal

in order to overcome these limitations (Brincker et al. 2005, Barzilai 2000). No further details are provided in this thesis about geophones, since they have not been used for any application.

When accelerometers are used for ambient vibration tests of civil structures, due to the low amplitude of the motion and the limited frequency range of the DUT, the best performance can be obtained by high-sensitivity accelerometers such as those ones usually used for seismic networks. However, frequency band and sensitivity are not the only parameters to be taken into account for a proper choice of sensors.

Before discussing sensor characteristics in view of their application in the OMA framework, it is worth noticing that the final choice is always the result of a number of factors. In this thesis, the use of seismic accelerometers is suggested because of their high performance and because of their flexibility, allowing recording of both weak and strong motions, which is relevant in particular for structural health monitoring applications in earthquake prone regions. The test engineer, however, should be aware that the market offers a large variety of sensors, characterized by a range of specifications and prices: thus, the final choice must take into account different factors, such as the final objective of measurements, the amplitude of motion to be measured, the characteristics of the sensors in relation to those ones of the data acquisition hardware and of the DUT, and, the last but not the least, the available budget.

### 3.2 THE MEASUREMENT CHAIN

---

First-rate accelerometers in the field of modal identification of civil engineering structures in output-only conditions are Force Balance (FB) accelerometers and seismic IEPE (Integrated Electronics Piezoelectric) accelerometers.

An accelerometer is a mechanical system which can be represented as a SDOF system, characterized by an oscillating mass, a spring and a dashpot, subjected to a ground motion. It can be equivalently represented in terms of its FRF.

In FB accelerometers the external force on the sensor mass is compensated by an electronically generated force in the opposite direction, so that the mass remains nearly stationary. Such a force is generated by a current through a coil: the current needed to balance the external force is proportional to it. Thus, by measuring the current (more precisely, a potential difference), a measure proportional to the external acceleration is obtained.

Piezoelectric accelerometers, instead, rely upon the piezoelectric effect of quartz or ceramic crystals to produce an electrical output proportional to the applied acceleration: in particular, the piezoelectric effect produces on the crystal a charge accumulation which is proportional to the applied force and, therefore, to the acceleration, according to the Newton's law of motion. In IEPE accelerometers, this charge is converted, by a built-in signal conditioning electronics, into a low-impedance voltage signal which can be transmitted, over ordinary two-wire or coaxial cables, to a data acquisition device.

About the frequency response of sensors, most of them are described to have a flat response within a given frequency band (Figure 3.1): in particular, because the widest frequency range with a near-uniform gain is obtained for a damping ratio equal to 0.707 (Bendat & Piersol 1986), certain type of high-gain accelerometers are designed with added damping in order to maximize their useful frequency range.

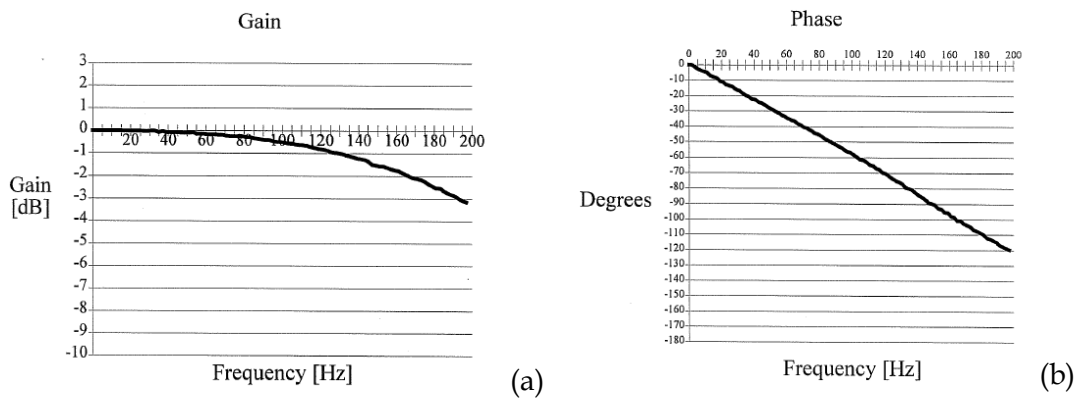


**Figure 3.1.** Typical frequency response for Force Balance accelerometers

In any case, being the frequency response nearly flat up to about the 20% of the undamped natural frequency of the accelerometer, apart from the damping ratio, it may happen that no specific design in terms of damping is adopted by the manufactures: in such a case, the useful frequency range is up to 20% of the natural frequency of the sensor.

In terms of phase, a value of 0.707 for damping ratio produces a near-linear phase function (on a linear scale) over the frequency range where the frequency response amplitude is nearly flat. The linear phase function corresponds to a simple time delay, which does not distort the time

### 3.2 THE MEASUREMENT CHAIN

---

history of the physical phenomenon being measured. Deviations from the above mentioned value of damping result, instead, in a phase distortion of the measured phenomenon: however, in these cases, the phase is zero up to 20% of the natural frequency of the sensor, which can be used in this limited frequency range without distortions of the measured phenomenon.

Sensor specifications must be, therefore, read carefully in order to use them properly. It is also worth noticing that some sensor characteristics, such as dynamic range or sensitivity, might be frequency dependent: thus, a sensor might show better specifications in a certain frequency band and worse specification elsewhere. This circumstance must be taken into account in sensor choice in order to state if it is suitable for application.

Sensitivity is usually given as the gain of the sensor (for example, 10 V/g) and it is in some way related to the smallest signal that can be resolved: however, it must be pointed out that such a signal is also limited by the noise generated in the electronics. Anyway, a high gain should be preferred since an amplified signal minimizes noise effects due to transmission over cables. Besides, it is important to verify that the maximum sensor output has a level fitting the recorder maximum input so that the sensor dynamic range is optimally used.

The dynamic range of a sensor (often expressed in dB) is, instead, the ratio between the largest and the smallest signal it can record. The best accelerometers have a dynamic range higher than 150 dB: however, a

usual dynamic range is equal to 120-140 dB, which is well adapted to the dynamic range of the average 24 bit digitizers.

An ideal sensor should behave linearly: thus, another important characteristic to be inspected in order to compare performance of different devices is linearity, which must be better than 1%. Cross axis sensitivity has to be also low (less than 2-5%).

Sensor self noise should be also quantified, because if the signal to be recorded is very small it may drown in the electronic noise of the sensor. This characteristic could be relevant in the case of very massive low-rise structures. Even if they were designed to deal with seismic background noise, Peterson noise curves (Peterson 1993) could be useful to judge about the applicability of a sensor in presence of very low levels of vibration. Starting from ground acceleration power spectral densities determined for noisy and quiet periods at 75 worldwide distributed digital stations, Peterson has derived two curves which represent upper and lower bounds of the cumulative compilation of such PSDs. If the sensor noise is below such curves, the output signal is not just electronic noise. Since the level of vibration of a structure in operational conditions is expected to be higher than the seismic background noise (even for massive structures in quiet environment), a sensor which accomplishes Peterson's model can be certainly applied for OMA tests.

For some kinds of measurement systems, as it will be clarified next, also the output bias voltage of the sensor must be taken into account, so that the data acquisition device can be chosen and operate properly.



## 3.2 THE MEASUREMENT CHAIN

---

### 3.2.2 Data acquisition hardware: choice of measurement system

Measuring analog signals by mean of a data acquisition device is usually not as simple as wiring the signal source leads to the data acquisition system: in fact, noise-free measurements can be obtained only by a proper knowledge of the nature of the signal source, a suitable configuration of the data acquisition hardware and an appropriate cabling scheme. The main difficulty is, therefore, related to the choice of an appropriate input configuration, also because most data acquisition devices provide some flexibility in their analog input stage configuration: as a consequence, appropriate knowledge of input configurations is needed in order to do accurate measurements and to choose the measurement system by taking into account the relative merits of different schemes. In this section, a general discussion about this topic is reported, in order to better understand the different configurations and to give a suggestion about their choice.

Signal conditioning systems usually produce an electrical signal in the form of voltage: this signal is then transferred to the data acquisition hardware for digitization. Sensors can, therefore, be interpreted as signal sources and grouped into two classes: grounded and floating signal sources.

When grounded (or ground-referenced) signal sources are considered (Figure 3.2), the voltage signal is referenced to the building system ground: it is the case of plug-in instruments. It is worth emphasizing that two

grounded signal sources are usually not at the same potential even if they are connected to the same building.

In a floating (or non-referenced) signal source, instead, the voltage signal is not referred to an absolute reference, such as earth or building ground, since each terminal of the signal source is independent of earth (Figure 3.2). Any device which has an isolated output is considered a floating signal source. Non-grounded accelerometers are an example of floating signal source.

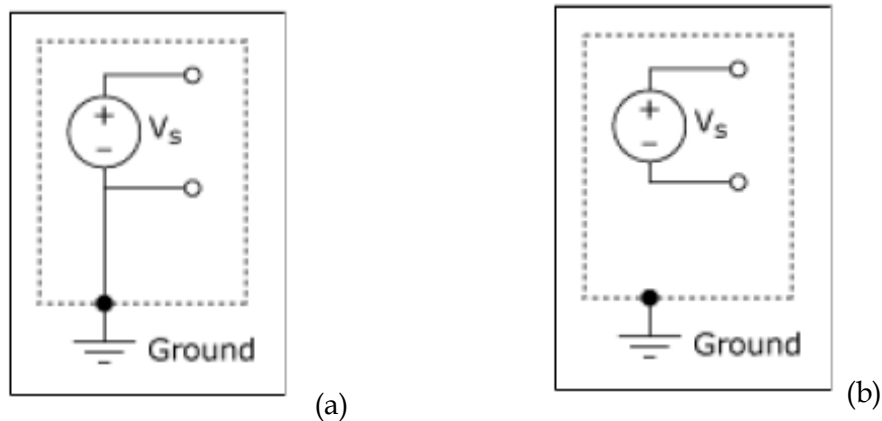


**Figure 3.2.** Grounded (a) and floating (b) signal sources  
(<http://zone.ni.com/devzone>)

A similar distinction can be done for measurement systems.

A differential (or non-referenced) measurement system has neither of its inputs tied to a fixed reference, such as earth or building ground.

A grounded (or ground-referenced) measurement system is similar to a grounded source, since measurements are referred to ground. This kind of system is also referred to as a single ended measurement system.

### 3.2 THE MEASUREMENT CHAIN

---

A third configuration, the pseudodifferential one, will be described later in this section in order to better understand similarities and differences with respect to the classical differential configuration.

While discussing advantages and limitations of the different measurement system types, it is necessary to deal with noise sources: different measurement systems shows different behaviour with respect to a certain type of noise source. Moreover, knowledge of noise sources provides some useful hints for carrying out high quality measurements.

An ideal differential measurement system responds only to the potential difference between its two terminals, the non-inverting terminal (+) and the inverting terminal (-). Any voltage measured with respect to the instrumentation amplifier ground which is present at both amplifier terminals is referred to as a common-mode voltage. Common-mode voltage is completely rejected by an ideal differential measurement system: however, actual devices have some limitations, described by some parameters such as the common-mode voltage range and the common-mode rejection ratio (CMRR). Anyway, this capability is useful in rejecting noise, since unwanted noise is often present in the form of common-mode voltage. Typical sources of common-mode voltage noise are 50/60 Hz signals from power lines, power supply ripple or electromagnetic fields. The CMRR is a measure of the ability of an instrument to reject interference from a common-mode signal: it is usually expressed in dB. Basically, CMRR describes the ability of a differential input measurement system to reject noise common to both inputs: the higher the CMRR, the

better the circuitry can extract differential signals in the presence of common-mode noise.

The common-mode voltage range, instead, limits the allowable voltage swing on each input with respect to the measurement system ground: violating this constraint can result not only in measurement errors but also in a possible damage to the data acquisition device. As an example, some devices, when dealing with IEPE sensors, provide an equation which limits the sum of common-mode voltage, bias voltage of the sensor and full scale voltage of the sensor to be in a predefined voltage range to ensure that the data acquisition device can be used with those sensors.

A grounded signal source is best measured with a differential measurement system. In fact, if a ground-referenced measurement system is adopted in this case, the measured signal is the sum of the signal voltage and of the potential difference between the signal source ground and the measurement system ground. The potential difference between the two grounds causes a current to flow in the interconnection: this current is called ground-loop current. Ground-loop introduced noise may have both AC and DC components, thus introducing offset errors as well as noise in the measurements. Such noisy measurements often show power line frequency components in the reading. Signal degradation due to ground-loop effects may be tolerable when connecting a single ended measurement system and a grounded signal source only in presence of signals characterized by a high voltage level and if the wires between source and measurement system have a low impedance.

### 3.2 THE MEASUREMENT CHAIN

---

Floating signal sources can be measured by both differential and single ended measurement systems: however, in the case of differential measurement systems, it is important to ensure that the common-mode input range of the measurement device is respected. Due to a number of phenomena, the voltage level of the floating source can move out of the valid range of the input stage of the data acquisition device: to anchor this voltage level to a reference, bias resistors connected between each lead and the measurement system ground have to be used, otherwise erratic or saturated readings may be obtained.

If a floating signal source is connected to a single ended measurement system, no ground-loop is created in this case, thus allowing the use of this measurement scheme.

As a general rule, differential measurement systems should be preferred because they reject not only ground-loop induced errors, but also the noise picked up in the environment up to a certain degree. Single ended measurement systems, however, provide twice the number of channels with respect to an equivalent differential measurement system, but their use can be justified only if the magnitude of the induced errors is smaller than the required accuracy of the data.

When differential input systems are considered, differences between the differential and the pseudodifferential configuration must be taken into account in order to optimize the measurement results.

Both differential and pseudodifferential configurations provide common-mode voltage rejection while single ended inputs do not: however,

differential systems provide both AC and DC common-mode rejection, while pseudodifferential devices provide only DC common-mode voltage rejection. A pseudodifferential measurement system is very similar to the differential one: however, in the case of pseudodifferential systems, all inputs are referred, but not directly tied because of the isolation provided by a resistor, to a common ground. The advantages of using a pseudodifferential system are that DC common-mode voltages are broken and that ground-loop effects can be minimized. In summary, pseudodifferential measurements can be recommended for floating signal sources and can be used also for grounded signal sources, even if differential systems provide more common-mode rejection. Grounded signal sources are recommended to be measured by differential systems; floating sources can be measured also, but additional connection to ground are needed to prevent signal drifts beyond the common-mode range.

Ground-loops and common-mode voltage are not the only noise sources, since there is always a certain amount of noise picked up from the environment: this is especially true for low level analog signals. It is necessary to comply with some rules of thumb in order to minimize these effects. First of all, mobile phones must be switched off and cables must be placed as far as possible from the computer screen during measurements. Cabling should be made by coaxial cables or twisted shielded cables: unshielded wires must be avoided for analog signal transmission due to the interchannel modulation (cross talk) and excessive background noise

## 3.2 THE MEASUREMENT CHAIN

---

problems. Moreover, cable motion can cause triboelectric effects, due to the charge generated on the dielectric within the cable, if it does not maintain contact with the cable conductors; in a few words, errors are due to changes in the magnetic field. The solution is to avoid dangling wires and to clamp the cabling.

If the measurement system has been properly defined and the installation and measurement process has been properly carried out, the last should result in good quality data, which can be eventually further improved by adopting adequate signal processing techniques for noise reduction. However, it is worth emphasizing that there is no substitute to good measurements: the acquired signal must carry on actual informations together with a certain amount of noise in order to apply successfully OMA techniques. Signal processing techniques and advanced modal analysis techniques have no effects if the recorded signal is just noise.

### 3.2.3 Data acquisition hardware: characteristics

The main characteristics of analog-to-digital converters (ADCs) are here summarized in order to compare different solutions.

The resolution of an ADC can be defined as the smallest step that can be detected, which is related to one change of the least significant bit (LSB). For high dynamic range digitizers, the order of magnitude is about 1  $\mu\text{V}$ . The number of bits of an ADC is also sometimes referred to as resolution. However, most ADCs have an internal noise higher than one count: in this

case, the number of noise free bits, rather than the total bit number, limits the effective resolution.

The sample rate is the number of samples acquired per second. For OMA applications in the civil engineering field, a maximum sampling rate of 100 Hz or 200 Hz is usually adopted.

The maximum input has to be chosen by taking into account sensor characteristics (see section 3.2.2).

The dynamic range is defined as the ratio between the largest and the smallest value the ADC can give and it is usually expressed in dB: however, for some digitizers the lowest bits contain only noise, so the dynamic range is defined as the ratio between the largest input voltage and the noise level of the digitizer. This number may be also dependent on the sampling frequency. Good digitizers have a dynamic range higher than 100 dB.

The absolute accuracy is a measure of all error sources. It is defined as the difference between the input voltage and the voltage representing the output. Ideally, this error should be  $\pm\text{LSB}/2$  (the quantization error, that is to say the error only due to the digitization steps).

The noise level is related to the number of bits occupied by noise when the input is zero: it is usually expressed in terms of RMS noise. A good 24-bit digitizer usually has just the last two bits corrupted by noise.

Conversion time, that is to say the minimum time required for a complete conversion, is defined just for converters based on a sample-and-hold architecture. However, currently a sigma-delta architecture is preferred



### 3.2 THE MEASUREMENT CHAIN

---

for 24-bit ADCs because of its higher performance: because of the different architecture of these converters, based on a continuous signal tracking, the conversion interval is not important. Without describing sigma-delta converters in details, it is worth noticing that their higher performance is basically obtained by sampling the input signal at a frequency much higher than the desired data rate: these samples are then applied to a digital filter which expands the data to 24 bits, rejects signal components greater than the Nyquist frequency associated to the desired sampling frequency, and digitally resamples the data at the chosen data rate. This combination of analog and digital filtering provides a very accurate representation of the signal. Usually, the built-in anti-aliasing filters automatically adjust themselves.

If several channels are available in the same digitizer, a signal recorded with one channel may be seen in another channel: this phenomenon is referred to as cross talk. The specification is given in dB and means how much lower the level is in the neighbouring channels. A good 24-bit digitizer has 120 dB of damping or better. Cheaper multichannel digitizers, instead, usually use a single ADC and an analog multiplexer, which connects different inputs sequentially to the ADC input. This limits the cross talk separation since analog multiplexers have limited performance. For high resolution digitizers, one digitizer per channel is therefore preferred.

Non-linearity is related to how two different signals at the input are intermodulated (so that the amplitude of a signal depends on the other) at

the output and it is expressed as a certain percentage of the full scale. This is usually not a problem with modern sigma-delta converters.

The offset is basically the DC level of the output when the input is zero. Some offset is always present, due to the ADC or to the connected devices, and it can be usually minimized. It is worth noticing, however, that any offset limits the dynamic range, since the ADC will reach its maximum value (positive or negative) for smaller input values than its nominal full-scale.

### **3.3 DATA PROCESSING SOFTWARE AND PROGRAMMABLE HARDWARE: CUSTOMIZED SOLUTIONS FOR OMA**

Several industrial softwares are currently available to carry out operational modal analysis according to a number of different methods. However, in order to build an own measurement and data processing system, a solution could be the adoption of appropriate data acquisition boards which can be controlled by LabView ([www.ni.com/labview](http://www.ni.com/labview)).

LabVIEW programs are called Virtual Instruments, or VIs, because their appearance and operation imitate physical instruments, such as oscilloscopes and multimeters. LabVIEW contains a comprehensive set of tools for acquiring, analyzing, displaying, and storing data, as well as tools for code troubleshooting (National Instruments 2005).

### 3.3 DATA PROCESSING SOFTWARE AND...

---

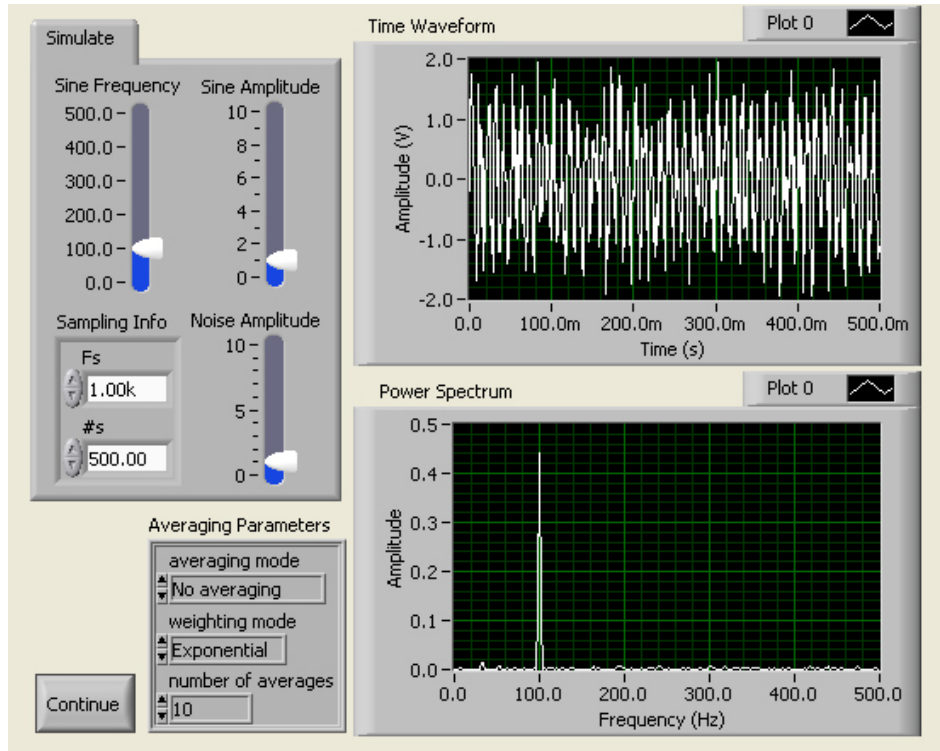


**Figure 3.3.** LabView Front Panel

In LabVIEW it is required to build a user interface, or Front Panel (Figure 3.3), with controls and indicators, which are the interactive input and output terminals of the VI, respectively. Controls are knobs, push buttons, dials, and other input mechanisms. Controls simulate instrument input mechanisms and supply data to the Block Diagram of the VI. Indicators are graphs, LEDs, and other output displays. Indicators simulate instrument output mechanisms and display data the Block Diagram acquires or generates. Types of controls and indicators include:

### 3. THE MEASUREMENT CHAIN

- numeric controls and indicators, such as slides and knobs, graphs, charts;
- Boolean controls and indicators, such as buttons and switches;
- strings, paths, arrays, clusters, listboxes, tree controls, tables, ring controls, enumerated type controls, containers, and so on.

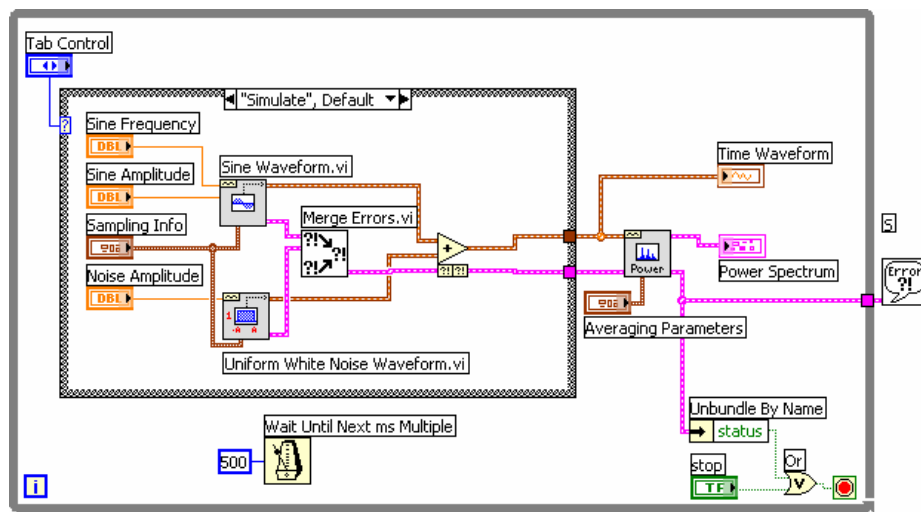


**Figure 3.4.** LabView Block Diagram

Associated to the interface, the user adds related code using VIs and structures to get the control of the front panel objects. The Block Diagram (Figure 3.4) contains this code. Objects on the Block Diagram include terminals and nodes. Block Diagrams are built by connecting the objects with wires. The colour and symbol of each terminal indicate the data type of the corresponding control or indicator. Constants are terminals that supply given data values to the Block Diagram.

### 3.3 DATA PROCESSING SOFTWARE AND...

---

LabVIEW can be used also to communicate with hardware such as data acquisition, vision, and motion control devices, as well as GPIB, PXI, VXI, RS232, and RS485 equipments. It can be both National Instruments and third part hardware. Hardware configuration is carried out through the Measurement and Automation eXplorer (MAX): here it is possible to test the hardware and configure it (Figure 3.5), before managing it through LabView.

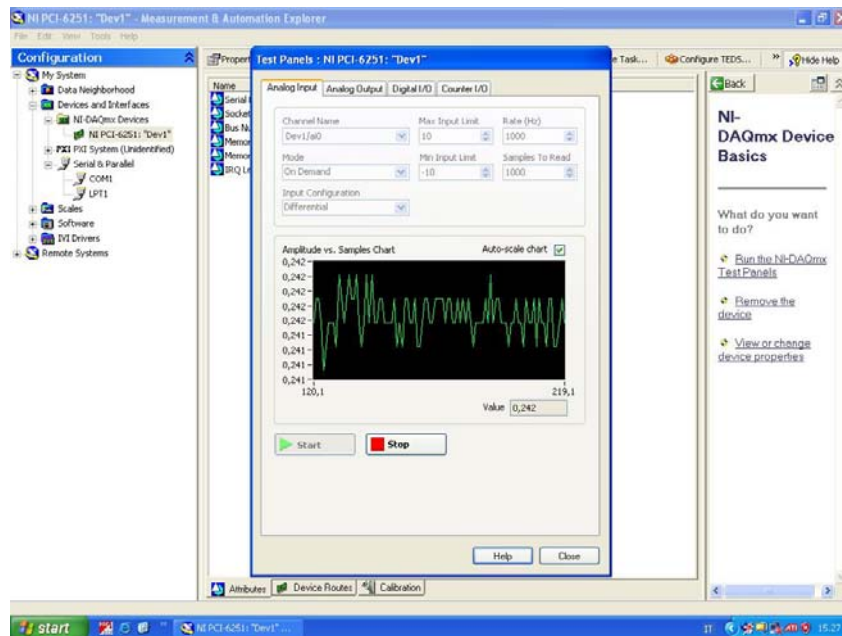


**Figure 3.5.** The Measurement and Automation eXplorer

LabVIEW adopts a dataflow model for running VIs. A Block Diagram node executes when it receives all required inputs. When a node executes, it produces output data and passes the data to the next node in the

dataflow path. The movement of data through the nodes determines the execution order of VIs and functions on the Block Diagram.

Visual Basic, C++, JAVA, and most other text-based programming languages follow a control flow model of program execution. In control flow, the sequential order of program elements determines the execution order of a program.

In LabVIEW, the flow of data, rather than the sequential order of commands, determines the execution order of block diagram elements. Therefore, it is possible to create Block Diagrams that have simultaneous operations.

Dataflow execution makes memory management easier than the control flow model of execution. In LabVIEW, the user typically does not allocate memory for variables or assign values to them. Instead, a Block Diagram with wires, that represent the transition of data, is created. VIs and functions that generate data automatically allocate the memory for that data. When the VI or function no longer uses the data, LabVIEW deallocates the associated memory. When new data are added to an array or a string, LabVIEW allocates sufficient additional memory to manage the new data.

Several tools for implementation of OMA methods are already available: for example, the Basic Frequency Domain method can be quickly implemented in LabView environment by mean of the available tools for spectral analysis. Also parametric identification techniques are already available in some tools; they are:

### 3.3 DATA PROCESSING SOFTWARE AND...

---

- Polynomial models: autoregressive, moving average, and autoregressive moving average models, together with a set of model-selection criteria to estimate the model order (Akaike's Information Criterion, Bayesian Information Criterion, Final Prediction Error Criterion, Minimal Description Length Criterion, Phi Criterion);
- Modal parametric models: basically the LSCE method;
- Stochastic state-space models.

Moreover, it is possible to implement any other algorithm thanks to a large family of VIs which allows computations in the fields of linear algebra (Singular Value Decomposition, QR Decomposition, DOT product, and so on), probability and statistics, fitting, signal processing (FFT, Filters, Windows), Time-Frequency Analysis and Wavelet Analysis.

In the following section the main aspects related to the implementation of an integrated hardware/software system for OMA are reviewed.

## 3.4 AN INTEGRATED OMA SYSTEM

### 3.4.1. Hardware selection

Programmable hardware can be a valuable low-cost solution for data acquisition in the field of Operational Modal Analysis. Since it seems to be useful for a deeper understanding of the basic concepts about hardware device choice previously outlined, development of an integrated system to carry out output-only modal tests is described.

### 3. THE MEASUREMENT CHAIN

---

A data acquisition system can be easily developed starting from a National Instruments Compact DAQ device managed by a data acquisition software implemented in LabView environment. In the present case, the system developed for acquisition of acceleration data through the NI9233 modules, gathered into a CDAQ chassis and linked via USB to a PC, is described. The obtained system is characterized by a 24-bit ADC of the sigma-delta type (with analog prefiltering). The internal master timebase  $f_M$  is 12.8 MHz while the data rate for sampling is in the range 2-50 kHz. The available data rates can be obtained by the following equations:

$$f_s = \frac{f_M/256}{n}, n = 2, \dots, 25 \text{ per } f_s \leq 25.65 \text{ kHz} \quad (3.1)$$

$$f_s = \frac{f_M/128}{n}, n = 2, 3 \text{ per } f_s > 25.65 \text{ kHz}$$

which has been implemented into the data acquisition software used to manage the recorder. The input coupling is AC and the AC cut-off frequency is 0.5 Hz at -3dB: as a consequence, this recorder is not suitable for very flexible structures, even if the adopted sensors have a suitable frequency range, in particular in terms of its lower bound. By the way, it can be used for a number of applications with confidence by taking into account this limitation. For flexible structures, a different solution, in terms of commercial or programmable hardware, must be adopted.



### 3.4 AN INTEGRATED OMA SYSTEM

---

The system can be used with IEPE accelerometers and provides an excitation current which must be compared with the range allowed by the sensors. Either ground-referenced or floating sensors can be used, since the system is based on a pseudodifferential configuration. The input range is  $\pm 5$  V and the incoming signal must comply with this range: sensor specifications must be, therefore, read carefully, also because the full scale voltage of the sensor and its bias voltage, together with the common mode voltage, must comply with an allowable voltage range defined in the specifications of the input module. CMRR is 56 dB (typical) while crosstalk value is -100 dB. The built-in antialiasing filters automatically adjust themselves according to the specified data rate. Good accuracy is also provided, and an offset error of a few mV. Also the dynamic range is quite good (102 dB).

The link between (floating) accelerometers and recorder has been made through a RG-58/U low impedance coaxial cable, to achieve the best accuracy.

If the above mentioned characteristics of the data acquisition hardware are compared with the best ones outlined in section 3.2.3, it is clear that a good compromise between hardware cost and quality has been obtained. However, a data acquisition software has to be developed, too, in order to manage the hardware.

#### **3.4.2. Software implementation: conceiving and organization**

A software for output-only modal parameter identification has been originally designed and implemented in the framework of the activities related to design and installation of the Structural Health Monitoring system of the School of Engineering Main Building at University of Naples (Rainieri et al. 2008a). Then, it has been slightly modified in order to get a versatile integrated instrument for data acquisition, pre-treatment and processing. It includes also some instruments for correlation of results of experimental tests with those ones of numerical modelling of structures, which are useful for model updating applications. The final result is a software able to get data from different sources, such as data acquisition hardware, databases or text files, and, for this reason, it can be employed in a lot of different applications. In particular, thanks to the possibility to get data from a remote database, it is fully integrated in the Structural Health Monitoring system of the School of Engineering Main Building at University of Naples. It is a useful field instrument, not only because of the opportunity to get data from a data acquisition hardware, but also because of the use of EFDD as data processing procedure, which allows a fast on-site processing of data and a first validation of measurements. By saving the raw data, it is possible to process them at another time with different methods, such as Cov-SSI and DD-SSI.

Finally, thanks to the possibility to read text files, the software is able to process data acquired by other people or by other data acquisition devices, if the text file is properly formatted. Therefore, a versatile software,

### 3.4 AN INTEGRATED OMA SYSTEM

---

characterized by an interactive user-friendly interface and employable for different applications, has been developed and is herein described.

#### 3.4.3. Data acquisition

During its implementation, the software has been organized into three main modules: data acquisition, data pre-treatment, and data processing.

About the first module, it is possible to get data from different sources, such as data acquisition hardware, databases or text files: as a result, a software employable in a lot of different applications has been designed and built.

The data acquisition phase is managed by a VI which allows the data source selection: employing “radio buttons” and a “case structure”, selection among the different data sources is operated and the VI corresponding to the selected source is opened.

About data acquisition from an appropriately formatted text file, the corresponding VI allows the selection of the path where the file is located and loads it; these data are then passed to the pre-treatment and data processing modules. By using a “While loop”, the user interface is easily managed.

When the data source is a remote MySQL database, like in the case of the School of Engineering Main Building Structural Health Monitoring system, communication with database is carried out by mean of the ActiveX technology. Thus, in the Block Diagram a specific library is used

### 3. THE MEASUREMENT CHAIN

in order to call the ActiveX Data Objects needed to communicate with the database: in particular, the “ADODB.Connection” library is called, in order to create a link with the ADO objects. Then, by working with methods, it is possible to interact with the database and execute queries. The “Open” method starts communication with database on the base of the specified DSN of the database, and of the UserID and Password to access it. The “Execute” method is used to send a query. The “GetString” method, applied to the recordset returned by the “Execute” method, gives the result of the query in the form of a string (Figure 3.6).

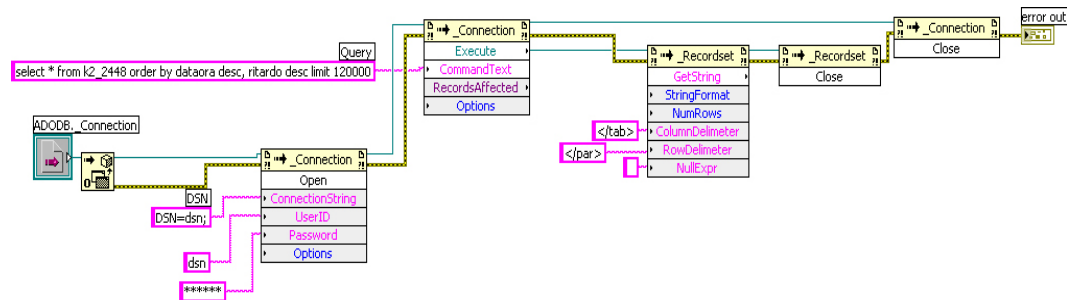


**Figure 3.6.** Connection to MySQL Database

Finally, the obtained acceleration data are converted into double precision numbers and formatted into a matrix form. Data are then passed to the data pre-treatment and processing modules.

When carrying out field measurements, it is sometimes important to evaluate the quality of recorded data and carry out a quick processing: thus, a data acquisition module, able to manage the measurement hardware described in section 3.4.1, and to store data during field tests, has been developed.

### 3.4 AN INTEGRATED OMA SYSTEM

In Figure 3.7 the user interface of the data acquisition management software is shown: when the “Start acquisition” button is pressed, communication with measurement hardware is started. The two charts on the left show the recorded accelerations for the couple of channels selected by using the controls on the right. The two indicators near the charts show the percentage of full scale range which is used during the acquisition process: if the acceleration value is higher than 90% of the full scale range, the indicator turns its colour from blue to red. Therefore, the user can have a first control on data before the pre-treatment phase and decide if a repetition of measurement is necessary.

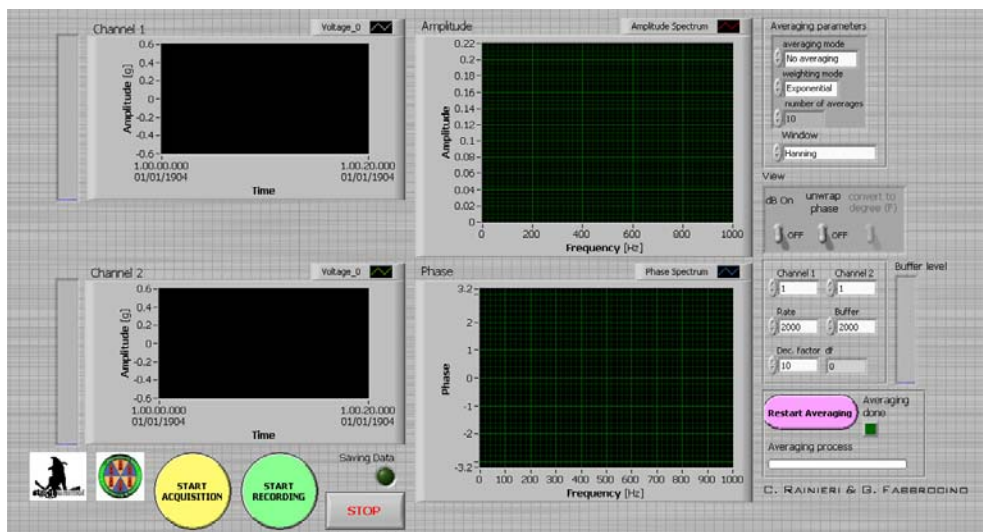


**Figure 3.7.** Data acquisition software

On the right there are the plots of the amplitude and phase spectrum for the selected couple of channels. By using the controls near the plots, a selection of the averaging mode and parameters and of the window to be

used in spectrum computation. Controls in “View”, instead, operate on visualization mode: for example, it is possible to convert the amplitude spectrum in dB scale. The “Averaging process” indicator shows the progress of the averaging process; when it ends, the “Averaging done” indicator turns on and the spectrum computation process stops. In order to restart it, the “Restart averaging” button has to be pressed: a new spectrum for the same couple of channels will be computed with the new data currently incoming from the measurement hardware. If one of the selected channels is changed, the averaging process restarts automatically. The “Rate” control allows the selection of the sampling frequency according to equations (3.1), while the “Buffer” control is used to set the buffer size; moreover, since the allowable sampling rate is usually set much larger than the desired frequency range, it is possible to further filter the data and set a decimation factor through the appropriate control. The frequency resolution of the computed spectra is given by the “ $\Delta f$ ” indicator. The “Buffer level” indicator shows how many samples are in the buffer waiting to be read: its colour turns from blue to red if more than 80% of the buffer size is filled by data. If the buffer size is set too low, the buffer becomes fully filled and the VI stops.

After having verified that all sensors are properly working and that meaningful spectra can be obtained, it is possible to store data into one or several files by pressing the “Start recording” button: during recording, the “Saving data” indicator turns on.

### 3.4 AN INTEGRATED OMA SYSTEM

---

This VI is based on a Producer/Consumer architecture. The Producer loop is used to initialize controls and indicators and to manage data acquisition from the measurement hardware. Data are then passed to the Consumer loop by creating an appropriate queue: data are enqueued in the Producer loop when the “Start Acquisition” button is pressed and are dequeued in the Consumer loop. If an error occurs, the VI is stopped. If no errors occur, data are shown in the charts and used to compute spectra; moreover, if the “Start recording” button is pressed, the “Rate”, “Buffer” and “Dec. factor” controls are disabled and greyed before the writing process starts.

#### 3.4.4. Data pre-treatment

A specific module for data pre-treatment has been developed, too: it is characterized by a state machine architecture which allows to pass from one state to the other. The software consists of a main VI, called “Data pre-treatment”, and four main subVIs.

In the first state, the “Remove mean” VI is loaded: since the DC component of the signal has no physical meaning in civil engineering applications (accelerometers are mounted on structures characterized by a null net acceleration, so the DC component of the signal is only due to sensor circuitry), it has to be removed. The VI shows the acceleration record before and after mean removal for each measurement channel and the offset value in a “mean” indicator.

The next step is trend removal: spurious trends may arise due to environmental (usually temperature) induced drifts in analog data acquisition instrumentation. Trends can be removed by computing first a fit to the record and then subtracting it from the same record. However, the higher the order of the fit, the higher is the probability of removing actual low frequency informations in the data (Bendat & Piersol 1986). The polynomial order (maximum 3) is user-selectable.

In the next state the probability density plots of the channels are shown in order to verify that data are approximately normally distributed and that measurements can be used for modal analysis because no anomalies are present (in Bendat & Piersol 1986 possible measurement anomalies are described together with their effect in terms of statistical distribution of recorded data). As an indicator of the probability distribution of data, also the Kurtosis index is computed: a value of 3 denotes a Gaussian distribution. Anyway, the probability density plot is computed and compared with a pure Gaussian distribution in order to validate data or recognize anomalies, such as signal clipping, intermittent noise, power line pickup, signal drop-outs. If a measurement channel cannot be used for processing, it can be removed from the dataset.

The last state is based on computation of the Short Time Fourier Transform (STFT) of each channel, since it can be useful to detect eventual non-linearities and, above all, spurious harmonic components, as reported in (Jacobsen et al. 2007).



### 3.4 AN INTEGRATED OMA SYSTEM

---

Pre-treated data are now ready to be processed according to the EFDD method or to SSI algorithms.

#### 3.4.5. Data processing

The data processing modules are able to carry out output-only modal analysis according to the BFD, EFDD, Cov-SSI and DD-SSI algorithms, as described in Chapter 1; some tools for validation of results and correlation with those ones deriving from finite element models of structures have been also implemented. Their structure is summarized by the flowcharts reported in Figure 3.8 and Figure 3.9. The flowchart for BFD is not explicitly reported, since it corresponds to the first three steps of the EFDD scheme.

As shown by the corresponding flowchart, implementation of the EFDD algorithm is based on seven main subVIs, each one corresponding to a specific action.

In the data loading step, it is possible to define some analysis parameters such as the amount of overlapping, the type of averaging and the type of window to be used in spectrum computation: a decimation factor can be eventually set. A further inspection to response time series is possible in the next step. Then, auto and cross-power spectra, in terms of amplitude and phase, and coherence functions for couples of channels, are computed and shown in different plots. A cursor allows the selection of a peak on the amplitude plot of the spectrum: two indicators near the amplitude plot

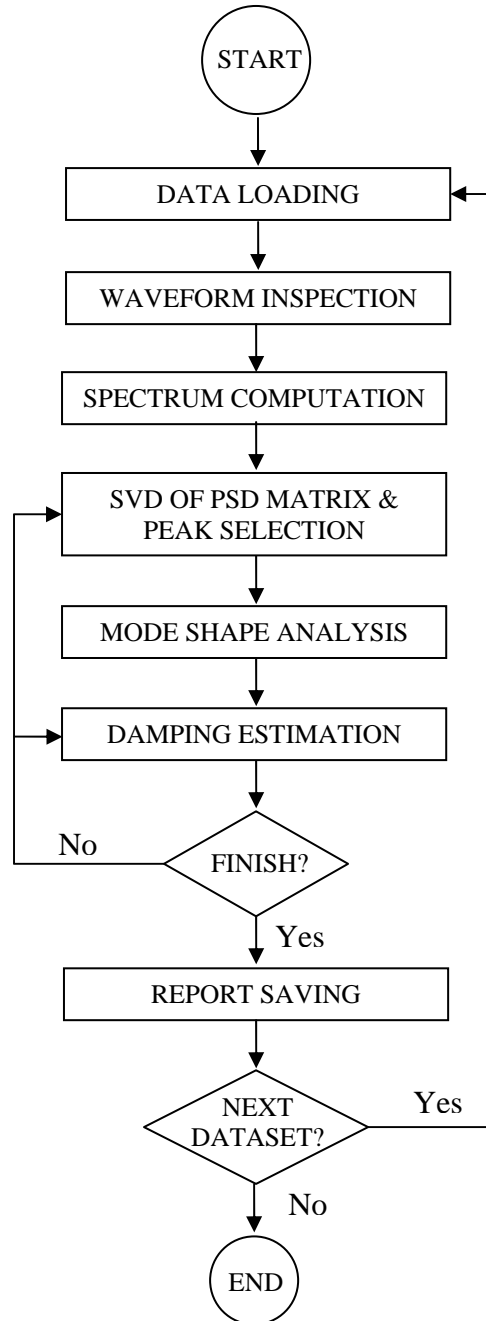


**Figure 3.8.** EFDD flowchart

### 3.4 AN INTEGRATED OMA SYSTEM

---

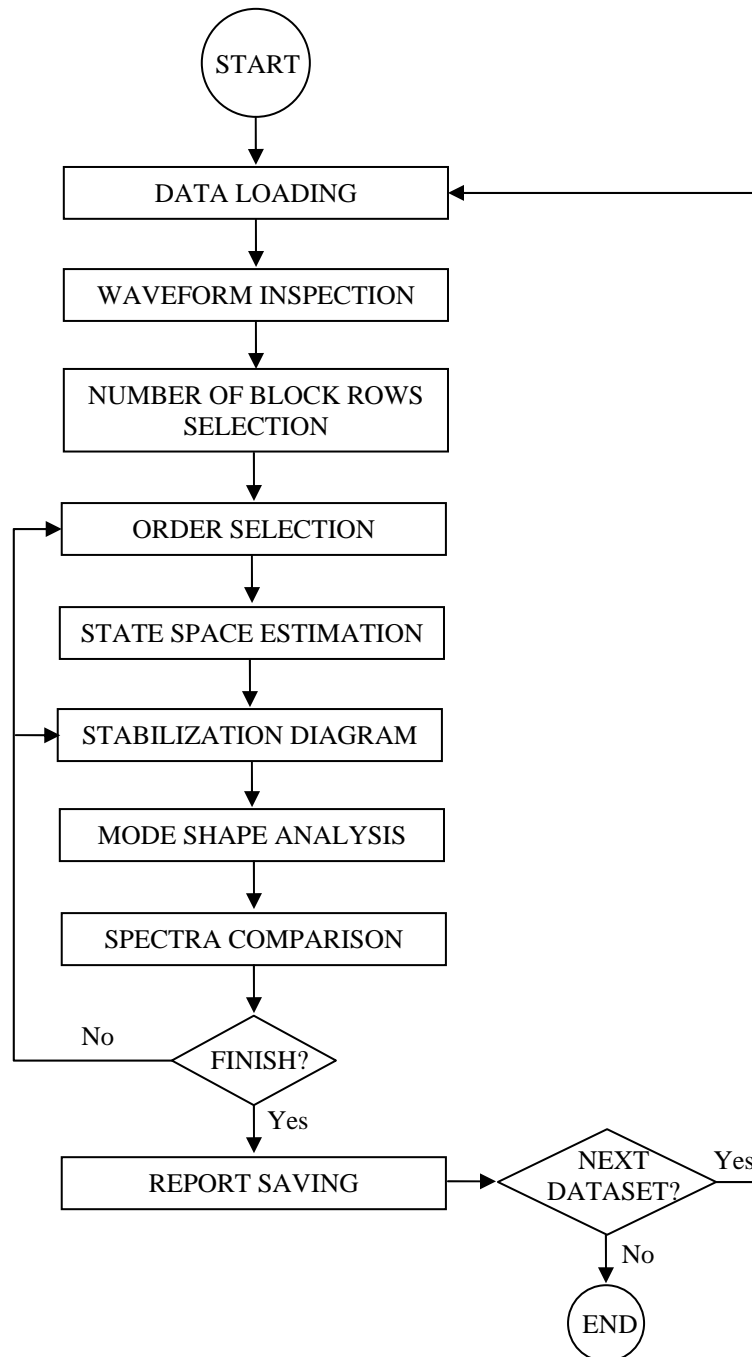


**Figure 3.9.** SSI flowchart

### 3. THE MEASUREMENT CHAIN

show the corresponding values of amplitude and frequency. The cursors in the phase plot and in the coherence plot are automatically placed at the same frequency line as in the amplitude plot: in this way, the values of phase and coherence corresponding to the selected peak in the amplitude plot can be read in the indicators near the corresponding plots. The Power Spectral Density matrix, which is an output of this subVI, can be saved on a spreadsheet .txt file and opened, for example, by Microsoft® Excel.

The SVD of the PSD matrix is computed in the next step and the singular value plots are shown. It is possible to select the peaks on the singular value plots through cursors which can be added or removed depending on the specific needs (Figure 3.10). This result can be easily obtained by working on the properties of graphs.

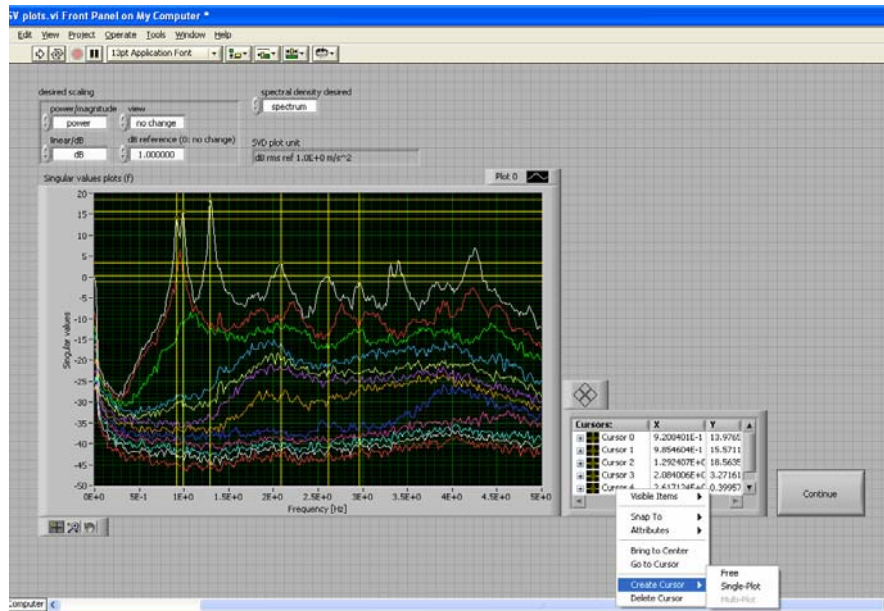


Figure 3.10. "Peak selection" subVI

### 3.4 AN INTEGRATED OMA SYSTEM

---

The obtained results in terms of mode shapes are shown in the next step together with 3D plots of MAC (Allemang & Brown 1982) and AutoMAC matrices and complexity plots. If numerical mode shapes are provided, the Normalized Modal Difference (Maia et al. 1997, Waters 1995) can be computed, too. Damping estimation is then carried out by defining the SDOF Bell function according to the user defined value of the MAC Rejection Level. The resulting SDOF Bell function and its Inverse FFT are shown in two separate graphs. Damping is computed by carrying out a linear regression in a semi-logarithmic plane of the extreme values of the inverse FFT of the SDOF Bell function. In the same graph, all extreme values are shown together with the regression line. The residue is used as an indicator of the quality of regression. The user can select the points to be used for damping evaluation, which is then carried out according to the classic logarithmic decrement method. Computation of natural frequency is carried out in a similar way but considering the zero-crossing of the Inverse FFT of the SDOF Bell function. After having estimated damping ratio and natural frequency for a certain mode, the user can save the results and continue with another mode. Finally, the results of identification in terms of natural frequencies, damping ratios and mode shapes can be visualized and saved in a report in the form of a .txt file.

The implementation of the SSI algorithms is, instead, based on nine main subVIs, each one corresponding to a specific action. In the data loading step, a decimation factor can be set; for the DD-SSI algorithm, it is possible to define also the way of computing the state matrix. A further inspection

to response time series is possible in the next step. Then, the user sets the number of block rows to be used for construction of the Hankel matrix, in the case of DD-SSI, or of the Toeplitz matrix, in the case of Cov-SSI. By inspecting the plot of the normalized singular values obtained from SVD of the Projection matrix, in the case of DD-SSI, or of Toeplitz matrix, in Cov-SSI, the user can set the maximum order of the model. Then the state space matrix and the output matrix are estimated, together with the modal parameters for different model orders: the results are used to construct the stabilization diagram. Here, it is possible to select the poles and, therefore, the corresponding modal parameters directly on the diagram. The obtained mode shapes can be inspected in the next step; complexity plots are also shown, together with 3D plots of the MAC and AutoMAC matrices. The quality of the estimated model can be assessed by looking at the comparison of the trace of the synthesized spectral matrix with the trace of the spectral matrix computed by applying the Welch's method to the recorded data. The estimated modal parameters can be, finally, saved into a report in the form of a .txt file.

#### **3.4.6. Software validation**

Before using field records, the software has been validated using simulated data obtained from numerical models: SAP2000® (Computers and Structures 2006) has been used as FEM software. A simple numerical model has been built and an artificially generated Gaussian white noise

### 3.4 AN INTEGRATED OMA SYSTEM

---

has been used as base excitation; the accelerations at some nodes, obtained from a linear modal time history analysis according to the method of mode superposition, have been used for the identification. No additional noise to simulate measurement noise has been considered at this stage. The FE model is a shear-type 15-stories 1-bay r.c. frame, characterized by well-separated modes and a constant value of damping ratio equal to 0.05. The case study is very simple but it has been useful for a first level of validation of the results of the software. Modal parameter identification has been carried out by considering acceleration records from only five nodes and, in the case of EFDD, by using the Hanning window in spectrum computation, with a 66% overlap. The total length of the simulated records was 600 sec, with a sampling frequency of 100 Hz. In Table 3.1, Table 3.2 and Table 3.3 comparisons between natural frequencies obtained from numerical analysis and those ones obtained from the simulated identification process is reported for the different methods; since very good results have been obtained, also in terms of mode shape estimation, the software has been then used to analyze actual records, as it will be described in Chapter 5.

Mode number	FE model frequency [Hz]	EFDD frequency [Hz]	Scatter [%]	Damping ratio [%]
1	1.07	1.08	0.9	5.02
2	3.21	3.17	-1.2	5.29
3	5.30	5.30	/	4.82

**Table 3.1.** Simulated identification (EFDD)

---

Mode number	FE model frequency [Hz]	Cov-SSI frequency [Hz]	Scatter [%]	Damping ratio [%]
1	1.07	1.08	0.9	5.01
2	3.21	3.18	-0.9	4.99
3	5.30	5.29	-0.2	5.1

**Table 3.2.** Simulated identification (Cov-SSI)

Mode number	FE model frequency [Hz]	DD-SSI frequency [Hz]	Scatter [%]	Damping ratio [%]
1	1.07	1.08	0.9	5.01
2	3.21	3.17	-1.2	5.03
3	5.30	5.31	0.2	5.03

**Table 3.3.** Simulated identification (DD-SSI)

### 3.5 REMARKS

Noisy measurements are a problem often encountered in Operational Modal Analysis. Since there is no substitute for high quality data and OMA procedures can recover informations only if the signal is not just noise, the main issues related to the measurement chain have been reviewed. Sensor and data acquisition hardware characteristics have been extensively described since a good measurement process starts from a proper selection of test equipment. An appropriate measurement scheme can reduce noise problems. There is not a unique choice for test equipment: it depends on several factors, including the available budget. However, advantages and limitations of the different measurement schemes must be taken into account in order to assess their applicability.



### 3.5 REMARKS

---

Finally, it is important to follow some rules of thumb during tests in order to minimize noise effects induced by the environment.

If a good measurement process has been carried out and high quality data have been obtained, a reliable identification process is possible.

Implementation of an integrated system for Operational Modal Analysis has been described: it consists of a data acquisition, a data pre-treatment and a data processing module.

Data pre-treatment is important in off-line analyses in order to remove spurious trends and to verify data quality.

The data processing module has been implemented so that output-only data can be processed according to different methods (BFD, EFDD, Cov-SSI, DD-SSI): validation of the software against simulated data has been described at the end of this chapter.

---

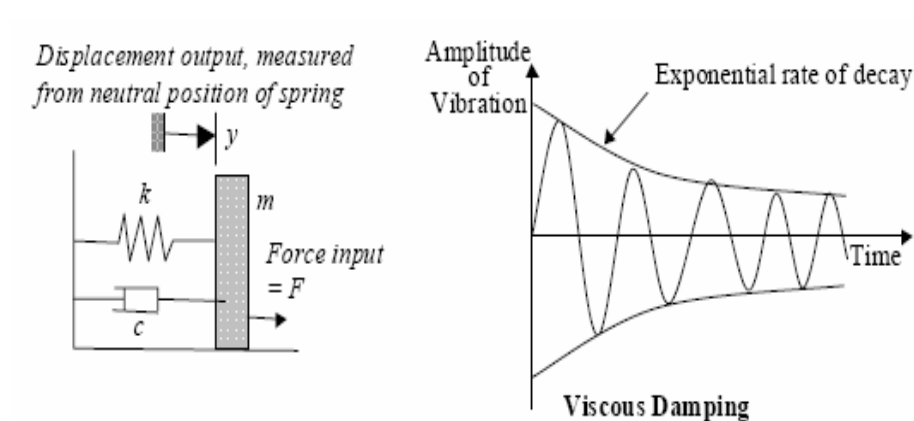
# 4

## Damping

---

*«All structures exhibit vibration damping, but despite a large literature on the subject, damping remains one of the least well-understood aspects of general vibration analysis. The major reason for this is the absence of a universal mathematical model to represent damping forces»*

*Jim Woodhouse*





## CHAPTER 4

### 4.1 INTRODUCTION

The fundamental law of motion, which governs structural dynamics, has been deeply investigated by many researchers, in particular to take into account the effect of damping on the dynamic behaviour of structures. Nevertheless, in despite of the large amount of literature available on this subject, damping is one of the least understood aspects of general vibration analysis. The main reason is the absence of a universal mathematical model to represent damping forces (Woodhouse 1998). However, damping strongly influences the structural response under dynamic loads: this circumstance affects both the ultimate limit state and the serviceability limit state of the structure itself. Wind forces and seismic excitation are fundamental aspects of structural design. In case of tall buildings, for example, wind-induced accelerations are of primary importance for occupant comfort concerns and they can be reduced by an increase in structural damping: thus, since vibration levels in serviceability conditions are to be taken into account for an effective design, an increasing attention has been recently focused on damping evaluation for

#### 4.1 INTRODUCTION

---

the purpose of designing vibration control devices. On the other hand, since dynamic displacements, strains and stresses in a structure subjected to seismic excitation are strongly influenced by damping, an accurate estimation of damping ratios is crucial also for a proper design of structures with respect to their ultimate limit state.

Although natural frequencies and mode shapes can be measured accurately with little difficulty by mean of dynamic tests, damping estimation still shows problems, and error bound in the experimental values can be large. On the other hand, mathematical models may predict natural frequencies and mode shapes of a structure: damping values, instead, cannot be predicted in an analytical way; damping values adopted for dynamic analyses are basically empirical values, based on experimental estimates of damping obtained from similar structures. However, it is worth noticing how structures are often only superficially similar, since they could be affected by substantial differences, for example, in arrangement, dimensions and use of materials.

When dynamic analyses are carried out, the response of the structure is obtained as the superposition of responses of independent viscously damped SDOF systems: in such a case, response amplitudes are inversely proportional to damping coefficients. Thus, the use of low damping values is conservative but it can result in an overdesigned structure. On the other hand, if the damping value used for the analyses is too much high, actual stresses in the structure subjected to dynamic loads are underestimated. It is, therefore, of primary importance the availability of a reliable prior

estimate of the damping capacity of a structure, in order to achieve both a safe and economical design of the structure itself.

This target can be accomplished by creating a large database of experimentally obtained damping values, so that correlations can be found allowing estimation of damping values for different structural typologies according to an empirical base. It is, therefore, necessary to define homogeneous classes of structures and the corresponding expected values for damping; obviously, it is important to have as low as possible error bounds. The main contribution in this sense given by the present thesis is related to the definition of possible criteria for a reliable damping estimation, within the limitations of the estimators, by reducing the scatter due to improper data processing; moreover, a literature review has been carried out in order to define typical values of damping for different typologies of structures. It is worth emphasizing since now that collected data are not enough to define any correlation, not only because of their quantity: damping mechanisms in structures are very complex, depending on several factors, but informations about these factors are rarely reported in the literature.

### 4.2 DAMPING MECHANISMS

Several damping mechanisms can be found on a certain structure. They can be generally classified as (Lagomarsino 1993):

- Damping intrinsic to the structural material;

## 4.2 DAMPING MECHANISMS

---

- Damping due to friction in the structural joints and between structural and non-structural elements;
- Energy dissipated in the foundation soil;
- Aerodynamical damping;
- Damping introduced by passive and active dissipation systems.

The function of damping is to dissipate energy and limit the magnitude of forced vibrations in a structure: in this sense, the specific damping capacity of a structure can be defined as the percentage of the total energy of vibration lost in a cycle.

Structural damping is usually mathematically modelled as one or as a combination of the following types of damping: viscous damping, hysteretic damping, friction (or Coulomb) damping, aerodynamic (or atmospheric) damping.

Viscous damping is assumed to be proportional to the velocity of the oscillatory motion: in such a case, the vibratory motion of the SDOF system is described by the following differential equation:

$$m\ddot{x}(t) + c\dot{x}(t) + kx(t) = F(t) \quad (4.1)$$

where  $m$  is the mass,  $c$  the viscous damping and  $k$  the stiffness of the SDOF system;  $F$  is the dynamic force acting on the system;  $\ddot{x}$ ,  $\dot{x}$  and  $x$  denote the system response in terms of acceleration, velocity and displacement, respectively.

When  $c$  is above the critical value  $c_{cr}$ :

$$c_{cr} = 2\sqrt{km} \quad (4.2)$$

the initially disturbed system will not oscillate but will simply return to the equilibrium position. It can be also defined as the smallest amount of damping for which no oscillations occur in the free response (Clough & Penzien 1975). This condition does not usually occur in practice (Fertis 1995).

Actual structures usually show a damping much lower than the critical damping (usually damping is lower than 10 % of critical value): in these cases, the frequency of vibration of a system (its damped frequency) is basically equal to the (undamped) natural frequency (Paz 1997). For an underdamped system, motion is oscillatory and characterized by an amplitude of vibration which decreases exponentially (Figure 4.1).

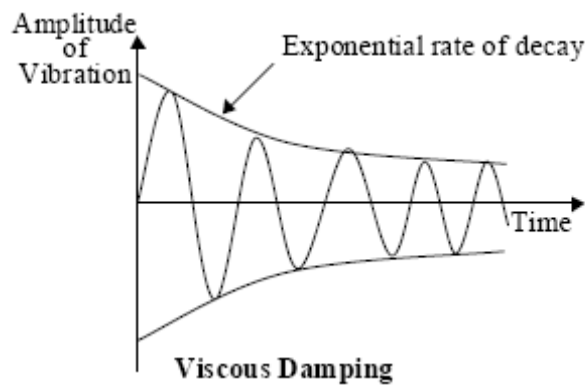


**Figure 4.1.** Decay curve for viscous damping



## 4.2 DAMPING MECHANISMS

---

The hysteretically damped SDOF system is, instead, described by the following differential equation:

$$m\ddot{x}(t) + k(1 + j\eta)x(t) = F(t) \quad (4.3)$$

where  $j = \sqrt{-1}$  and  $\eta$  is the hysteretic damping factor. Hysteresis is basically due to inelastic behaviour: thus an equivalent damping ratio can be obtained from the area inside the hysteresis loop (Figure 4.2); the hysteretic damping is a function of frequency but, unless it is a strong function of frequency, the portion of the response curve around the natural frequency will be similar to that one for viscous damping: this circumstance makes the two types of damping practically indistinguishable.

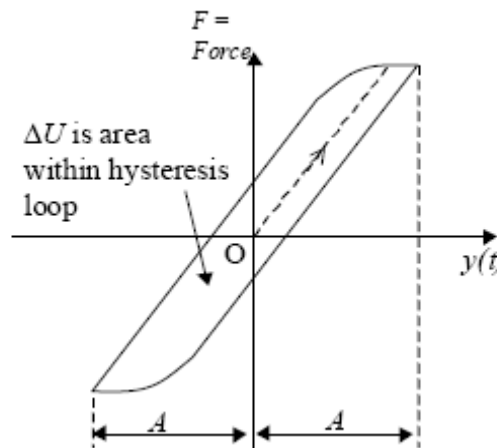


**Figure 4.2.** Hysteresis loop

Tests on hysteretic systems show that there is also a dependence from amplitude, in particular for soils. Material damping is another example of hysteretic damping. For concrete or soils, damping inherent to the material may be relevant (0.05 is the typical value for concrete); for structural metals, instead, the damping capacity is quite small (usually less than 0.005): for metallic structures, therefore, this damping mechanism is almost negligible.

A SDOF system characterized by friction damping is described by the following differential equation:

$$m\ddot{x}(t) + kx(t) + R x(t)/|x(t)| = F(t) \quad (4.4)$$

Friction damping is the result of rubbing and sliding between vibrating dry surfaces. It is proportional to amplitude and changes its sign according to the sign of motion. A freely vibrating system subjected to pure friction damping shows a linearly decaying amplitude (Figure 4.3).

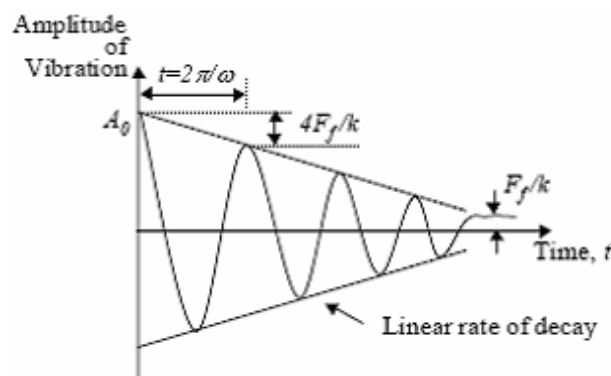


**Figure 4.3.** Decay curve for friction damping

## 4.2 DAMPING MECHANISMS

---

Much of the energy dissipated in vibrating structures is due to friction. However, a structure usually exhibits a combination of hysteretic and friction damping which is usually referred to as structural damping. This kind of combination is pointed out by an initial increase and a subsequent decrease of damping capacity with increasing amplitude of motion (Brownjohn 1988).

Aerodynamic damping arises as a result of the drag and lift forces on an object in air: such forces are proportional to the square of the velocity of the object with respect to the air stream.

In the literature it is possible to find some relationships for prediction of aerodynamic damping (Brownjohn 1988). Even if aerodynamic damping is much lower than other types of damping mechanisms, it gives a relevant contribution to the overall damping for some kinds of structures (tall building or some kinds of bridges).

Actual dynamic systems show, in general, a combination of linear (that is to say, damping independent of amplitude of motion) and non-linear (namely, damping depending on amplitude) damping mechanisms. As a consequence, there is not a single way to describe mathematically all vibrating structures. In engineering practice, due to the difficulty of defining the true damping characteristics of typical structural systems, a viscous damping model is usually used because it leads to linear equations of motion. Even when viscous damping may be not operating, an equivalent viscous damping model is assumed, thus creating a certain amount of confusion because it is usually not specified in the literature

whether pure viscous damping exists or whether equivalent viscous damping has been assumed.

In most design codes, damping is usually assigned based on the construction material. For example, the Italian Seismic Code (Consiglio Superiore dei Lavori Pubblici 2008) gives a spectrum computed for a damping value of 5% and suggests a formulation to modify the spectrum when the actual damping is different from it: however, in the Code there is no mean to define the actual damping value; it is just said that its evaluation has to be based on construction materials, structural typology and type of foundation soil. For wind applications, the ISO Code (ISO 4354:1997) suggests damping ratios of 1% and 1.5% for steel and concrete structures, respectively.

It is worth noticing that damping has been observed to increase with amplitude in full-scale data sets. This circumstance may be explained by taking into account that the equivalent viscous damping model is usually adopted in the equations of motion to represent all the different damping mechanisms. However, this model is non-ideal under a wide range of amplitudes of motion and, if it is assumed, actual structures may exhibit non-linearity, or a damping that changes with amplitude. Thus, a model for total damping with respect to amplitude level of motion (Figure 4.4) has been proposed (see, for example, Jeary 1986): in fact, by assuming that frictional losses give a large contribution to energy dissipation in structures, at low levels of motion, there are no significant slipping phenomena in the structure. Once a sufficient number of interfaces are

## 4.2 DAMPING MECHANISMS

---

activated, they will dissipate energy in proportion to their relative displacements, accounting for the linear increase. At high amplitude levels of motions, all interfaces have been activated and friction forces become constant even for increasing amplitude, thus defining the maximum level of damping that should not be exceeded unless damage occurs within the structure. In fact, in large amplitude regime, damping ratio can increase only if there are additional sources of damping forces: there is the possibility of damage to secondary elements, but a lot of design codes does not allow this kind of damage, at least for certain level of excitations. Thus, in such cases, higher damping ratios cannot be expected for structures vibrating within their elastic limit. If, instead, the amplitude exceeds this limit, the contribution of plastic-hysteretic damping may become predominant.

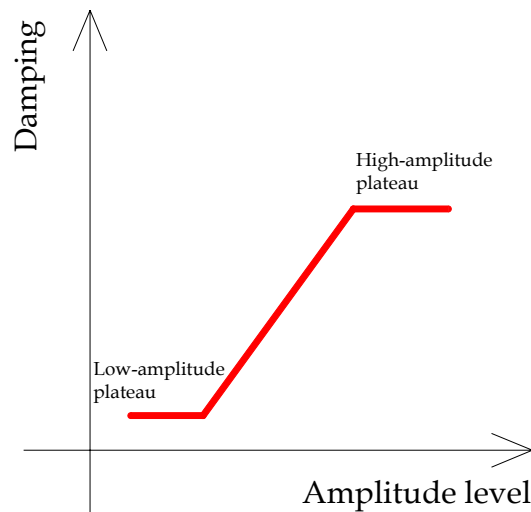


**Figure 4.4.** Model for total damping vs. amplitude level

### 4.3 EXPERIMENTAL DAMPING ESTIMATION

There are several methods allowing damping estimation from measurement of the structural response to forced, transient or ambient excitation. In Ewins (Ewins 1984), several techniques requiring the knowledge of the force input are described. Such techniques are extensively applied in laboratory testing in the field of aerospace and mechanical engineering: the most popular procedures are based on the FRF curve-fit or on the Nyquist diagram circle-fit. These curve fitting methods probably provide the most accurate estimation of damping for a given structure: however, they cannot be easily applied to large civil structures such as tall buildings, bridges or dams, due to the need of artificially induced vibrations large enough to overcome the ambient noise, but not too large, since non-linearities can arise. Other methods described by Ewins and working in time domain are, instead, the Ibrahim Time Domain technique and methods based on auto-regressive models.

When forced or transient vibration tests are used for damping estimation, shakers or instrumented hammers are used in order to excite the structure. Sometimes, snap-back techniques are used, by elastically deforming the structure and suddenly releasing it in order to measure damping from free decay oscillations. However, when the input is applied by a hammer, the transient response is the sum of the response of several modes of vibration; when snap-back techniques are applied, instead, response is mainly due to the mode (usually the fundamental mode of the structure)

#### 4.3 EXPERIMENTAL DAMPING ESTIMATION

---

whose shape best resembles the statically deformed configuration of the structure.

If a shaker is used, a run-down test can be carried out: after having identified a resonant frequency and having reached a steady-state forced vibration, the shaker is switched off and the resulting decaying vibrations are measured. In such a case, damping is obtained by applying the logarithmic decrement method. If, instead, the response spectrum is available, the half-power bandwidth method can be applied, but it requires well-separated modes and it has been proved that it can lead to inaccurate damping estimates, in particular in the case of ambient vibration tests (Brownjohn 1988). Curve fitting techniques seems to be more reliable with respect to the problem of damping estimation, since all available points are used for the fit instead of just three points like in the half power bandwidth method.

The recent improvements in data processing and measurement hardware performance have made forced vibration testing less popular than ambient vibration testing in the case of large civil structures, also because excitation of civil structures at very low frequencies is impractical or impossible with shakers, being the first natural frequencies of such structures well below the operating range of the exciter.

When ambient vibration tests are used for damping estimation, since there is no control over the input force, there is also a lack of knowledge about the spectral distribution of its energy. Thus, the options are to use time domain modelling techniques, or to determine the frequency content of

response data and use frequency domain techniques, such as half-power bandwidth or curve fitting. However, the assumptions about the input in ambient vibration tests are not always satisfied and, in any case, it is impossible to judge their validity: thus, damping estimates are affected by errors not only due to the noise in the signal and, eventually, to the errors caused by windowing in spectral analysis, but also due to the erroneous assumptions about input.

Measurement noise affects the quality of fit in curve fitting procedures and, as a consequence, reliability of damping estimation. The use of the Hanning window in order to reduce leakage effects in spectral analysis of ambient vibration records, instead, yields a bias error with respect to the true damping value. In order to minimize this effect, a fine frequency spacing must be adopted. In order to have a good estimation of the response spectrum a high number of averages is also required (Brincker et al. 2003): it has been shown (Brownjohn 1988) that, by increasing the number of averages, the damping estimates converge to a value depending on the type of curve fit, but if fewer than 10-15 averages are used, the damping estimates are significantly lower than this converged value. Frequency resolution, instead, affects the number of data points used for the fit. Brownjohn (Brownjohn 1988) suggested to use at least 16 points in the fit, based on the results of a number of numerical simulations. As a consequence, a reliable damping estimation in the frequency domain cannot leave out of consideration long records of the structural response, in order to compute spectra characterized by a high



#### 4.3 EXPERIMENTAL DAMPING ESTIMATION

---

number of averages and a fine frequency resolution. A total record length equal to 1000-2000 times the first natural period of the tested structure is usually suggested. In Brincker et al. (Brincker et al. 2003), a simplified formulation to compute the total record length on the base of the expected first natural frequency and damping ratio is proposed: it is defined so that a high number of averages in spectrum estimation is obtained. About the bias error introduced by windowing, Brownjohn (Brownjohn 1988) has proposed a procedure to correct damping estimation, but it requires calibration.

#### 4.4 DAMPING DATABASES AND EMPIRICAL PREDICTIONS

Since a model for structural damping analogous to those ones for mass or stiffness determination cannot be defined, the only alternative is to develop empirical expressions. In order to have reliable prior estimates of damping based on empirical formulations, a very large database of experimental damping values is necessary. However, availability of damping data in the literature is not very large, in comparison with other data such as natural frequencies. Most of the available data are of limited value because variances are not reported or very large and because of the lack of descriptive data about the tested structure in terms, for example, of dimensions, characteristics of soil and foundations, architectural finishing and non-structural members, vibration amplitude. These characteristics,

together with those ones of structural materials, test method and damping evaluation procedure, contribute significantly to the dispersion of damping data. Moreover, it is worth emphasizing how short test times or low quality data can result in large errors in damping estimation and, sometimes, in meaningless results: thus, such data cannot be included into a damping database aiming at the definition of empirical correlations.

Over the years, a number of individuals or research groups have collected estimates of damping from their own tests or from published data. Some of these collections are reported in the papers by Jeary (Jeary 1986) for tall buildings, while Davenport (Davenport 1981) and Eyre & Tilly (Eyre & Tilly 1977) have collected data about bridges. On the base of these data, some empirical expressions for damping estimation have been proposed. For example, Davenport & Hill-Carroll (Davenport & Hill-Carroll 1986) have proposed a simple formulation which correlates damping to the amplitude of vibration and to the building height. A more complex model, taking into account building dimensions and its fundamental frequency, has been proposed by Jeary (Jeary 1986): base dimensions have been considered in this model to take into account the effects of radiation damping in the soil.

When bridges are considered, a strong correlation between the estimated damping and the natural frequency of the lowest vertical and lateral modes has been found for suspension bridges, based on the data acquired by Davenport (Davenport 1981). For cable-stayed bridges, instead, a constant value has been proposed.

#### 4.4 DAMPING DATABASES AND EMPIRICAL PREDICTIONS

---

However, only recently some databases for damping values have been systematically organized: in particular, the Japanese Damping Database collects the dynamic properties of more than 200 steel and reinforced concrete buildings: they are mainly tall buildings (higher than 100 m); an international database featuring the dynamic properties of 185 buildings in Asia, Europe and North America has been also issued by Lagomarsino & Pagnini (Lagomarsino & Pagnini 1995). Such databases include informations about the buildings (location, usage, shape, height, dimensions, number of stories, structural type and foundation characteristics) and about dynamic properties (natural frequencies and damping ratios, together with informations about excitation type, measurement method, data processing procedure and amplitude of vibrations). The main results obtained from processing of informations included in these databases are herein briefly summarized.

Various vibration testing methods have been used to measure the dynamic properties of buildings: they belong to the two classes previously defined according to the nature of excitation (artificial or natural). Almost all data have been obtained from measurements at low vibration amplitude. Both frequency and time domain methods have been used for damping estimation.

A dependency of damping from building height has been observed: in particular, it becomes smaller when the height increases. Moreover, damping ratios much higher for reinforced concrete structures than for steel structures have been found.

An increase of damping with the first natural frequency of the building has been also observed. Such a dependency is larger in the case of pile foundations: thus, radiation damping seems to give a high contribution to the overall damping for buildings supported with a pile foundation. The influence of soil-structure interaction and, therefore, of radiation damping on the overall damping of buildings is witnessed also by the higher scatter in damping values found for low-rise buildings (for which these effects are more important) with respect to high-rise ones.

The effect of non-structural members has been taken into account in an indirect way by mean of the building usage informations: in fact, it has an influence, for example, on the number of partitions. Thus, higher values of damping have been found for hotel and apartments, characterized by several partitions, than for office buildings.

By looking at translational modes of office buildings, it has been found that the damping ratio in the longer direction of such buildings is usually larger than in the shorter direction: this tendency is not clear in the case of buildings characterized by different usage.

A number of empirical expressions have been derived starting from these results: they basically correlate damping with the fundamental natural frequency and the height of the building. However, even if they allows a first evaluation of damping in a structure, the actual level of damping can be quite different because of the influence of other variables such as foundation type, soil conditions, quantity and arrangement of non-structural members. Moreover, due to the considerable scatter in the data,

#### 4.4 DAMPING DATABASES AND EMPIRICAL PREDICTIONS

---

quality of correlations can be improved only by defining a standard and effective procedure for damping estimation.

#### 4.5 DAMPING ESTIMATION BY EFDD AND SSI: MAIN ISSUES

In the framework of ambient vibration tests, EFDD and SSI are techniques widely used for modal parameter estimation. However, in order to obtain a reliable estimation of such parameters and, in particular, of damping ratios, some basic test and data processing rules should be defined.

Being the EFDD method based on computation of spectra from recorded data, long records are needed to keep low the error on spectrum estimation (Bendat & Piersol 1986) and, therefore, to extract modal parameters in a reliable way. As previously mentioned, a high number of averages and a fine frequency resolution are crucial for an effective estimation of damping ratios, apart from the bias introduced by windowing.

The effect of frequency resolution on the estimates of damping, when the EFDD procedure is applied, has been extensively studied by Tamura et al. (Tamura et al. 2005): they have shown that estimated damping ratios for all identified modes decrease when the frequency resolution improves. In particular, they have found that damping estimates converge for a frequency resolution equal to 0.01 Hz or better. Moreover, the bias in damping estimation is kept low by inverse Fourier transforming the

identified SDOF Bell functions and by fitting the data related only to the first few cycles of the obtained correlation functions for the identified modes.

Even if the EFDD technique is, in principle, able to deal with closely spaced modes, damping estimation in such a case seems to be not very reliable. Partial identification of SDOF Bell functions, beating phenomena and errors due to windowing can significantly bias damping estimates.

A more refined estimation of damping in presence of close modes can be obtained by mean of SSI methods. This ability is crucial above all for very flexible structures, characterized low frequencies and damping ratios and by several close modes. SSI methods are used to provide estimates of modal parameters also in presence of limited amounts of data, since no averages are required. However, it is worth noticing that, in principle, an unbiased estimate of modal parameters can be obtained only by mean of infinite records. Nevertheless, reliable estimations of natural frequencies are provided by such methods also in the case of records characterized by limited durations. Even if record length seems to be less critical for this class of methods, longer durations allow a more stable and reliable identification of modal parameters and, in particular, of damping ratios. Pridham & Wilson (Pridham & Wilson 2003) have carried out a numerical study using ERA pointing out that at least 4000 data points are necessary for a reasonable identification of system frequencies lower than 1 Hz and damping ratios lower than 1%.

#### 4.5 DAMPING ESTIMATION BY EFDD AND SSI: MAIN ISSUES

---

When describing practical applications of Operational Modal Analysis in the next chapter, some results of sensitivity analyses of modal parameters to record durations are reported, pointing out the (sometimes relevant) bias introduced by short datasets. Sensitivity analyses have been carried out also in order to investigate the effect of the number of block rows on the estimated modal properties: in fact, the number of block rows, multiplied by the number of measurement channels, defines the maximum model order which can be selected during inspection of singular values of the Hankel or Toeplitz matrix. Even if the product of the number of block rows times the number of measurement channels is large enough to ensure that all modes in a certain frequency range can be identified, sensitivity analyses carried out on actual data point out that estimation of modal parameters and, in particular, of damping improves when the number of block rows increases, converging to a certain value. Also the stabilization diagram becomes clearer. However, if the number of block rows is set too much high, spurious poles appear close to physical ones and they are erroneously identified as stable. Nevertheless, sensitivity analyses, carried out in order to investigate the influence of the number of block rows on the estimates, can help to better define this parameter and to evaluate the level of uncertainty affecting the identified modal properties.

#### 4.6 BUILDING A DATABASE OF MODAL PROPERTIES

During the present research, an extensive literature research has been carried out in order to build a database of natural frequencies and damping ratios for different kinds of structures. The results have been mainly used as references during modal identification tests: it is, in fact, instructive to compare damping estimates from tests with those ones measured on similar structures, so that obvious errors or anomalies can be recognized. Recurrent values for some structural typologies have been, thus, identified: no empirical correlations have been defined, due to the scarcity of available data and the lack of informations about the level of uncertainty affecting the estimates, neither they have been used to verify available correlations. A first look at damping values, reported in Appendix B, however, allows also the identification of anomalous estimates. The database has grown over time, by adding the results of tests carried out during the present research and those ones found in the literature. Damping values, however, are often not reported: thus, construction of a large database results in a very difficult job. When it will be large enough, some acceptance criteria could be defined for homogeneous classes of structure in order to reject anomalous data, which could be due, for example, to poor testing and data processing procedures: in this way it is possible to reduce the influence of such factors on the scatter naturally affecting damping estimates. The resulting cleaned database will be useful to further improve the knowledge about damping mechanisms. Since data are gathered by including informations about



#### 4.6 BUILDING A DATABASE OF MODAL PROPERTIES

---

building location, a database of damping ratios and natural frequencies for Italian structures could be defined in the future: it will be useful to improve design criteria with respect to dynamic excitations.

#### 4.7 REMARKS

The main problems related to damping estimation have been reviewed in this chapter. Damping data are scattered due to a number of different reasons, related, on one hand, to structural and soil characteristics and to the need of defining a unique damping value which takes into account the different damping mechanisms that can arise in a structure, and, on the other hand, to inherent limitations of data processing methods or to errors in testing procedures (low quality data, short records).

Some criteria for a reliable experimental estimation of damping values have been identified, based on simulation results reported in the literature and sensitivity analyses carried out on actual measurements. Definition of testing protocols can reduce the influence of testing procedures on the scatter affecting damping estimates: this circumstance allows to focus attention on the actual sources of uncertainty. A database of modal properties for different kinds of structures has been built over time, pointing out again the variability of damping values and, above all, the difficulty to find them in the literature. Whenever data about damping are provided, they may be inconsistent due to the lack of informations about

the tested structure: thus, a large and consistent database can result only from a longer work and the execution of standardized tests.

#### 4.7 REMARKS

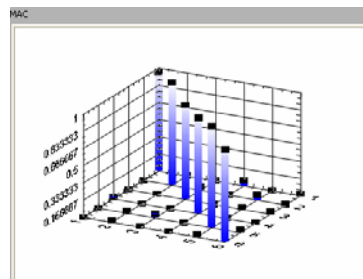
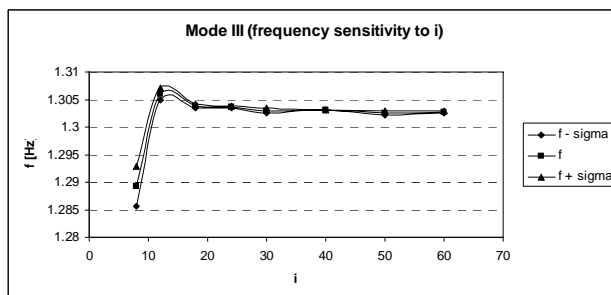
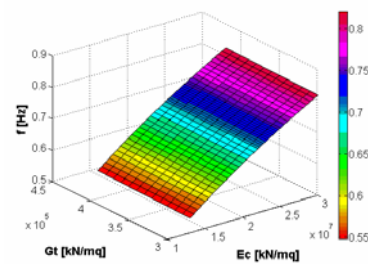
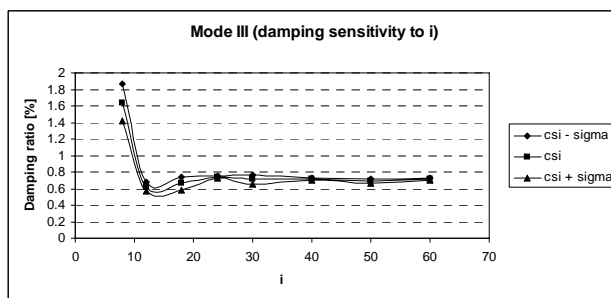
---

# 5

## Applications

«Someone told me that Operating Modal Analysis  
produces better results and that damping  
is much more realistic...»

Pete Avitabile





## CHAPTER 5

### 5.1 INTRODUCTION

Italy is characterized by a very large cultural heritage, spread all over its territory, but it is also affected by a high seismic risk. Thus, effective measures have to be taken in order to protect constructions at risk and to mitigate losses due to seismic events. The need for protection does not affect only ordinary constructions, in view of life safety, but also historical ones, to mitigate loss of unique artefacts.

From the structural engineering perspective, this objective can be reached by increasing the knowledge of structural behaviour, in particular with respect to dynamic loads. However, this is particularly difficult in the case of historical structures, where several uncertainties affect material properties and structural schemes, so that a reliable model cannot be easily identified, or cannot be identified at all.

The theme of assessment and reduction of seismic risk of historical constructions is becoming more and more important in Italy, due to the huge number of potentially vulnerable heritage structures. The effects of recent earthquakes (Umbria-Marche, 1997; Molise, 2002) on a number of

## 5.1 INTRODUCTION

---

historical structures pointed out these issues as crucial and a number of Codes and guidelines have been produced since then.

Increasing attention has been paid in seismic codes towards historical constructions, which have some common characteristics with existing structures but also some peculiar ones: thus, it is not possible to treat them according to the current building practice without a preliminary evaluation of the effects of such approach. In the current National seismic Code (Direttiva P.C.M. 2007, Consiglio Superiore dei Lavori Pubblici 2008) specific recommendations about interventions on heritage constructions are reported.

The guidelines for assessment and reduction of seismic risk of historical structures provide general principles and specific suggestions, depending on the type of construction. As a general rule, interventions must be as limited as possible and they must be based on increasing levels of knowledge. The methodological path is summarized in Figure 5.1. Limited or extensive interventions are possible, but a high level of confidence in the knowledge of structural behaviour is necessary. Therefore, a number of tests and surveys are needed in order to define a representative model of the structural behaviour, or even to demonstrate that a global approach cannot be pursued and simplified assumptions on limited portions of the construction can be used to support decisions on the extension and nature of interventions.

Destructive tests must be limited in number, due to the valuable characteristics of historical constructions. Conversely, non destructive and

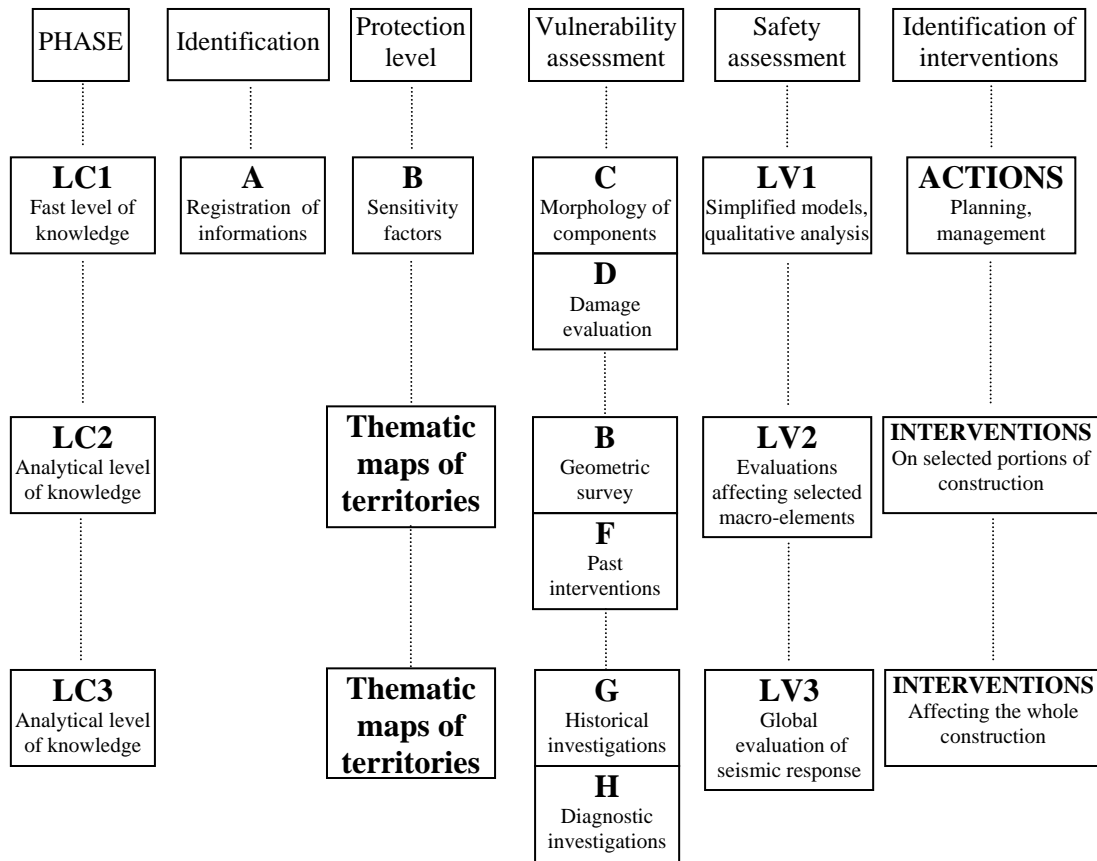


**Figure 5.1.** Methodological path for interventions on historical constructions

non invasive tests are, of course, preferred. Dynamic tests under environmental excitation, in conjunction with model updating techniques, can be considered an effective non-destructive tool for the assessment of the dynamic behaviour of existing and, in particular, historical constructions. Repeated in time tests can be helpful also to evaluate the health state of a structure. Modal-based structural health monitoring is, in fact, becoming a reliable and widely accepted technology for damage



## 5.1 INTRODUCTION

---

detection in structures and for evaluation of seismic performance in the early earthquake aftershock.

Stated that dynamic tests are an effective tool to increase the knowledge about the dynamic behaviour of existing structures, the methodology for test execution is also an issue.

The current Italian Code recognizes the relevance of experimental modal analysis, above all in the case of important structures from the historical or architectural point of view, because of the unique structural techniques which affect a large part of these constructions (Ministero per i Beni e le Attività Culturali 2006). Besides, uncertainties about geometry and materials make accurate structural analyses and assessment of the effective behaviour of structures in operational conditions difficult. Knowledge of modal properties of historical structures is very important, in particular for the evaluation of structural performance in presence of extreme load conditions, such as during an earthquake (Gentile 2005).

The traditional techniques based on the knowledge of the input source are now well-developed, reliable and widely accepted, also due to their extensive application to a large variety of structures in the last thirty years. In recent years, however, increasing attention has been paid to techniques for modal parameter identification based on ambient vibrations which, among the rest, allow the evaluation of dynamic properties of structures in actual service conditions (Cunha & Caetano 2005) without any external excitation. When historical structures are considered, output-only techniques are preferred (Gentile 2005), since artificial excitation often

exhibits problems of test execution and input control while environmental loads are always present. In addition, tests are cheaper and faster with respect to traditional experimental modal analysis and imply a minimum interference with the normal use of the structure (Mohanty 2005). Thus, an increasing number of applications of OMA techniques for modal identification of historical constructions are appearing in the literature (Ramos et al. 2007, Schmidt 2007, Gentile 2005): the identified modal parameters, representative of the structural behaviour in operational conditions, are used to validate or update finite element models, or to detect structural modifications or damage. However, few applications are reported about the possibility to use updated analytical models for an effective evaluation of seismic risk of the considered structure.

In the following sections, a number of ambient vibration tests carried out on different typologies of heritage structures will be described and the main results will be discussed. Most of the datasets obtained from these ambient vibration tests have been also used to test the automated modal parameter identification procedure described in the next chapter.

## 5.2 THE MASONRY STAR VAULT (LECCE)

### 5.2.1 Research background and motivations

Interest in ancient masonry buildings arises from the need of preservation of cultural heritage and of its service utilization, assuring a sufficient level of safety with respect to both vertical loads and earthquake actions

## 5.2 THE MASONRY STAR VAULT (LECCE)

---

(Direttiva P.C.M. 2007, Consiglio Superiore dei Lavori Pubblici 2008). When, in particular, seismic performances are considered, a number of aspects have to be taken into account:

- the presence of degraded materials, with a consequent reduction of local and global stiffness and strength;
- extended and substantial structural alterations, carried out throughout the life of the construction, ignoring their effect on seismic performance;
- historical masonry constructions are built on the basis of local traditions and experience, without taking into account specific rules for earthquakes resistance (Cardoso et al. 2005).

In this case study, attention is focused on a monumental building, representative of historical-cultural heritage of Lecce's "City Centre" in Southern Italy. In a recent work (Aiello et al. 2007) a vulnerability assessment of the whole structure to seismic actions has been carried out.

The incomplete experimental characterization of strength and stiffness parameters of masonry and the complexity of geometrical configuration, with the presence of singular structural elements such as masonry vaults, have suggested a new phase of detailed research work. Thus, an experimental campaign has been started in the framework of the INTERREG M.E.E.T.I.N.G. Project aiming at characterize the structure and its dynamic behaviour through indirect methods. The complex structural configuration, the large variety of materials and the relevant dimensions

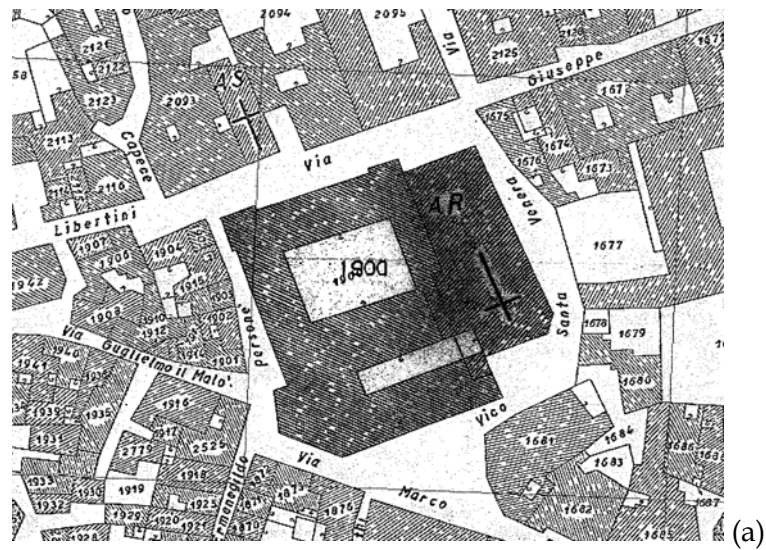


**Figure 5.2.** “Convento dei Carmelitani scalzi”: cadastral view (a); view from Libertini street (b)

## 5.2 THE MASONRY STAR VAULT (LECCE)

---

A short review of the history of the building can give an idea about its high degree of complexity.

The structure, located in the Historical Centre of Lecce, is known as "*Convento dei Carmelitani Scalzi*", since it was built in 1627 as the residence of the religious congregation of the "Teresiani" Fathers. The cadastral view (Figure 5.2a) points out the large extension of the building: it covers, together with the neighbouring Church of St. Teresa, a wide area of 65m x 50m, called the "*Island of St. Venera*" because the monumental block is entirely surrounded by roads. In particular, the main façade of the building is on one of the main streets of the City Centre of Lecce, known as "Libertini" Street (Figure 5.2b).

An historical research (Conte 2006) allowed the identification of the main structural modifications which affected the structure during its life and that can influence its seismic response:

- in 1813, the building was submitted to the City, and converted to a military residence;
- in 1826, minute maintenance works were made in the military residence, affecting only the functionality of the building without producing any modification of the original configuration;
- in 1841-1871, some repair interventions were carried out, with application of tie rods to ensure an effective connection between old and new masonry walls (built in order to separate the

military building from the Church of St. Teresa) and to balance the lateral actions in the vaulted systems.;

- in 1875-1889, the masonry columns of the central cloister underwent some interventions from the static point of view, with the construction of a new foundation and repair of damaged masonry panels located around the cloister. Continuous maintenance works were carried out in order to reinforce the original building structure;
- in 1894-1970, the works for architectural modification and for the new functional organization of the building (started together in the 19th century) were finished: these works caused the loss of the original architectural configuration (external and internal façades);
- in 1970s, the building underwent some other interventions and was converted to school residence;
- in 1994-1997, an experimental campaign was carried out in order to define the static performance of the foundation soil (physical-mechanical properties); restoration and recovery works were also carried out, aiming at preserve the school destination.

The historical research points out that substantial alterations occurred between the 19th and the 20th centuries, when the religious construction became a military residence (known as “*Caserma Cimarrusti*”).

## 5.2 THE MASONRY STAR VAULT (LECCE)

---

From a structural point of view, the structure was built on a “pietra leccese” quarry and it consists of two above-ground floors and some inaccessible underground rooms, discovered during a recent geological survey. In particular, the ground floor and the first floor are organized around a central cloister, with main entrance from “Libertini” Street. A preliminary global visual inspection of the current state of the construction has provided essential qualitative informations about the main structural characteristics:

- the roofs at both levels consist of different types of vaults – *barrel vaults*, *pavilion vaults*, *cross vaults* and *star vaults* – that alternate without a rational organization, defining the unique architectural scheme of the construction; just some roofs, at the first level and along the perimeter of the cloister, are made of plain reinforced-concrete;
- most of the masonry walls are characterized by an irregular texture and the predominant cross section is of the so called “*sack masonry*” typology, made by two external layers of regular stone blocks and a core filled with incoherent materials, without adequate connections between the two external layers.

The structural complexity, also due to the large number of interventions, each one reflecting the knowledge and tradition of its time, does not allow a reliable structural modelling of the whole building. On the other hand, the possibility to consider only a portion of the structure at a time requires the validation of simplified assumptions about the interaction of each

substructure with the neighbouring ones. Dynamic tests can be helpful in formulating or validating such assumptions.

In the present case study, attention has been focused on the vaults: in fact, assessment of vaulted systems and of their peculiar geometry, and the physical-mechanical characterization of masonry play a primary role in estimating the actual structural performance of the building under dead as well as seismic actions.

### 5.2.2 The star vault: increasing the first level of knowledge

The first level of knowledge, which is a starting point in order to plan the next actions, has been reached according to the methodological path for interventions on historical construction reported in Figure 5.1: informations about the structure, morphology of components and existing damages have been identified as outlined in the previous section. Safety assessment according to simplified models has been carried out by Aiello et al. (Aiello et al. 2007).

In order to increase the level of knowledge from LC1 to LC2 (Figure 5.1) a complete geometrical survey and identification of all past interventions that affected the structure are required. From the safety assessment point of view, selected macro-elements can be considered. Since the star vault is typical of local culture in Lecce (it is also known as “*volta a spigolo leccese*”) and represents the predominant structural element in the building, attention has been focused on one of these vaults.



## 5.2 THE MASONRY STAR VAULT (LECCE)

---

In order to comply with requirements of the LC2 level of knowledge, a detailed geometrical study of the curved shapes defining the vault has been necessary: it has been useful also for the finite element modeling of the vault.

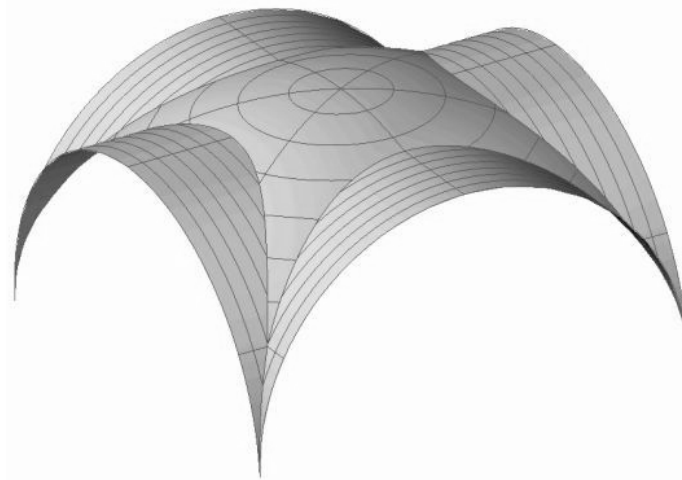


**Figure 5.3.** 3D definition of the star vault

The star vault is a type of cross vault, where the four barrel groins do not meet at the crown but are moved backwards leaving at the centre a portion with double curvature with a star shape. The complexity of the star vault is associated to the “lines of discontinuity” between the groins and the double curvature. A survey of the exact 3D shape (Figure 5.3) has been carried out, and geometry of the tested vault has been recovered according to the following steps:

- design of two cylinders (barrel vaults) with defined dimensions;

- intersection of the two cylinders and achievement of a cross vault;
- design of ellipsoidal surface with defined dimensions;
- intersection of the ellipsoidal surface with the cross vault, thus obtaining the final geometry of the star vault.

The image of the vault shown in Figure 5.3 does not reproduce the entire “masonry cell”: the boundary arches, representing the extension of the barrel groins, and the masonry piers have been defined directly in the FE model (Conte et al. 2008). The FE model of the vault is actually a simplified model, which does not take into account the interaction with the adjacent vaults: it has been used just to have a lower bound of natural frequencies. In fact, having neglected the constraint due to the presence of the adjacent vaults and of the wall in between two piers, and taking into account all masses referring to the considered vault due to finishing materials (filler of vault extrados, screed, floor), a model characterized by a lower stiffness than the actual structure has been obtained. As a result, a first natural frequency of 3.51 Hz has been obtained. By comparing this value with the AC cut-off frequency response of the NI 9233 module used for data acquisition (Figure 5.4), it is possible to see that just a little attenuation is obtained (about -0.1 dB). Since the first natural frequency is expected to be higher than this value, the use of the above mentioned data acquisition system is justified in this case. The frequency response of the accelerometers used for the present application (PCB Piezotronics® model 393B31) is flat until values lower than 0.5 Hz, corresponding to the lower

## 5.2 THE MASONRY STAR VAULT (LECCE)

---

bound of the -3dB bandwidth of the data acquisition module: thus, no further limitations are provided by the sensors.

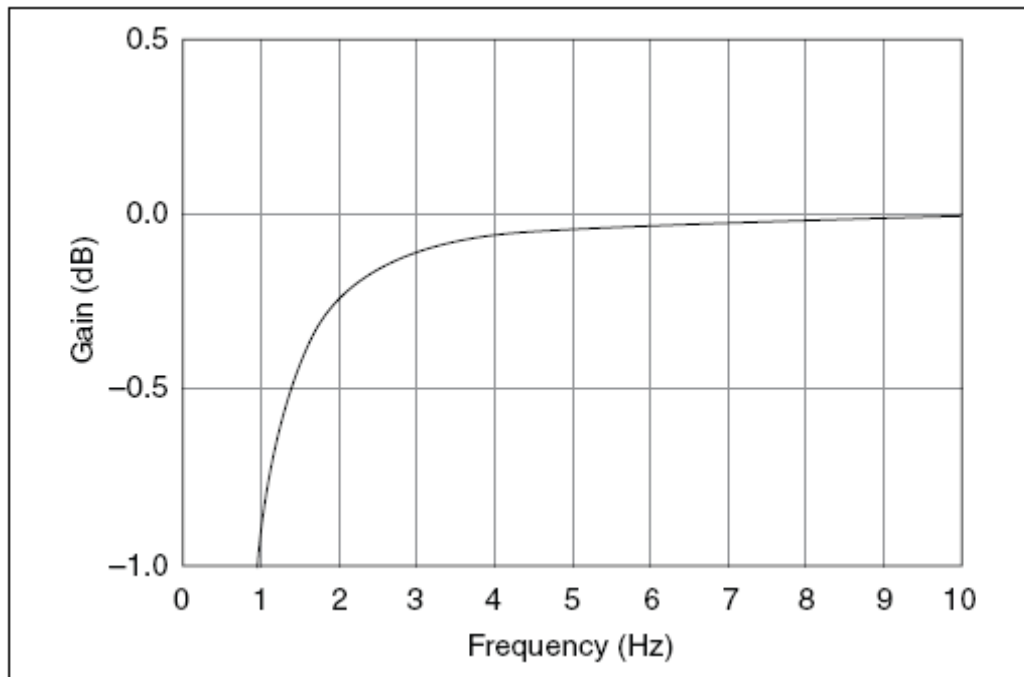


**Figure 5.4.** AC cut-off frequency response of the data acquisition modules

The final data acquisition system, therefore, was made of ten piezoelectric accelerometers whose data were acquired through three NI 9233 modules mounted on a NI 9172 chassis, which was linked to a PC via USB cable. The system was managed by the data acquisition software described in the previous chapter. As already mentioned, the data acquisition modules are characterized by a 24 bit sigma-delta ADC with a dynamic range of 102 dB and an on-board anti-aliasing filter. The link between accelerometers and recorder has been made through RG-58/U coaxial cables. Particular

attention has been devoted to avoid any noise source as much as possible: cables were fixed to the structure, mobile phones were switched off and specific attention has been paid to the connections with the data acquisition modules, by preventing the metal shells of BNC connectors from touching each other. The sensors installed on the vault are seismic, ceramic shear, high sensitivity ICP accelerometers, characterized by a bandwidth from 0.1 to 200 Hz, by a 10 V/g sensitivity and by a resolution of 0.000001 g rms.

Because of the specifications of data acquisition system and sensors and taking into account the value of the first natural frequency given by the simplified FE model, it was expected that the data acquisition system was adequate for the present application and able to properly resolve the response signals, even if in presence of low levels of vibrations due to ambient noise.

The mode shapes given by the simplified FE model are obviously not realistic, since the actual stiffness has been underestimated and the constraint due to the adjacent structural elements has been neglected: thus, this model cannot be used as such for a model updating application. However, a certain degree of reliability has been assured by an accurate evaluation of the masses directly affecting the vaults and of the mass and stiffness properties of masonry by mean of some destructive tests. The masonry properties obtained by the tests are summarized in Table 5.1. More details about destructive tests on masonry, mortar and stone samples constituting the building are reported in (Conte et al. 2008).

## 5.2 THE MASONRY STAR VAULT (LECCE)

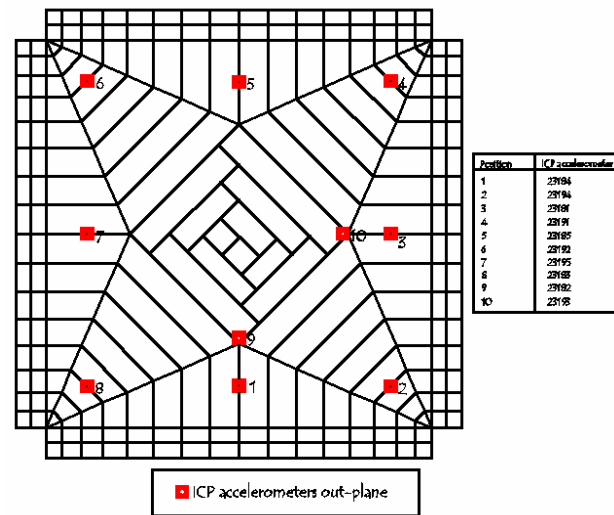
---

<i>Property</i>	<i>Average value</i>
Density $\gamma$ [kN/m <sup>3</sup> ]	16
Compressive strength $f_m$ [MPa]	3,5
Young modulus E [MPa]	3500
Shear modulus G [MPa]	1400

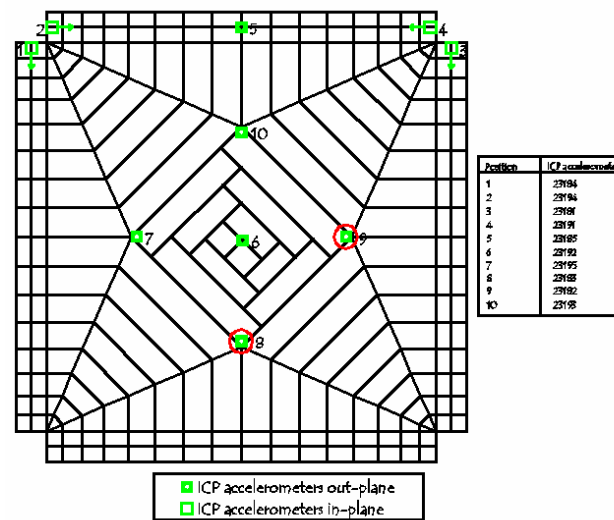
**Table 5.1.** Masonry properties

Since the actual level of constraint could not be defined in an univocal way, it was decided to look at the experimental mode shapes in order to have further indications for FE modelling. Therefore, even if, in its original plan, the main objective of the experimental campaign was the identification of a number of consecutive star vaults in order also to better understand their interaction, in the first phase, which is described here (the experimental campaign is still in progress), measurements have been carried out only on a single vault: the results have provided some indications about its effective behaviour. Such results, together with those ones of dynamic tests on the adjacent vaults, will give the opportunity to improve the FE model of the vault, in view of a model updating application. In this section the main results of dynamic tests on a single vault are reported and the main lessons learned from experimental results are described.

The dynamic response of the structure has been measured by ten accelerometers placed at the intrados of the vault (setup A) and, in a second configuration, also on two column heads (setup B). The first and the second test setups are reported in Figure 5.5.



(a)



(b)

**Figure 5.5.** Test setups: setup A (a) and setup B (b)

Sensor placement has taken into account the results of the preliminary FE model in a limited way, being it based on very simplified and not realistic assumptions. In order to overcome the uncertainties about the effective

## 5.2 THE MASONRY STAR VAULT (LECCE)

---

behaviour of the vault a quite regular mesh, covering as much as possible all elements of the vault consistently with the limited number of available sensors, has been adopted. Due to the limited number of sensors, a second test setup was necessary in order to characterize the behaviour of the columns on which the vault stands. It allowed also a further verification of the fundamental modal properties identified in the first phase. The ten accelerometers have been placed in contact with the vault surface through a little anchor plate where the sensor has been screwed: each sensor has been mounted orthogonally to the vault surface and, in the second configuration, four sensors have been placed parallel to the main directions of the columns, in order to get their translation.

The modal parameter identification has been carried out on the base of two different records: the first one was related to setup A while the second one to setup B. They are characterized by a length of 25 minutes and 30 minutes, respectively, and have been acquired by adopting a sampling frequency of 2 kHz; then, filtering and decimation have been carried out in order to obtain a final sampling frequency of 100 Hz for the setup A record, and of 200 Hz for the setup B record.

Before processing, a data pre-treatment has been carried out: data standardization has been used in order to verify that data were approximately normally distributed and that measurements could be used for modal analysis (no problems of clipping, drop-out and so on occurred). Moreover, treatment of records aimed at mean and trend removal has been carried out.

The modal parameters have been evaluated according to the EFDD algorithm in frequency domain, and according to the Cov-SSI and the DD-SSI methods in time domain. In the first case, spectra were computed using a Hanning window, with a 66% overlap. A final resolution of 0.01 Hz has been obtained.

The results, in terms of natural frequencies and damping ratios for the first two fundamental modes, obtained by applying these methods, are in good agreement each other and reported in Table 5.2, Table 5.3 and Table 5.4.

Damping ratios in time domain have been computed by carrying out sensitivity analyses on the number of block rows, according to the procedure which will be better explained in section 5.3.8 and section 5.4.

Mode number	Test setup	Frequency [Hz]	Damping ratio [%]
1	A	4.35	1.4
	B	4.31	1.5
2	A	4.96	1.05
	B	4.94	1.3

**Table 5.2.** Star vault: results of modal identification (EFDD)

Mode number	Test setup	Frequency [Hz]	Damping ratio [%]
1	A	4.34	1.7
	B	4.31	1.7
2	A	4.98	0.9
	B	4.95	1.1

**Table 5.3.** Star vault: results of modal identification (Cov-SSI)



## 5.2 THE MASONRY STAR VAULT (LECCE)

---

Mode number	Test setup	Frequency [Hz]	Damping ratio [%]
1	A	4.32	1.3
	B	4.31	1.4
2	A	4.99	0.9
	B	4.95	1.0

**Table 5.4.** Star vault: results of modal identification (DD-SSI)

The identification process has been stopped after having obtained the first two modes, since a reliable identification of higher modes was complicated by the effects of the interaction with the adjacent vaults. For a reliable estimation of such modes a new experimental campaign has been planned but not carried out yet: the aim of this campaign aims at a characterization also of the close vaults in order to try to filter out the interaction effects. The last series of tests, instead, will be specifically devoted to the study of interactions.

The results obtained in terms of mode shapes by applying EFDD and Cov-SSI are also in good agreement, as pointed out by values of CrossMAC higher than 0.99; the CrossMAC matrices for setup A and setup B obtained from the estimates of mode shapes given by the Cov-SSI and the DD-SSI methods are shown in Figure 5.6, as an example. The identified mode shapes for the first two modes are shown in Figure 5.7. The AutoMAC matrix (Figure 5.8), instead, points out that sensor placement was adequate to distinguish such mode shapes, which are normal, as shown by the Complexity plots (Figure 5.9 and Figure 5.10).

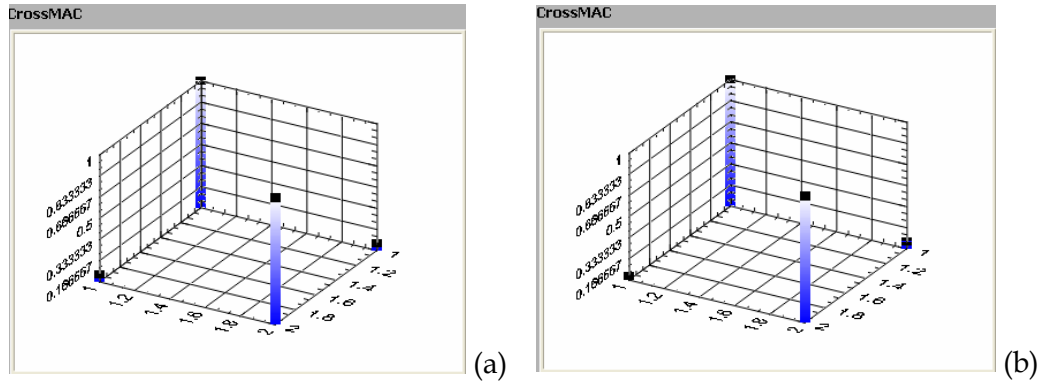


**Figure 5.6.** CrossMAC matrices (DD-SSI vs. Cov-SSI): setup A (a) and setup B (b)

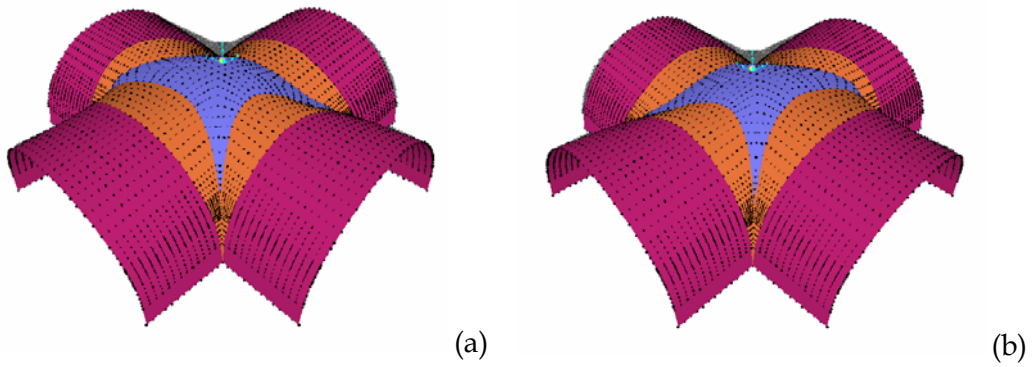


**Figure 5.7.** Identified mode shapes: mode 1 (a) and mode 2 (b)

## 5.2 THE MASONRY STAR VAULT (LECCE)

---

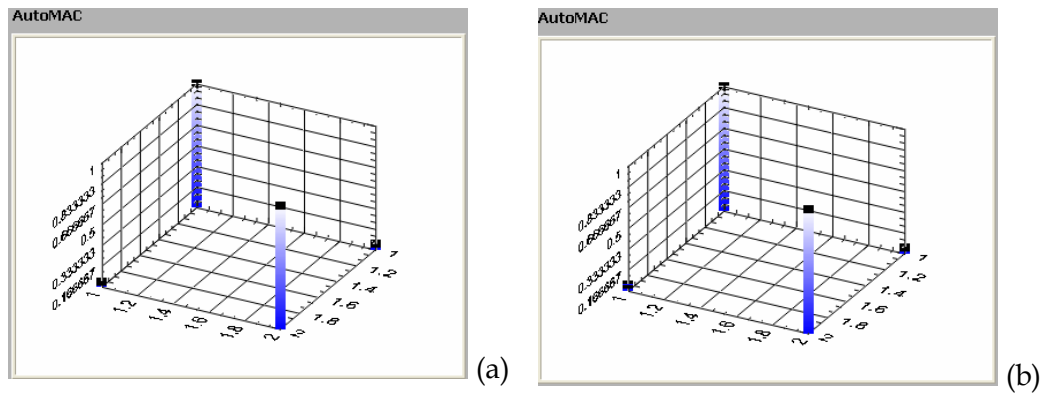


**Figure 5.8.** AutoMAC matrices: setup A (a) and setup B (b)

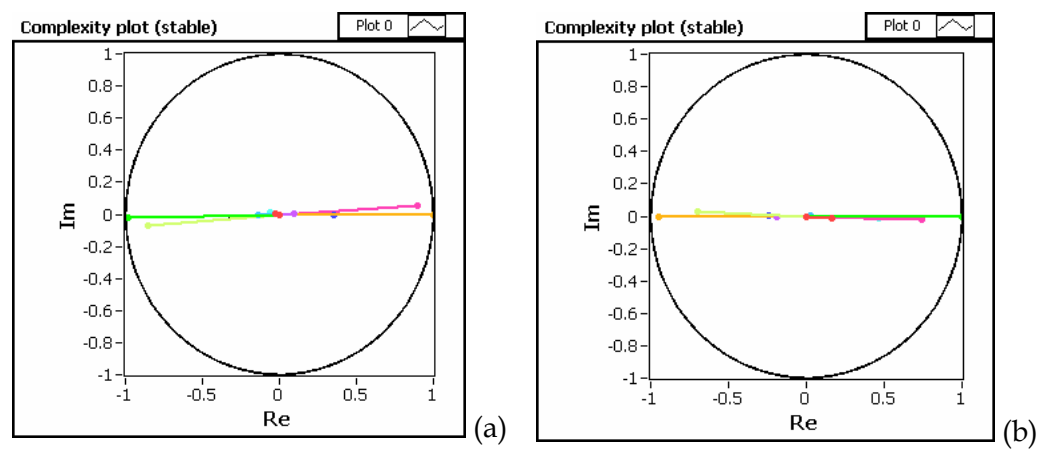


**Figure 5.9.** Complexity plots (Setup A): mode 1 (a) and mode 2 (b)

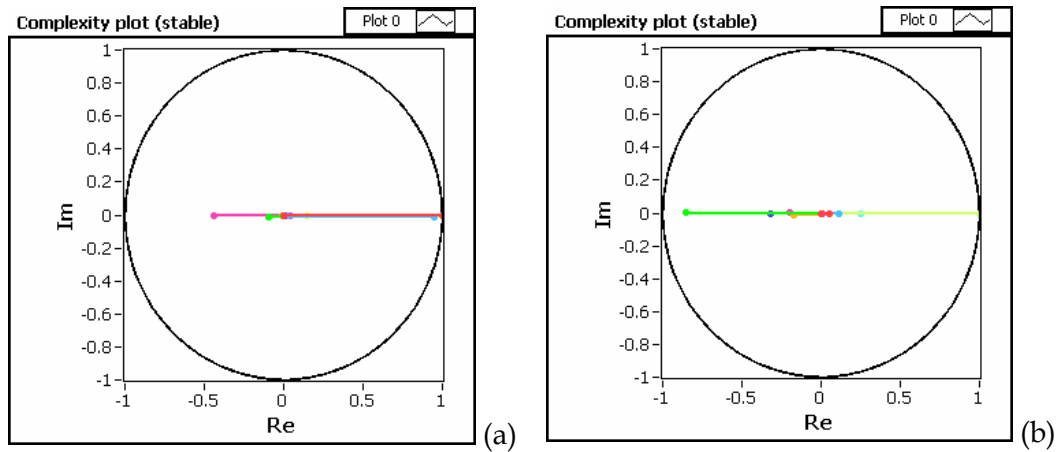


**Figure 5.10.** Complexity plots (Setup B): mode 1 (a) and mode 2 (b)

By looking at the obtained mode shapes, some indications about model refinement have been obtained: in fact, the two rear piers, characterized by the presence of a masonry wall in between, show very limited modal displacements and can be probably considered as fixed. Moreover, the shapes seem to be defined by the relative displacements of the other two piers with respect to the rear ones: in particular, the actual shape is determined by the direction of movement of those piers, determining a compression against the constraints of the vault. However, further investigations are needed about interaction with the close vaults, since, in correspondence of the identified frequencies for the studied vault, they seem to behave as a kind of constraint. Since they are characterized by different dimensions, it is possible that there is no synchronization among them at a certain frequency: this aspect seems to be confirmed by some

## 5.2 THE MASONRY STAR VAULT (LECCE)

---

peaks in the spectra (and spurious poles in the stabilization diagram) not corresponding to actual modes of the instrumented vault.

The higher stiffness of the vault with respect to its FE model is pointed out by the values of natural frequencies of the identified modes: as expected, the interaction with the close structural elements (vaults and wall) acts as a constraint for the vault and causes an increase in the stiffness of the system. The inadequacy of the simplified FE model to reproduce the actual behaviour of the vault is pointed out also by a poor correlation between experimental and numerical mode shapes. It is worth emphasizing, however, that reproduction of the structural behaviour was not the main aim of this model: an effective correlation with numerical results is possible only after having implemented a new model by taking into account the informations obtained from this first experimental campaign. Even if the study is far from being finished, this results show how numerical modelling and OMA tests can be strongly interrelated in order to better define experimental setups and to get a deeper knowledge about the dynamic behaviour of very complex systems, such as historical structures.

## 5.3 THE TOWER OF THE NATIONS (NAPLES)

### 5.3.1 Research motivations

The present research describes the use of Operational Modal Analysis for the evaluation of modal parameters of an important historical structure

such as the Tower of the Nations, located within the Mostra D'Oltremare area in Naples. In particular, it can be placed in the framework of the activities aiming at designing an appropriate restoration and seismic upgrading intervention for the Tower, taking into account the valuable characteristics of the structure itself, and therefore the need of improving the knowledge of the structural characteristics of the building.

Because of the valuable characteristics of the structure, a high level of knowledge was necessary in order to build a reliable FE model: different sources of information (design drawings, survey, non-destructive tests) have been taken into account. In order to reduce as much as possible modelling uncertainties, dynamic measurements have been carried out, aiming at optimize the numerical model adopted for structural analyses.

Assessment of the building structure has been undertaken evaluating a number of sources of information, in compliance with relevant National (Consiglio Superiore dei Lavori Pubblici 2008) and International (European Committee for Standardization 2003) Codes concerning seismic evaluation of existing constructions. It has been divided into the following three different phases:

- Geometric investigation, to completely define the geometric characteristics of the structure in terms of structural and non-structural elements;
- Structural investigation, aiming at the definition of the structural scheme and of the steel reinforcement in structural elements;

### 5.3 THE TOWER OF THE NATIONS (NAPLES)

---

- Investigation about materials, aiming at the evaluation of mechanical characteristics of concrete and steel;
- Evaluation of the structural response in the case of dead loads and under earthquake loading.

The first three phases can be considered as preliminary to the numerical evaluation of the structural response under dead loads and earthquake loading: they can be synthesized in the examination of structural drawing and execution of visual inspection and survey and of non-destructive tests. Data collected in these phases have been used in the implementation of the numerical model: anyway, some modelling hypotheses had to be confirmed.

#### 5.3.2 The Tower of the Nations

The Tower of the Nations is one of the most important and representative buildings located within the Mostra D'Oltremare area in Naples. It is a reinforced concrete building designed by the architect Venturino Ventura, after a national competition. The building has two opposed blind and two completely see-through façades. The 35.6 m wide by 36.1 m long by 43.7 m height building was built as a r.c. (reinforced concrete) frame, as shown in Figure 5.11, with elevator shafts and stairs located in the center of the building. Apart from the first, the second and third floor, the remaining portion of the building was built so that the visitor can look from one floor to another of the exposition levels.

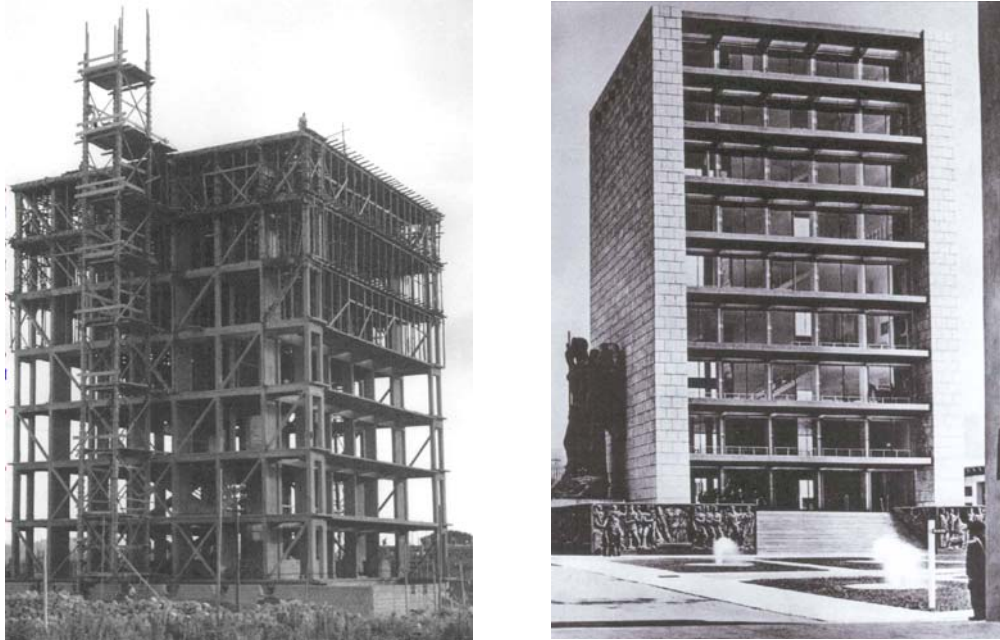


**Figure 5.11.** The Tower of the Nations: under construction (left), at completion (right)

As shown in Figure 5.12, the first level is characterized by a whole floor, which can be accessed, from outside or from the basement, by two couples of one flight stairs or by the central elevator. The second level can be accessed only through two interior stairs and it has two balconies from which one can see the first level. The third level, like the first one, is characterized by a whole floor, which can be accessed by two couples of one flight stairs or by the central elevator. The remaining levels, except the tenth, are characterized by alternate levels which cover just an half of the imprint area of the building, as shown in Figure 5.13. They are linked by the central elevator or by a one flight stair. The tenth level (the roof) is



### 5.3 THE TOWER OF THE NATIONS (NAPLES)

---

characterized by a whole floor which can be accessed only through a one flight stair.

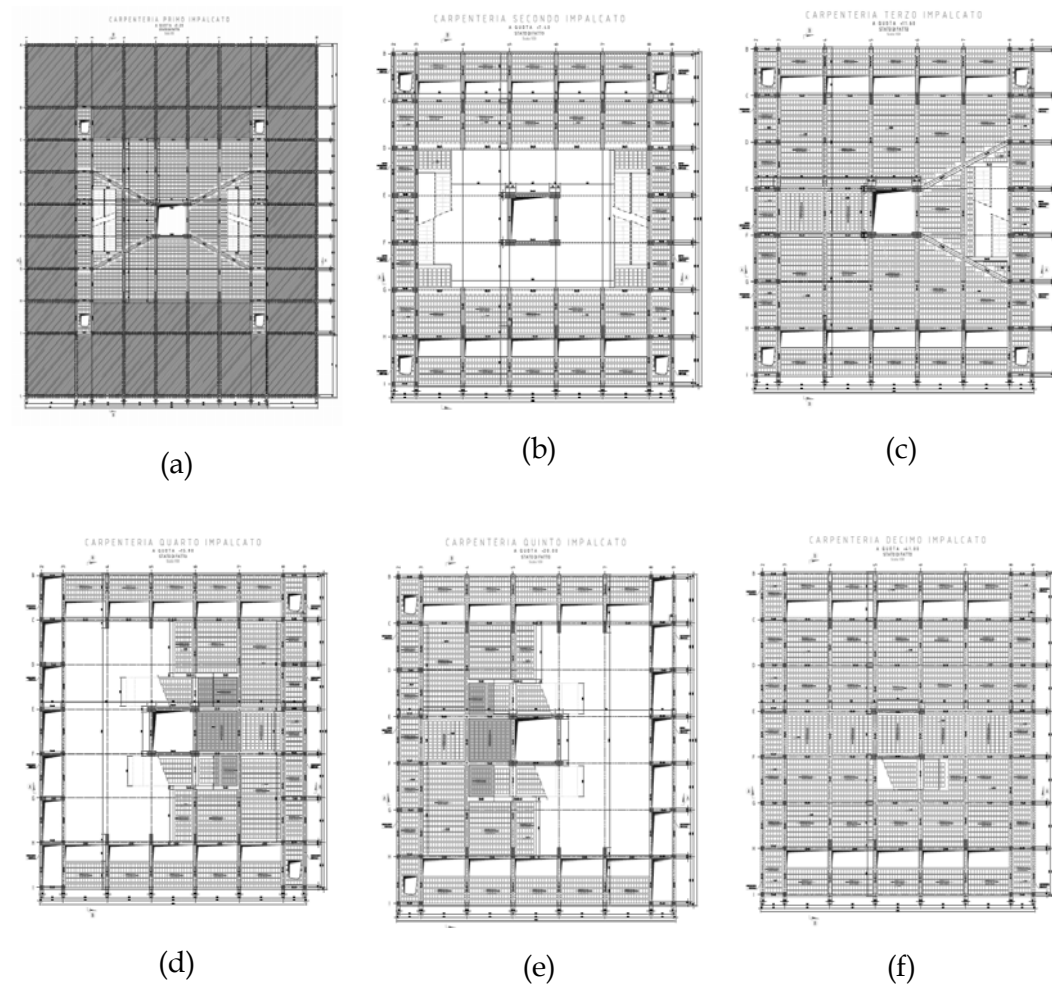


**Figure 5.12.** Carpentries: the first floor and the basement (a), the second floor (b), the third floor (c), the fourth floor (d), the fifth floor (e), the tenth floor (f)

The structural system is very interesting and can be addressed as innovative, taking into account the time of original design and erection. It

is made, in the longitudinal direction, by two couples of frames with reinforced concrete diagonals, to increase stiffness, and tuff masonry within the fields of the frames, as shown in Figure 5.13. In the transverse direction, instead, the structural system is characterized by the presence of the elevator within a three-dimensional one-bay r.c. frame with r.c. walls in the above mentioned direction.

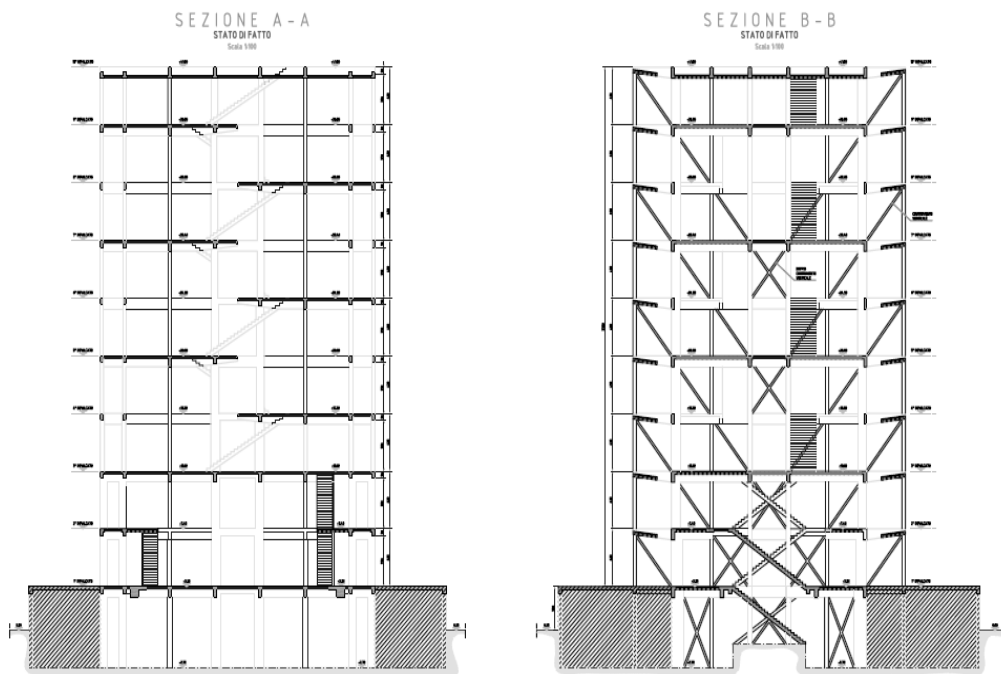


**Figure 5.13.** Transversal (left) and longitudinal (right) section

The geometric assessment of the structure has been carried out through a visual inspection of the structure at the various floors. The structure has a central body (the Tower) which does not change in elevation while at the first level there is a basement along the whole perimeter with an extension

### 5.3 THE TOWER OF THE NATIONS (NAPLES)

---

of 6.0 m outside the edge of the Tower. The link between basement and Tower is made by a short deep beam. The Tower has a nearly square shape (about 23.10 x 23.60 m) and an height of 41.0 m with respect to the soil level. It has ten floors with constant height (4.20 m) while the first level is 5.90 m tall. The total height of the Tower from the foundations level is 43.7 m.

Even if the structure was designed only to bear gravity loads, its characteristics are interesting also from a seismic point of view. In fact, in the transversal direction there are two systems of exterior frames: each system is characterized by two near frames (2.00 m) and each frame has seven bays, 3.30 m wide, with relatively small beams (0.35 x 0.50 m); the columns have variable dimension from 0.30 x 0.60 m to 0.30 x 0.30 m. The two frames are connected in the transversal direction by beams with cross section of 0.30 x 0.80 m, by the floor, where it is present, and by r.c. walls, 0.15 m thick and located between two close columns. There are eight walls at the first level, six at the second and the third level, and four at the remaining ones. Moreover, about the systems of two close frames, only the exterior one is characterized by the presence of r.c. diagonals and of tuff masonry walls within the fields of the frame (Figure 5.14a).

In the longitudinal direction, the structure is even more complex because of the presence of r.c. walls and of alternate levels. There are two types of walls: the first ones have small thickness, as described above, and link the two frames which constitute the exterior systems; the second ones have larger dimensions and are located near the elevator at the center of the

building. The two exterior systems and the central one are linked by the floor, where present, and, along the two exterior sides of the building, by two frames characterized by bays 3.95 m wide, beams with cross section of  $0.25 \times 0.80$  m, and columns with variable cross section from  $0.45 \times 1.10$  m at the first level to  $0.30 \times 0.80$  m at the last level. Most of the floors are plotted in the longitudinal direction, with a height of 0.23 m. From the third to the ninth level, the roofs are characterized by the presence of a false ceiling 0.04 m thick and linked to the floors by a steel net and steel rods (Figure 5.14b).

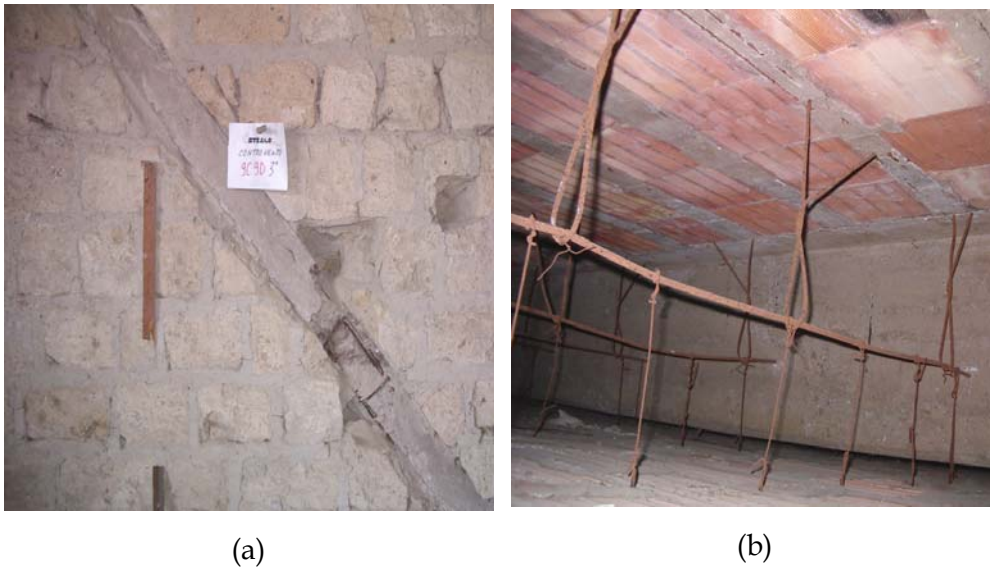


**Figure 5.14.** Views from survey: r.c. diagonals and tuff walls (a), false ceiling linked to the floors (b)

### 5.3 THE TOWER OF THE NATIONS (NAPLES)

---

#### 5.3.3 Test program

A visual inspection of the structure has been carried out in order to assess geometry. Some non-destructive tests, instead, have been carried out to assess material properties and reinforcement details: these informations, together with those ones related to the structural scheme, are crucial for implementation of the numerical model. In order to get these data, the following procedure has been adopted.

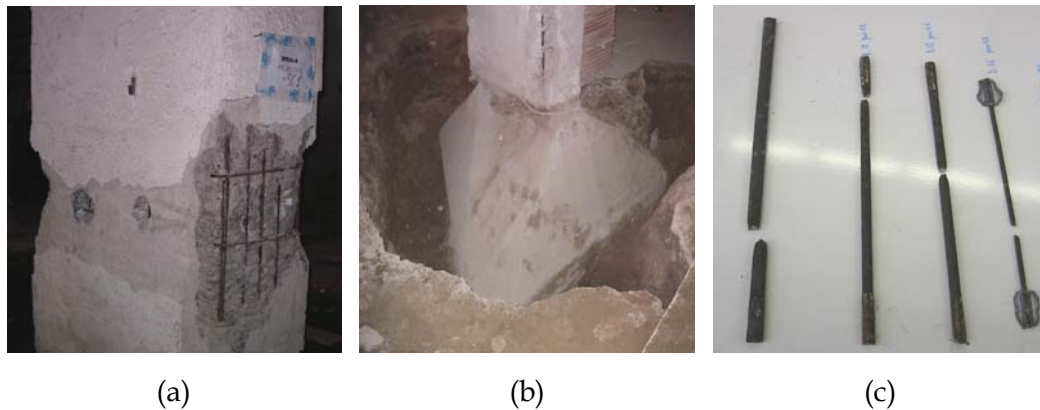


**Figure 5.15.** Views from survey: column reinforcement (a), foundation geometry (b), tested smooth rebars (c)

An appropriate investigation has been carried out in order to identify geometry and reinforcement of all structural elements. As regards beams, reinforcement has been evaluated in three sections (one at the center and the others at the ends) while, as regards columns, only a midspan section has been considered (Figure 5.15a). Moreover, geometry of foundations has been assessed: they are made by prismatic blocks on circular piles (Figure 5.15b). The comparison between the results of simulated design of

the structure and field investigations has confirmed that the structure was designed to bear only gravity loads. According to Italian seismic code provisions, a 'knowledge level' LC2 has been reached.

Combining destructive and non-destructive tests, the mechanical characteristics of materials have been defined. As regards concrete, some logs have been extracted and SonReb tests have been conducted to evaluate the compressive strength: values ranging from 10.64 MPa and 25.98 MPa have been obtained, with a mean value of 15.26 MPa but a very high scatter (see also Rainieri et al. 2008b for more details). As regards the steel reinforcement, some specimens have been extracted from structural elements, obtaining an average yielding strength of 275 MPa. The bars were smooth and oxidized, in particular at the first level and the roof (Figure 5.15c).

All these tests have been carried out to support the numerical model of the building and the development of non-linear static push-over analyses to assess its seismic capacity, besides modal dynamic analyses. More details can be found in (Cosenza et al. 2006). In order to validate some modelling hypotheses and obtain a reliable model of the structure at present stage, some dynamic measurements have been carried out, in order to get the modal parameters of the structure in operational conditions.

### 5.3.4 Dynamic tests: setup

The dynamic response of the structure has been measured at the fourth and the fifth level of the building and at the roof. The roof and the fifth

### 5.3 THE TOWER OF THE NATIONS (NAPLES)

---

level have been instrumented in two corners: at each corner two Force Balance accelerometers (Kinemetrics EpiSensor ES-U2) have been placed. Another couple of accelerometers has been placed at the fourth floor. Figure 5.16 shows the adopted test layout.

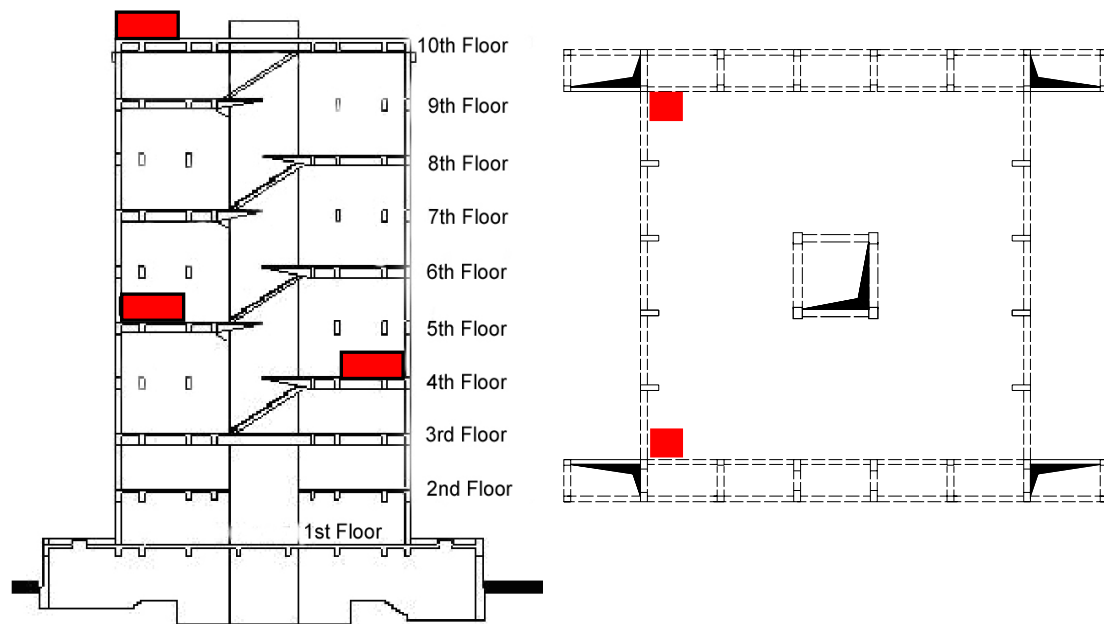


**Figure 5.16.** Test layout

The ten accelerometers have been placed directly in contact with the concrete slab and parallel to the main directions of the building, in order to get both translational and torsional modes of the structure. The sensors have a bandwidth (-3 dB) of about 200 Hz (starting from DC) and a high dynamic range (140 dB). The full scale range can be set by the user and can vary from  $\pm 4$  g (0.625 V/g as sensitivity) and  $\pm 0.25$  g (10 V/g as

sensitivity): values of sensitivity are related to a single-ended configuration and  $\pm 2.5$  V output. In this application a full scale range of  $\pm 0.25$  g has been adopted, due to the weak vibrations induced on the structure by ambient noise. A Kinematics K2 Digital Recorder, characterized by a 24-bit DSP, an analog anti-aliasing filter and a high dynamic range ( $>114$  dB at 200 sps), has been used for data acquisition. The link between accelerometers and recorder has been made through a 24 AWG cable made by individually shielded twisted pairs.

Modal parameter identification has been carried out on the base of a record characterized by a length of about 5 minutes and a sampling frequency of 200 Hz. Due to its short duration, only natural frequencies and mode shapes could be estimated with a certain degree of accuracy: estimates of damping ratios, instead, were not reliable. Anyway, informations about natural frequencies and mode shapes are sufficient for model refinement. Other two measurements, characterized by a length of 30 minutes and 1 hour, respectively, with a sampling frequency of 100 Hz, have been carried out two years later and have not been used for model refinement but for damping ratio estimation. Results obtained from the last two records are discussed at the end of this section: they have been used also for testing of the automated modal parameter identification procedure described in the next chapter.



## 5.3 THE TOWER OF THE NATIONS (NAPLES)

---

### 5.3.5 Experimental results

Data pre-treatment and processing has been carried out by mean of the software described in the previous chapter.

Modal parameter estimation in frequency domain has been carried out by using a Hanning window for spectrum computation, with a 66% overlap: a final frequency resolution of 0.01 Hz has been obtained.

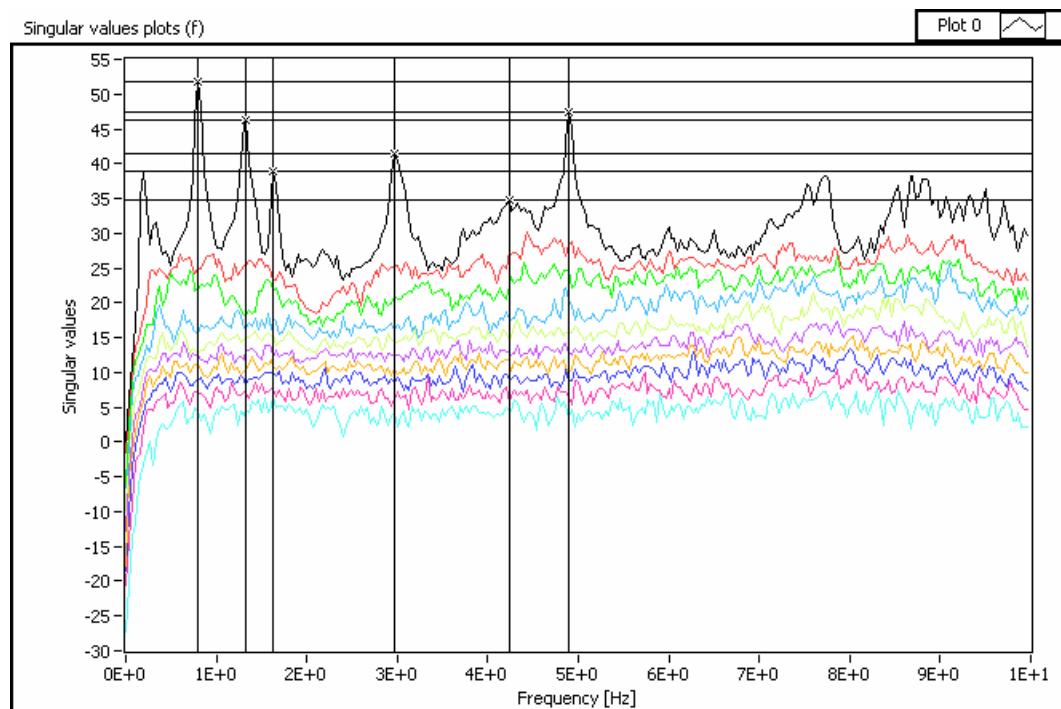


**Figure 5.17.** Singular Value plots

In Figure 5.17 the Singular Value plots obtained by applying the EFDD method are reported, and peaks relative to the first six modes are indicated: the first singular value plot points out that the structure is characterized by well-separated modes. The results of identification

process in terms of natural frequencies, damping ratios and mode shapes are reported in Table 5.5. It is possible to recognize that the first and the fourth mode are translational modes parallel to the open side of the building; the second and the fifth mode are, instead, translational modes parallel to the blind side; finally, the third and the sixth mode are torsional modes.

Mode number	Type	Frequency [Hz]
1	Translation (open side)	0.80
2	Translation (blind side)	1.33
3	Torsion	1.66
4	Translation (open side)	2.96
5	Translation (blind side)	4.23
6	Torsion	4.90

**Table 5.5.** Results of identification (EFDD)

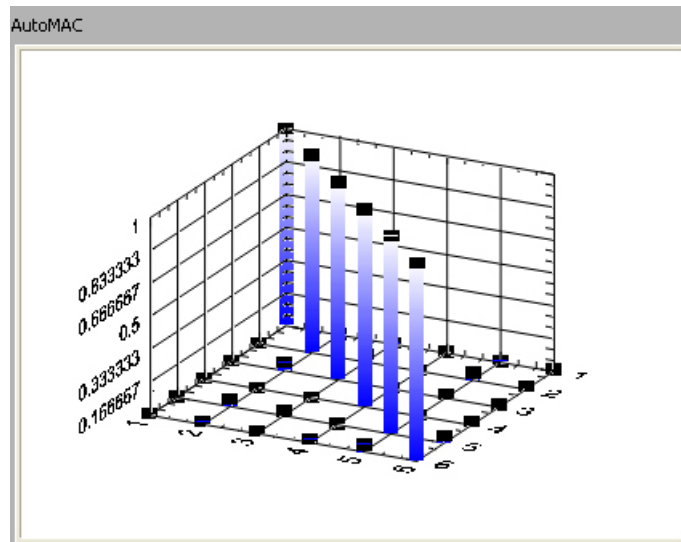


**Figure 5.18.** AutoMAC matrix

### 5.3 THE TOWER OF THE NATIONS (NAPLES)

---

In Figure 5.18 a 3D histogram of the AutoMAC matrix is reported: it points out the effectiveness of experimental setup. Another check of the obtained mode shapes has been carried out by the complexity plots: these plots are useful in order to verify if mode shapes are normal or not. As shown in Figure 5.19, all modes are normal or nearly normal (i.e., the fifth and the sixth mode: however, they are not very well excited, so, probably, imaginary components are mainly a noise effect).

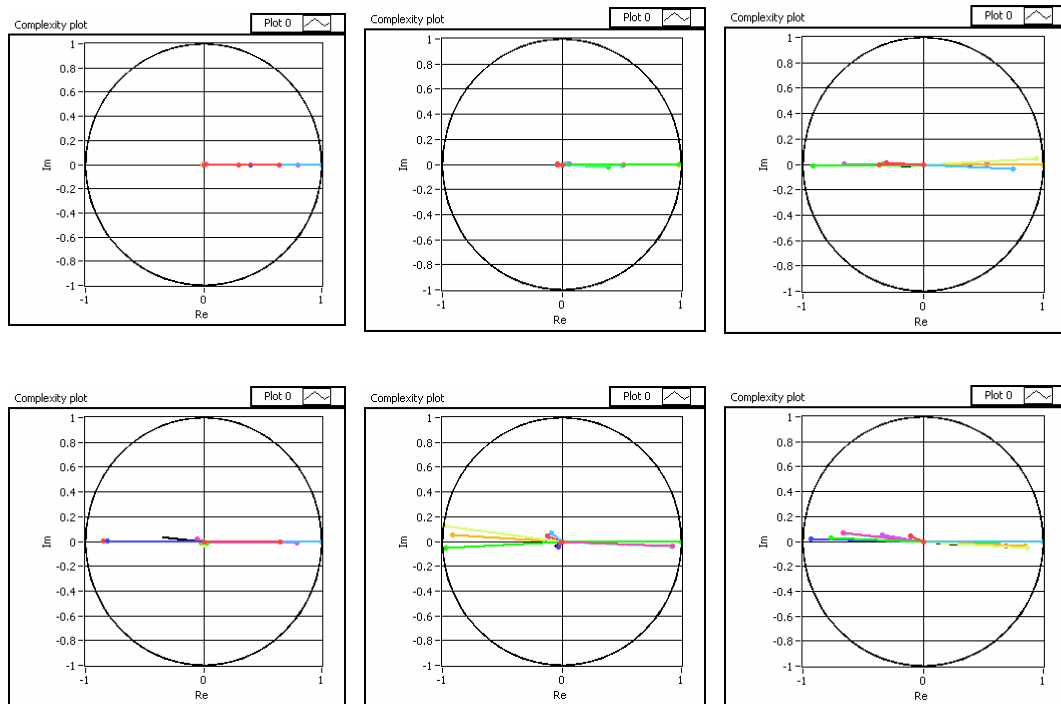


**Figure 5.19.** Complexity plots

The same record has been analyzed again according to the Cov-SSI and DD-SSI methods. In Table 5.6 the eigenfrequencies obtained by applying the different methods are compared: a good agreement among them has

been obtained. Similar results have been obtained also by comparing the different estimates of mode shapes, as pointed out by the CrossMAC matrices (Figure 5.20), characterized by values close to 1 along the main diagonal and close to 0 elsewhere.

Mode number	Type	Frequency (Cov-SSI) [Hz]	Frequency (DD-SSI) [Hz]	Frequency (EFDD) [Hz]
1	Translation (open side)	0.81	0.80	0.80
2	Translation (blind side)	1.33	1.33	1.33
3	Torsion	1.65	1.65	1.66
4	Translation (open side)	2.98	2.98	2.96
5	Translation (blind side)	4.24	4.23	4.23
6	Torsion	4.90	4.90	4.90

**Table 5.6.** Identified natural frequencies: comparison from different methods

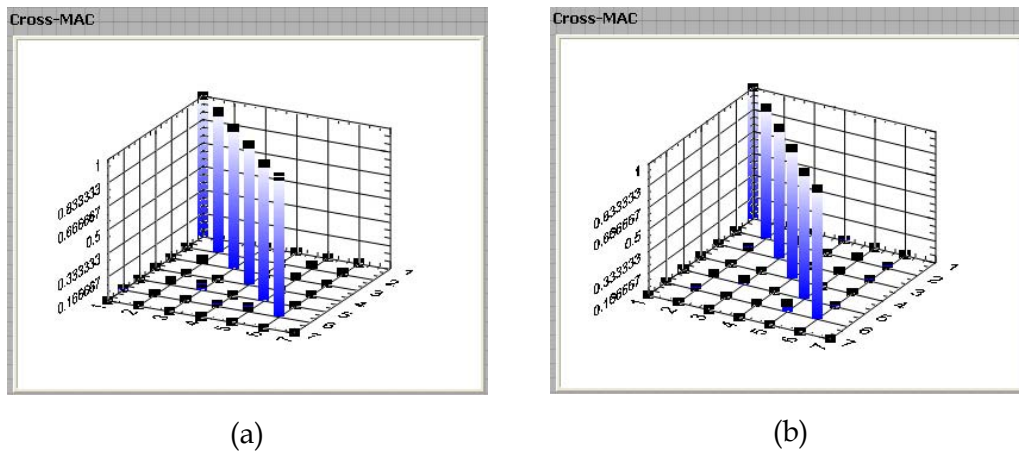


**Figure 5.20.** CrossMAC matrices: Cov-SSI vs. EFDD (a), DD-SSI vs. EFDD (b)

### 5.3 THE TOWER OF THE NATIONS (NAPLES)

---

#### 5.3.6 The Finite Element model

The dynamic response of the structure has been characterized numerically by the implementation of some FE models of the Tower and carrying out modal analyses through the SAP2000® software (Computers and Structures 2006). The geometric and structural model of the building represents in details, under different modelling assumptions, the geometric and mechanic characteristics of the structural elements and the mass distribution on plain and along height. The unique structural system, characterized by the absence of repetitive floors and by a particular distribution of stairs, had influence on the construction of the FE model, with a different configuration at each floor (Figure 5.21).

Position and geometry of structural elements at each floor are defined according to the results of in-situ investigations. One-dimensional elements (columns, beams, braces) are modelled by “beam” elements. Bi-dimensional elements (r.c. walls, stairs, tuff walls) are modelled by “shell” elements. At each floor, shell elements, 0.05 m thick, are put in every field of carpentry. In Figure 5.21 the modelling phases for the first four levels are shown: comparison with Figure 5.12 points out the detailed modelling of the structure.

About restraints, absence of soil-structure interaction has been assumed. As regards, instead, mass assignment, in the case of r.c. structural elements, mass has been implicitly considered in compliance with the specific mass of the material (concrete) and the geometric dimensions of the elements. Floors and stairs, in a similar way, are characterized by a

uniform area mass. This mass has been evaluated according to section geometry and, in compliance with the present state of the structure, no live loads have been applied. As regards tuff masonry walls, an externally applied linear mass has been considered acting on the beams.

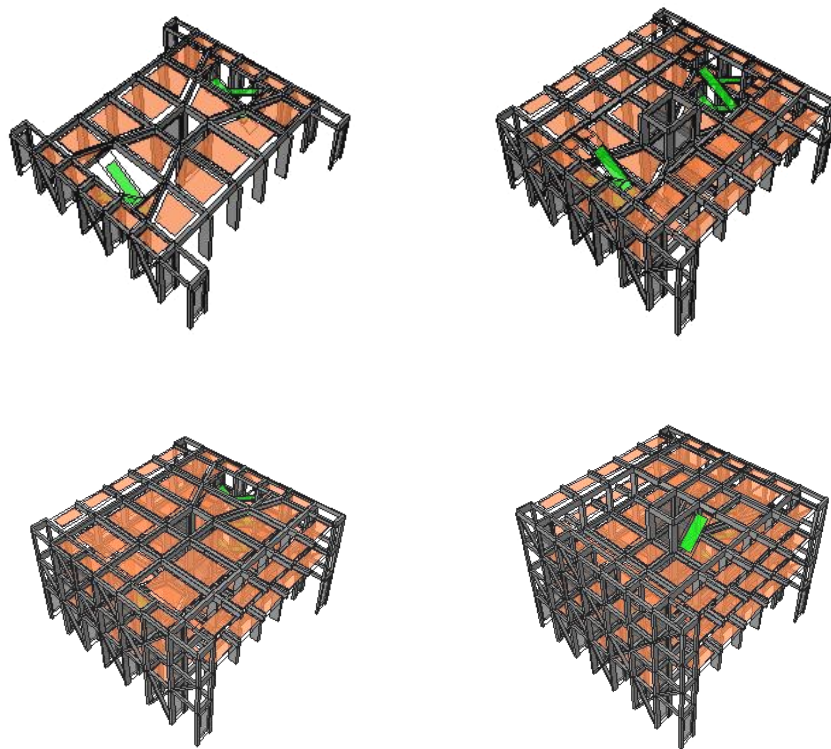


**Figure 5.21.** Construction of the FE model (from the 1<sup>st</sup> to the 4<sup>th</sup> level)

Correlation with experimental results has been evaluated by defining a number of model classes according to the following modelling assumptions:

- Absence vs. presence of tuff masonry walls;

### 5.3 THE TOWER OF THE NATIONS (NAPLES)

---

- Absence vs. presence of the basement parallelepiped structure;
- Floor modelling: shell elements vs. rigid diaphragm.

Their definition is related to the main uncertainties affecting numerical modelling of the structure: thus, correlation with results of dynamic tests has been useful, first of all, to assess the effectiveness of different modelling hypotheses. In particular, the main objectives were related to the evaluation of the influence of curtain walls on the dynamic behaviour of the structure, the characterization of the level of interaction between Tower and surrounding basement, to assess sensitivity to different assumptions about in-plane stiffness of the floors.

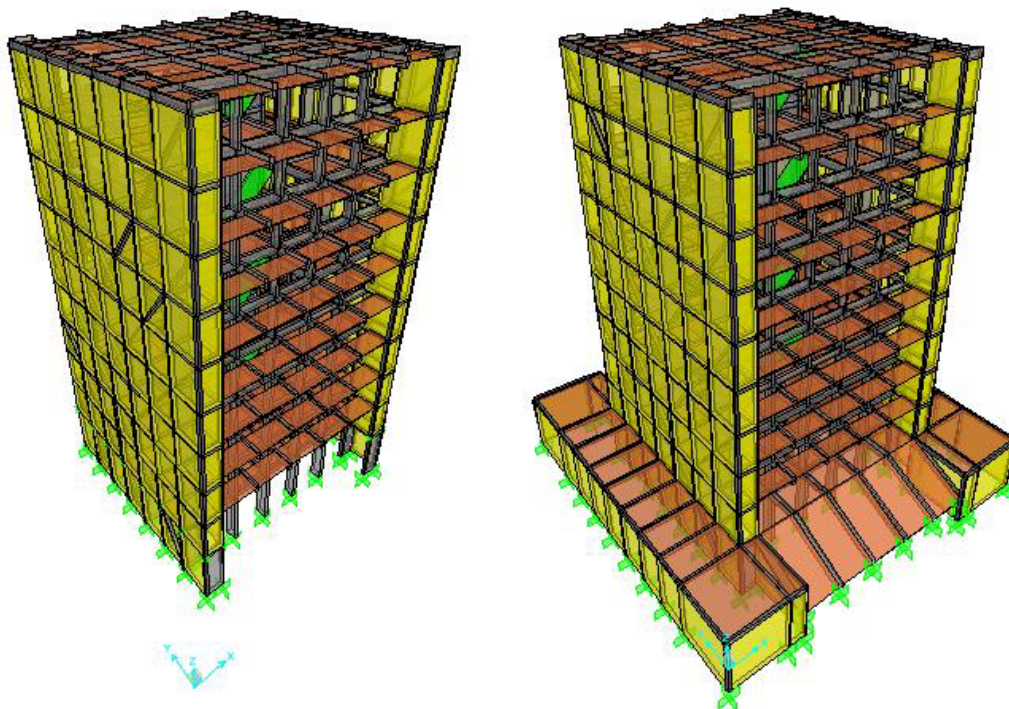


**Figure 5.22.** FE model without (left) and with (right) basement

Uncertainties related to the above mentioned hypotheses are due to a number of different reasons:

- about tuff masonry walls, correlation with the model characterized by absence of curtain walls has been evaluated in compliance with a traditional assumption in structural design; however, due to the low level of excitation, it is evident that the dynamic response of the structure in operational conditions is not negligibly influenced by the presence of masonry walls: this circumstance has been demonstrated also by the poor correlation between experimental and numerical results obtained for the model without walls. Thus, being this assumption not meaningful, models without masonry walls will be no further mentioned;
- as regards the basement parallelepiped structure, the main source of uncertainty is related to the particular link with the Tower; a simplified approach, based on the assumption that the basement can be considered as a translational restraint along the perimeter of the first level of the central tower, has been considered (Figure 5.22): this assumption can be justified by taking into account the high transversal stiffness of the basement, due to the presence of perimeter r.c. walls and r.c. stairs for the access to the Tower, and its reduced height, with respect to that one of the Tower, whose effect is a low contribution in terms of participating mass. On the other hand,



### 5.3 THE TOWER OF THE NATIONS (NAPLES)

---

because of the low level of vibrations in operational conditions, also the effect of a full interaction between Tower and basement has been considered: this condition affects, in particular, the participating mass, whose effect on natural frequency cannot be neglected, in particular at higher modes;

- about floors, they can be modelled both by shell elements and by diaphragms. Their respective influence on modal properties of the structure has been evaluated, in order to define the error due to these different assumptions. However, slightly better results were expected when floors were modelled by shell elements: in fact, since masonry walls have influence on the structural response at low levels of excitation, the ratio between the in-plane stiffness of floors and the stiffness of walls is such that floors cannot be rigorously considered as infinitely stiff in their plane.

By combining the above mentioned modelling assumptions, the following four classes of models have been defined:

- Floor = Diaphragm – With basement
- Floor = Shell – With basement
- Floor = Diaphragm – Without basement
- Floor = Shell – Without basement

Within each class, the selected updating parameters were the elastic modulus of concrete and the shear modulus (which is correlated to the elastic modulus) of tuff masonry.

The elastic modulus of concrete has been taken in the range:

$$E_{c,min}=13000 \text{ MPa}, E_{c,max}=30000 \text{ MPa}$$

in compliance with the high scatter shown by compressive tests on concrete.

The shear modulus of tuff masonry has been, instead, taken in the range:

$$G_{t,min}=300 \text{ MPa}, G_{t,max}=420 \text{ MPa}$$

provided by the National Seismic Code for existing constructions (Consiglio Superiore dei Lavori Pubblici 2008). The corresponding values for the elastic modulus of tuff masonry are:

$$E_{t,min}=900 \text{ MPa}, E_{t,max}=1260 \text{ MPa}.$$

By adopting a fine increment for the values of elastic modules and considering all possible combinations of values of elastic modules of tuff masonry and concrete, a total number of 2132 models has been obtained. These models have been automatically generated and analyzed starting from a basic model for each class by mean of a software developed on purpose in LabView environment. Since the SAP2000® libraries are not open for free use, modal analyses have been carried out by controlling it by mean of the Microsoft® Windows™ user32.dll library.

### 5.3 THE TOWER OF THE NATIONS (NAPLES)

---

As a result, sensitivities of the different model classes to material property changes have been evaluated. An example of response surfaces in terms of natural frequencies of the first six modes with respect to the values of elastic modules of concrete and tuff masonry is reported in Figure 5.23. It is worth noticing, by looking at the response surfaces, how the natural frequencies of the first and the fourth mode are mainly influenced by the elastic modulus of concrete. A stronger influence of the shear modulus of tuff masonry can be, instead, observed for the remaining modes, as expected.

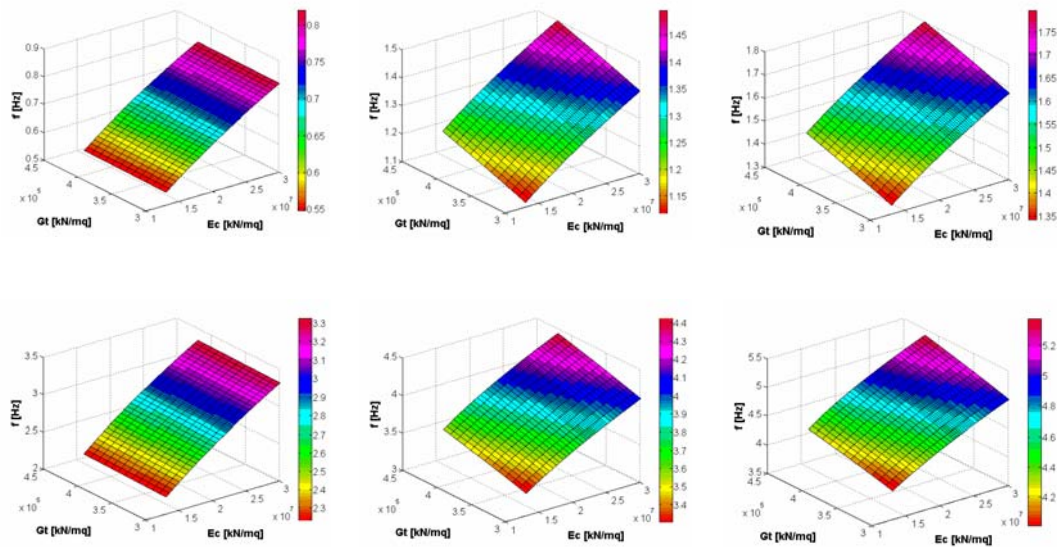


**Figure 5.23.** Sensitivity of natural frequencies to elastic modulus changes (Floor = Shell – With basement)

**5.3.7 Model refinement**

Starting from sensitivity analyses carried out for each class of models, correlations with experimental results have been evaluated in order to validate modelling assumptions and to define a refined model, namely a model which reproduces as close as possible the experimental values of the modal properties of the structure.

In order to update the FE model, objective functions have to be chosen and their value minimized: this choice has been done according to the results of sensitivity analyses. Widely used objective functions are defined in terms of scatter between analytical and numerical values of natural frequencies:

$$J_f = \frac{100}{N_m} \sum_{i=1}^{N_m} \left| \frac{f_i^e - f_i^a}{f_i^e} \right| \quad (5.1)$$

or, taking into account also mode shape correlation:

$$J_{f,\phi} = \frac{100}{N_m} \sum_{i=1}^{N_m} \left[ \left| \frac{f_i^e - f_i^a}{f_i^e} \right| + NMD(\phi_i^e, \phi_i^a) \right] \quad (5.2)$$

$$J_{f,\phi} = \frac{100}{N_m} \sum_{i=1}^{N_m} \left[ \left| \frac{f_i^e - f_i^a}{f_i^e} \right| + MAC(\phi_i^e, \phi_i^a) \right] \quad (5.3)$$

### 5.3 THE TOWER OF THE NATIONS (NAPLES)

---

where  $N_m$  is the number of identified modes, and:

$$\Delta f[\%] = \left| \frac{f_i^e - f_i^a}{f_i^e} \right| \cdot 100 \quad (5.4)$$

is the scatter between the analytical value  $f_i^a$  and the experimental value  $f_i^e$  of natural frequency of the  $i^{\text{th}}$  mode, while correlation between the corresponding analytical  $\{\phi_i^a\}$  and experimental  $\{\phi_i^e\}$  mode shapes is defined through the Modal Assurance Criterion (MAC), defined as (Allemang & Brown 1982):

$$MAC(\{\phi_i^e\}, \{\phi_i^a\}) = \frac{|\{\phi_i^e\}^H \{\phi_i^a\}|^2}{\{\phi_i^e\}^H \{\phi_i^e\} \{\phi_i^a\}^H \{\phi_i^a\}} \quad (5.5)$$

or in terms of Normalized Modal Difference (Maya et al. 1997, Waters 1995), defined as:

$$NMD(\{\phi_i^e\}, \{\phi_i^a\}) = \sqrt{\frac{1 - MAC(\{\phi_i^e\}, \{\phi_i^a\})}{MAC(\{\phi_i^e\}, \{\phi_i^a\})}} \quad (5.6)$$

In practice, the NMD is a close estimate of the average difference between the components of the two vectors  $\{\phi_i^a\}$  and  $\{\phi_i^e\}$ . It seems to be much more sensitive to mode shape differences than the MAC and, therefore, it

can be used to better highlight the differences between highly correlated mode shapes, as in the present case study. In fact, sensitivity analyses carried out on the different models of the Tower of the Nations point out that mode shapes are little sensitive to changes in the elastic properties of materials. Moreover, since the obtained numerical mode shapes are very similar each other and always highly correlated to the experimental ones for all classes of models, the minimization process has been based upon the objective function defined by equation (5.1). However, informations in terms of mode shapes have been indirectly taken into account by mean of the values of participating masses, used as weights in the updating process, as it will be clarified in the following.

The participating mass ratio of a mode is a very important parameter, since it provides a measure of how important a mode is for computing the response of the modelled structure to the acceleration loads in each of the three global directions defined into the model. Thus it is useful for determining the accuracy of response spectrum analyses and seismic time-history analyses. The National Seismic Code states that, when carrying out a dynamic modal analysis, all modes characterized by a participating mass ratio higher than 5% or, alternatively, a number of modes characterized by a total participating mass ratio higher than 85% must be taken into account. This rule can give also an indication about the number of modes to be taken into account during model refinement: however, it often happens that the identified modes are not enough to respect Code regulations. In such a case, obviously, the experimental results are a

### 5.3 THE TOWER OF THE NATIONS (NAPLES)

---

constraint of the model updating procedure. In order to better clarify this concept, the values of mass participating ratios and their cumulative sums for different models of the Tower of the Nations are reported in Table 5.7, Table 5.8, Table 5.9, Table 5.10:

Mode number	Period	UX	UY	SumUX	SumUY	RZ	SumRZ
	Sec	Unitless	Unitless	Unitless	Unitless	Unitless	Unitless
1	1.264569	0.60189	8.53E-07	0.60189	8.528E-07	0.25373	0.25373
2	0.732622	7.36E-07	0.6375	0.60189	0.6375	0.24686	0.50059
3	0.610582	1.49E-08	0.00118	0.60189	0.63868	0.11037	0.61096
4	0.312541	0.17312	3.35E-06	0.77501	0.63869	0.07347	0.68444
5	0.248155	3.16E-06	0.15933	0.77502	0.79801	0.06538	0.74981
6	0.204284	4.53E-08	1.3E-05	0.77502	0.79803	0.0232	0.77301

**Table 5.7.** Participating mass ratios (Floors = Shell - With basement)

Mode Number	Period	UX	UY	SumUX	SumUY	RZ	SumRZ
	Sec	Unitless	Unitless	Unitless	Unitless	Unitless	Unitless
1	1.274395	0.59401	2.95E-06	0.59401	0.00000295	0.25077	0.25077
2	0.731478	2E-06	0.62921	0.59401	0.62921	0.24008	0.49085
3	0.610722	3.25E-08	0.00175	0.59401	0.63096	0.11203	0.60289
4	0.310474	0.17726	3.68E-06	0.77127	0.63097	0.0753	0.67819
5	0.239113	5.24E-06	0.15978	0.77128	0.79075	0.06564	0.74382
6	0.199508	2.21E-08	3.57E-05	0.77128	0.79078	0.02413	0.76795

**Table 5.8.** Participating mass ratios (Floors = Diaphragm - With basement)

Mode Number	Period	UX	UY	SumUX	SumUY	RZ	SumRZ
	Sec	Unitless	Unitless	Unitless	Unitless	Unitless	Unitless
1	1.252382	0.6515	8.12E-07	0.6515	8.12E-07	0.28088	0.28088
2	0.739044	7.3E-07	0.70727	0.6515	0.70728	0.27958	0.56046
3	0.616204	3.4E-08	0.00131	0.6515	0.70858	0.12527	0.68573
4	0.300601	0.16857	3.37E-06	0.82007	0.70859	0.07322	0.75895
5	0.242692	3.0E-06	0.14304	0.82007	0.85163	0.05993	0.81888
6	0.201599	1.3E-10	1.25E-05	0.82007	0.85164	0.0212	0.84008

**Table 5.9.** Participating mass ratios (Floors = Shell - Without basement)

Mode Number	Period	UX	UY	SumUX	SumUY	RZ	SumRZ
	Sec	Unitless	Unitless	Unitless	Unitless	Unitless	Unitless
1	1.249946	0.6811	4.32E-06	0.6811	4.3E-06	0.29309	0.29309
2	0.736663	2.34E-06	0.74746	0.6811	0.74746	0.28952	0.58262
3	0.616499	4.26E-08	0.00215	0.6811	0.74961	0.13613	0.71875
4	0.293002	0.17785	6.72E-06	0.85896	0.74962	0.07713	0.79588
5	0.23281	7.14E-06	0.15578	0.85896	0.90539	0.06467	0.86055
6	0.196982	4.49E-10	5.99E-05	0.85896	0.90545	0.02436	0.88491

**Table 5.10.** Participating mass ratios (Floors = Diaphragm - Without basement)

They point out that, in almost all cases, six modes are not sufficient to get a total mass participating ratio higher than 85%; however, higher modes than the fifth one are characterized by mass participating ratios lower than 5%. As a result, it is possible to focus model refinement on the first six modes of the Tower.

By comparing the results of numerical models in terms of natural frequencies with the experimental values, it is possible to compute the values of the objective function defined by equation (5.1). The number of



### 5.3 THE TOWER OF THE NATIONS (NAPLES)

---

modes  $N_m$  to be taken into account is equal to six. The minimization process has given the results shown in Table 5.11:

Solution	Scatter [%]							
	<i>I</i>	<i>II</i>	<i>III</i>	<i>IV</i>	<i>V</i>	<i>VI</i>	<i>First three</i>	<i>First six</i>
Floor = Diaphragm - Without basement (22500 - 310)	3.08	0.01	2.45	11.56	0.08	1.99	5.54	19.17
Floor = Shell - Without basement (19500 - 390)	10.66	0.68	1.50	0.91	2.98	0.59	12.84	17.31
Floor = Diaphragm - With basement (24250 - 300)	6.05	0.03	2.25	4.07	3.43	0.008	8.32	15.83
Floor = Shell - With basement (24000 - 360)	8.03	2.11	0.008	0.65	4.86	0.12	10.15	15.78

**Table 5.11.** Optimization results (minimization of cumulative error on six modes)

Thus, it has provided an optimum solution for each class of models, but two main drawbacks should be noted. First of all, in almost all cases, the maximum error affects the fundamental mode of the structure, which is also characterized by a high mass participating ratio and, as such, contributes significantly to the structural response. An alternative solution

could be obtained by defining an additional constraint on the minimization process: for example, a maximum scatter, in terms of natural frequency, lower than 5% for each mode involved in the model updating process. When considering this additional constraint, just one class of models gave a possible solution: that one reported in Table 5.12 is obtained from the combination of the limit on the cumulative error on six modes and the limit on the error for each mode. The result obtained in this case is, however, characterized by a slightly higher cumulative error with respect to the previously obtained solution for the same class of models.

Solution	Scatter [%]							
	<i>I</i>	<i>II</i>	<i>III</i>	<i>IV</i>	<i>V</i>	<i>VI</i>	<i>First three</i>	<i>First six</i>
Floor = Shell - With basement (22500 - 310)	4.52	2.31	0.21	4.32	4.75	0.003	7.05	16.12

**Table 5.12.** Optimization results (minimization of cumulative error on six modes and maximum scatter lower than 5% for the single mode)

Moreover, when looking at the cumulative errors of the first six modes, their values are very similar each other, in particular for models characterized by the presence of the basement. Since the first three modes are characterized by a mass participating ratio much higher than the second three modes, a different solution to the refinement problem could be to minimize the cumulative error of the first three modes and to look at

### 5.3 THE TOWER OF THE NATIONS (NAPLES)

---

the errors on the second three modes (Table 5.13). However, the obtained solutions are characterized by a higher error on six modes. Thus, the solution to the minimization problem is not unique and a final choice without additional informations is not easy.

Solution	Scatter [%]							
	<i>I</i>	<i>II</i>	<i>III</i>	<i>IV</i>	<i>V</i>	<i>VI</i>	<i>First three</i>	<i>First six</i>
Floor = Diaphragm - Without basement (24000 - 310)	0.004	1.81	0.69	15.04	1.46	3.60	2.50	22.62
Floor = Shell - Without basement (24750 - 310)	0.19	1.48	0.64	12.14	2.67	1.23	2.32	18.35
Floor = Diaphragm - With basement (26500 - 300)	1.91	2.53	0.25	8.57	1.21	2.29	4.70	16.77
Floor = Shell - With basement (28000 - 300)	1.15	2.37	0.27	7.85	4.81	0.10	3.80	16.56

**Table 5.13.** Optimization results (minimization of cumulative error on the first three modes)

The minimization process has been, then, repeated by weighting the scatter in terms of natural frequency for each mode by the corresponding mass participating ratio for all the models in the different classes. In such a

case, the solutions obtained during the minimization process are unique within each class, apart from the number of considered modes. The optimum models for the four classes are shown in Table 5.14:

Solution	Scatter [%]							
	<i>I</i>	<i>II</i>	<i>III</i>	<i>IV</i>	<i>V</i>	<i>VI</i>	<i>First three</i>	<i>First six</i>
Floor = Diaphragm – Without basement (24000 – 300)	0.04	1.08	1.40	14.96	0.61	2.75	2.52	20.84
Floor = Shell – Without basement (24750 – 300)	0.24	0.75	1.35	12.04	3.41	0.46	2.34	18.27
Floor = Diaphragm – With basement (27500 – 300)	0.13	3.64	1.33	10.51	0.25	3.29	5.10	19.15
Floor = Shell – With basement (28500 – 300)	0.30	2.90	0.79	8.77	4.33	0.40	3.99	17.49

**Table 5.14.** Optimization results (weighted)

This procedure has, therefore, provided, for each class of models, the solution that minimizes the scatter with respect to experimental data and, at the same time, gives the best results in terms of response spectrum and seismic time-history analyses: it is evident that it is not simply the solution

### 5.3 THE TOWER OF THE NATIONS (NAPLES)

---

minimizing the cumulative scatter. Moreover, by looking at Table 5.14, it is clear that the better agreement with experimental data is obtained by modelling floors as shell elements. The need to calibrate optimization on the first six modes shows that the refined model is characterized by presence of the basement, floors modelled as shells,  $E_c = 28500$  MPa,  $G_t = 300$  MPa. This result is confirmed also by the correlation between analytical and experimental mode shapes, expressed in terms of NMD in Table 5.15:

Solution	NMD					
	<i>I</i>	<i>II</i>	<i>III</i>	<i>IV</i>	<i>V</i>	<i>VI</i>
Floor = Shell - Without basement (24750 - 300)	0.242	0.076	0.319	0.306	0.140	0.352
Floor = Shell - With basement (28500 - 300)	0.207	0.060	0.309	0.285	0.126	0.347

**Table 5.15.** Mode shape correlation

The MAC matrix between experimental and numerical mode shapes for the identified optimum model is shown in Figure 5.24.

In conclusion, this case study points out how an optimization process can be better driven by the objectives of seismic analyses, allowing a clearer definition of the optimum solution. In particular, due to their importance for seismic analyses, modal mass participating ratios have been

considered as weights for the updating process. The obtained results in terms of elastic properties of materials (the parameters of the updating process) are reasonable. Thus, dynamic measurements based on environmental vibrations, together with effective model refinement procedure, constitute an opportunity, in particular in the case of heritage structures, for minimization of the impact of structural assessment on existing constructions. However, efficiency of numerical procedures adopted to extract modal parameters and a quantification of the error of estimates are still an issue in the field, even if in the literature some attempts of model refinement aiming at deal with uncertainties affecting both the models and the experimental results (Gabriele et al. 2007, Hanns 2005) can be found.

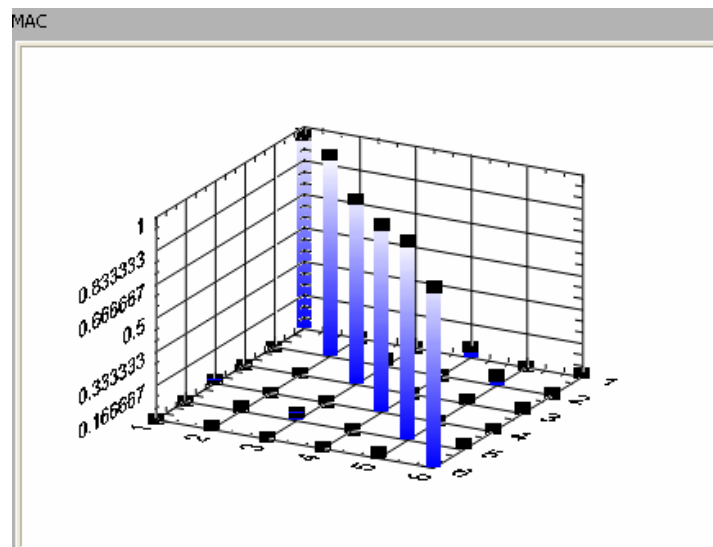


Figure 5.24. MAC matrix for the refined FE model

### 5.3 THE TOWER OF THE NATIONS (NAPLES)

---

In the present case study, the optimization process has allowed also the investigation of different modelling aspects, pointing out, first of all, the importance of curtain walls on the dynamic response of a structure, at least for low levels of excitation. About modelling of floors, sensitivity analyses have shown that, for the present case study, the two different assumptions were nearly equivalent, but the actual response of the structure was better reproduced by the models characterized by floors modelled by shell elements, keeping the other modelling assumptions constant. Finally, the basement has a not negligible importance on the global dynamic behaviour of the structure, in particular when higher modes are considered.

#### 5.3.8 Other OMA tests

Two years after the first dynamic test, a second one has been carried out. Two records of the structural response in operational conditions, indicated as TdN1 and TdN2 and characterized by a length of about 25 minutes and 40 minutes, respectively, and a sampling frequency of 100 Hz, have been obtained. They have not been used in the model refinement application but for damping estimation. The modal parameters obtained from these measurements by applying EFDD and SSI methods are reported here also because these records have been used to test the fully automated modal parameter identification procedure described in the next chapter.

Just eight sensors have been used: four of them were placed at the fifth floor and the others on the roof. Results of modal identification obtained by applying the EFDD method are reported in Table 5.16.

Record	Number of averages	Mode number	Type	Natural frequency [Hz]	Damping ratio [%]
TdN1	42	I	Translation	0.813	0.75
		II	Translation	1.375	1.09
		III	Torsion	1.758	0.88
TdN2	69	I	Translation	0.812	0.94
		II	Translation	1.362	1.42
		III	Torsion	1.727	1.21

**Table 5.16.** Tower of the Nations: results of modal identification (EFDD)

When damping has been evaluated by mean of EFDD, a high number of averages and a fine frequency resolution (0.01 Hz) have been considered, in compliance with the criteria outlined in Chapter 4.

Modal parameter estimation by SSI methods has been carried out by mean of sensitivity analyses of natural frequency and damping estimates with respect to the number of block rows  $i$ . Mean and standard deviation of natural frequencies and damping ratios have been computed by considering all stable poles for each mode and each value of  $i$ . Results of modal identification are reported in Table 5.17 for Cov-SSI and Table 5.18 for DD-SSI.

Sensitivity analyses have shown that stabilization improves by increasing the value of  $i$ , thus reducing the variance of estimates, which converge to a certain value. However, if it is set too high, spurious poles can appear



### 5.3 THE TOWER OF THE NATIONS (NAPLES)

---

close to physical ones and they can be erroneously identified as stable. By stopping sensitivity analyses at values of  $\delta$  preventing such phenomenon, stable values of modal parameter estimates, characterized by moderate variance, can be identified.

Record	Number of block rows	Mode number	Type	Natural frequency [Hz]	Damping ratio [%]
TdN1	40	I	Translation	0.812	0.40
		II	Translation	1.375	1.17
		III	Torsion	1.757	0.63
TdN2	40	I	Translation	0.812	0.68
		II	Translation	1.362	1.31
		III	Torsion	1.730	0.77

**Table 5.17.** Tower of the Nations: results of modal identification (Cov-SSI)

Record	Number of block rows	Mode number	Type	Natural frequency [Hz]	Damping ratio [%]
TdN1	40	I	Translation	0.812	0.44
		II	Translation	1.375	1.09
		III	Torsion	1.756	0.59
TdN2	40	I	Translation	0.812	0.74
		II	Translation	1.361	1.19
		III	Torsion	1.733	0.64

**Table 5.18.** Tower of the Nations: results of modal identification (DD-SSI)

Estimates in good agreement each other have been obtained from the different methods: however, EFDD seems to provide a slight overestimation of damping with respect to SSI methods. The influence of tuff masonry walls infilled in the r.c. frames is pointed out by the higher

value of damping ratio for the second mode in comparison with other modes.

#### **5.4 THE SCHOOL OF ENGINEERING MAIN BUILDING (NAPLES)**

The School of Engineering Tower in Naples is a tall r.c. building of thirteen stories of which the first two are underground: further details about the building are reported in section 6.3.

The building has been instrumented with a permanent Structural Health Monitoring system, whose main characteristics will be described in the next chapter. Here just the results of output-only modal identification are reported based on different datasets: the first record, named RC0, has been taken during the night of an ordinary day in the middle of the week; the second record, RC1, is equivalent to the first one but relative to morning hours, when the level of ambient vibrations is higher; the last two records, RC2 and RC3, have been, instead, taken during two crowded football matches at the close stadium. Record durations are 20' for RC0 and RC1, 55' for RC2, 63'20" for RC3: the sampling frequency is 100 Hz for all records. Hanning window and 66% overlap have been used for spectrum computation: a frequency resolution of 0.01 Hz has been obtained. Results of modal identification by applying EFDD and SSI methods will be useful to assess performance of the automated modal identification algorithm described in the next chapter.

#### 5.4 THE SCHOOL OF ENGINEERING MAIN BUILDING (NAPLES)

---

Twelve sensors have been used for modal identification: four of them were placed at the fourth floor of the building, four at the seventh floor and the others on the roof.

Results of modal identification obtained by applying the EFDD method are reported in Table 5.19:

Record	Number of averages	Mode number	Type	Natural frequency [Hz]	Damping ratio [%]
RC0	33	I	Prev. transl. (long side)	0.921	1.03
		II	Prev. transl. (short side)	0.982	1.25
		III	Prev. torsion.	1.299	1.03
RC1	33	I	Prev. transl. (long side)	0.920	1.08
		II	Prev. transl. (short side)	0.985	1.59
		III	Prev. torsion.	1.299	0.76
RC2	96	I	Prev. transl. (long side)	0.933	1.50
		II	Prev. transl. (short side)	0.990	0.93
		III	Prev. torsion.	1.310	0.94
RC3	111	I	Prev. transl. (long side)	0.926	1.40
		II	Prev. transl. (short side)	0.990	1.48
		III	Prev. torsion.	1.304	0.79

**Table 5.19.** School of Engineering: results of modal identification (EFDD)

Modal parameter estimation by SSI methods has been carried out by mean of sensitivity analyses of natural frequency and damping estimates with respect to the number of block rows  $i$ , as described in the previous section.

Results of modal identification are reported in Table 5.20 for Cov-SSI and Table 5.21 for DD-SSI.

Estimates in good agreement each other have been obtained from the different methods: also in this case, however, EFDD provides a slight overestimation of damping ratios with respect to SSI methods. This is probably an effect of partial identification of SDOF Bell functions in presence of close modes and of windowing, which is mitigated in presence of a high number of averages and a fine frequency resolution, but not completely removed.

Record	Number of block rows	Mode number	Type	Natural frequency [Hz]	Damping ratio [%]
RC0	40	I	Prev. transl. (long side)	0.922	1.07
		II	Prev. transl. (short side)	0.982	1.08
		III	Prev. torsion.	1.298	0.82
RC1	40	I	Prev. transl. (long side)	0.920	1.32
		II	Prev. transl. (short side)	0.985	1.02
		III	Prev. torsion.	1.299	0.64
RC2	60	I	Prev. transl. (long side)	0.932	1.37
		II	Prev. transl. (short side)	0.991	0.84
		III	Prev. torsion.	1.310	0.71
RC3	60	I	Prev. transl. (long side)	0.927	1.05
		II	Prev. transl. (short side)	0.990	1.19
		III	Prev. torsion.	1.303	0.71

**Table 5.20.** School of Engineering: results of modal identification (Cov-SSI)

#### 5.4 THE SCHOOL OF ENGINEERING MAIN BUILDING (NAPLES)

Record	Number of block rows	Mode number	Type	Natural frequency [Hz]	Damping ratio [%]
RC0	60	I	Prev. transl. (long side)	0.921	0.98
		II	Prev. transl. (short side)	0.981	1.00
		III	Prev. torsion.	1.298	0.83
RC1	40	I	Prev. transl. (long side)	0.921	1.27
		II	Prev. transl. (short side)	0.984	0.92
		III	Prev. torsion.	1.301	0.61
RC2	40	I	Prev. transl. (long side)	0.936	1.21
		II	Prev. transl. (short side)	0.991	0.84
		III	Prev. torsion.	1.311	0.64
RC3	40	I	Prev. transl. (long side)	0.926	1.06
		II	Prev. transl. (short side)	0.989	1.07
		III	Prev. torsion.	1.304	0.71

**Table 5.21.** School of Engineering: results of modal identification (DD-SSI)

Seeking for completeness, sensitivity of natural frequencies and damping ratios to the number of block rows for one of the considered records (RC3) is reported in Figure 5.25, Figure 5.26, Figure 5.27: these results have been obtained by applying the Cov-SSI method, but similar results are given by DD-SSI.

Correlation among mode shapes provided by the different methods is very high, as pointed out by the CrossMAC matrices shown in Figure 5.28.

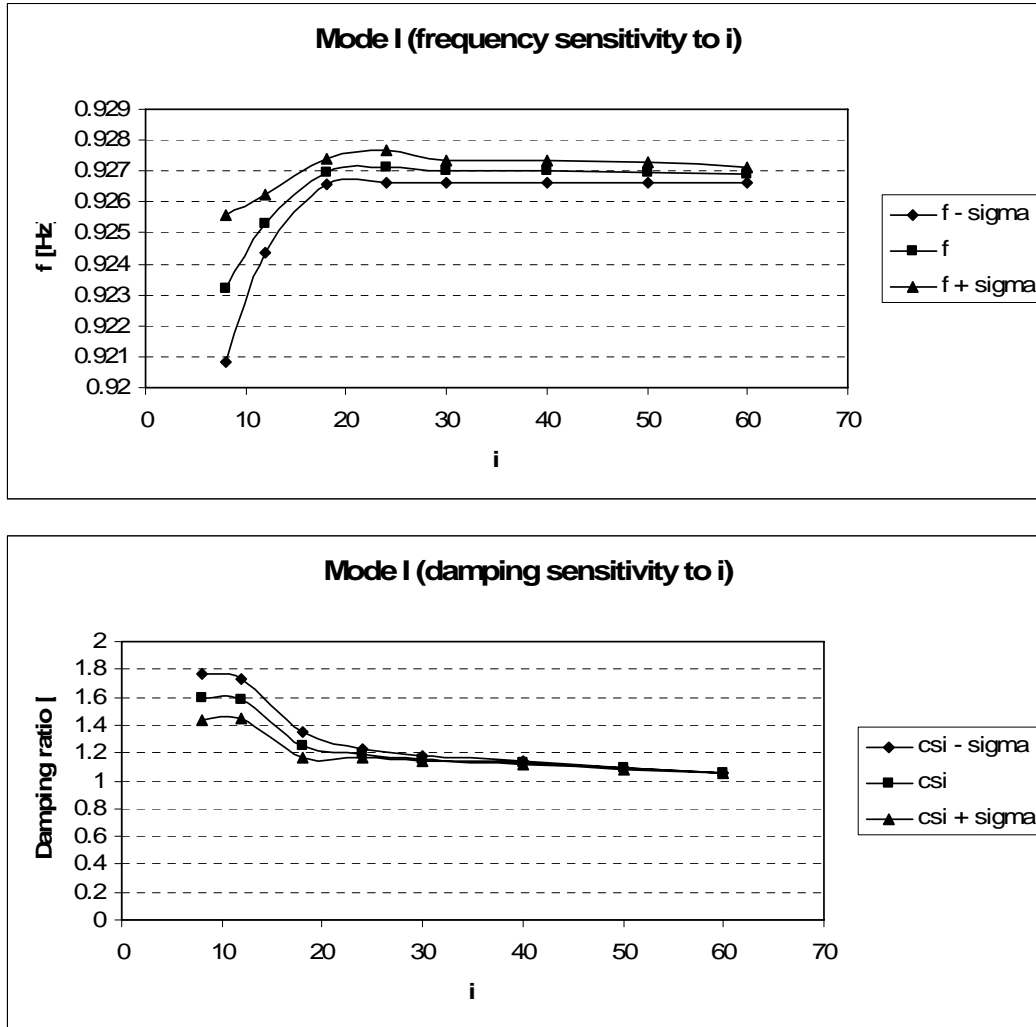


**Figure 5.25.** Influence of the number of block rows on natural frequency and damping ratio estimates (mode 1 – RC3 – Cov-SSI)

## 5.4 THE SCHOOL OF ENGINEERING MAIN BUILDING (NAPLES)

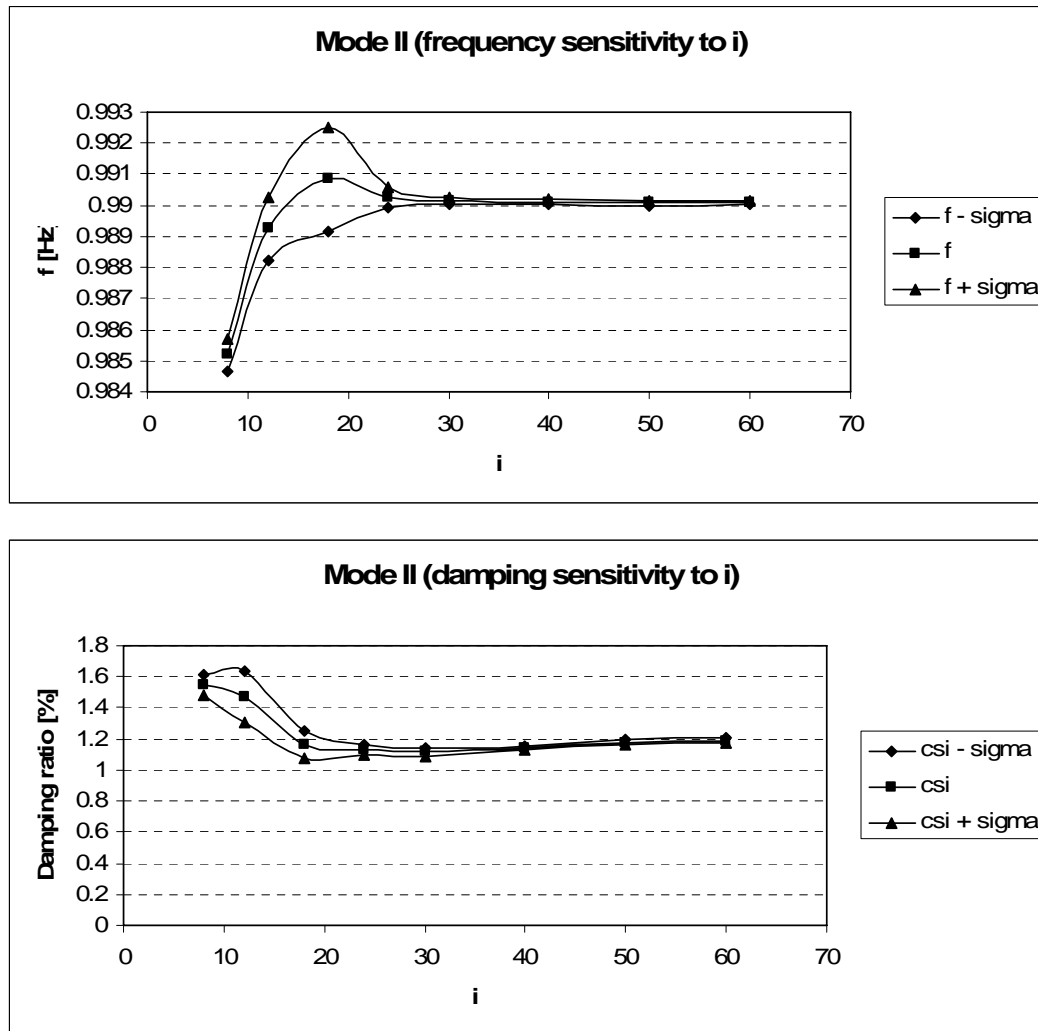


**Figure 5.26.** Influence of the number of block rows on natural frequency and damping ratio estimates (mode 2 - RC3 - Cov-SSI)

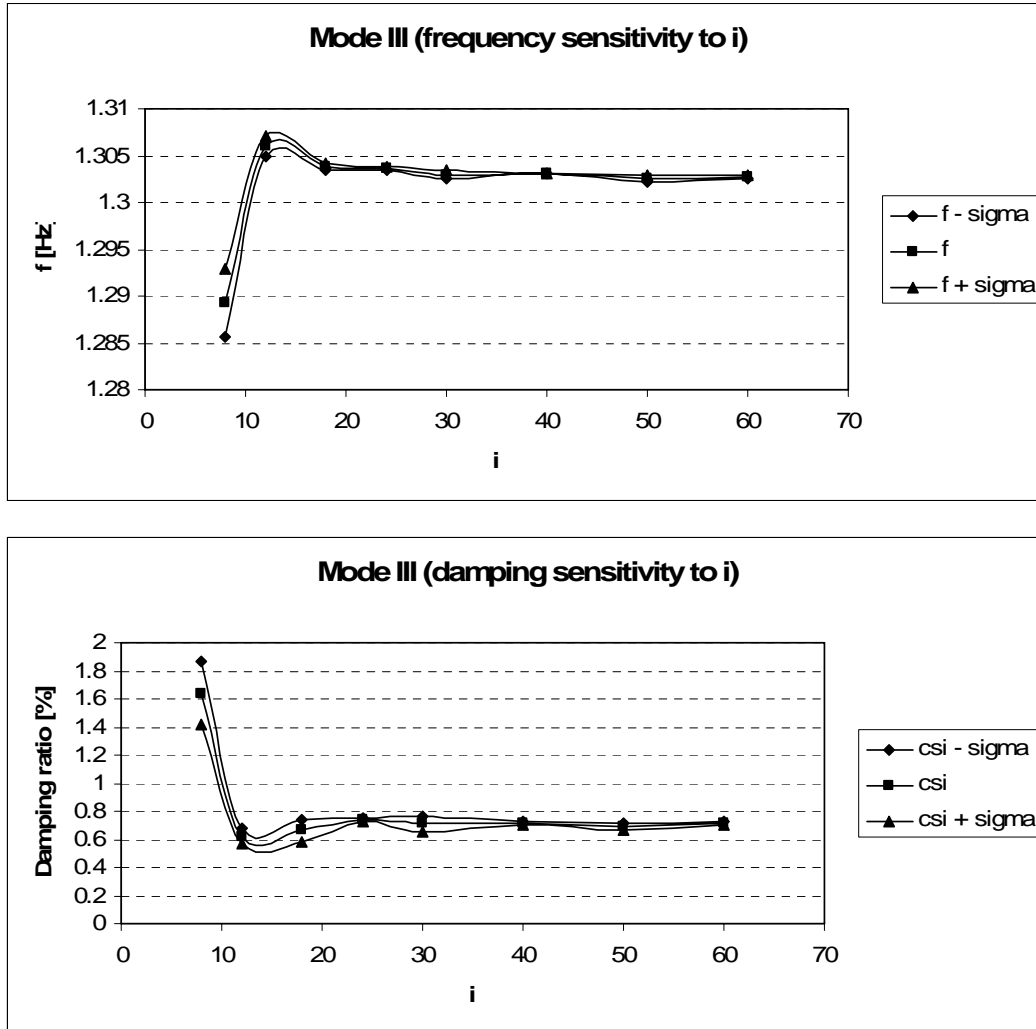
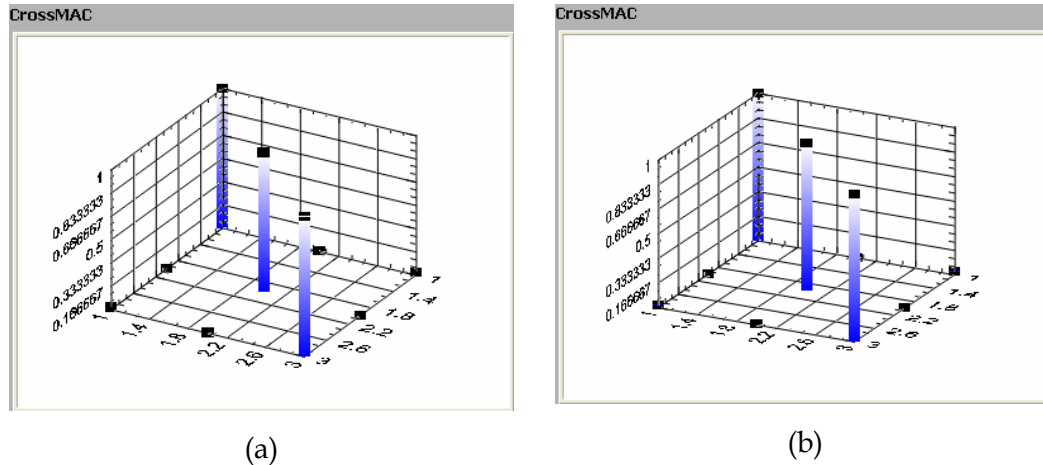


**Figure 5.27.** Influence of the number of block rows on natural frequency and damping ratio estimates (mode 3 - RC3 - Cov-SSI)



## 5.4 THE SCHOOL OF ENGINEERING MAIN BUILDING (NAPLES)

---



In Figure 5.29 a picture of the bell tower is shown; it is worth noticing that the tower is not separated from the surrounding structures.



**Figure 5.29.** S. Maria del Carmine bell tower – courtesy of Ceroni F.

A number of tests has been carried out in order to investigate the mechanical properties of materials (Ceroni et al. 2006, Ceroni et al. 2007) to be used in the numerical model of the structure. Moreover, some dynamic tests have been carried out in order to refine the FE model. Particular

## 5.5 “S. MARIA DEL CARMINE” BELL TOWER (NAPLES)

---

attention has been focused on mode shapes of the first two bending modes, because of their importance in linear and non-linear static analyses.

Sensors used for the present application are EpiSensors ES-U2 by Kinemetrics Inc., like in the case of the Tower of the Nations. However, a National Instrument PXI-4472 system has been used for data acquisition.

The first two modes of the structure, obtained from output-only modal identification, are bending modes characterized by a natural frequency of 0.70 Hz and 0.76 Hz, respectively. Figure 5.30 shows the singular value plots obtained by applying EFDD to the time histories courteously made available by Dr. Ceroni (University of Sannio). Results of modal identification by applying the different algorithms are reported in Table 5.22, Table 5.23, Table 5.24.

Mode number	Frequency [Hz]	Damping ratio [%]
1	0.70	0.99
2	0.76	1.0

**Table 5.22.** S. Maria del Carmine bell tower: results of identification (EFDD)

Mode number	Frequency [Hz]	Damping ratio [%]
1	0.70	0.9
2	0.76	0.8

**Table 5.23.** S. Maria del Carmine bell tower: results of identification (Cov-SSI)

Mode number	Frequency [Hz]	Damping ratio [%]
1	0.70	0.9
2	0.76	0.7

**Table 5.24.** S. Maria del Carmine bell tower: results of identification (DD-SSI)

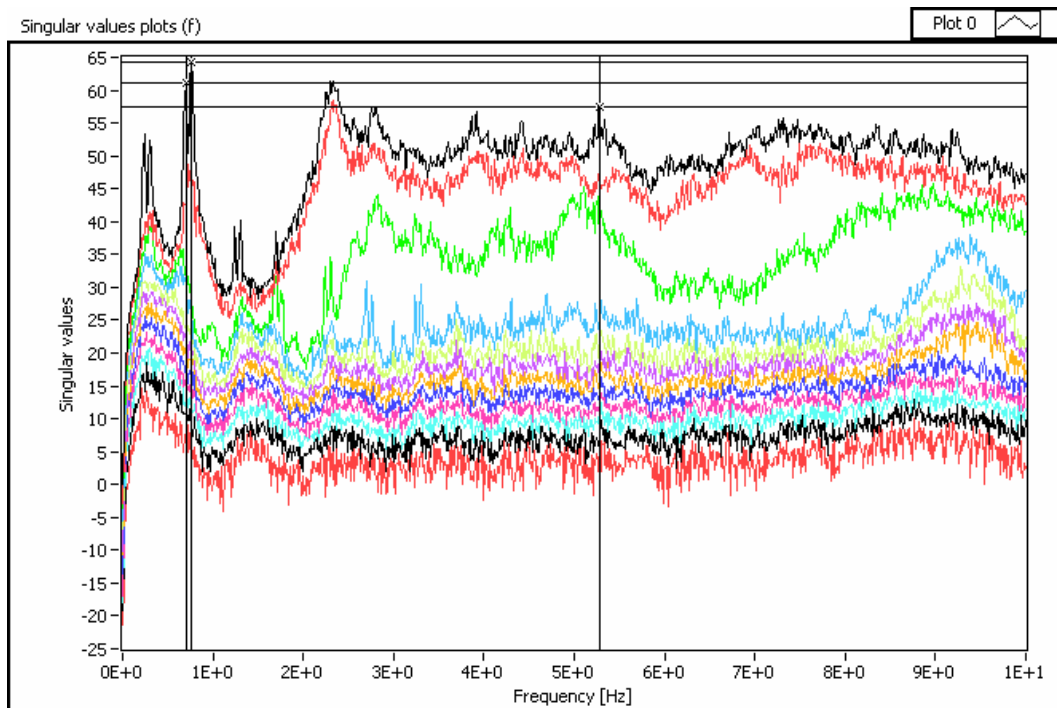


**Figure 5.30.** S. Maria del Carmine bell tower: Singular Value plots (EFDD)

Also this record has been used to test the automated modal parameter identification procedure described in the next chapter.

### 5.6 REMARKS

The above described case studies show that a reliable estimation of model parameters is provided by both time and frequency domain methods.

The first two case studies point out potentialities of OMA as a tool for model refinement, but also of FE modelling as a tool for design of test setups.

OMA, in combination with FE model updating, can be considered as a non-destructive technique for structural assessment; the optimized model, moreover, allows an accurate definition of the performance of structures under dynamic (and, in particular, seismic) loads. Updating techniques play a relevant role, in particular towards historical constructions, where destructive tests must be as limited as possible: thus, informations obtained from dynamic tests in operational conditions can provide fundamental knowledge about these unique structures, allowing a better definition of structural schemes and, in some cases, an indirect identification of material properties. Refined models are valuable also for optimized design of interventions. Finally, an accurate definition of the mode shape of the fundamental mode of the structure is useful also for definition of the system of static forces proportional to the first mode shape to be used in pushover analyses.

---

# 6

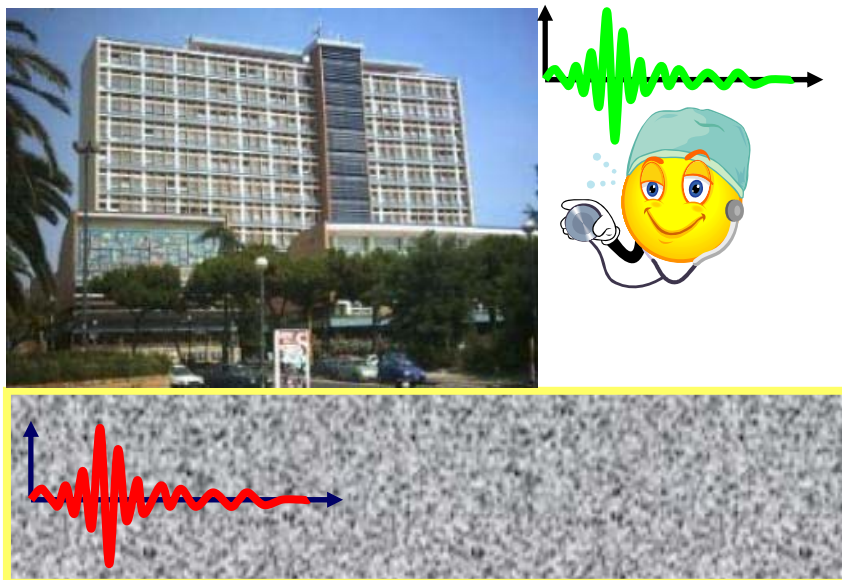
## OMA and SHM

---

*«So we can do OMA efficiently.*

*Now what?»*

*James Brownjohn*





## CHAPTER 6

### 6.1 INTRODUCTION

Structural Health Monitoring (SHM) and damage identification are assuming larger and larger importance in civil, mechanical and aerospace engineering. Structural Health Monitoring for civil structures, in particular, is becoming increasingly popular in Europe and worldwide, also because of the opportunities that it offers in the fields of construction management and maintenance. The main advantages related to implementation of such techniques are: reduction of inspection costs; research, resulting in the possibility to better understand the structural behaviour under dynamic loads; seismic protection; real or near real-time observation of the structural response and of damage evolution; possibility to develop post-earthquake scenarios and support rescue operations.

SHM is defined as the use of in-situ, non-destructive sensing and analysis of structural characteristics in order to identify if damage has occurred, to define its location and to estimate its severity, to evaluate its consequences on residual life of the structure (Silkorsky 1999). Even if SHM is a



## 6.1 INTRODUCTION

---

relatively new paradigm in civil engineering, the assessment of the health state of a structure by tests and measurements is a common practice, so that evaluation and inspection guidelines are available since a long time (Mufti 2001): SHM objectives are consistent with the practice of periodic tests but it takes advantage of the new technologies in sensing, instrumentation, communication and modelling in order to integrate them into an intelligent system. Even if periodic tests are still carried out, lots of new applications are appearing: they take advantage of web based technologies and advances in communications for real-time or near real-time continuous monitoring of structures. However, the increasing development of new and reliable high performance hardware, including also sensing and measurement systems, does not match with an equally fast progress in data processing algorithms, in particular with respect to reliability of damage extension estimation and prediction of residual life of the monitored structure.

Structural Health Monitoring is a very multidisciplinary field, where a number of different skills (seismology, electronic and civil engineering, computer science) and institutions can work together in order to increase performance and reliability of such systems, whose promising perspectives seem to be almost clearly stated.

Informations obtained from such systems can be useful for maintenance or structural safety evaluation of existing structures, rapid evaluation of conditions of damaged structures after an earthquake, estimation of residual life of structures, repair and retrofitting of structures,

## 6. OMA AND STRUCTURAL HEALTH MONITORING

---

maintenance, management or rehabilitation of historical structures. As reported in (Aktan et al. 1999, Chang 1999), reduction of down time and improvement in reliability enhance the productivity of the structure: monitoring results can be used also to have a deeper insight in the structural behavior, thus improving design of future structures.

In order to get all these objectives, an effective Structural Health Monitoring system should be based on integration of several types of sensors in a modular architecture. Moreover, the advances in the field of Information and Communication Technology assure data transmission also in critical conditions. It is worth noticing, however, that availability of procedures able to reduce transmission data volumes is a key aspect for reliability and sustainability of such systems, in particular when several constructions are monitored at the same time and supervised by a single network control centre.

In the following sections, worldwide SHM systems are reviewed and open issues in the field are reported, together with a description of the SHM system installed on the School of Engineering Main Building at University of Naples. Data continuously coming from this system have been crucial for successful implementation and testing of fully automated OMA procedures, which play a primary role into SHM strategies.

### 6.2 SHM: STATE-OF-THE-ART AND OPEN ISSUES

A monitoring system consists of a variety of sensors to monitor the environment and the structural response to loads. A typical architecture of monitoring systems is based on remote sensors wired directly to a centralized data acquisition system. However, the expensive nature of this architecture, due to high installation and maintenance costs associated with system wires (Lynch 2002), is causing replacement of wire-based systems with new low-cost wireless sensing units by spreading knowledge over the entire monitoring network. As a consequence, a larger effort is currently required in order to build effective data processing algorithms, taking into account such a new architecture. Another relevant task is related to the strategies to be implemented in order to manage data and combine informations coming from a variety of sensors and, therefore, related to different physical variables.

In the field of damage detection, a lot of algorithms has been proposed on the base of several different mechanical and physical principles (Doebbling et al. 1996, Farrar et al. 2007). However, they can be classified into two main classes: a first group of techniques, the so-called “modal-based” algorithms, aims at tracking changes in structural response directly or indirectly related to the mechanical characteristics (such as natural frequencies, mode shapes, etc.) of the structure before and after damage. Conversely, the second approach is based on post-processing of data to detect anomalies directly from measurements (ARMAV modelling, wavelet decomposition, etc.). In both cases, the trend is in using methods

able to automate the detection process by taking advantage of the recent advances in information technologies (Aktan et al. 2005, Rainieri et al. 2007a, Brincker et al. 2007). In this framework, identification of modal parameters of structures under operational conditions plays a primary role. Recently, some strategies have been set up in order to automate identification and tracking of modal parameters, thus allowing a full integration of modal identification within SHM systems. Such techniques will be discussed in the following.

Reliable procedures are necessary also towards data reduction and transmission, in particular when a limited communication bandwidth is available, such as after an earthquake: wavelet-based approaches seems to be particularly promising in this field (Li et al. 2007, Mizuno & Fujino 2007). However, real-time interpretation of data can fail due to their poor quality and, in particular, in case of sensors failure: therefore, in case of automated applications, this verification must be conducted by the data processing system itself. Recently, some interesting approaches have been proposed to this aim (Kraemer & Fritzen 2007).

The most recent and innovative applications concern of possible interaction among earthquake early warning, structural health monitoring and structural control. However, unlike traditional seismic monitoring, an event driven monitoring system is not useful: continuous condition assessment and performance-based maintenance of civil infrastructures are necessary in order to assess the short-term impact due to earthquakes and the long-term deterioration process due to physical aging and routine

## 6.2 SHM: STATE-OF-THE-ART AND OPEN ISSUES

---

operation. In this framework, a monitoring system can be used also for disaster and emergency management, traffic control, damage evaluation, post-earthquake scenario definition. The use of monitoring systems on underground pipeline systems may be considered as an example of post-earthquake emergency management: damaged gas utilities, in fact, can cause secondary disasters and, as a consequence, serious losses. In this case, informations about abnormal pressure changes in gas pipelines can lead to an emergency shut-off. Similar controls can affect traffic, if informations about structural integrity of infrastructures are available. Knowledge of still operable bridges can help decision makers to arrange a route to the disaster area for rescue personnel and goods.

A comprehensive SHM system should be based on an appropriate number of sensors, usually of different types and performance, but, above all, on an efficient data processing system which acquires sensor outputs, processes data and eventually provides an alarm: thus, data processing, reduction and storage, sampling frequency and simultaneous sampling are fundamental issues, in particular in presence of a large number of sensors installed on the monitored structure. For a real time response of the system, data must be collected, stored, assessed for validity and processed within a very short time. This is crucial in particular for those applications where SHM systems are in conjunction with structural control systems (Kanda et al. 1994).

Sampling frequency has to be accurately chosen in order to acquire and retain an optimized amount of data: together with filtering, this is an issue

## 6. OMA AND STRUCTURAL HEALTH MONITORING

---

related to data reduction and storage which cannot be neglected. Moreover, if several sensors are connected to a single unit, a significant time delay with respect to the response of the structure could arise, thus affecting the real-time behavior of the monitoring system.

The problem of simultaneous sampling is easily solved when a single data logger is used: in fact, data synchronization is governed by the switch rate of the data logger (McConnell & Reiley 1987). If two or more loggers are used, instead, particular strategies have to be adopted in order to ensure simultaneous sampling. Since the number of sensors is rapidly increasing and their type differentiating, modular architectures are spreading. Redundancy is another important characteristic of the last applications in the SHM field which increases the number of sensors and communication systems to be managed. All these reasons, together with the new wireless sensor networks, make simultaneous sampling a fundamental task for design and implementation of SHM systems.

Sensor choice depends on the structure and the monitoring requirements: no sensor can be assumed as the best system for every SHM application. A network of different types of sensors may often be necessary for a given monitoring application. Thus, the first task in design and installation of a monitoring system is related to the choice of appropriate sensors (strain gauges, accelerometers, FBG sensors, temperature sensors, anemometers, load cells and so on) and to definition of the main issues related to installation and data processing (additional mass due to sensors and wires, maintenance of sensors, data volume and processing time).

## 6.2 SHM: STATE-OF-THE-ART AND OPEN ISSUES

---

Protection of sensors, wires and connections is fundamental to ensure durability of the SHM system and data quality. For some types of sensors, electromagnetic radiation (EMR) effects must be considered. Fiber Optic Sensors (FOS) are being more and more used because they can overcome this drawback. A comprehensive description of FOS can be found in (Fixter & Williamson 2006) together with a comparison with traditional strain gauges. Other interesting trends are the miniaturization of sensors, represented by the so-called Micro Electro-Mechanical Systems (MEMS), and the adoption of wireless techniques (De Stefano 2007, Lynch 2002). Wireless sensing is quickly spreading because remote interrogation provides huge benefits for applications characterized by a difficult access to the structure. However, simultaneous sampling and data losses are not fully overcome drawbacks. MEMS, instead, allow also the introduction of active elements, in order to obtain the so-called active sensors, which can work both as sensors and actuators. Currently, they are widely used in aerospace but their use is spreading also in civil engineering.

SHM systems have been applied to a variety of structures, such as buildings, bridges, pipelines ([www.ishmii.org/News/2004\\_07\\_15\\_FOSpipeline.html](http://www.ishmii.org/News/2004_07_15_FOSpipeline.html)), wind turbine blades (Sørensen et al. 2002). A synthesis is reported in Table 6.1.

SHM of bridges can provide a reduction in maintenance costs and confidence in the performance of the structure. Several applications of health monitoring to bridges are reported in the literature (Seim & Giacomini 2000, Omenzetter et al. 2004, Liu et al. 2007, Enckell 2007).

## 6. OMA AND STRUCTURAL HEALTH MONITORING

Country	Structure	Year	N° of sensors	Seismic zone	Sensor type	Main features
Canada	Pipelines	2004	N.A.	No	FOS	N.A.
Denmark	Wind turbine	2002	N.A.	No	FOS, MEMS accelerometers	N.A.
USA	Prestressed concrete pile	2008	8 (4 + 4)	No	Accelerometers, Strain gauges	Embedded wireless sensors
USA	Golden Gate Bridge	2000-06	64 nodes	Yes	Wireless accelerometers	The largest wireless sensor network for SHM
China	Donghai Bridge	2006	8	Yes	GPS Antennas	GPS-based SHM system
Sweden	Gröndal Bridge	2004	$\geq 30$	No	FOS, LVDT's	Comparison FOS-LVDT
Portugal	Historical structures	2005	$\leq 10$	Yes	Accelerometers	SHM of historical structures
Italy	School of Engineering Tower	2006	$\leq 30$	Yes	Accelerometers	Automated OMA

**Table 6.1.** Worldwide SHM systems

The Donghai Bridge SHM system in China (Liu et al. 2007) is an interesting example of application of GPS antennas in structural monitoring: however, low sampling rates (10 Hz maximum) are currently available and, therefore, GPS is not yet suitable for a wide range of applications. In Täljsten et al. (Täljsten et al. 2007) a performance comparison between FOS and LVDT's for SHM applications points out the effectiveness of FOS but also the high



## 6.2 SHM: STATE-OF-THE-ART AND OPEN ISSUES

---

cost of a FOS-based monitoring system: thus, it seems to be more suitable for periodic than for continuous monitoring.

Geotechnical applications of FOS are reported in (Habel et al. 2007), where such sensors have been used extensively in Geosynthetics and, above all, in micro piles for corrosion and damage detection purposes. However, a few applications of embedded sensors in piles are reported in the literature. Song & Zhou (Song & Zhou 2007) have monitored steel reinforcement and soil stresses for static purposes. Szyniszewski et al. (Szyniszewski et al. 2008), instead, installed wireless sensors during casting of prestressed concrete piles in order to monitor stresses and accelerations during driving: however, their interest was focused only on preventing microcracking of piles during driving, thus extending life of such elements in a marine environment. Use of SHM systems for assessment of performance of geotechnical structures is, therefore, not very spread: however, the dynamic behaviour of special structures, such as flexible retaining walls, under seismic load conditions or soil-structure interaction effects is currently not fully understood. In order to overcome this lack of knowledge in the geotechnical field, an innovative SHM system, combining structural, geotechnical and seismological skills, has been recently designed at University of Molise (Fabbrocino et al. 2008) and it is currently under implementation. At the present time, two adjacent piles of a flexible retaining wall have been already instrumented by embedded accelerometers and functionality tests have been carried out; moreover, at completion, the system will cover several interesting aspects, ranging from the dynamic behaviour of buildings and flexible retaining

walls to soil-structure interactions and site specific early warning: thus, it seems to be a promising application in the field of Structural Health Monitoring.

Monitoring of buildings is desirable particularly in areas prone to earthquakes and strong winds, or for historical or heritage structures (Ramos et al. 2007, Glisic et al. 2007, Turek & Ventura 2007, Thibert et al. 2007). In Mita et al. (Mita et al. 2006) an automatic data management system based on Matlab Web Server, with several buildings monitored at the same time, is described. The School of Engineering Tower SHM system in Naples is an example of Italian application in this field. It is an example of integration between structural monitoring and seismic early warning (Rainieri et al. 2006, Rainieri et al. 2007b).

### 6.3 THE SCHOOL OF ENGINEERING MAIN BUILDING SHM SYSTEM

The main characteristics of the SHM system, designed and implemented at University of Naples and installed at the School of Engineering Main Building, are herein outlined since they are functional to the description of the automated modal identification procedures described in the following. The SHM system of the School of Engineering in Naples has been designed and implemented in the framework of a specific research project aiming at integration of Structural Health Monitoring and Earthquake Early Warning of strategic structures and infrastructures. It is currently

### 6.3 THE SCHOOL OF ENGINEERING MAIN BUILDING SHM SYSTEM

---

undergoing some interventions in order to allow its integration with that one under implementation at University of Molise (Fabbrocino et al. 2008). The following description of the system architecture takes into account changes due to the new design process.



**Figure 6.1.** The School of Engineering Main Building

The School of Engineering Tower in Naples (Figure 6.1) is a tall building of thirteen stories of which the first two are underground: the floor-to-floor height is about 4.2 m. The original design of the building was made by L. Cosenza ([www.luigicosenza.it](http://www.luigicosenza.it)) according to obsolete National design codes. It was originally characterized by a reinforced concrete structure, designed and built during early 1960s to bear gravity loads and wind: two exterior walls give stiffness in the short direction of the structure, along which there are only three orders of columns. After the

Irpinia Earthquake (1980) the framed r.c. structure underwent some minor interventions in order to strengthen it with respect to seismic loads.

The building is located in a very urbanized area, near some surface and underground railways and near the stadium: thus, employment of high sensitivity sensors in combination with a good level of ambient excitation allows a continuous monitoring of the health state of the structure in its operational conditions. Moreover, the structure is located in a high seismic risk area, such as the Neapolitan area of Campi Flegrei, classified as second seismic category. The seismic activity of the area is monitored by the national seismic network of Istituto Nazionale di Geofisica e Vulcanologia (INGV) and also by the seismic network implemented by the Regional Center of Competence on Analysis and Monitoring of Environmental Risk (CRdC-AMRA) (Weber et al. 2006). It is worth emphasizing that the School of Engineering Main Building is located not too far (about 100 km) from the Irpinia fault and that the above cited regional seismic network is real-time.

The continuous availability of good levels of ambient excitation and the closeness with a fault and with a real-time seismic network have provided the ideal conditions for implementation of a combined SHM-EWS system.

A schematic representation of the designed system is reported in Figure 6.2. The local server has to store, validate and process data, and transmit the results of analyses to the master server, where these results are stored and used for definition of maintenance or rescue strategies. On the master

### 6.3 THE SCHOOL OF ENGINEERING MAIN BUILDING SHM SYSTEM

---

server, a “history” of each structure and of the working conditions of sensors is kept through a second database.



**Figure 6.2.** SHM system architecture: (a) Monitored constructions, (b) local server, (c) data transmission, (d) satellite communication and seismic network, (e) master server

The main characteristics of such a system can be summarized as follows:

- Integration
- Redundancy
- Scalability
- Durability

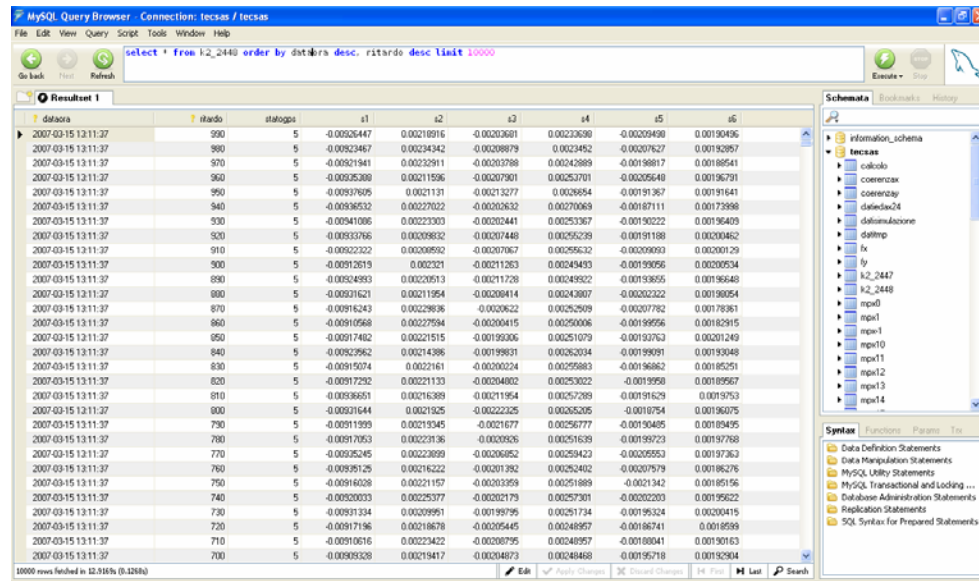
and their practical implementation is clarified by the description of the parts of the monitoring system.

Basically, a monitoring system combining structural, geotechnical and seismological model has been designed. It is an open system, being expandable through various data acquisition and transmission systems. It consists of a variety of sensors (mainly accelerometers) to monitor the environment, the soil and the structural response to loads. Integration among different models is achieved by implementing opportune data processing procedures on the local server. Moreover, the SHM system is embedded in the Regional Seismic Network issued by CRdC-AMRA: seismological models allow to foresee the characteristics of the incoming events and send these informations to the local server in order to start early warning procedures. Moreover, combining seismological, geotechnical and structural data, a deeper knowledge about site effect phenomena and propagation of seismic waves can be obtained.

A primary role for integration of data coming from different sensors is played by the database working on the local server, which is used for storage of raw data. It is a MySQL relational database (Figure 6.3)

### 6.3 THE SCHOOL OF ENGINEERING MAIN BUILDING SHM SYSTEM

organized in different tables depending on the type of data and, therefore, of sensor.



The screenshot displays the MySQL Query Browser interface. The title bar indicates the connection is to 'tccsas / tccsas'. The menu bar includes File, Edit, View, Query, Script, Tools, Window, and Help. The toolbar contains buttons for Go back, Next, Refresh, Execute, and Stop. The query editor shows the following SQL query: `select * from i2_2448 order by data desc, ritardo desc limit 10000`. The 'Resultset 1' tab is active, displaying a table with 10 columns: data, ritardo, status, s1, s2, s3, s4, s5, s6, and s7. The data is sorted by 'data' in descending order, with the most recent entry at the top. The 'Schema' pane on the right shows the database structure, including the 'information\_schema' and 'tccsas' databases. The 'Syntax' pane at the bottom provides a list of SQL syntax rules for various statements.

data	ritardo	status	s1	s2	s3	s4	s5	s6	s7
2007-03-15 13:11:37	990	5	-0.00236447	0.00210916	-0.00206081	0.00222630	-0.00205490	0.00190436	
2007-03-15 13:11:37	990	5	-0.00234467	0.00234342	-0.00208879	0.00234852	-0.00207627	0.00193957	
2007-03-15 13:11:37	970	5	-0.00219441	0.00232911	-0.00202786	0.00242869	-0.00198817	0.00188541	
2007-03-15 13:11:37	960	5	-0.00235308	0.00211596	-0.00207901	0.00252701	-0.00205648	0.00196791	
2007-03-15 13:11:37	960	5	-0.00237605	0.0021131	-0.00213277	0.00236954	-0.00191367	0.00191641	
2007-03-15 13:11:37	940	5	-0.00236532	0.00227022	-0.00202632	0.00270069	-0.00187111	0.00173998	
2007-03-15 13:11:37	930	5	-0.00241086	0.00223303	-0.00202441	0.00253367	-0.00190222	0.00196409	
2007-03-15 13:11:37	920	5	-0.00233766	0.00209832	-0.00207448	0.00255239	-0.00191188	0.00200462	
2007-03-15 13:11:37	910	5	-0.00222322	0.00208592	-0.00207067	0.00255632	-0.00209993	0.00200129	
2007-03-15 13:11:37	900	5	-0.00212615	0.0022321	-0.00211263	0.00243493	-0.00199956	0.00200534	
2007-03-15 13:11:37	890	5	-0.00244993	0.00220513	-0.00211728	0.00249522	-0.00193855	0.00193648	
2007-03-15 13:11:37	880	5	-0.00231621	0.00211954	-0.00206414	0.00242807	-0.00202222	0.00198854	
2007-03-15 13:11:37	870	5	-0.00218243	0.00223636	-0.00206622	0.00252609	-0.00207782	0.00175961	
2007-03-15 13:11:37	860	5	-0.00219568	0.00227594	-0.00200415	0.00250006	-0.00199556	0.00182915	
2007-03-15 13:11:37	850	5	-0.00217482	0.00221515	-0.00199306	0.00251079	-0.00193763	0.00201249	
2007-03-15 13:11:37	840	5	-0.00229562	0.00214386	-0.00199831	0.00262034	-0.00198991	0.00193048	
2007-03-15 13:11:37	830	5	-0.00215074	0.0022161	-0.00200224	0.00259883	-0.00196862	0.00185251	
2007-03-15 13:11:37	820	5	-0.00217292	0.00221133	-0.00204802	0.00253022	-0.00199590	0.00189567	
2007-03-15 13:11:37	810	5	-0.00236651	0.00216389	-0.00211954	0.00257289	-0.00191629	0.0019753	
2007-03-15 13:11:37	800	5	-0.00231644	0.0021925	-0.00222325	0.00255205	-0.0018754	0.00196075	
2007-03-15 13:11:37	790	5	-0.00211939	0.00219345	-0.0021677	0.00256777	-0.00190495	0.00189495	
2007-03-15 13:11:37	780	5	-0.00217053	0.00223136	-0.00209505	0.00251639	-0.00199723	0.00197768	
2007-03-15 13:11:37	770	5	-0.00235245	0.00222899	-0.00206952	0.00259423	-0.00205553	0.00197363	
2007-03-15 13:11:37	760	5	-0.00209729	0.00216222	-0.00201292	0.00252402	-0.00207979	0.00186276	
2007-03-15 13:11:37	750	5	-0.00216028	0.00221157	-0.00203359	0.00251889	-0.0021342	0.00185156	
2007-03-15 13:11:37	740	5	-0.00202033	0.00225377	-0.00202179	0.00257301	-0.00202203	0.00195622	
2007-03-15 13:11:37	730	5	-0.00231334	0.00209951	-0.00199796	0.00251734	-0.00195324	0.00200415	
2007-03-15 13:11:37	720	5	-0.00217196	0.00218678	-0.00205445	0.00248957	-0.00186741	0.0018559	
2007-03-15 13:11:37	710	5	-0.00210616	0.00223422	-0.00208795	0.00248957	-0.00188041	0.00190163	
2007-03-15 13:11:37	700	5	-0.00209538	0.00219417	-0.00204873	0.00248488	-0.00195718	0.00192504	

Figure 6.3. The remote database

Moreover, it contains data about the status of GPS, used for time synchronization, and informations on settings of sensors (i.e. sensitivity, full scale, engineering unit). It is a high performance database, allowing not only data storage but also error checking and recovery of corrupted tables. Data in operational conditions are kept for a week before deletion; in the case of a seismic event, pointed out by the seismic network, the related data are stored in different tables to avoid deletion. In this framework, the database allows integration of structural health monitoring procedures in operational conditions, which can tolerate a reasonable delay, and seismic early warning and emergency support

procedures, which have to work in real-time. Thus, in case of a seismic event, data are stored apart and just the strictly necessary ones can be used for the early warning procedures, in order to restrain the computational burden and allow a real-time response of the system.

Redundancy of the system is related to sensor placement and data transmission.

About acceleration sensors mounted on the structure, the School of Engineering Tower has been instrumented at the upper levels with two type of accelerometers: uniaxial force-balance accelerometers by Kinemetrics inc. (model FBA ES-U2; 2.5 V/g of sensitivity,  $\pm 1g$  of full scale range; 5 V/g of sensitivity,  $\pm 0.5g$  of full scale range), uniaxial piezoelectric accelerometers by PCB Piezotronics inc. (models 393B04 and 393A03; 1 V/g of sensitivity;  $\pm 5g$  of full scale range). Geotechnical parameters are monitored through a Kinemetrics EpiSensor ES-T, mounted at the base of the building (2.5 V/g of sensitivity,  $\pm 1g$  of full scale range), and through three Kinemetrics Shallow Borehole EpiSensor SBEPI (2.5 V/g of sensitivity,  $\pm 1g$  of full scale range), which are mounted underground at a vertical distance of 10 m each other until 30 m of deepness: such sensors are managed by the geotechnical research group from University of Calabria.

The instrumented storeys are the third, the seventh and the roof (Figure 6.4); sensors are placed along the north-south direction and the east-west direction in two opposite corners of the building and in two opposite corners nearby the stairs. Preliminary evaluations about sensors



### 6.3 THE SCHOOL OF ENGINEERING MAIN BUILDING SHM SYSTEM

---

placement have been carried out by setting up a finite element model of the structure (Rainieri et al. 2007c) on the base of original design drawings, visual inspections and local investigations: the final settlement of sensors on the building has been selected in order to get both translational and torsional modes of the structure. It is worth noticing that, at each position, there is a couple of Kinemetrics EpiSensors FBA ES-U2, which are used for monitoring in operational conditions, and a couple of PCB Piezotronics accelerometers, characterized by a higher full scale range and, therefore, more suitable to the extreme conditions of an earthquake which can saturate the previous sensors.

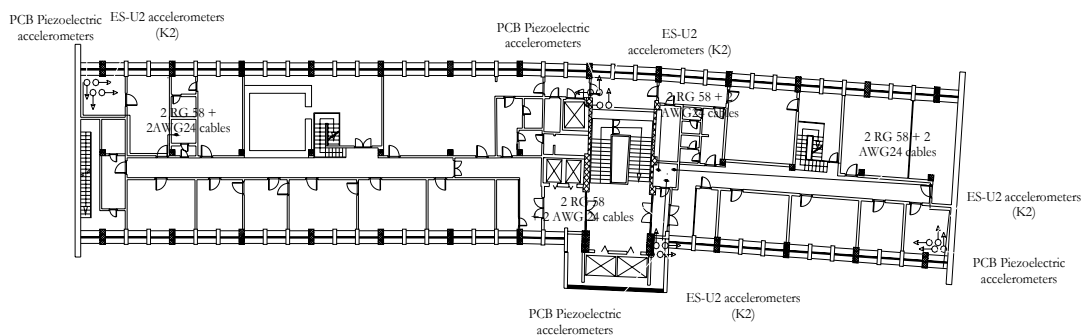


**Figure 6.4.** Roof sensors

Since data collected during seismic events allow a deeper knowledge of the structural behavior and can be used for real-time evaluation of the level of safety of the building in the early earthquake aftershock (in this sense, the system is oriented to produce earthquake scenarios and to support decision making processes), the architecture of the monitoring

system has been designed so that it is able to transmit data also in critical conditions, such as during an earthquake: redundant vectors for data transmission (DSL, traditional and cellular phone, satellite) are employed to this aim.

Scalability and durability of the designed SHM system are strictly related to the local database. In fact, due to its presence, the SHM system is easily expandable: new hardware can be added only by setting up an appropriate driver in order to transfer data on the database. The independence from the hardware platform, thanks to the database, is related also to the durability of the monitoring system: in fact, obsolete hardware can be easily and quickly replaced without modifications in the overall architecture of the system.

Scalability makes the system suitable also for monitoring of gigantic structures; durability and redundancy, instead, give a life span to the SHM system comparable to that one of the monitored structure.

### **6.4 AUTOMATED MODAL PARAMETER IDENTIFICATION: LITERATURE REVIEW**

The last few years have seen a large effort in the development of vibration based damage detection techniques (Doebeling et al. 1996). In fact, since the dynamic behaviour of a structure is influenced by damage, it is possible to detect occurrence of relevant damage levels through the evolution of modal parameters (Swamidas & Chen 1995, Hermans et al. 1999).

## 6.4 AUTOMATED MODAL PARAMETER IDENTIFICATION...

---

However, changes in environmental and operational conditions can affect modal parameter estimation (Peeters 2000) as well. In this framework, an automated modal identification and tracking procedure represents a relevant aspect related to the applicability of damage detection techniques as a part of monitoring practices. This is not a trivial task since traditional modal identification always requires extensive interaction from an experienced user (Verboven et al. 2003). Nevertheless, computational loads have to be taken into account in order to assess applicability of modal identification techniques for damage detection purposes. In fact, fast on-line data processing is crucial for quickly varying in time systems (such as a rocket burning fuel). However, a number of vibration-based condition monitoring applications are carried out at very different time scales, resulting in satisfactory time steps for on-line data analysis. Interesting examples are related to structural monitoring of large structures, such as bridges (Peeters & De Roeck 2000, Doebling et al. 1996) or offshore platforms (Doebling et al. 1996, Brincker et al. 1995). Currently, there are some advancements in the field of automated Operational Modal Analysis, with the development of methods based on control theory (both in time and frequency domain) and methods based on conventional signal processing.

The first proposal for automated identification of modal properties is by Verboven et al. (Verboven et al. 2002) but it is just in the last two years that an increasing attention has been paid to this issue, determining a number of proposals for automated identification and tracking of modal

parameters (Brincker et al. 2007, Deraemaeker et al. 2008, Rainieri et al. 2007a).

As methods based on control theory are concerned, the model order is usually over-specified to get all physical modes present in the frequency range of interest, according to classical modal analysis. However, physical and mathematical modes have to be distinguished. This practice requires large interaction with an expert user (Soderstrom 1975). Thus, classical modal analysis takes advantage of very relevant and effective tools, such as the stabilization diagram, which is a useful mean to distinguish physical from mathematical modes. However, selection of physical poles is not a trivial task: it may be difficult and time-consuming depending on the quality of data, the performance of the estimator (even if there are interesting advancements in this field; see Lanslots et al. 2004) and the experience of the user. Extensive interaction between tools and user is basically inappropriate for monitoring purposes.

The first proposal for automated modal identification was based on the Least Square Complex Frequency (LSCF) method (Verboven et al. 2003). In this case selection of physical poles from a high order model is based on a number of deterministic and stochastic criteria and a fuzzy clustering approach. However, the algorithm for pole selection is quite complex and computational demanding.

In 2008 Deraemaeker et al. (Deraemaeker et al. 2008) have proposed an automated operational modal analysis procedure based on the Stochastic Subspace Identification (SSI) technique. It is suitable as tracking method

## 6.4 AUTOMATED MODAL PARAMETER IDENTIFICATION...

---

but it always requires user interaction because an initial set of modal parameters, using stochastic subspace identification and the stabilization diagram, has to be identified before launching the tracking procedure.

Andersen et al. (Andersen et al. 2007), instead, proposed, in 2007, a fully automated method for extraction of modal parameters adopting the SSI technique. It is based on the clear stabilization diagram obtained according to a multipatch subspace approach. Poles extraction is carried out by the graph theory. This algorithm seems to be very fast, so that it can be used for a monitoring routine, but further work is still needed in order to improve the numerical efficiency of the method.

About methods based on conventional signal analysis, Guan et al. (Guan et al. 2005) proposed in 2005 the so-called Time Domain Filtering method, which is a tracking procedure based on the application of a band-pass filter to the system response in order to separate the single modes in the spectrum. However, the frequency limits of the filter are static and, above all, user-specified according only to the Power Spectral Density (PSD) plots of the response signals; if excitation is unknown, it is sometimes difficult to identify the regions where certain modes may be located according only to power spectrum plots. Moreover, in the case of close modes, it is very difficult, or even impossible, to correctly define such limits in a way able to follow the natural changes in modal frequencies.

In 2007 Brincker et al. (Brincker et al. 2007) presented an algorithm for automation of the Frequency Domain Decomposition procedure in order to remove any user interaction and use it as modal information engine in

SHM systems. It is based on identification of the modal domain around each identified peak in the singular value plot according to predefined limits for the so-called modal coherence function and modal domain function. A good initial value for such limits would be 0.8. However, if the limit value for the modal coherence indicator is somehow justified (Brincker et al. 2007) on the base of the standard deviation of correlation between random vectors and of the number of measurement channels, few indications are reported for the modal domain indicator.

In 2008, the approach to automated modal parameter identification proposed by Brincker et al. has been slightly modified and applied to the permanent monitoring of the “Infante D. Henrique” bridge (Magalhães et al. 2008). In this case, also an automated procedure based on Cov-SSI and on a clustering algorithm for stable pole selection has been proposed. In the case of the modified FDD algorithm, however, Magalhães et al. have shown that, when the level of noise in the spectra increases, the procedure for automatic identification loses efficiency. Moreover, after having defined the frequency resolution and the frequency interval under analysis, the MAC rejection level has to be set: its values has to be identified for each monitored structure by mean of a number of sensitivity tests and, therefore, its calibration could be time consuming. Magalhães et al. have proposed to use a very small value (0.4) but it can be inadequate if the number of sensors is small and similar mode shape vectors for adjacent natural frequencies result from the identification process. The automated Cov-SSI method proposed by the same Authors, instead, seems

## 6.4 AUTOMATED MODAL PARAMETER IDENTIFICATION...

---

to be more efficient in the case of closely spaced modes but it shows lower ability in the identification of poorly excited modes. The application of the clustering algorithm allows a reliable identification of structural modes: however, also in this case, a number of parameters has to be set after a calibration phase of the system.

Automated modal identification algorithms have been recently proposed also for the SOBI method and for the transmissibility based method.

Automation of SOBI has been proposed by Poncelet et al. (Poncelet et al. 2008): identification of structural modes is based on rejection of all modes out of the frequency range of interest and of time series of sources characterized by a fitting error higher than 10%; finally, selection of actual structural modes is based on the computation of a confidence factor. The main advantage of the proposed procedure is a lower computational load with respect to SSI methods; moreover, selection of model order is not necessary. The main drawback is, instead, related to the need of a number of sensors greater or equal than the number of active modes. Moreover, at now the algorithm has been applied only against simulated data: so, its effectiveness in the case of actual measurements has to be verified.

The automated OMA procedure using transmissibility functions is, instead, based on the combination of SVD and stabilization diagram for selection of structural modes (Devriendt et al. 2008). Computation of the stabilization diagram from transmissibility functions results in stable vertical lines but not all of them correspond to actual system poles, even if they are related to structural characteristics. Thus, another selection tool is

needed. The Authors have proposed to compute the SVD of a two column matrix where each column consists of a transmissibility function evaluated for a particular load condition. Since all transmissibility functions converge to the same unique values at the system poles, the matrix will be of rank one in correspondence of each system pole. Thus, by looking at the plot of the inverse of the second singular value, it is possible to distinguish actual structural modes from its peaks. Peak selection can be carried out by defining a threshold: however, in presence of measurement noise this approach is not very reliable. In order to overcome this drawback the Authors have proposed the use of a smoothing function, but it has to be used carefully to avoid distortion. Further refinements of the proposed algorithm are, therefore, needed.

### 6.5 FULLY AUTOMATED OMA: LEONIDA

#### 6.5.1 The algorithm background

In the present section theoretical aspects related to the development of a fully automated OMA algorithm are reported.

It is based on a classical output-only modal identification procedure, such as the Enhanced Frequency Domain Decomposition (Brincker et al. 2000b). However, the following discussion mainly refers to the Complex Mode Indicator Function (CMIF) (Fladung & Brown 1992), of which the EFDD is the corresponding extension to the output only case, taking into account



## 6.5 FULLY AUTOMATED OMA: LEONIDA

---

the relation between the Frequency Response Function (FRF), the input and the output.

For a Single Degree of Freedom (SDOF) system, the transfer function can be expressed as (Heylen et al. 2002):

$$H(p) = \frac{A_1}{(p - \lambda_1)} + \frac{A_1^*}{(p - \lambda_1^*)} \quad (6.1)$$

with:

$$A_1 = \frac{1/M}{j2\omega_1} \quad (6.2)$$

where the residue  $A_1$  is a constant,  $M$  is the mass,  $\omega_1$  is the damped natural frequency,  $\lambda_1$  and  $\lambda_1^*$  the two complex conjugate roots of the system characteristic equation. For a Multi Degree of Freedom (MDOF) system, residues are related to the mode shapes  $\{\psi\}$ :

$$[H(p)] = \sum_{r=1}^N \left( \frac{\mathcal{Q}_r \{\psi\}_r \{\psi\}_r^T}{(p - \lambda_r)} + \frac{\mathcal{Q}_r^* \{\psi\}_r^* \{\psi\}_r^{*T}}{(p - \lambda_r^*)} \right) \quad (6.3)$$

where  $*$  and  $^T$  denote complex conjugate and transpose, respectively, and each residue is:

$$[A]_r = Q_r \{\psi\}_r \{\psi\}_r^T \quad (6.4)$$

After a number of mathematical manipulations, the FRF matrix can be expressed as:

$$[H(p)] = [V][p[I] - [\Lambda]]^{-1} [Q][V]^T \quad (6.5)$$

where  $[I]$ ,  $[\Lambda]$  and  $[Q]$  are diagonal and:

$$[V] = [\{\psi\}_1 \dots \{\psi\}_N \{\psi\}_1^* \dots \{\psi\}_N^*] \quad (6.6)$$

Expression (6.5) can be compared to the SVD of the FRF matrix at a specific frequency:

$$[H(j\omega_k)] = [P_k][\Sigma][R_k]^*{}^T \quad (6.7)$$

where the orthonormal columns  $[P_k]$  are the left singular vectors, while  $[\Sigma]$  is the diagonal matrix holding the singular values. When multiple roots do not exist, as  $\omega_k$  approaches the system pole  $\lambda_k$ , the quantity  $\frac{1}{(j\omega_k - \lambda_r)}$  reaches a maximum. In fact, since  $[V]$  and  $[Q][V]^T$  are constant,

the amplitude information depends only on the  $\frac{1}{(j\omega_k - \lambda_r)}$  terms, or on

the singular values, when SVD of the FRF matrix is considered, being the singular vectors of unity length. In particular, near a resonance, the FRF matrix is dominated by the corresponding term:

$$[H(j\omega_r)] = \{\psi\}_r \frac{Q_r}{(j\omega_r - \lambda_r)} \{\psi\}_r^T \quad (6.8)$$

and, therefore, just one singular value is relevant.

If corresponding singular vectors in the mode bandwidth are considered, being  $\{\psi\}_r$  constant in the bandwidth of the mode, the MAC index (Allemang & Brown 1982) computed at the same frequency line between the two first singular vectors derived from two subsequent records should be constant and equal to 1 for a stationary and ergodic system:

$$MAC(\{\psi_1^{t_0}(\bar{\omega})\}, \{\psi_1^{t_0+n\Delta T}(\bar{\omega})\}) = \frac{|\{\psi_1^{t_0}\} \{\psi_1^{t_0+n\Delta T}\}^H|^2}{(\{\psi_1^{t_0}\} \{\psi_1^{t_0}\}^H) (\{\psi_1^{t_0+n\Delta T}\} \{\psi_1^{t_0+n\Delta T}\}^H)} \quad (6.9)$$

where  $\{\psi_1(\bar{\omega})\}$  denotes the first singular vector at frequency  $\bar{\omega}$ , and the superscript  $t_0$  and  $t_0 + n\Delta t$  denote the starting time of the first and of the  $n$ -th records. The superscript  $H$  denotes hermitian.

It is not the case of actual records, since measures are affected by noise, so that specific selection criteria and tolerances must be set.

When considering EFDD, only output measurements are available for modal parameter estimation. In such a case, the SVD of the PSD matrix, instead of the FRF matrix, gives un-scaled mode shapes. However, being the algorithm based on the MAC index, a constant multiplier does not affect results, so the proposed procedure can be applied without changes to the output-only case.

### 6.5.2 Implementation

As discussed in the last part of the previous section, the algorithm moves from the SVD of the output PSD matrix, this is the core of the EFDD method. After applying decomposition, the first singular vector at each frequency line is obtained. This step is repeated for a number of subsequent records. Afterwards, the MAC between the two singular vectors at the same frequency line obtained from two different records is computed. However, the MAC index is quite sensitive to noise, as it will be discussed later; thus, noise of measures must be processed. In order to reduce the effect of noise, the average MAC vs. frequency plot is computed.

Averaged MAC vs. frequency plot can be seen as a coherence function; where a certain mode is located, points are located very close each other and to 1 and a nearly flat shape is obtained, as shown in Figure 6.5.

## 6.5 FULLY AUTOMATED OMA: LEONIDA

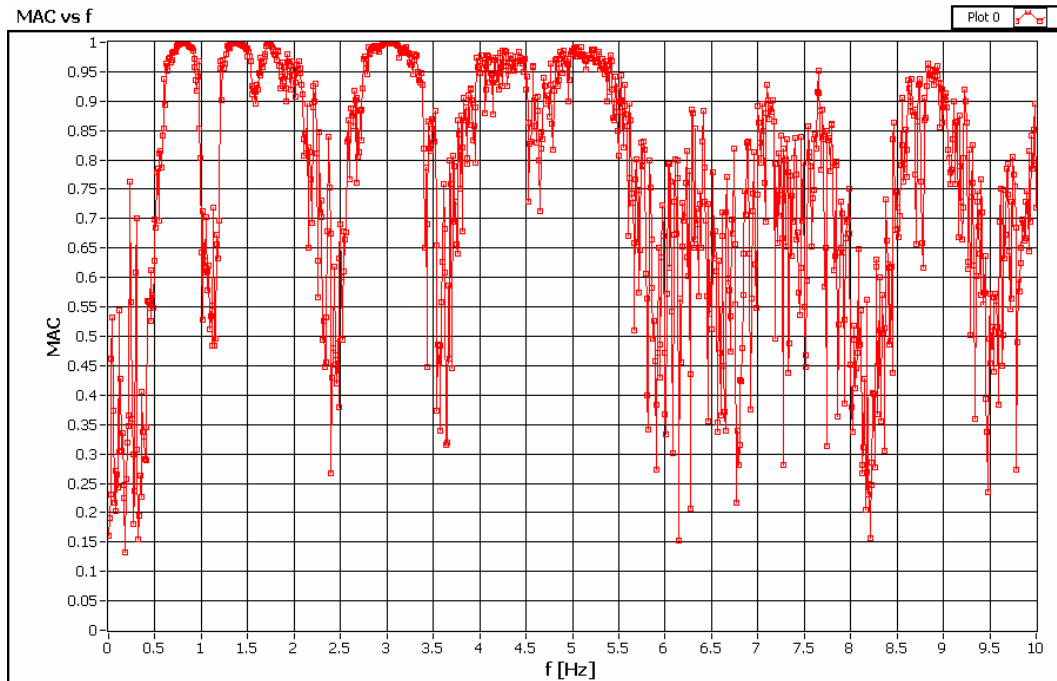


**Figure 6.5.** Averaged MAC vs. frequency plot

Identification of the bandwidth of each mode is carried out evaluating some statistical parameters related to the MAC value at each frequency line and to the difference between MAC values at two subsequent steps. Mean and standard deviation are the statistical parameters assumed for mode bandwidth identification. In order to have a good estimation of such parameters, at least ten steps are generally taken into account.

As shown in Figure 6.6, the MAC function is nearby horizontal only at the frequency lines located within a mode bandwidth (Figure 6.6b). It has been assumed that such function is horizontal if the assumed parameters satisfy some predefined limits: in particular, for a given number of step, the MAC must have an average value higher than 0.95 and a standard

## 6. OMA AND STRUCTURAL HEALTH MONITORING

deviation lower than 0.01; moreover, the difference between two subsequent values of MAC must be, on average, lower than 0.01, with a standard deviation lower than 0.01. These limits are the results of a calibration process, independent of measurement hardware characteristics, level of noise in measurements and number of averages in computation of MAC vs.  $f$  plot. However, such limits should be related at least to the number of averages, since the scatter in MAC values decreases when it increases. A high number of averages results in a strict and more refined definition of such limits and, thus, in a mode bandwidth identification less sensitive to noise effects.

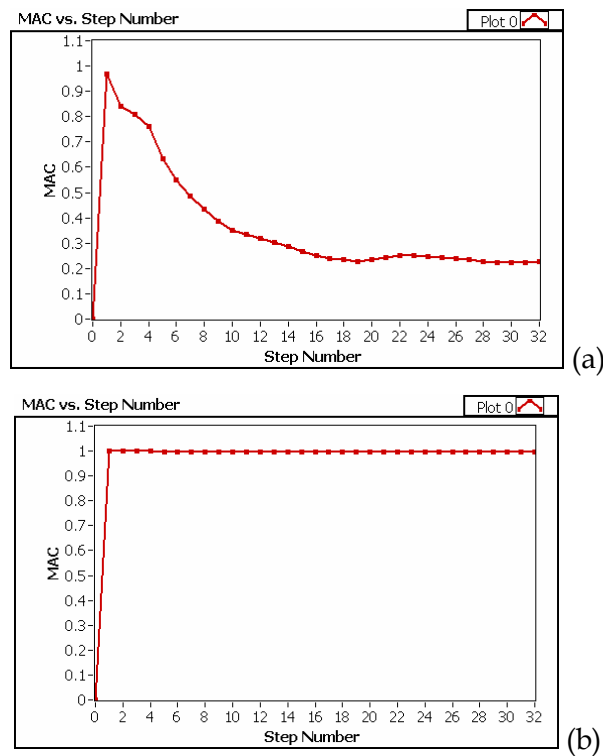


**Figure 6.6.** Averaged MAC vs. step number: (a) noise, (b) mode bandwidth

## 6.5 FULLY AUTOMATED OMA: LEONIDA

---

In the current implementation of the algorithm, frequency resolution and record length are held constant and equal to 0.01 Hz and 10 minutes for each step, respectively. This record length for the single step seems to be the minimum one providing a sufficiently averaged spectrum, thus resulting in a good compromise between accuracy and computational time. However, longer records can result in improved definition of spectra, where most of the noise is averaged out, and therefore of estimated mode shapes, thus reducing noise effects on MAC. A higher number of averages is necessary also to reduce the effects of transients, if they are expected: in fact, they can affect mode shape estimation, resulting in a lower value of MAC: even if the MAC slightly changes due to transient signal effects, it may happen that, due to its variation, the above defined limits are no more satisfied. As a consequence, in particular in presence of close coupled modes, it is possible that a mode is not identified.

The assumed limits for statistical parameters and record length have given satisfactory results. However, further work and data are necessary for an accurate and robust calibration of such values.

From the averaged MAC vs. frequency plot, the bandwidth of a number of modes can be identified. Within each bandwidth, use of peak detection algorithms over the corresponding portion of the first singular value plot leads to the identification of natural frequency for that mode. The corresponding singular vector at that frequency line is a good estimation of the mode shape of the structure (Brincker et al. 2000b). Starting from the

SDOF Bell function of the mode (Brincker et al. 2000b), damping and natural frequency can be determined in an automated way from the correlation function of the isolated SDOF system using only a portion of such function down to a certain decay level, as suggested in (Brincker et al. 2007).

A synthesis of the proposed algorithm is shown in Figure 6.7. It has been implemented into a software, named Leonida, developed in LabView environment and firstly tested against simulated data (Rainieri et al. 2008c). A state machine architecture has been adopted for software implementation since well-defined stages can be identified.

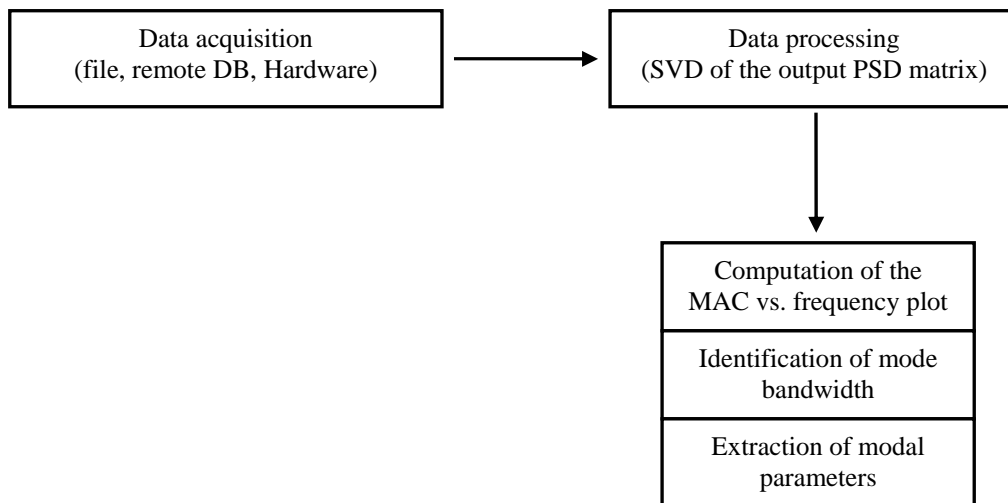


**Figure 6.7.** The algorithm for automated modal parameter identification

At first there is the start-up phase (Figure 6.8) where the user can define the data source. In particular, data can be retrieved from file, but also from



## 6.5 FULLY AUTOMATED OMA: LEONIDA

a remote MySQL database or directly from a measurement hardware, thus allowing integration of the software within a fully automated structural health monitoring system. If data are retrieved from file, the number of steps cannot be controlled but it depends on the length of the record. Later on, it will be shown that more than one hour long records can assure a good number of averages and, therefore, are necessary to obtain the clearest results.

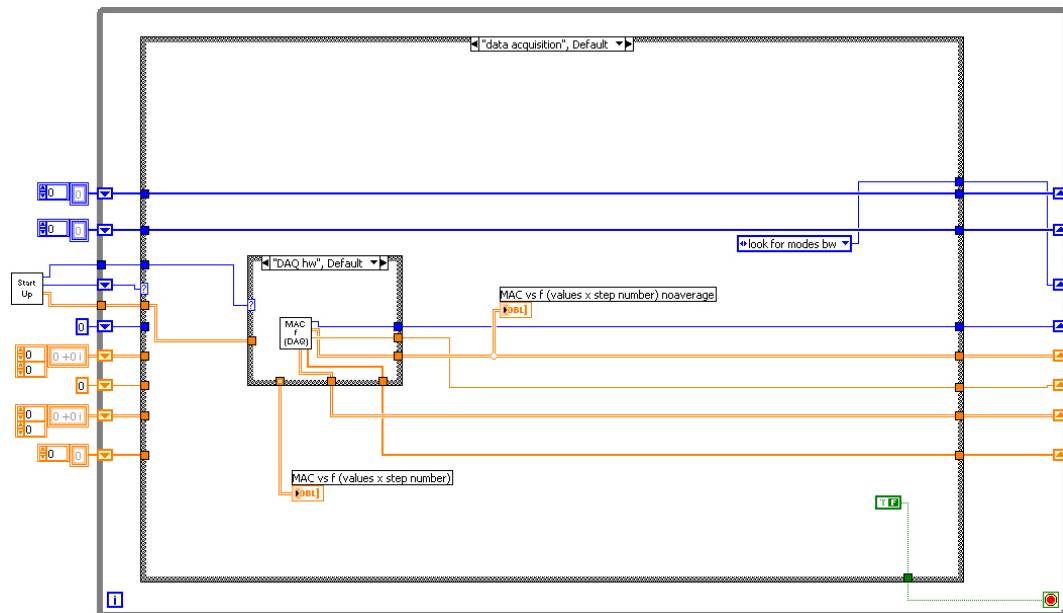


**Figure 6.8.** Leonida software: state machine architecture and start-up phase

In the first state the MAC vs. frequency plot is computed over a number of subsequent records according to the previously selected data source (Figure 6.9). Computational time is optimised adopting parallel recording and processing procedures. Moreover, a partial overlap between

subsequent records can be considered in the case of data retrieved from file in order to increase the number of averages.

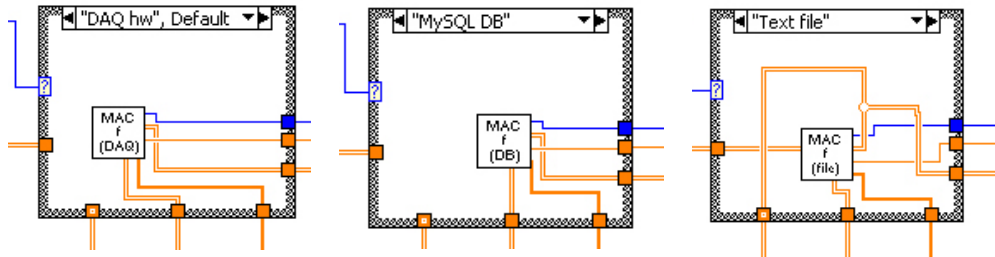


**Figure 6.9.** Leonida software: data sources

In the second state, mode bandwidths are identified according to the above mentioned predefined limits. At the end of this state, a number of bandwidths are identified through their limit values of frequency.

In the third state modal parameters are extracted in a fully automated way by focusing only on the frequency lines defining a certain mode bandwidth.

This software can be used for single applications, in order to define the fundamental modes of the structure under test, or as modal information engine for a modal tracking procedure, as described in the following sections. In this second case, starting from the identified mode shapes for a number of modes, it is possible to track natural frequencies and mode shapes of those modes over time, thus performing an effective structural health monitoring.

### 6.5.3 Applications

Some applications of the proposed algorithm are herein reported, in order to show effectiveness and limitations. Promising results have been obtained in detecting fundamental modes of a number of different structures, thus pointing out potentialities of the proposed procedure. The following applications also show the limitations of the algorithm, in particular at higher modes and when the effects of noise become important. However, if higher modes are not properly excited or noise is relevant, also an expert user probably runs into a number of problems.

Different record lengths, measurement hardware and structural typologies have been considered for testing the algorithm. A number of different case studies and hardware characteristics has been taken into account.

The first application concerns the measurements carried out on the Tower of the Nations (see also section 5.3). Records TdN1 and TdN2 have been both used for modal identification. TdN1 record is 25 minutes long, TdN2 is 40 minutes long. In both cases, a sampling frequency of 100 Hz has been adopted. Hardware characteristics and record lengths are summarized for completeness in Table 6.2.

Structure	Sensors	Data acquisition hardware	Records	Duration [s]	Sampling frequency [Hz]
Tower of the Nations	Kinematics Epi-Sensor FBA ES-U2	Kinematics K2	TdN1	1500	100
			TdN2	2400	100

**Table 6.2.** The Tower of the Nations: summary

## 6. OMA AND STRUCTURAL HEALTH MONITORING

Results of tradition (manual) identification have been shown in section 5.3.8. Leonida has been then applied to such records by adopting a frequency resolution in spectrum computation equal to 0.01 Hz. The averaged MAC vs. frequency plots are shown in Figure 6.10, while identified mode bandwidths are shown in Figure 6.11.

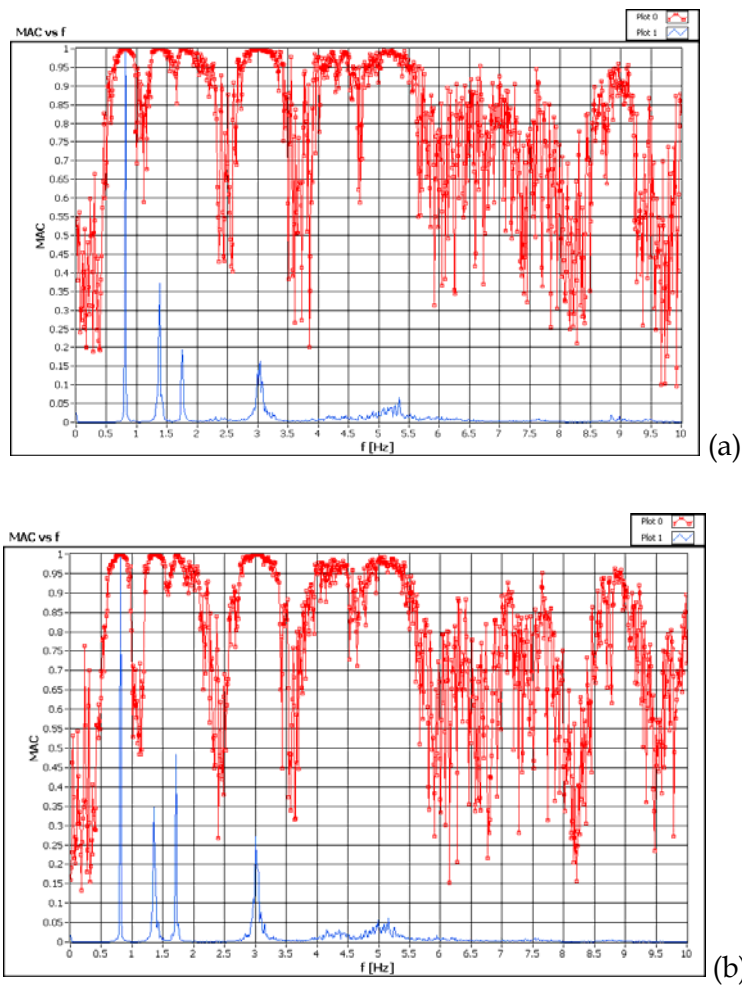


**Figure 6.10.** The Tower of the Nations: averaged MAC vs. frequency plot for TdN1 (a) and TdN2 (b) record

## 6.5 FULLY AUTOMATED OMA: LEONIDA

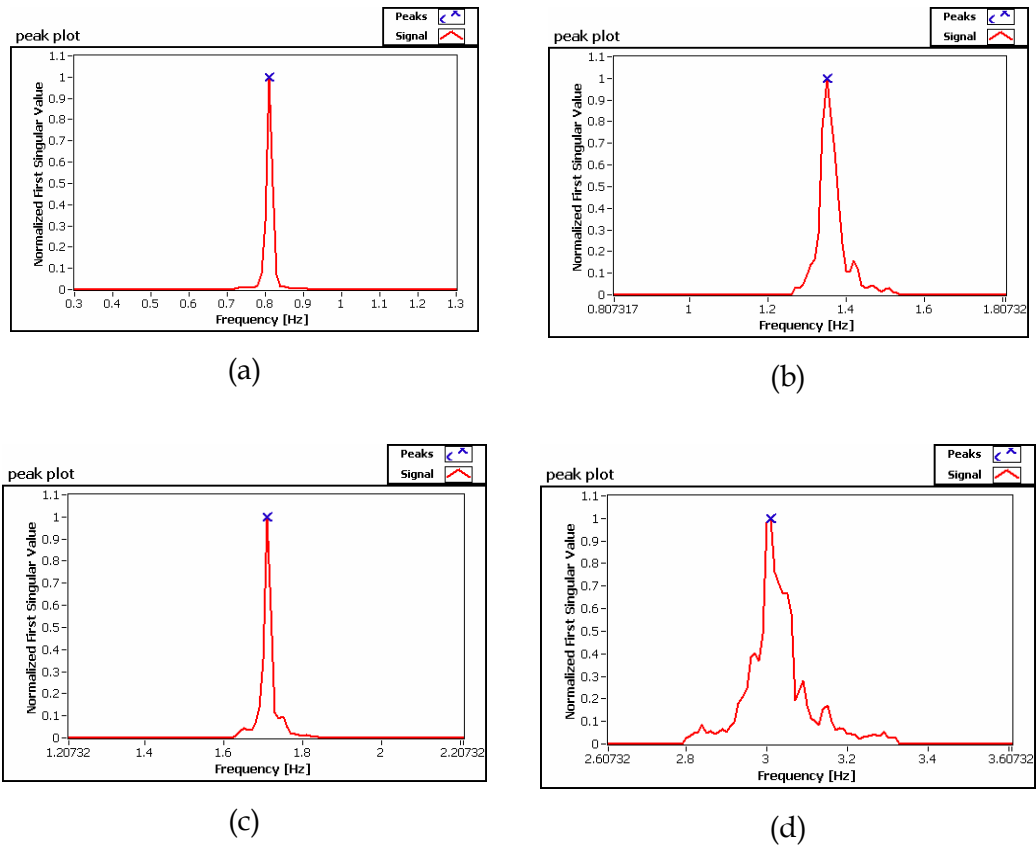


**Figure 6.11.** The Tower of the Nations: Identified bandwidths (TdN2) for mode I (a), II (b), III (c) and IV (d)

Results of automated identification are reported in Table 6.3, in comparison with those ones of traditional (manual) output-only identification.

Thus, the automated procedure has been able to clearly identify the first four modes of the structure. This is a basic case study, being the structure characterized by well-separated modes.

## 6. OMA AND STRUCTURAL HEALTH MONITORING

Record	Mode number	Natural frequency (EFDD) [Hz]	Natural frequency (Leonida) [Hz]
TdN1	I	0.813	0.81
	II	1.375	1.38
	III	1.758	1.75
	IV	3.025	3.04
TdN2	I	0.812	0.81
	II	1.362	1.35
	III	1.727	1.71
	IV	3.023	3.01

**Table 6.3.** The Tower of the Nations: results of automated modal identification

About higher modes, where a confident manual identification is also difficult, the bandwidths of the modes are not so clearly identified. They have been divided into a number of sub-ranges, due to noise effects, but they should be a whole. Differences in values of natural frequencies are related to the fact that, at the current stage of implementation of the software, a basic peak picking algorithm and a fixed frequency resolution have been considered; identification of natural frequencies through the EFDD technique or the SSI algorithms is, instead, independent of frequency resolution.

A second application has been carried out by using the two records obtained from the ambient vibration test on the masonry star vault in Lecce (see section 5.2.2). Hardware characteristics and record lengths are summarized in Table 6.4.

## 6.5 FULLY AUTOMATED OMA: LEONIDA

---

Structure	Sensors	Data acquisition hardware	Records	Duration [s]	Sampling frequency [Hz]
Star vault	PCB Piezotronics 393B31	cDAQ NI9233	Setup A	1500	100
			Setup B	1800	200

**Table 6.4.** The star vault: summary

Results of automated modal identification, corresponding to a frequency resolution of 0.01 Hz, are reported in Table 6.5, in comparison with those ones of traditional (manual) output-only identification.

Record	Mode number	Natural frequency (EFDD) [Hz]	Natural frequency (Leonida) [Hz]
Setup A	I	4.35	4.35
	II	4.96	4.98
Setup B	I	4.31	4.30
	II	4.94	4.93

**Table 6.5.** The star vault: results of automated modal identification

The automated procedure has been able to clearly identify the first two fundamental modes of the structure. Higher modes have not been considered since manual identification has been stopped after having identified the first two modes, as described in section 5.2.2.

The automated procedure has been, then, applied to S. Maria del Carmine Bell Tower data (see section 5.5). It is an onerous case study, because of the presence of two close, even if not coupled, bending modes and of relevant

## 6. OMA AND STRUCTURAL HEALTH MONITORING

---

noise effects corrupting data. Hardware characteristics and record lengths are summarized in Table 6.6.

Structure	Sensors	Data acquisition hardware	Records	Duration [s]	Sampling frequency [Hz]
S. Maria del Carmine bell tower	Kinemetrics Epi-Sensor FBA ES-U2	NI PXI-4472	Single record	1800	100

**Table 6.6.** S. Maria del Carmine bell tower: summary

Results of automated modal identification are reported in Table 6.7 in comparison with those ones of traditional (manual) output-only identification.

Record	Mode number	Natural frequency (EFDD) [Hz]	Natural frequency (Leonida) [Hz]
Single record	I	0.70	0.70
	II	0.76	0.76

**Table 6.7.** S. Maria del Carmine bell tower: results of automated modal identification

The last case study concerns the School of Engineering Main Building: since this test case is relevant to point out the effectiveness of the proposed procedures in presence of close coupled modes and the possibility of its integration within SHM systems, it will be discussed apart.



## 6.6 AUTOMATED MODAL TRACKING: AFDD-T

### 6.6.1. Algorithm

An approach to automated tracking of modal parameters, based on the Enhanced Frequency Domain Decomposition procedure, is described here. Modal tracking by EFDD can be easily automated if the mode shapes of the monitored structure are known, as shown in the flow chart in Figure 6.12: in fact, the mode shapes can be used for spatial filtering of data.

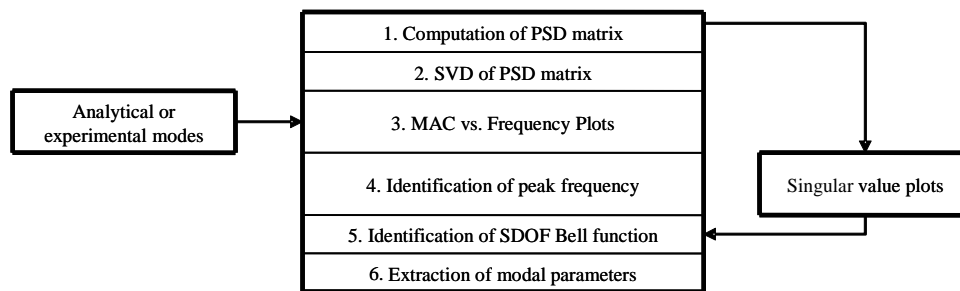


**Figure 6.12.** AFDD-T: algorithm for automated modal tracking

The main difference with respect to traditional applications of spatial filtering, like in the Frequency-Spatial Domain Decomposition (see section 2.4.2), is related to the fact that mode shapes are not applied to the PSD matrix, but each mode shape vector is used to identify a filter for the mode of interest starting from the singular vectors obtained at each frequency line by SVD of the PSD matrix. Thus, the  $k$ -th mode of interest can be identified through the MAC vs. frequency plot, where the MAC index is computed between a reference mode shape and the singular vectors resulting from SVD of the PSD matrix at each frequency line. Under the

assumption of absence of noise, this plot shows an absolute maximum at the frequency of the mode itself, where the singular vector obtained from SVD of the PSD matrix approximates the effective mode shape of the structure (Figure 6.13a). The presence of noise, however, can spread the values of the resulting frequencies, as shown in Figure 6.13b: in fact, near a peak in the spectrum, the corresponding singular vectors give similar values of MAC with respect to the reference mode shape (the plot of MAC vs. frequency is nearly flat in a certain range near the peak frequency). Presence of noise causes a variation of the last significant digits so that, if only the frequency associated to the maximum value of MAC is considered, the resulting values of frequency are spread, in particular in the case of a reduced number of sensors. By the way, it is possible to use the reference mode shape as a filter characterized by an adaptive bandwidth, by selecting all points characterized by a MAC value higher than a user-defined MAC Rejection Level, i.e. 80÷90% of the maximum MAC found in the MAC vs. frequency plot.

As a consequence, the algorithm for the peak detection can be applied only to the filtered data. Once the peak frequency is identified, the mode characterization can be carried out according to the standard FDD procedure. In some cases, excitation of the structure could be affected by harmonic components. The role of harmonic excitations can be different depending on the relative distance between structural frequencies of interest and harmonic excitation. Whenever the latter is far away from a structural mode, the operating deflection shape results as a combination of

## 6.6 AUTOMATED MODAL TRACKING: AFDD-T

---

several excited modes and the forces acting on the structure: thus, low MAC values are obtained.

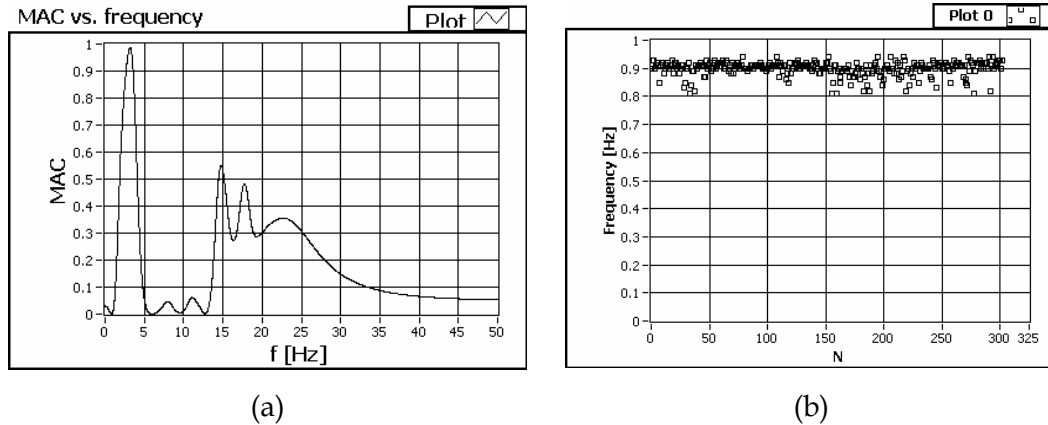


**Figure 6.13.** MAC vs. frequency plot (a) and dispersion of values due to noise (b)

Conversely, if the harmonic component is close to a structural mode, MAC values point out a high correlation and the estimated modal parameters can be biased. A structural and functional assessment of the monitored building is, therefore, necessary in order to identify presence of harmonic excitations. In such cases, implementation of specific algorithms able to identify and remove harmonic components (Jacobsen et al. 2007) is needed, resulting in increased computational efforts and hardware requirements.

Another relevant issue concerns the minimum number of sensors to be used for an effective spatial filtering. Figure 6.14 shows that, by increasing the number of sensors, the effectiveness of spatial filtering improves.

## 6. OMA AND STRUCTURAL HEALTH MONITORING

Results of simulations and actual applications show that, in presence of a minimum number of sensors, local maxima appear in the MAC vs. frequency plot: however, the absolute maximum is reached in the bandwidth of the considered mode defined by the reference mode shape. Thus, starting from identification of the absolute maximum, the spatial filter can be defined in a reliable way and, as a consequence, an effective extraction of modal parameters can be carried out. Applications to actual data have shown that such a filtering procedure is effective also when applied to short records (a few minutes), yielding a reduced number of averages in spectrum computation and, therefore, noisier spectra. As a consequence, by adopting an appropriate architecture for data processing, modal parameters can be estimated also every three-five minutes.

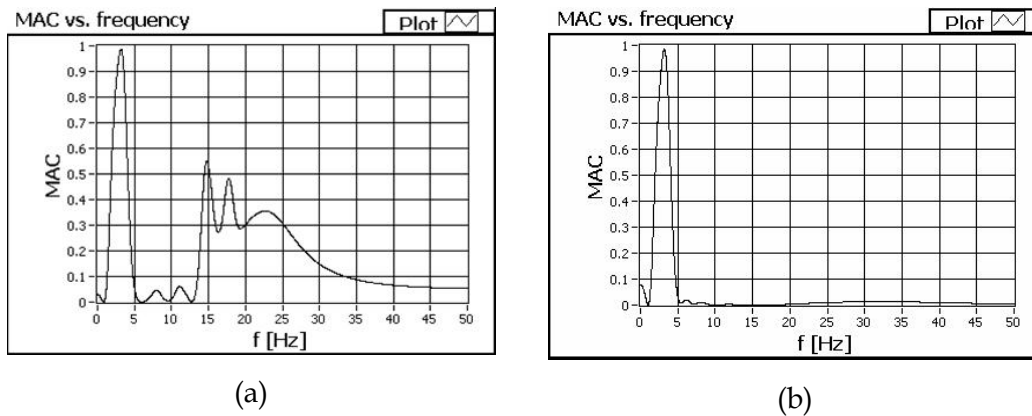


**Figure 6.14.** Effect of number of sensors: poor spatial definition (a); improved spatial definition (b)

### 6.6.2. Numerical validation

The automated modal tracking procedure has been tested using a number of numerical models implemented by mean of SAP2000® computer program. For each model, simulated data have been obtained by numerical analyses.

The first structural model used for validation of the modal tracking procedure is a shear-type 15-stories 1-bay r.c. frame with a Young's modulus of 250000 kg/cm<sup>2</sup> and characterized by well-separated modes. A Gaussian white noise has been generated and used as base excitation. Errors due to measures have been intentionally excluded. The effect of the number of sensors has been also investigated.

The results seem to be not affected by the number of sensors if mode observability is assured. The only effect is the presence of other relative maxima in the MAC vs. frequency plot together with the absolute maximum, as outlined in the previous section. Table 6.8 shows the results of identification by using simulated records relative to only five nodes: the reference mode shapes are those ones obtained by the Finite Element model. A good agreement between estimated and calculated values can be observed.

Mode Number	FE model [Hz]	AFDD-T [Hz]
1	1.07	1.07
2	3.21	3.2
3	5.30	5.27

**Table 6.8.** AFDD-T validation: simulated data, shear type frame

## 6. OMA AND STRUCTURAL HEALTH MONITORING

Moreover, a sensitivity analysis has been carried out by changing the concrete Young's modulus (from 100000 to 250000 kg/cm<sup>2</sup>) for a number of columns in the intermediate floors of the frame but assuming a unique set of reference mode shapes for the identification process (those ones obtained from the FE model of the structure in its initial configuration). The effect of the number of sensors has been also evaluated: plots reported in Figure 6.15 show that AFDD-T is able to detect changes of the natural frequency with reduced errors (max 10% with a very low number of sensors) without updating the reference mode shape.

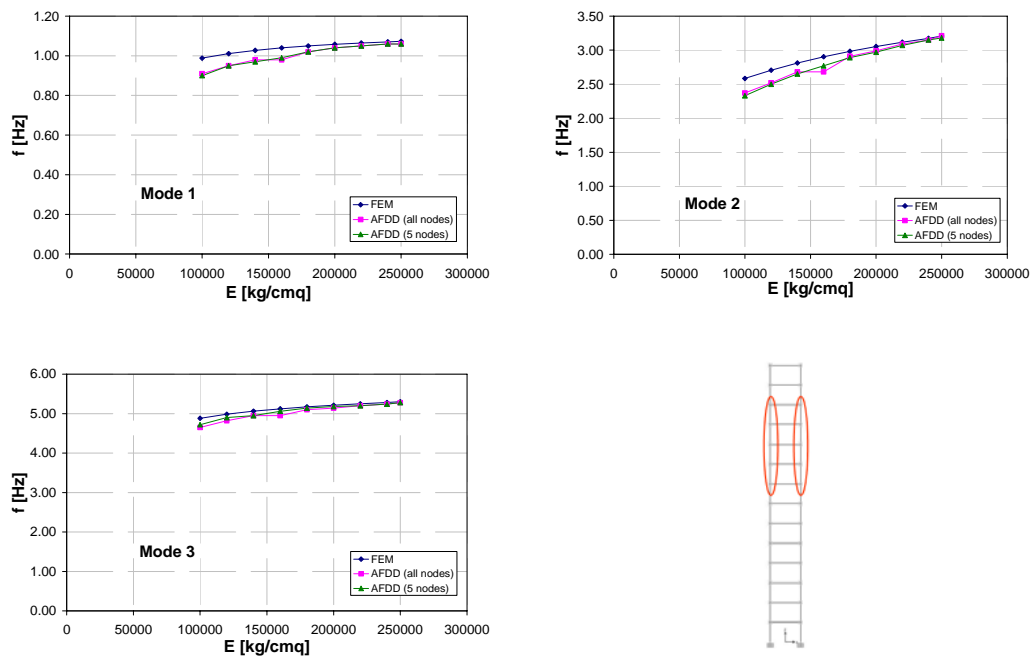


**Figure 6.15.** AFDD-T sensitivity analyses: simulated data, shear type frame

## 6.6 AUTOMATED MODAL TRACKING: AFDD-T

---

Similar results have been obtained considering a 3D two stories r.c. frame characterized by a rigid diaphragm at each floor and subjected to white noise as base excitation. Eight simulated records (x and y accelerations in two opposite corners of each floor) have been used for the analysis. This is a more complex case study, because the model is characterized by two close coupled modes, and mode shape estimation by the EFDD method is not so reliable in this case. The results of automated identification of the structure in its initial condition and using FE mode shapes as references are reported in Table 6.9. A good agreement has been obtained also in this case, but the maximum value of MAC for the second mode ( $\approx 0.6$ ) was lower than for the other modes (higher than 0.95) because of the limits of the EFDD procedure in mode shape estimation of close coupled modes (Brincker et al. 2000b). This circumstance suggests, in the case of close coupled modes and a few sensors, to use mode shape estimates obtained directly from identification through FDD-based algorithms, in order to improve the effectiveness of spatial filtering in presence of noise.

Mode Number	FE model [Hz]	AFDD-T [Hz]	FE vs. AFDD-T scatter [%]
1	3.58	3.52	1.78
2	4.01	4.06	1.21
3	5.75	5.78	0.46

**Table 6.9.** AFDD-T validation: simulated data, 3D frame

Two types of sensitivity analyses have been carried out on this model. In the first case, the Young's modulus of three columns, chosen in order to

## 6. OMA AND STRUCTURAL HEALTH MONITORING

increase the coupling between the first two modes, has been changed from 0 (absence of columns) to 300000 kg/cm<sup>2</sup>. Changes in natural frequencies (Figure 6.16) have been detected with moderate errors (max 4.6%). In the second simulation, M22 and M33 moments at one end of an increasing number of columns have been released. Changes in natural frequencies of the first three modes have been detected with a maximum scatter within 3% (Figure 6.17).

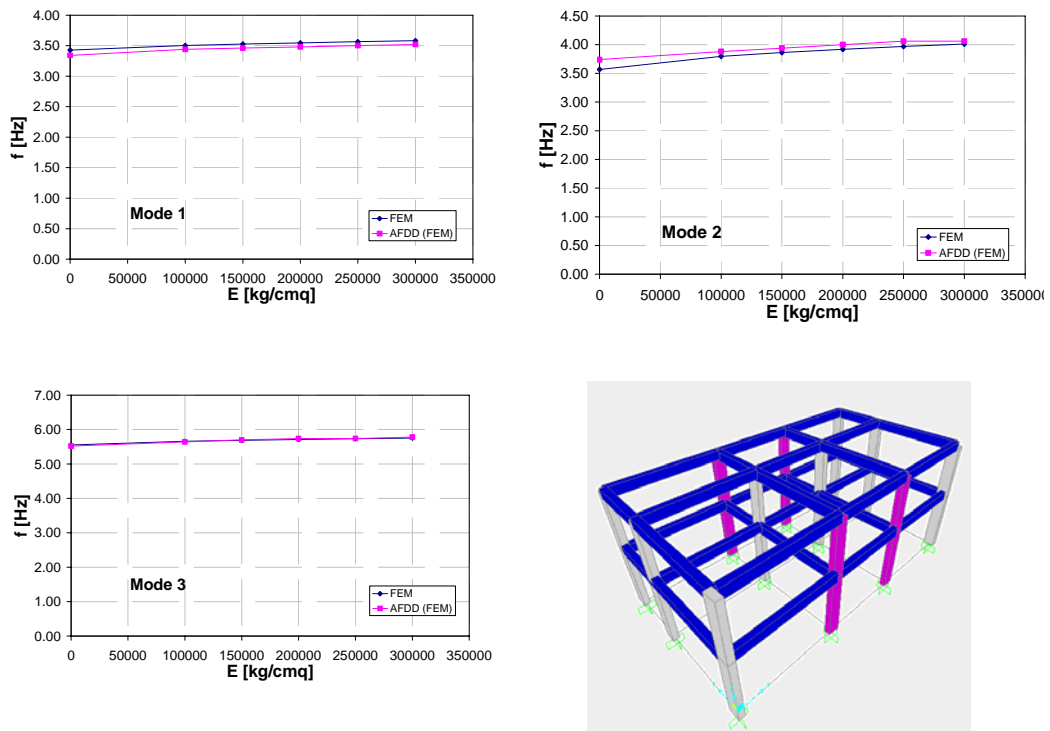


**Figure 6.16.** AFDD-T sensitivity analyses: simulated data, 3D frame (stiffness change)



## 6.6 AUTOMATED MODAL TRACKING: AFDD-T

---

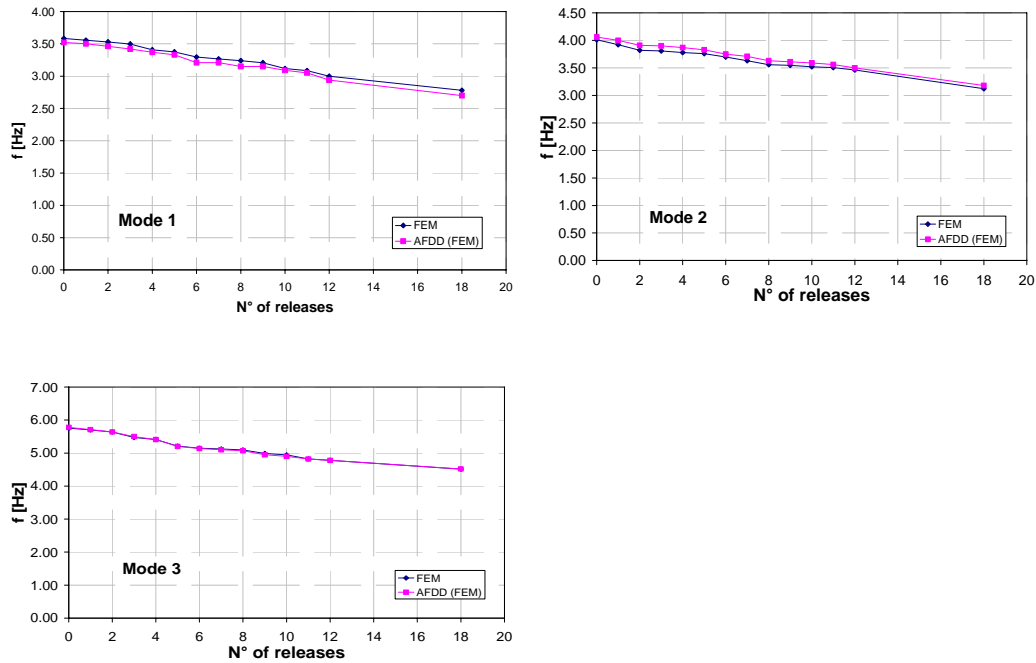


**Figure 6.17.** AFDD-T sensitivity analyses: simulated data, 3D frame (moment release)

These analyses show the importance of spatial filtering with respect, for example, to a traditional filtering. Application of a bandpass filtering may suffer some limitations: identification of the bandwidth of a mode according only to PSD plots or SV plots may be difficult; moreover, filter limits are static: as a consequence, only limited variations of natural frequencies can be observed, in particular in presence of close or multiple roots. A proof based on actual data is herein reported. In section 5.4 it has been shown that the School of Engineering Main Building is characterized by two close coupled modes having natural frequency equal to 0.92 Hz and 0.99 Hz, respectively. However, modal tracking during summer has

## 6. OMA AND STRUCTURAL HEALTH MONITORING

shown that such values can decrease until 0.89-0.9 Hz for the first mode, and 0.95-0.97 Hz for the second one. Calibration of a bandpass filter on the base of the SV plots obtained during modal identification results in a limit value equal to 0.95 (Figure 6.18) in order to separate such modes.

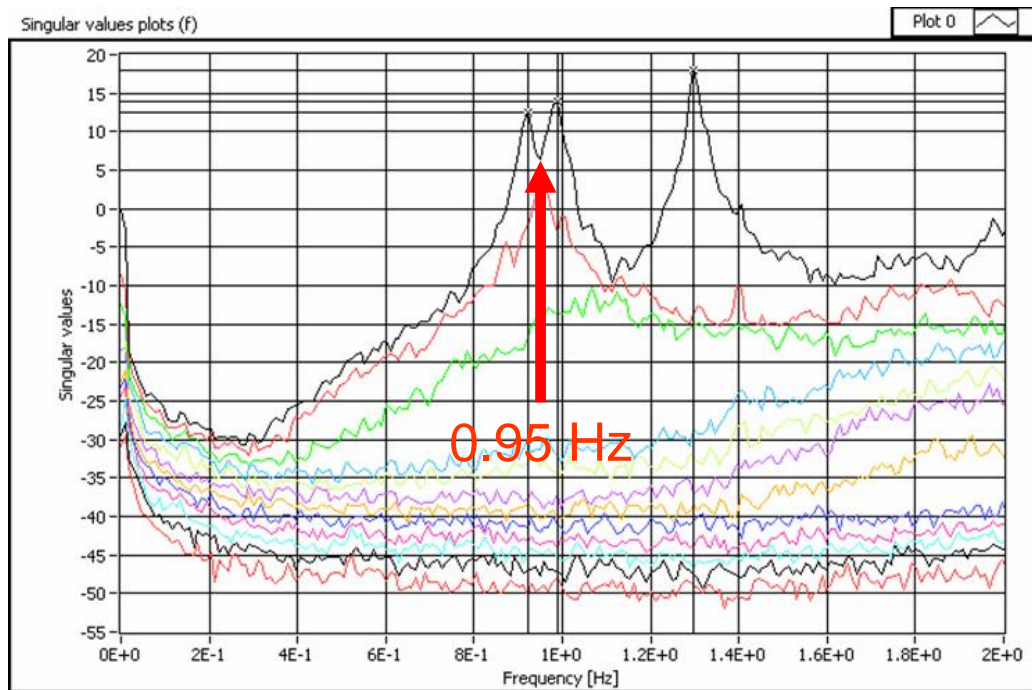


**Figure 6.18.** Mode bandwidth limit according to visual inspection of the first Singular Value plot

As a consequence, a bandpass filter is not adequate for modal parameter tracking in presence of close modes, since the natural changes of modal parameters due to environmental effects can move the natural frequencies outside the limits of the filter, thus causing an error in the estimates. By applying, instead, AFDD-T, the limits of the filter are set at each iteration

and changes in modal parameters can be followed in an automated way, thus allowing an effective and reliable modal tracking. Moreover, in presence of repeated roots, the spatial filtering can be applied to both the first and the second singular value plots.

### 6.6.3. Implementation

After testing, AFDD-T has been implemented in a stand-alone software, running on the local server of the School of Engineering Main Building SHM system and interfaced with its MySQL database. It has been implemented in LabView environment and it is characterized by a graphic interface showing location and activity of sensors on the structure, acceleration waveforms and results of identification in terms of natural frequencies vs. time. At each iteration a dataset is downloaded from the database and used to get natural frequencies and mode shapes for the first three modes, which are the most significant in terms of participating mass as pointed out by the numerical model of the structure (Rainieri et al. 2007c).

Since damage detection algorithms based on changes in modal damping ratios are less developed than natural frequency and mode shape approaches, also because fundamental understanding of the influence of damage on damping in structures has not been thoroughly established, tracking of damping ratio has not been taken into account.

In Figure 6.19 a picture of the software interface is reported: on the left side the plot of the first singular value (obtained by SVD of the PSD

## 6. OMA AND STRUCTURAL HEALTH MONITORING

matrix) vs. frequency is reported; in the middle plots of natural frequency vs. time for the first three modes are shown; on the right two dynamic charts, showing accelerations recorded by the sensors which are blinking at that time, are reported. Working sensors are denoted by a green light while out-of-order sensors by a red light.

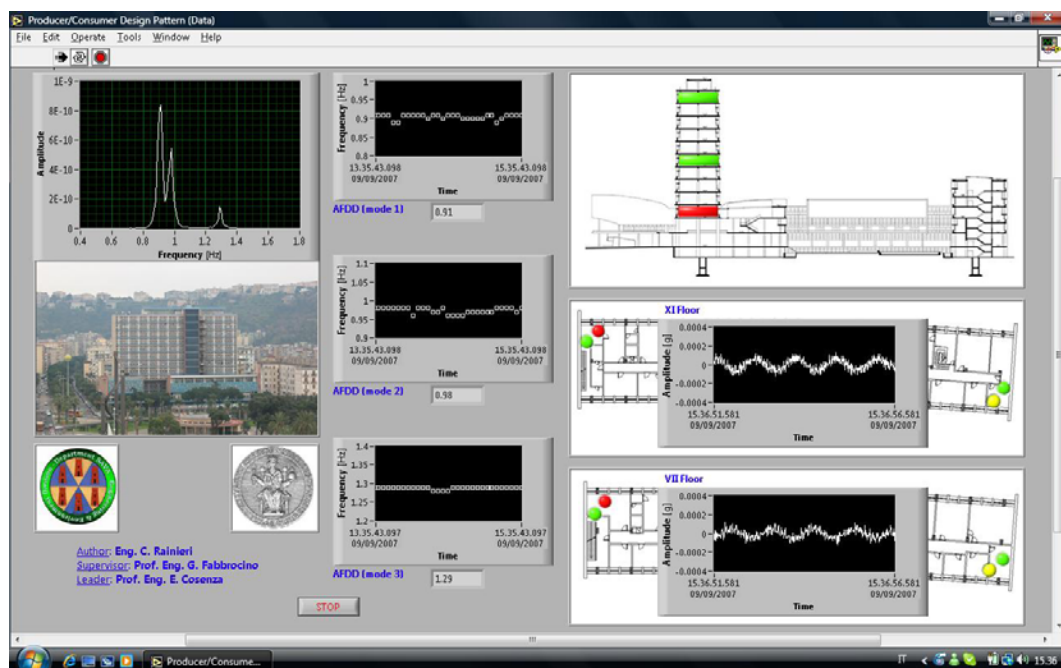


Figure 6.19. AFDD-T: software interface

The software is characterized by a producer/consumer architecture: the producer cycle is used to get data from the database while the consumer cycle processes these data and shows the output on screen.

The application of the procedure for automated modal parameter extraction is allowing an effective tracking of such parameters and,

## 6.6 AUTOMATED MODAL TRACKING: AFDD-T

---

indirectly, of the health state of the structure: a database of dynamic characteristics of the structure is progressively growing over the time. Currently, the procedure is applied considering only six sensors placed at two opposite corners of the seventh floor and on the roof of the monitored building. Experimental mode shapes obtained from an environmental vibration test using FDD have been used to apply the automated procedure. As the role of the number of sensors is concerned, results of modal tracking confirm that only 6 sensors, among those ones installed on the School of Engineering Tower, provide a robust identification of modes if observability is assured.

## 6.7 AUTOMATED OMA FOR SHM: LEONIDA + AFDD-T

### 6.7.1 Leonida applied to the School of Engineering Main Building data

Leonida has been extensively applied also to data continuously coming from the permanent SHM system installed on the Main Building of the School of Engineering at University of Naples. The possibility to retrieve data directly from a data acquisition hardware or from a remote database allows an easy integration of the software into a structural health monitoring system. In this section, results obtained from the repeated application of the algorithm to a number of datasets recorded in different days and having different lengths but related to the same structure are reported, and the effect of record length on the clearness and stability of results is discussed.

## 6. OMA AND STRUCTURAL HEALTH MONITORING

The considered records have been referred to as RC1, RC2 and RC3 in section 5.4. Duration of each record is reported in Table 6.10, together with hardware characteristics.

The first two fundamental modes of the structure are two close coupled modes, as shown in section 5.4. Continuous monitoring of modal parameters over different periods of the year has shown that natural frequencies of the first three modes vary in the ranges reported in Table 6.11.

Structure	Sensors	Data acquisition hardware	Records	Duration [s]	Sampling frequency [Hz]
School of Engineering Main Building	Kinematics Epi-Sensor FBA ES-U2	Kinematics K2	RC1	1200	100
			RC2	3300	100
			RC3	3800	100

**Table 6.10.** The School of Engineering Main Building: summary

Mode number	Observed frequency range [Hz]	Mode of observed natural frequency [Hz]
I	0.89-0.95	0.92
II	0.95-1.01	0.99
III	1.27-1.32	1.29

**Table 6.11.** The School of Engineering Main Building monitoring results: observed values of natural frequencies

Results obtained by applying Leonida, with a spectrum frequency resolution equal to 0.01 Hz, to the above mentioned three records are reported in Table 6.12.

## 6.7 AUTOMATED OMA FOR SHM: LEONIDA + AFDD-T

Record	Mode number	Natural frequency (EFDD) [Hz]	Natural frequency (Leonida) [Hz]
RC1	I	0.920	0.92
	II	0.985	0.98
	III	1.299	1.29
RC2	I	0.933	0.93
	II	0.990	1.00
	III	1.310	1.31
RC3	I	0.926	0.92
	II	0.990	0.99
	III	1.304	1.31

**Table 6.12.** School of Engineering Main Building: results of automated modal identification

The software has been, therefore, able to identify in a reliable way the natural frequencies of the first three fundamental modes in all test cases. Also the extension of mode bandwidths is quite stable in all cases apart from record length, as reported in Table 6.13.

Record	Mode number	Mode bandwidth (Leonida) [Hz]
RC1	I	0.87-0.94
	II	0.97-1.05
	III	1.21-1.51
RC2	I	0.88-0.96
	II	0.98-1.02
	III	1.27-1.34
RC3	I	0.87-0.95
	II	0.97-1.02
	III	1.26-1.37

**Table 6.13.** The School of Engineering Main Building: automated identification of mode bandwidth

## 6. OMA AND STRUCTURAL HEALTH MONITORING

---

When higher modes are considered, a number of wrongly identified frequency ranges disappears for a sufficiently long duration of the record, as a result of noise averaging.

Application of Leonida to data coming from the SHM system installed on the School of Engineering Main Building at University of Naples shows that a reliable identification is possible also in presence of close coupled modes. Different record durations have been also considered, in order to investigate the effects of record length on the reliability of results: fundamental modes have been correctly identified in all cases, apart from record length. When also higher modes are considered, as a result of noise, bandwidths are not clearly identified. However, a number of wrongly identified frequency ranges disappear for a sufficiently long duration of the record as a result of noise averaging, while regions where modes are actually located remain stable notwithstanding record duration. Thus, definition of a minimum record length can assure a complete modal identification. Actually, it is worth noticing that a large number of civil structures are characterized by moderate irregularities. In such cases, the first modes are affected by a large amount of participating mass, so they play a primary role in the dynamic response to earthquakes: as a consequence, the number of measures and the cost of tests and monitoring systems can be optimized, without loss of reliability, on the estimation of modal properties of such modes. Conversely, specific attention has to be paid when strongly irregular structures are considered and the role of higher modes cannot be easily neglected.



The issue of identification of higher modes is closely related to sensitivity of mode shapes, and therefore of MAC, to noise. Spectrum averaging is an effective way to reduce noise influence. In the above described applications, spectra are computed by using ten minutes long records because this length for the single step seems to be the minimum one providing a sufficiently averaged spectrum, thus resulting in a good compromise between accuracy and computational time. However, longer records can result in improved definition of spectra, where most of the noise is averaged out, and, therefore, of estimated mode shapes, thus reducing noise effects on MAC.

### **6.7.2 Integration of automated modal identification and tracking**

In the previous section it has been shown that Leonida is able to carry out a reliable modal identification of the School of Engineering Main Building. Due to the need to process a large amount of data, it is a time demanding procedure: however, it could be applied as such for modal tracking since, for civil structures, fast on-line data processing may be considered not crucial. However, if the SHM system is used also to assess the health state of a structure in the early earthquake aftershock, a faster data processing becomes relevant. Thus, integration of Leonida within a fully automated SHM system can be obtained by combining it with AFDD-T. Leonida can be applied to carry out a single output-only modal identification test: thus, it works as modal information engine for the modal parameter tracking procedure (AFDD-T). In fact, the mode shapes provided by Leonida are

## 6. OMA AND STRUCTURAL HEALTH MONITORING

---

used as references for the continuous modal tracking procedure. Periodically or on demand, a new reference can be obtained by Leonida and used to confirm the previous one or to replace it.

In Figure 6.20 a sample of monitoring results in terms of natural frequencies for the first three modes of the School of Engineering Main Building at University of Naples is reported. In Table 6.14 a synthesis of results of automated tracking is shown, pointing out the effectiveness of the algorithm for autonomous modal parameter monitoring (success rate higher than 99%, using data from only six sensors, among those ones actually installed on the building, and short datasets): statistics have been computed over 7130 samples for each mode; they are referred to data collected from the beginning to late summer 2008.

Mode number	Mode [Hz]	Mean [Hz]	Standard deviation [Hz]	Success rate [%]
I	0.92	0.92	0.00979	99
II	0.99	0.99	0.008094	99
III	1.29	1.29	0.008367	99

**Table 6.14.** School of Engineering Main Building: synthesis of monitoring results (summer 2008)

These data can be useful also for a deep characterization of the structure in its health state: in particular, the effect of temperature can be studied in order to find a model describing the variations of modal parameters due to temperature so that these effects can be depurated when applying damage identification procedures.

## 6.7 AUTOMATED OMA FOR SHM: LEONIDA + AFDD-T

---

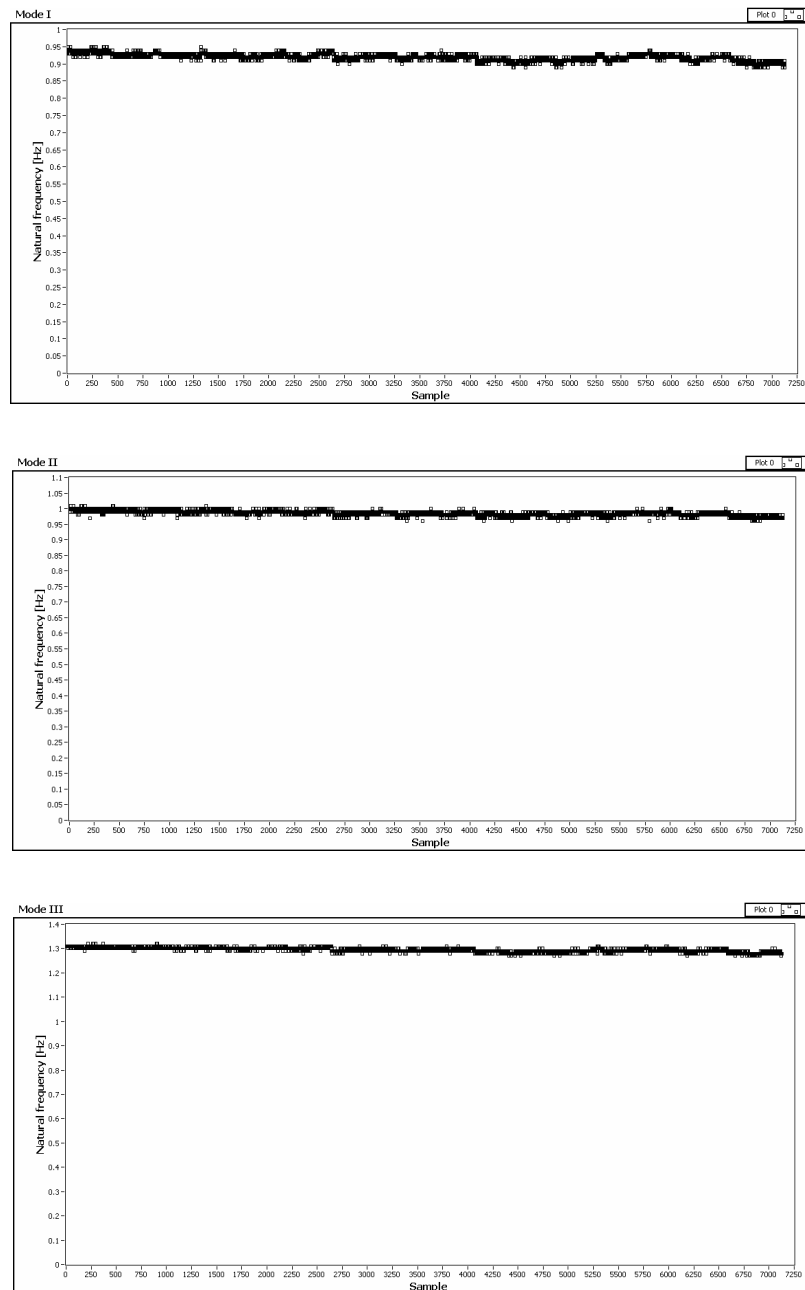


**Figure 6.20.** School of Engineering Main Building: plots of monitoring results (summer 2008)

## 6. OMA AND STRUCTURAL HEALTH MONITORING

---

Even if such a study has not been carried out yet for the monitored structure, a certain influence of temperature on the dynamic characteristics of the structure (in particular, natural frequencies) has been observed: in fact, in summer, during extremely hot periods, a decrease of the values of natural frequency for the first three modes has been observed: since, after these periods, they have assumed the original values, such variations seems to be due to temperature effects rather than to an actual damage. The low values of standard deviation of natural frequencies reported in Table 6.14 point out that the influence of environmental variables on this structure is relatively small (standard deviations lower than 0.01 Hz) and that it is quite uniform for all modes. Environmental effects, however, have been useful to verify reliability and robustness of the modal tracking procedure also in presence of close coupled modes. Identification of the region where a certain mode is located prior to extract the corresponding modal parameters seems to be a more efficient strategy with respect to threshold based peak detection followed by bandwidth definition, since it is less influenced by the relative strength of modes. Therefore, an effective tracking of modal parameters in presence of environmental effects, such as those ones due to temperature, or damage is possible and this circumstance makes OMA a relevant instrument in the field of Structural Health Monitoring in earthquake prone regions.

### 6.8 REMARKS

Opportunities given by Operational Modal Analysis in the field of Structural Health Monitoring have been investigated. The main drawback related to the extensive use of OMA procedures within fully automated SHM system is related to the need of a user intervention: a proposal for automated modal parameter identification and tracking has been, thus, described. The related algorithms have been implemented into software packages and, after a validation phase based on simulated and actual data, have been integrated within the SHM system of the School of Engineering Main Building in Naples. Some results have been also presented, pointing out the effectiveness of the procedure for continuous monitoring of structures in earthquake prone regions.

---

# 7

## Conclusions

---

*«The future does not belong to those who are content with today [...] timid and fearful in the face of bold projects and new ideas. Rather, it will belong to those who can blend passion, reason and courage in a personal commitment to great enterprises [...]»*

*Robert F. Kennedy*





## CHAPTER 7

### 7.1 CONCLUSIONS

In the present thesis, Operational Modal Analysis techniques and their application for seismic protection of structures have been investigated. The reliability and high versatility of such techniques, which do not require knowledge about the excitation that causes structural vibrations, has been demonstrated by applying them to a number of different case studies. Moreover, the present research work does not consist only of applications of available theory to civil engineering structures, but also of new developments which enhance potentialities of OMA above all in the field of Structural Health Monitoring. Extensive literature reviews allowed the definition of the framework of the present research and its innovative approach. The work has been organized so that opportunities given by OMA in the field of seismic engineering are pointed out: in particular, OMA tests, FE modelling and updating and the requirements of seismic analyses can be combined, thus defining criteria for definition of test setups and model refinement. Opportunities in the field of seismic protection of historical or heritage structures have been investigated. Some



## 7.1 CONCLUSIONS

---

criteria for a proper test execution have been defined, and an extensive literature review has been carried out in order to build a database of modal properties which can be used as a reference for validation of experimental results.

The main conclusions, chapter-by-chapter, of this thesis are the following:

- An extensive literature review has been crucial for the identification of effective procedures of Operational Modal Analysis; the mathematical background and the main characteristics of the methods have been deeply discussed in order to find similarities and differences; algorithms of the implemented procedures have been described in details;
- The main issues affecting data quality have been investigated and some criteria for measurement hardware choice have been defined; an home-made solution for OMA has been described; the implemented procedures have been validated against simulated data obtained from Finite Element models;
- Damping is the most difficult modal parameter to be estimated: thus, damping mechanisms and factors influencing structural damping have been investigated; procedures for a reliable estimation of damping in output-only conditions have been proposed, starting from the results of a literature review and from personal experience; a database of modal properties for different kinds of structures has been created in order to identify typical values of modal properties;

- Some case studies have been presented: in particular, the relationship between experimental tests and Finite Element modelling has been described by mean of two case studies: in the first one, the role of Finite Element modelling for proper definition of test setup is highlighted; in the second one, instead, the use of experimental data for model refinement has been described, pointing out how this procedure can be driven by the requirements of seismic analyses; some other case studies have been also described because of their role for implementation and validation of fully automated output-only modal identification and tracking procedures.
- Potentialities of OMA in the field of Structural Health Monitoring have been discussed; an algorithm for fully automated modal parameter identification and tracking has been developed, implemented into a software package and integrated into the SHM system of the School of Engineering Main Building in Naples; results of monitoring have been discussed, pointing out the effectiveness of the proposed procedure.

### 7.2 FUTURE RESEARCH

Even if some useful results have been obtained during the present research work and some useful criteria for proper test execution have been

## 7.2 FUTURE RESEARCH

---

identified, further work is needed, for example, for the definition of a standard procedure allowing accurate damping estimates, by defining durations and parameter settings for the different methods. In particular, definition of a criterion for identification of record length and number of block rows in SSI methods without the need of carrying out sensitivity analyses is of fundamental importance. Deep studies on damping mechanisms and on factors influencing its value are also crucial, because of the effects of damping on the amplitude of structural response under dynamic loads and, therefore, on structural design.

Characterization of typical values and of errors on damping estimates allows also a more reliable use of damping in SHM strategies. In such a case, a reliable fully automated SSI algorithm can solve the problem of continuous monitoring of damping ratios. Creation of large databases of modal parameters in operational conditions and after extreme events can be useful also to better understand the dynamic behaviour of structures and to gauge modal-based SHM strategies.

---

**A**

**Fundamental Property of NExT**

---



## APPENDIX A

In this section the fundamental property used in the NExT method is derived.

Said  $R_{ijk}(T)$  the cross-correlation function between two responses  $x_{ik}$  and  $x_{jk}$  at i and j due to a white-noise input at a location k, by definition  $R_{ijk}(T)$  is the expected value of the product between  $x_{ik}$  and  $x_{jk}$  evaluated with a time delay T:

$$R_{ijk}(T) = E[\{x_{ik}(t+T)\}\{x_{jk}(t)\}] \quad (\text{A.1})$$

where E is the expectation operator. For measured signals, the correlations can be computed as:

$$R_{ijk}(T) = \lim_{T \rightarrow \infty} \frac{1}{T} \int_{-T/2}^{T/2} x_{ik}(t)x_{jk}(t-T)dt \approx \frac{1}{n} \sum_{\alpha=1}^n x_{ik}(t_{\alpha}+T)x_{jk}(t_{\alpha}) \quad (\text{A.2})$$

Substituting the expression of the structural response to a certain input f in terms of its convolution with the Impulse Response Function:

$$x_{ik}(t) = \sum_{r=1}^N \phi_{ri} \phi_{rk} \int_{-\infty}^t f_k(\tau) g_r(t-\tau) d\tau \quad (\text{A.3})$$

into equation (A.1), the following expression is obtained:

$$R_{ijk}(T) = E \left( \sum_{r=1}^N \sum_{s=1}^N \phi_{ri} \phi_{rk} \phi_{sj} \phi_{sk} \int_{-\infty}^t \int_{-\infty}^{t+T} g_r(t+T-\sigma) g_s(t-\tau) f_k(\sigma) f_k(\tau) d\sigma d\tau \right) \quad (\text{A.4})$$

By taking into account that the expectation of the product between a random function  $a(t)$  and a non-random function  $b(t)$  satisfies (Mohanty 2005):

$$E[a(t)b(t)] = b(t)E[a(t)] \quad (\text{A.5})$$

and using this property in equation (A.4) where  $f_k(t)$  is a random function and  $x(t)$  is a non-random time function, the following equation is obtained:

$$R_{ijk}(T) = \sum_{r=1}^N \sum_{s=1}^N \phi_{ri} \phi_{rk} \phi_{sj} \phi_{sk} \int_{-\infty}^t \int_{-\infty}^{t+T} g_r(t+T-\sigma) g_s(t-\tau) E[f_k(\sigma) f_k(\tau)] d\sigma d\tau \quad (\text{A.6})$$

Using the definition of the autocorrelation function (A.1) and assuming  $f(t)$  to be white noise, the following relation is obtained:

$$R_{ffk}(\tau - \sigma) = E[f_k(\tau)f_k(\sigma)] = \alpha_k \delta(\tau - \sigma) \quad (\text{A.7})$$

where  $\alpha_k$  is a constant and  $\delta(t)$  the Dirac delta function. Substitution of equation (A.7) in (A.6) yields:

$$R_{ijk}(T) = \sum_{r=1}^N \sum_{s=1}^N \alpha_k \phi_{ri} \phi_{rk} \phi_{sj} \phi_{sk} \int_{-\infty}^t g_r(t+T-\sigma) g_s(t-\sigma) d\sigma \quad (\text{A.8})$$

Equation (A.8) can be further simplified by making a change of the integration variable: in fact, imposing  $\lambda = t - \sigma$ , then  $d\lambda = -d\sigma$  and the limits of integration for  $\lambda$  are  $+\infty$  and 0. Equation (A.8) then becomes:

$$R_{ijk}(T) = \sum_{r=1}^N \sum_{s=1}^N \alpha_k \phi_{ri} \phi_{rk} \phi_{sj} \phi_{sk} \int_0^{\infty} g_r(\lambda+T) g_s(\lambda) d\lambda \quad (\text{A.9})$$

Using the definition of  $g_r$ :

$$g_r(t) = \frac{1}{m_r \omega_r (1 - \xi_r^2)^{1/2}} e^{-\xi_r \omega_r t} \sin(\omega_r \sqrt{1 - \xi_r^2} t) \quad (\text{A.10})$$

it is possible to separate the terms depending on  $\lambda$  and the ones depending on T as follows:



$$\begin{aligned}
 g_r(\lambda + T) = & \left[ e^{-\xi_r \omega_r T} \cos(\omega_r \sqrt{1 - \xi_r^2} T) \right] \frac{e^{-\xi_r \omega_r \lambda} \sin(\omega_r \sqrt{1 - \xi_r^2} \lambda)}{m_r \omega_r (1 - \xi_r^2)^{1/2}} + \\
 & + \left[ e^{-\xi_r \omega_r T} \sin(\omega_r \sqrt{1 - \xi_r^2} T) \right] \frac{e^{-\xi_r \omega_r \lambda} \cos(\omega_r \sqrt{1 - \xi_r^2} \lambda)}{m_r \omega_r (1 - \xi_r^2)^{1/2}}
 \end{aligned} \tag{A.11}$$

Substitution of (A.11) in (A.9), by using the definition (A.10), yields:

$$R_{ijk}(T) = \sum_{r=1}^N \left[ G_{ijk}^r e^{-\xi_r \omega_r T} \cos(\omega_r \sqrt{1 - \xi_r^2} T) + H_{ijk}^r e^{-\xi_r \omega_r T} \sin(\omega_r \sqrt{1 - \xi_r^2} T) \right] \tag{A.12}$$

where  $G_{ijk}^r$  and  $H_{ijk}^r$  are independent of T and are given by:

$$\begin{Bmatrix} G_{ijk}^r \\ H_{ijk}^r \end{Bmatrix} = \sum_{s=1}^N \frac{\alpha_k \phi_{ri} \phi_{rk} \phi_{sj} \phi_{sk}}{m_r \omega_r \sqrt{1 - \xi_r^2} m_s \omega_s \sqrt{1 - \xi_s^2}} \int_0^\infty e^{(-\xi_r \omega_r - \xi_s \omega_s) \lambda} \sin(\omega_s \sqrt{1 - \xi_s^2} \lambda) \begin{Bmatrix} \sin(\omega_r \sqrt{1 - \xi_r^2} \lambda) \\ \cos(\omega_r \sqrt{1 - \xi_r^2} \lambda) \end{Bmatrix} d\lambda$$

(A.13)

Equation (A.12) is the key result of this derivation: it shows that the cross-correlation function is a linear combination of decaying sinusoids similar to the impulse response function of the original system (see equation (2.11)); thus, the cross-correlation functions can be handled as impulse response functions and processed with time-domain identification

techniques to estimate the modal parameters of the system. It is worth emphasizing that in this approach the amplitude of the random inputs are not measured so that the constant  $\alpha_k$  in (A.13) is unknown. As a consequence the modal masses  $m_r$  cannot be estimated.

## APPENDIX A

---

---

**B**

**Damping Database**

---



## APPENDIX B

STRUCTURE	N° Floors	H [m]	h interstorey [m]	f1 [Hz]	f2 [Hz]	f3 [Hz]	$\xi_1$ [%]	$\xi_2$ [%]	$\xi_3$ [%]
BUILDING 23	26.00	98.80	3.80	0.41	1.27	2.20	2.22	1.95	2.66
	26.00	98.80	3.80	0.41	1.26	2.23	1.39	1.84	1.75
	26.00	98.80	3.80	0.42	1.27	2.23	1.70	1.94	2.08
	26.00	98.80	3.80	0.45	1.32	2.32	2.83	2.27	3.12
	26.00	98.80	3.80	0.42	1.27	2.24	1.68	1.91	1.91
	26.00	98.80	3.80	0.42	1.32	2.31	1.87	2.13	3.70
BUILDING 34	60.00	257.00		0.34	0.34		0.90	1.40	
	60.00	257.00		0.28	0.28		4.90	2.20	
BUILDING 37	13.00	61.00		0.76	0.76		3.40	2.30	

**Table B.1.** Building-like structures: steel – earthquake

STRUCTURE	N° Floors	H [m]	h interstorey [m]	A [m <sup>2</sup> ]	f1 [Hz]	f2 [Hz]	$\xi_1$ [%]	$\xi_2$ [%]
BUILDING 33	30.00	94.00	3.13		0.38	0.38	11.60	15.50
BUILDING 35	12.00	57.00	3.13		0.45	0.45	2.70	2.70
BUILDING 69	14.00	54.70	3.91	1682.83	0.46	0.47	3.10	3.60
	14.00	54.70	3.91	1682.83	0.45	0.46	4.00	4.10

**Table B.2.** Building-like structures: r.c. – earthquake

## APPENDIX B

STRUCTURE	N° Floors	H [m]	A [m <sup>2</sup> ]	f1 [Hz]	f2 [Hz]	f3 [Hz]	ξ1 [%]	ξ2 [%]	ξ3 [%]
TOWER 1		35	17	1.28	1.83	3	1.22	3.56	1.17
		35	17	1.28	1.82	3.03	1.75	2.11	1.23
TOWER 4		74		0.586	0.708	2.456	2.05		1.59
		74		0.598	0.708	2.417	2.05		1.59
TOWER 5		52		2.3	3.43	4.4	0.74	2.09	0.3
TOWER 7		71.41	155.48	0.793	0.814	1.995	3.253	2.555	1.126
		71.41	155.48	0.785	0.814	1.953	3.253	2.555	1.126
TOWER 9		20.4	21.15	2.15	2.58	4.98	2.68	1.71	2.05
		20.4	21.15	2.56	2.76	7.15	1.25	1.42	1.16
TOWER 10		34.05		2.133	2.473	6.557	0.61	0.85	1.53
TOWER 11		104		0.839	0.9356	1.008	1.24	1.282	1.088
TOWER 12		91		1.213	1.383	1.629	2.111	1.618	1.877
TOWER 13		70		1.085	1.469	1.813	0.8226	0.9184	0.7205
TOWER 14		50		1.062	1.466	2.669	2	1.362	1.617
TOWER 16		48		1.486	1.589	3.593	1.43	1.26	1.04
TOWER 17		55		0.88	1.08	1.64	1.18	1.17	2.18
		55		0.88	0.98	1.64	1.18	1.17	2.18
		55		0.85	0.88	3.62	1.18	1.17	1.97
BUILDING 26		24	2800	3.69	5.12	6.29	2.34	1.11	1
		24	2800	3.68	5.04	6.3	1.26	2.68	0.82
BUILDING 38		120		0.8	1.61	1.68			
BUILDING 66	3			4	4.39	5.12			
TOWER 2		21	16.6	1.72	5.81	12.9			
TOWER 3		38.2	72.38	1.38	4.86	10.2			
TOWER 7		71.41	155.48	0.786	0.803	1.95			
TOWER 15		25.5		2.3	2.4	5.5			
TOWER 16		48		1.465	1.582	3.633			
TOWER 30		34.95	11.9	1.05	1.15	2.5			
TOWER 33		30	300	3.63	4.41	7.98			

**Table B.3.** Building-like structures: masonry – operational conditions

## APPENDIX B

STRUCTURE	N° Floors	H [m]	h interstorey [m]	A [m <sup>2</sup> ]	f1 [Hz]	f2 [Hz]	f3 [Hz]	ξ1 [%]	ξ2 [%]	ξ3 [%]
TOWER 18		230.00			0.40	0.41	1.47	0.18	0.30	0.83
		230.00			0.40	0.41	1.47	0.24	0.39	0.30
TOWER 19		108.00			0.54	0.57	1.87	0.30	0.20	0.14
TOWER 20		80.00			1.18	1.19	3.21	0.23	0.34	0.25
TOWER 25		37.00			2.69	2.80	4.36	1.56	1.20	0.56
TOWER 26		35.00			2.22	2.22	4.49	0.29	0.31	0.25
TOWER 32		336.00			0.23	0.43	1.02	2.80	2.00	0.70
BUILDING 2					3.41	5.13	7.02	0.47	0.64	0.80
BUILDING 13		59.10			0.76	0.85	1.11	0.65	0.74	0.84
BUILDING 24	26.00	98.80	3.80		0.42	1.28	2.27	2.98	2.96	3.98
	26.00	98.80	3.80		0.39	1.17	1.97	1.57	2.27	3.37
	26.00	98.80	3.80		0.41	1.30	2.31	1.49	2.24	2.20
	26.00	98.80	3.80		0.39	1.19	2.05	1.44	1.83	2.46
	26.00	98.80	3.80		0.43	1.30	2.29	1.62	2.49	2.59
	26.00	98.80	3.80		0.39	1.19	2.04	2.05	1.93	2.58
	26.00	98.80	3.80		0.42	1.30	2.30	1.58	2.44	2.07
BUILDING 25	5.00			1497.60	1.42	2.60	3.00	1.61	1.34	1.03
	5.00			1497.60	1.42	2.65	3.00	1.61	0.79	1.03
	5.00			1497.60	1.42	2.60	2.98	1.61	1.34	0.80
	5.00			1497.60	1.42	2.60	2.99	1.61	1.34	0.63
	5.00			1497.60	1.42	2.65	2.98	1.61	0.79	0.80
BUILDING 28	2.00			2283.88	4.13	6.66	7.51	1.00	0.30	0.60

**Table B.4.** Building-like structures: steel – operational conditions



## APPENDIX B

STRUCTURE	N° Floors	H [m]	h interstorey	A [m <sup>2</sup> ]	f1 [Hz]	f2 [Hz]	f3 [Hz]
BUILDINGS 67	5	15.30	3.06	180.18	2.48	3.00	7.19
	5	16.30	3.26	155.00	2.38	3.23	7.81
	5	17.30	3.46	244.20	3.03	3.03	8.70
	5	16.00	3.20	142.60	2.42	3.07	7.35
	6	12.60	2.10	298.75	3.57	4.76	
	14	42.40	3.03	457.60	0.89	1.15	2.80
	14	42.40	3.03	364.00	0.89	1.23	2.80
	11	34.70	3.15	515.16	1.89	1.92	5.99
	6	18.40	3.07	377.40	3.13	3.13	
	5	15.30	3.06	377.40	3.45	3.45	
	18	61.00	3.39		0.67	0.79	2.17
	15	54.00	3.60	309.60	1.02	1.28	3.18
	12	37.40	3.12	52.60	1.35	1.41	4.27
BUILDING 1					3.24	4.00	4.46
BUILDING 18	4			702.72	2.50	3.60	7.00
BUILDING 19	2				2.50	3.50	4.30
BUILDING 20	12				0.55	0.59	0.91

**Table B.5.** Building-like structures: steel – operational conditions

## APPENDIX B

STRUCTURE	N° Floors	H [m]	h interstorey [m]	A [m <sup>2</sup> ]	f1 [Hz]	f2 [Hz]	f3 [Hz]	ξ1 [%]	ξ2 [%]	ξ3 [%]
TOWER 8		310			0.234	0.734	1.273	1.37	0.28	0.64
BUILDING 3		27.5		374.85	1.253	1.873	4.048	4.61	3.381	2.278
BUILDING 17	6				2.34	2.69	3.17	3.91	5.86	5.08
	6				2.34	2.69	3.17	1.53	0.843	0.595
	6				2.38	2.74	3.23	6.21	3.66	2.93
	6				2.38	2.74	3.23	0.614	0.368	0.454
BUILDING 25	5	29.18	5.84	1650	2.75	2.87	3.88	4.13	5.07	4.46
BUILDING 29	25			2754	0.712	0.79	0.919	0.5	0.8	0.6
BUILDING 30	42			1792	0.315	0.415	0.471	1.6	1.1	0.7
BUILDING 32	46			115	0.31	0.35	0.65	3.86	2.36	1.67
BUILDING 40	7	29.89	4.27		2.69	2.93	3.65	2.2	2.6	2.2
BUILDING 41	4				11.57	12.84	17.05	2.03	2.5	4.91
	4				11.52	12.88	17.1	3.61	3.12	5.34
	4				7.36	10.04	11.07	4.13	2.32	2.03
	4				7.36	9.94	10.96	4.2	7.2	3.24
	4				11.89	14.2	15.74	3.33	2.37	2.54
	4				11.81	14.33	15.85	3.74	8.76	2.68
BUILDING 44	12				1.05	1.28	1.89	1.05	0.97	0.58
	12				1.05	1.28	1.89	0.69	0.94	0.53
BUILDING 49	4			1565.19	0.88	0.94	1.26	5.66	6.94	6.01
BUILDING 51	6	16.9	2.82	376.2	1.1765	1.515		6.6	6.8	
BUILDING 58	5	15.5	3.10	238.386	1.1236	1.408		6.5	6.9	
BUILDING 59	11				1.91	2.48	6.63	1.51	1.39	1.34
BUILDING 60	5				3.07	3.34	3.77	4.19	1.88	1.88
BUILDING 61	3				1.88	3.12	5.56	11.4	4.18	2.99
BUILDING 62	3				2.58	2.92	3.24	5.48	4.39	2.67
BUILDING 64					1.6	1.78	2.21	1.2	1	1
BUILDING 65					2.87	3.65	4.1	1.27	3.32	1.12
					2.88	3.6		3.72	3.59	

**Table B.6.** Building-like structures: r.c. – operational conditions

## APPENDIX B

STRUCTURE	N° Spans	Lenght [m]	Span Lenght [m]	f1 [Hz]	f2 [Hz]	f3 [Hz]	$\xi_1$ [%]	$\xi_2$ [%]	$\xi_3$ [%]
BRIDGE 8	11	370.7	33.7	4.97	6.6	8.31	5.4	4.2	1.9
BRIDGE 14	1	9	9	16.9	25.5	49	4.7	0.9	0.7
BRIDGE 57	7	322	46	3.631	4.1311	8.366	1.55	1.92	1.58
BRIDGE 28	1	30	30	4.8	5.05	11			
BRIDGE 60	3	125	25-50-50	2.44	3.32	4.88			

**Table B.7.** Bridges: steel-concrete composite – operational conditions

STRUCTURE	N° Spans	Lenght [m]	Span Lenght [m]	f1 [Hz]	f2 [Hz]	f3 [Hz]	$\xi_1$ [%]	$\xi_2$ [%]	$\xi_3$ [%]
BRIDGE 40	1	50	50	1.02	1.22	2.08	6.25	2.8	1.41
BRIDGE 62	1	189.1	189.1	0.61	0.81	0.87	6.5	6	4.5
BRIDGE 34	1			0.7	1.2	1.86			
	1			0.7	1.21	1.86			
BRIDGE 36	4	455	40,5-220-134- 60,5	1.53	2.16	1.36			
	4	455	40,5-220-134- 60,5	2.22	2.49	1.98			
	4	455	40,5-220-134- 60,5	1.58	1.64	3.34			
	4	455	40,5-220-134- 60,5	1.26	2.72	2.23			

**Table B.8.** Bridges: steel (cable stayed) – operational conditions

STRUCTURE	N° Spans	Lenght [m]	Span Lenght [m]	f1 [Hz]	f2 [Hz]	f3 [Hz]	$\xi_1$ [%]	$\xi_2$ [%]	$\xi_3$ [%]
BRIDGE 7	3	220	55-110-55	0.97	1.15	1.44	2.27	1.82	1.63
BRIDGE 10				0.89	1.15	2.44	4	3	5
BRIDGE 12	1	23.5	23.5	4.8	13.3	16.9	7.8	4.9	2
BRIDGE 13	1	19.5	19.5	6.4	14.7	18.5	9.3	4.5	2.5
BRIDGE 15	1	21	21	5.4	18.8	19.2	6.1	2.8	1.8
BRIDGE 16	1	6	5.75	15			2		
BRIDGE 17	1	11	11.44	13.7	16.5	26.2	7.7	4.7	3
BRIDGE 29	2	81	40.395	3.4	4.1	4.92	1	2	2
BRIDGE 32	6	91.2	15.2	7.37	8.04	11.48	1.54	1.19	1.13
	6	91.2	15.2	7.463	8.01	11.54	1.26	0.58	0.68
BRIDGE 33	4	51	8,75-16,75- 16,75-8,75	5.47	7.62	12.89	2.94	3.69	2.08
BRIDGE 52	3	60	13,7-32,6-13,7	3.24	5.32	8.4	0.7	3.6	1.5
BRIDGE 55	7	231	25,5-36-36-36- 36-36-25,5	2.158	2.58	3	0.71	0.72	0.72
BRIDGE 56	4	538	44,78-117,87- 235-140	0.15	0.3	0.62	2.93	0.18	0.43
BRIDGE 58	6	535	59,02-90- 116,25-116,25- 90,1-63,46	1.86	2.69	3.1	1.86	1.23	0.79
	6	535	59,02-90- 116,25-116,25- 90,1-63,47	1.84	2.66	3.11	2.45	1.54	1.57
BRIDGE 61	4	180	70-130-70	0.82	1.92	3.54	1.31	3.87	1.53
BRIDGE 63	4	268	40-60-80-88	0.68	1.32	1.66	4.4	1.6	1.64
	4	268	40-60-80-88	0.68	1.34	1.71	3.4	1.46	1.61

Table B.9. Bridges: r.c. – operational conditions

## APPENDIX B

STRUCTURE	N° Spans	Lenght [m]	Span Lenght [m]	f1 [Hz]	f2 [Hz]	f3 [Hz]	$\xi_1$ [%]	$\xi_2$ [%]	$\xi_3$ [%]
BRIDGE 19	1	181	181	0.961	1.022	1.099	1.04	2.35	0.01
BRIDGE 37	2	180		0.9	1.3	2.5	3.1	1.6	
BRIDGE 39	1	100	100	1.18	1.52	1.71	0.7	1.2	0.9
BRIDGE 41	3	1710	280-1400- 530	0,311	0,481	0,591	1,47	1,14	0,92
	3	1710	280-1400- 530	0,311	0,481	0,591	1,55	1,28	0,83
BRIDGE 43	1	140	140	0.786	1.224	2.328	0.66	0.46	1.06
	1	140	140	0.779	1.228	2.316	2.5	0.56	2.87
BRIDGE 54	4	829.2	62-420-70,6- 72	0.303	0.339	0.458	1.246	0.333	0.262
BRIDGE 35	3	790	150-490-150	0.342	0.45	0.613	1.8	2	3.1
BRIDGE 5	6	387	42-105-126- 30-42-42	0.645	0.996	1.33			
BRIDGE 30	2	152	26-126	0.67	1.17	1.45			
BRIDGE 43	1	140	140	0.781	1.221	2.344			
	1	140	140	0.781	1.23	2.344			
BRIDGE 54	4	829.2	62-420-70,6- 72	0.303	0.339	0.458			
BRIDGE 59	3	270	70-130-70	0.43	0.431	0.458			
BRIDGE 6	1	90	90	3.2	3.44	4.02			

**Table B.10.** Bridges: r.c. (cable stayed) – operational conditions

## REFERENCES

- Aenlle M.L., Villa García L.M., Canteli A.F. & Brincker R. (2005). Scaling Factors Estimate by the Mass Change Method. *Proceedings of the 1<sup>st</sup> IOMAC*. Copenhagen, Denmark.
- Aenlle M.L., Brincker R., Fernández P.F. & Canteli A.F. (2007). Load Estimation from Modal Parameters. *Proceedings of the 2<sup>nd</sup> IOMAC*. Copenhagen, Denmark.
- Aiello M.A., Conte C. & Valente L. (2007). Analysis and seismic retrofit of Historical Masonry Building under earthquake loading: a case study, *Proceedings of the 4th International Specialty Conference on the Conceptual Approach to Structural Design*, Venice, Italy.
- Akaike H. (1974). Stochastic theory of minimal realization, *IEEE Transactions on Automatic Control*, 19, pp. 667-674.
- Aktan A.E., Ciloglu S.K., Grimmelsman K.A., Pan Q. & Catbas F.N. (2005). Opportunities and challenges in health monitoring of constructed systems by modal analysis, *Proceedings of the International*

## REFERENCES

---

- Conference on Experimental Vibration Analysis for Civil Engineering Structures*, Bordeaux, France.
- Aktan A.E., Tsikos C.J., Catbas F.N., Grimmelsman K. & Barrish R. (1999). Challenges and Opportunities in Bridge Health Monitoring, *Proceedings of the 2<sup>nd</sup> International Workshop on Structural Health Monitoring*, Stanford, CA, USA.
  - Allemang R.J. & Brown D.L. (1982). A correlation coefficient for modal vector analysis, *Proceedings of the 1<sup>st</sup> SEM International Modal Analysis Conference*, Orlando, FL, USA.
  - Allemang R.J. & Brown D.L. (1998). A unified matrix polynomial approach to modal identification, *Journal of Sound and Vibration*, 211(3), pp. 301-322.
  - Andersen P., Brincker R. & Kirkegaard P.H. (1996). Theory Of Covariance Equivalent Arma Models Of Civil Engineering Structures, *Proceedings of the 14th International Modal Analysis Conference (IMAC)*, Dearborn, Michigan, USA.
  - Andersen P. (1997). *Identification of Civil Engineering Structures using Vector ARMA models*. Ph.D. Thesis. Aalborg: Department of Building Technology and Structural Engineering, Aalborg University.

## REFERENCES

---

- Andersen P. & Brincker R. (1999). Estimation Of Modal Parameters And Their Uncertainties, *Proceedings of the 17th International Modal Analysis Conference (IMAC)*, Kissimmee, Florida, USA.
- Andersen P., Brincker R., Goursat M. & Mevel L. (2007). Automated Modal Parameter Estimation For Operational Modal Analysis of Large Systems, *Proceedings of the 2<sup>nd</sup> International Operational Modal Analysis Conference*, Copenhagen, Denmark, Vol. 1, pp. 299-308.
- Asmussen J.C. (1997). *Modal Analysis based on the Random Decrement technique – Application to civil engineering structures*, PhD Thesis, Department of Building Technology and Structural Engineering, Aalborg University, Aalborg, Denmark.
- Baptista M.A., Mendes P. & Oliveira S. (2005). Use of ambient vibration tests for structural identification: 3 case studies, *Proceedings of the 1st International Operational Modal Analysis Conference*, Copenhagen, Denmark.
- Bartlett M.S. (1946). The theoretical specification and sampling properties of autocorrelated time series, *Journal of Royal Statistical Society*, B 8, pag. 24-41.
- Barzilai A. (2000). *Improving a Geophone to Produce an Affordable broadband Seismometer*, PhD Thesis, Mechanical engineering, Stanford University, USA.



## REFERENCES

---

- Belouchrani A., Abed-Meraim K., Cardoso J.-F. & Moulines E. (1997). A blind source separation technique using second order statistics, *IEEE Transactions on Signal Processing*, Vol. 45, n. 2.
- Bendat, J.S. & Piersol, A.G. (1986). *Random Data: Analysis and Measurement Procedures*, John Wiley & Sons, New York, USA.
- Bendat J.S. & Piersol A.G. (1993). *Engineering Applications of Correlation and Spectral Analysis*, Second Edition, John Wiley & Sons, New York, USA.
- Benedettini F., Alaggio R. & Manetta P. (2005). Arch bridges in Provincia di Teramo: tests, identification and numerical models, *Proceedings of the 1st International Operational Modal Analysis Conference*, Copenhagen, Denmark.
- Brincker R., Kirkegaard P.H., Andersen P. & Martinez M.E. (1995). Damage detection in an offshore structure, *Proceedings of the 13<sup>th</sup> SEM International Modal Analysis Conference*, Nashville, Tennessee, USA, pp. 661-667.
- Brincker R. & Andersen P. (1999a). ARMA Models in Modal Space, *Proceedings of the 17th International Modal Analysis Conference (IMAC)*, Kissimmee, Florida, USA.

## REFERENCES

---

- Brincker R. & Andersen P. (1999b). Ambient Response Modal Analysis for Large Structures, *Proceedings of the Sixth International Congress on Sound and Vibration*, Copenhagen, Denmark.
- Brincker R., Andersen P., Møller N. & Herlufsen H. (2000a). Output Only Testing Of a Car Body Subject To Engine Excitation, *Proceedings of the 18th International Modal Analysis Conference (IMAC)*, San Antonio, Texas, USA.
- Brincker R., Zhang L. & Andersen P. (2000b). Modal identification from ambient responses using frequency domain decomposition, *Proceedings of the 18th SEM International Modal Analysis Conference*, San Antonio, TX, USA.
- Brincker R., Ventura C.E. & Andersen P. (2003). Why Output-Only Modal Testing is a Desirable Tool for a Wide Range of Practical Applications, *Proceedings of the 21st International Modal Analysis Conference (IMAC)*, Kissimmee, Florida, USA.
- Brincker R., Lagö T., Andersen P. & Ventura C.E. (2005). Improving the Classical Geophone Sensor Element by Digital Correction, *Proceedings of the 23rd International Modal Analysis Conference (IMAC)*, Orlando, Florida, USA.

## REFERENCES

---

- Brincker R., Andersen P. & Jacobsen N.J. (2007). Automated Frequency Domain Decomposition for Operational Modal Analysis, *Proceedings of the 25<sup>th</sup> SEM International Modal Analysis Conference*, Orlando, FL, USA.
- Brown D.L., Allemang R.J., Zimmerman R. & Mergeay M. (1979). Parameter estimation techniques for modal analysis. *SAE Technical Paper Series* No. 790221.
- Brown R.G. (1983). *Introduction to Random Signal Analysis and Kalman Filtering*, John Wiley & Sons, USA.
- Brownjohn J.M.W. (1988). *Assessment of structural integrity by dynamic measurements*, PhD Thesis, University of Bristol, Bristol, England.
- Brownjohn J.M.W. (2005). Long-term monitoring of dynamic response of a tall building for performance evaluation and loading characterization, *Proceedings of the 1st International Operational Modal Analysis Conference*, Copenhagen, Denmark.
- Büyüköztürk O. & Yu T.-Y. (2003). Structural Health Monitoring and Seismic Impact Assessment. *Proceedings of the 5<sup>th</sup> National Conference on Earthquake Engineering*. Istanbul, Turkey.
- Cantieni R. (2005). Experimental methods used in system identification of civil engineering structures, *Proceedings of the 1st International Operational Modal Analysis Conference*, Copenhagen, Denmark.

## REFERENCES

---

- Cardoso R., Lopes M. & Bento R. (2005). Seismic evaluation of old masonry building. Part I: Method description and application to case-study, *Engineering Structures* 27, pp. 2024-2035.
- Cauberghe B. (2004). *Applied frequency-domain system identification in the field of experimental and operational modal analysis*. PhD Thesis, Department of Mechanical Engineering, V.U. Brussels, Brussels, Belgium.
- Cawley P. & Adams R.D. (1979). The location of defects in structures from measurements in natural frequencies. *Journal of Strain Analysis for Engineering Design*. Vol. 14. pp. 49-57.
- Ceroni F., Pecce M. & Voto S. (2006). Historical, architectonic and structural investigations of the bell tower of Santa Maria del Carmine, *Proceedings of the XXXIV IAHS world congress on sustainable house design*, Naples, Italy.
- Ceroni F., Pecce M., Manfredi G. & Palmaccio F. (2007). Analisi sismica del Campanile del Carmine in Napoli, *Proceedings of the XII ANIDIS Conference*, Pisa, Italy (in Italian).
- Chang F.K. (1999). *Structural Health Monitoring*, Proceedings of the 2<sup>nd</sup> International Workshop on Structural Health Monitoring, Stanford, CA, USA.

## REFERENCES

---

- Chia W.L. (2007). *Multiple-Input Multiple-Output (MIMO) blind system identification for operational modal analysis using the Mean Differential Cepstrum (MDC)*. PhD thesis, University of New South Wales, Sydney, Australia.
- Chopra A.K. (2001). *Dynamics of structures – Theory and Applications to Earthquake Engineering*, Prentice Hall, New Jersey, USA.
- Clough R.W. & Penzien J. (1975). *Dynamics of structures*, McGraw-Hill, New York, USA.
- Computers and Structures (2006). *SAP2000® v.11*, manual, Computers and Structures Inc., Berkeley, California, USA.
- Consiglio Superiore dei Lavori Pubblici (2008). *Nuove Norme Tecniche per le Costruzioni*, D.M. Infrastrutture 14/01/2008, published on S.O. n. 30 at the G.U. 04/02/2008 n. 29 (in Italian).
- Conte C. (2006). *Analysis and seismic adjustment by innovative technique of existent masonry building*, Graduation Thesis, University of Salento, Lecce, Italy.
- Conte C., Rainieri C., Aiello M.A., Fabbrocino G. (2008). On-site assessment of masonry vaults: dynamic tests and numerical investigation, *Rudarsko-Geološko-Naftni Zbornik*, Vol. 20, n. 1.

## REFERENCES

---

- Cosenza E., Fabbrocino G., Manfredi G., Parretti R., Prota A. & Verderame G.M. (2006). Seismic Assessment and Retrofitting of the Tower of the Nations, Paper 0997, *Proceeding of the 2<sup>nd</sup> International fib Congress*, Naples, Italy.
- Cunha A. & Caetano E. (2005). From Input-Output to Output-Only Modal Identification of Civil Engineering Structures, *Proceedings of the 1st International Operational Modal Analysis Conference*, Copenhagen, Denmark.
- Davenport A.G. (1981). Reliability of long span bridges under wind loading, *Proceedings of ICOSSAR*, Trondheim, Norway.
- Davenport A.G. & Hill-Carroll P. (1986). Damping in tall buildings: its variability and treatment in design, *ASCE spring convention*, Seattle, USA.
- De Roeck G. (2005). Damage Identification of Civil Engineering Structures Based on Operational Modal Data, *Proceeding of the 1st International Operational Modal Analysis Conference (IOMAC)*, Copenhagen, Denmark.
- De Roeck G., Claesen W. & Van den Broeck P. (1995). DDS-methodology applied to parameter identification of civil engineering structures, *Proceedings of Vibration and Noise '95*, Venice, Italy.

## REFERENCES

---

- De Stefano A. (2007). Structural identification and health monitoring on the historical architectural heritage, *Key Engineering Materials*, Vol. 347, pp. 37-54.
- Deraemaeker A., Reynders E., De Roeck G. & Kullaa J. (2008). Vibration-based structural health monitoring using output-only measurements under changing environment, *Mechanical Systems and Signal Processing*, 22, pp. 34-56.
- Devriendt C. & Guillaume P. (2007). The use of transmissibility measurements in output-only modal analysis, *Mechanical Systems and Signal Processing*, Vol. 21, Issue 7, pp. 2689-2696.
- Devriendt C., De Troyer T., De Sitter G. & Guillaume P. (2008). Automated operational modal analysis using transmissibility functions, *Proceedings of ISMA 2008*, Leuven, Belgium.
- Direttiva P.C.M. (2007). *Direttiva del Presidente del Consiglio dei Ministri del 12/10/2007 per la valutazione e la riduzione del rischio sismico del patrimonio culturale con riferimento alle norme tecniche per le costruzioni*, published at the G.U. 29/01/2008 n.24 (in Italian).
- Doebling S.W., Farrar C.R., Prime M.B. & Shevitz D.W. (1996). Damage Identification and Health Monitoring of Structural and Mechanical Systems from Changes in their Vibration Characteristics: A Literature

## REFERENCES

---

- Review, *Technical Report LA-13070-MS, UC-900*, Los Alamos National Laboratory, New Mexico 87545, USA.
- Enckell M. (2007). Structural Health Monitoring of bridges in Sweden, *Proceedings of the 3<sup>rd</sup> International Conference on Structural Health Monitoring of Intelligent Infrastructure*, Vancouver, Canada.
  - European Committee for Standardization (2003). *Eurocode 8: Design of structures for earthquake resistance EN 1998-1:2003*, European Standard.
  - Ewins D.J. (1984). *Modal Testing: Theory and Practice*, Research Studies Press Ltd., Letchworth, Hertfordshire, UK.
  - Eyre R. & Tilly G.P. (1977). Damping measurements on steel and composite bridges, *Symposium on dynamic behaviour of bridges*, Crowthorne, Berks, USA.
  - Fabbrocino G., Laorenza C., Rainieri C. & Santucci de Magistris F. (2008). Seismic Monitoring of Structural and Geotechnical Integrated Systems, *Proceedings of the 2nd Asia-Pacific Workshop on Structural Health Monitoring*, Melbourne, Australia.
  - Farrar C.R. & Doebling S.W. (1999). *Damage Detection II: Field Applications to Large Structures, Modal Analysis and Testing. Nato Science Series*. Dordrecht, the Netherland: Kluwer Academic Publisher.



## REFERENCES

---

- Farrar C.R., Worden K., Todd M.D., Park G., Nichols J., Adams D.E., Bement M.T. & Farinholt K. (2007). Nonlinear System Identification for Damage Detection. *Technical Report LA-14353-MS*. Los Alamos National Laboratory, Los Alamos, New Mexico, USA.
- Fassois D. (2001). MIMO LMS-ARMAX identification of vibrating structures – part I: the method, *Mechanical Systems and Signal Processing*, 15(4), pp. 723-735.
- Felber A.J. (1993). *Development of a Hybrid Bridge Evaluation System*, PhD Thesis, University of British Columbia, Vancouver, Canada.
- Fertis D.G. (1995). *Mechanical and Structural Vibrations*, John Wiley & Sons, New York, USA.
- Fixter L. & Williamson C. (2006). State of the Art Review – Structural Health Monitoring, *QINETIC/S&DU/T&P/E&M/TR0601122*, UK.
- Fladung W. & Brown D. (1992). Multiple Reference Impact Testing, *Proceedings of ISMA 17*, Leuven, Belgium, pp. 257-272.
- Fujino Y. & Siringoringo D.M. (2007). Monitoring of bridges and transportation infrastructures using vibration techniques, *Keynote paper at the Experimental Vibration Analysis for Civil Engineering Structures Conference (EVACES)*, Porto, Portugal.

## REFERENCES

---

- Fukuzono K. (1986). *Investigation of Multiple Reference Ibrahim Time Domain Modal Parameter Estimation Technique*, M.S. Thesis, Department of Mechanical and Industry Engineering, University of Cincinnati, USA.
- Gabriele S., Valente C. & Brancaloni F. (2007). An Interval Uncertainty Based Method for Damage Identification. *Key Engineering Materials*. Vol. 347. pp. 551-556.
- Gentile C. (2005). Operational Modal Analysis and assessment of historical structures, *Proceedings of the 1st International Operational Modal Analysis Conference*, Copenhagen, Denmark.
- Gentile C. (2007). Operational Modal Analysis of curved cable-stayed bridges, *Proceedings of the 2nd International Operational Modal Analysis Conference*, Copenhagen, Denmark.
- Glisic B., Posenato D., Casanova N., Inaudi D. & Figini A. (2007). Monitoring of heritage structures and historical monuments using long-gage fiber optic interferometric sensors – an overview, *Proceedings of the 3<sup>rd</sup> International Conference on Structural Health Monitoring of Intelligent Infrastructure*, Vancouver, Canada.
- Golub G.H. & Van Loan C.F. (1996). *Matrix Computations*, Third Edition, The John Hopkins University Press, Baltimore, MD, USA.

## REFERENCES

---

- Gouttebroze S. & Lardiès J. (2001). On using the wavelet transform in modal analysis, *Mechanics Research Communications*, 28(5), pp. 561-569.
- Guan H., Karbhari V.M. & Sikorski C.S. (2005). Time-domain output only modal parameter extraction and its application, *Proceedings of the 1<sup>st</sup> International Operational Modal Analysis Conference*, Copenhagen, Denmark, pp. 577-584.
- Guillaume P, Pintelon R. & Schoukens J. (1996). Parametric identification of multivariable systems in the frequency domain - a survey. *Proceedings of ISMA 21*. Leuven, Belgium.
- Guillaume P., Verboven P. & Vanlanduit S. (1998). Frequency Domain Maximum Likelihood Identification of Modal Parameters with Confidence Levels. *Proceedings of ISMA 23*. Leuven, Belgium.
- Guillaume P., Verboven P., Vanlanduit S., Van der Auweraer H. & Peeters B. (2003). A polyreference implementation of the least-square complex frequency domain estimator. *Proceeding of IMAC XXI*. Kissimmee, FL, USA.
- Habel W.R., Schallert M., Krebber K., Hofmann D., Dantan N. & Nöther N. (2007). Fibre optic sensors for long-term SHM in civil engineering applications, *Proceedings of the 3<sup>rd</sup> International Conference on Structural Health Monitoring of Intelligent Infrastructure*, Vancouver, Canada.

## REFERENCES

---

- Han J.-G., Ren W.-X. & Xu X.-X. (2005). Wavelet-based modal parameter identification through operational measurements, *Proceedings of the 1st International Operational Modal Analysis Conference*, Copenhagen, Denmark.
- Hanson, D., Randall R.B., Antoni J., Thompson D.J, Waters T.P. & Ford R.A.J. (2007a). Cyclostationarity and the cepstrum for operational modal analysis of mimo systems – Part I: Modal parameter identification, *Mechanical Systems and Signal Processing*, 21(6), pp. 2441-2458.
- Hanson, D., Randall R.B., Antoni J., Thompson D.J, Waters T.P. & Ford R.A.J. (2007b). Cyclostationarity and the cepstrum for operational modal analysis of mimo systems – Part II: Obtaining scaled mode shapes through finite element model updating, *Mechanical Systems and Signal Processing*, 21(6), pp. 2459-2473.
- Hanss M. (2005). *Applied Fuzzy Arithmetics: An Introduction with Engineering Applications*. Springer, Berlin, Germany.
- Hearn G. & Testa R.B. (1991). Modal Analysis for Damage Detection in Structures. *Journal of Structural Engineering*. Vol. 117. pp. 3042-3062.
- Hermans L. & Van der Auweraer H. (1997). On the use of auto- and cross-correlation functions to extract the modal parameters from

## REFERENCES

---

- output-only data, *Proceedings of the Sixth International Conference on Recent Advances in Structural Dynamics*, Southampton, UK.
- Hermans L., Van Der Auweraer H. & Guillaume P. (1998). A frequency domain Maximum Likelihood approach for the extraction of modal parameters from output-only data. *Proceedings of ISMA 23*. Leuven, Belgium.
  - Hermans L., Van Der Auweraer H. & Mevel L. (1999). Health monitoring and detection of a fatigue problem of a sports car, *Proceedings of the 17th International Modal Analysis Conference*, Kissimmee, FL, USA, pp. 42-48.
  - Heylen W., Lammens S. & Sas P. (2002). *Modal Analysis Theory and Testing*. Katholieke Universiteit Leuven, Leuven, Belgium.
  - Ibrahim S.R. & Mikulcik E.C. (1977). A Method for the Direct Identification of Vibration Parameters from the Free Response. *The Shock and Vibration Bulletin* No. 47.
  - Ibsen L.B. & Liingaard M. (2005). Output-only modal analysis used on new foundation concept for offshore wind turbine, *Proceedings of the 1st International Operational Modal Analysis Conference*, Copenhagen, Denmark.
  - ISO 4354:1997 (1997). *Wind Actions on Structures*, International Organisation of Standardisation.

## REFERENCES

---

- Jacobsen N.J., Andersen P. & Brincker R. (2007). Using EFDD as a robust technique for deterministic excitation in Operational Modal Analysis, *Proceedings of the 2<sup>nd</sup> International Operational Modal Analysis Conference*, Copenhagen, Denmark.
- Jeary A.P. (1986). Damping in Tall Buildings - A Mechanism and a Predictor, *Earthquake Engineering and Structural Dynamics*, 14, pp. 733-750.
- Juang J.-N. & Pappa R. (1984). An Eigensystem Realization Algorithm (ERA) for Modal Parameter Identification. *NASA/JPL Workshop on Identification and Control of Flexible Space Structures*. Pasadena, CA, USA.
- Juang J.-N. (1994). *Applied System Identification*, Prentice Hall Englewood Cliffs, New Jersey, USA.
- Kanda K., Kobori T., Ikeda Y. & Koshida H. (1994). The development of a pre-arrival transmission system for earthquake information applied to seismic response controlled structures, *Proceedings of the 1<sup>st</sup> World Conference on Structural Control*, California, USA.
- Kerschen G., Poncelet F. & Golinval J.C. (2007). Physical interpretation of independent component analysis in structural dynamics, *Mechanical Systems and Signal Processing*, Vol. 21, n. 4, pp. 1561-1575.

## REFERENCES

---

- Kim J.H., Jeon H.S. & Lee C.W. (1992). Application of the Modal Assurance Criteria for Detecting and Locating Structural Faults. *Proceedings of IMAC X*. San Diego, CA, USA.
- Klepka A. & Uhl T. (2008). Hardware and software tools for in-flight flutter testing, *Proceedings of ISMA 2008*, Leuven, Belgium.
- Klinkov M. & Fritzen C.-P. (2007). An Updated Comparison of the Force Reconstruction Methods. *Key Engineering Materials*. Vol. 347. pp. 461-466.
- Kraemer P. & Fritzen C.-P. (2007). Sensor fault identification using autoregressive models and the Mutual Information concept, *Key Engineering Materials*, Vol. 347, pp. 387-392.
- Lagomarsino S. (1993). Forecast models for damping and vibration periods of buildings, *Journal of Wind Engineering and Industrial Aerodynamics*, 48, pp. 221-239.
- Lagomarsino S. & Pagnini L.C. (1995). Criteria for modelling and predicting dynamic parameters of buildings, *Report ISC-II, 1*, Istituto di Scienza delle Costruzioni, University of Genoa, Genoa, Italy.
- Lanslots J., Rodiers B. & Peeters B. (2004). Automated Pole-Selection: Proof-of-Concept and Validation, *Proceedings of International Conference on Noise and Vibration Engineering*, Leuven, Belgium.

## REFERENCES

---

- Lardiès J. (1997). Modal parameter identification from output-only measurements, *Mechanics Research Communications*, 24(5), pp. 521-528.
- Lardiès J. (2008). Relationship between state-space and ARMAV approaches to modal parameter identification, *Mechanical Systems and Signal Processing*, 22, pp. 611-616.
- Li J., Zhang Y. & Zhu S. (2007). A wavelet-based structural damage assessment approach with progressively downloaded sensor data, *Smart Materials and Structures* 17(2008) 015020 (11 pp.).
- Lieven N.A.J. & Ewins D.J. (1988). Spatial Correlation of Mode Shapes: The Coordinate Modal Assurance Criterion (COMAC). *Proceedings of IMAC VI*. Kissimmee, FL, USA.
- Link M., Weiland M. & Seckert T. (2008). Computational Model Updating for Damage Identification in the Time Domain, *Proceedings of ISMA 2008*, Leuven Belgium.
- Liu C., Meng X. & Yao L. (2007). A Real-Time Kinematic GPS Positioning Based Structural Health Monitoring System for the 32 km Donghai Bridge in China, *Proceedings of the 6<sup>th</sup> International Workshop on Structural Health Monitoring*, Stanford, CA, USA.
- Ljung L. (1999). *System Identification: Theory for the User*, Second Edition, Prentice Hall, Upper Saddle River, NJ, USA.



## REFERENCES

---

- Lynch J.P. (2002). Decentralization of wireless monitoring and control technologies for smart civil structures, Blume Earthquake Engineering Center, *Technical Report #140*, Stanford University, Stanford, CA, USA.
- Magalhães F., Cunha A. & Caetano E. (2008). Permanent monitoring of “Infante D. Henrique” bridge based on FDD and SSI-COV methods, *Proceedings of ISMA2008*, Leuven, Belgium.
- Maia N.M.M., Silva J.M.M., He J., Lieven N.A.J., Lin R.M., Skingle G.W., To W.-M. & Urgueira A.P.V. (1997). *Theoretical and Experimental Modal Analysis*, Edited by Maia N.M.M. and Silva J.M.M., Research Studies Press, Taunton, Somerset, UK.
- Marulo F., Franco F., Ficca A. & Piterà A. (2005). Experiences in using operational modal analysis, *Proceedings of the 1st International Operational Modal Analysis Conference*, Copenhagen, Denmark.
- McConnell K.G. & Reiley W.F. (1987). Strain-gage instrumentation and data analysis, in *Handbook on experimental mechanics*, Ed. A.S. Kobayashi, Prentice-Hall, pp. 79-116.
- Messina A., Jones I.A. & William E.J. (1992). Damage Detection and Localization using Natural Frequency Changes. *Proceedings of the 1st Conference on Identification*. Cambridge, England.

## REFERENCES

---

- Ministero per i Beni e le Attività Culturali (2006). *Linee guida per la valutazione e la riduzione del rischio sismico del patrimonio culturale*, (in Italian). ISBN: 8849211651.
- Mita A., Inamura T. & Yoshikawa S. (2006). Structural Health Monitoring system for buildings with automatic data management system, *Proceedings of the 4<sup>th</sup> International Conference on Earthquake Engineering*, Taipei, Taiwan.
- Mizuno Y. & Fujino Y. (2007). Wavelet decomposition approach for archiving and querying large volume of Structural Health Monitoring data, *Proceedings of the 3<sup>rd</sup> International Conference on Structural Health Monitoring of Intelligent Infrastructure*, Vancouver, Canada.
- Mohanty, P. (2005). *Operational Modal Analysis in the presence of harmonic excitations*, Ph.D. Thesis, Technische Universiteit Delft, The Netherlands.
- Møller N., Herlufsen H., Brincker R. & Andersen P. (2000). Modal Extraction On a Diesel Engine In Operation, *Proceedings of the 18<sup>th</sup> International Modal Analysis Conference (IMAC)*, San Antonio, Texas, USA.
- Mufti A. (2001). *Guidelines for Structural Health Monitoring*, University of Manitoba, ISIS, Canada.

## REFERENCES

---

- National Instruments (2005). "LabView Fundamentals", LabView manual.
- Omenzetter P., Brownjohn J.M.W. & Moyo P. (2004). Identification of unusual events in multi-channel bridge monitoring data, *Mechanical Systems and Signal Processing*, Vol. 18, pp. 409-430.
- Pandey A.K., Biswas M. & Samman M.M. (1991). Damage Detection from Changes in Curvature Mode Shapes. *Journal of Sound and Vibration*. Vol. 145. pp. 321-332.
- Pandit S.M. & Wu S.M. (1984). Time series and system analysis with applications, *The Journal of the Acoustical Society of America*, Vol. 75, Issue 6.
- Pandit S.M. (1991). *Modal and Spectrum Analysis: Data Dependent Systems in State Space*, John Wiley & Sons, New York, USA.
- Parloo E. (2003). *Application of frequency-domain system identification techniques in the field of operational modal analysis*. PhD Thesis, Department of Mechanical Engineering, V.U. Brussels, Brussels, Belgium.
- Paz M. (1997). *Structural Dynamics: Theory and Computations*, Chapman & Hall, New York, USA.

## REFERENCES

---

- Peeters B. (2000). *System Identification and Damage Detection in Civil Engineering*, Ph.D. Thesis. Katholieke Universiteit Leuven, Leuven, Belgium.
- Peeters B. & De Roeck G. (2000). One year monitoring of the Z24 Bridge: environmental influences versus damage events, *Proceedings of the 18<sup>th</sup> SEM International Modal Analysis Conference*, San Antonio, TX, USA, pp. 1570-1576.
- Peeters B. & Van der Auweraer H. (2005). PolyMAX: a revolution in Operational Modal Analysis, *Proceedings of the 1st International Operational Modal Analysis Conference*, Copenhagen, Denmark.
- Peeters B., Van der Auweraer H., Guillaume P. & Leuridan J. (2004). The PolyMAX frequency-domain method: a new standard for modal parameter estimation?, *Shock and Vibration*, Special Issue dedicated to Professor Bruno Piombo, 11, pp. 395-409.
- Peeters B., Olofsson M. & Nilsson P. (2007). Test-based dynamic characterizing of a complete truck by operational modal analysis, *Proceedings of the 2nd International Operational Modal Analysis Conference*, Copenhagen, Denmark.
- Peterson, J. (1993). Observation and modelling of seismic background noise. *US Geological Survey Open-File Report 93-322*, 95 pp, USA.

## REFERENCES

---

- Pintelon R. & Schoukens J. (2001). *System Identification: a Frequency Domain Approach*, IEEE Press, New York, USA.
- Pintelon R., Guillaume P., Rolain Y., Schoukens J. & Van Hamme H. (1994). Parametric identification of transfer functions in the frequency domain – a survey, *IEEE Transactions on Automatic Control*, AC-39(11), pp. 2245-2260.
- Poncelet F., Kerschen G., Golinval J.C. & Verhelst D. (2007). Output-only modal analysis using blind source separation techniques, *Mechanical Systems and Signal Processing*, Vol. 21, n. 6, pp. 2335-2358.
- Poncelet F., Kerschen G. & Golinval J.C. (2008). In-orbit vibration testing of spacecraft structures, *Proceedings of ISMA 2008*, Leuven, Belgium.
- Pridham B.A. & Wilson J.C. (2003). A study on errors in correlation-driven stochastic realization using short data sets, *Probabilistic Engineering Mechanics* 18, pp.61-77.
- Rainieri C., Fabbrocino G., Manfredi G. & Cosenza E. (2006). Integrated technologies for seismic protection: an Italian experience, *Proceedings of Cansmart 2006 International Workshop*, Toronto, Canada.
- Rainieri C., Fabbrocino G. & Cosenza E. (2007a). Automated Operational Modal Analysis as structural health monitoring tool:

## REFERENCES

---

- theoretical and applicative aspects. *Key Engineering Materials*. Vol. 347. pp. 479-484.
- Rainieri C., Fabbrocino G., Cosenza E. & Manfredi G. (2007b). Structural Monitoring and earthquake protection of the School of Engineering at Federico II University in Naples, *Proceedings of ISEC-04*, Melbourne, Australia.
  - Rainieri C., Fabbrocino G., Manfredi G. & Cosenza E. (2007c). Structural monitoring and assessment of the School of Engineering Main Building at University of Naples Federico II, *Proceedings of the 3<sup>rd</sup> International Conference on Structural Health Monitoring of Intelligent Infrastructure*, Vancouver, Canada.
  - Rainieri C., Fabbrocino G. & Cosenza E. (2008a). Hardware and software solutions for continuous near real-time monitoring of the School of Engineering Main Building in Naples, *Proceedings of IABSE Conference on Information and Communication Technology (ICT) for Bridges, Buildings and Construction Practice*, Helsinki, Finland.
  - Rainieri C., Fabbrocino G., Verderame G.M., Cosenza E. & Manfredi G. (2008b). Structural and dynamic assessment and model updating of heritage buildings, *Proceedings of ISMA 2008*, Leuven, Belgium.
  - Rainieri C., Fabbrocino G. & Cosenza E. (2008c). An approach to automated modal parameter identification for structural health

## REFERENCES

---

- monitoring applications, *Proceedings of The Ninth International Conference on Computational Structures Technology*, Athens, Greece.
- Ramos L., Marques L., Lourenco P., De Roeck G., Campos-Costa A. & Roque J. (2007). Monitoring historical masonry structures with operational modal analysis: two case studies, *Proceedings of the 2<sup>nd</sup> International Operational Modal Analysis Conference*, Copenhagen, Denmark.
  - Randall R.B. (2008). New cepstral methods of operational modal analysis, *Proceedings of ISMA 2008*, Leuven, Belgium.
  - Reynolds P., Mohanty P. & Pavic A. (2005). Use of Operational Modal Analysis on empty and occupied stadia structures, *Proceedings of the 1st International Operational Modal Analysis Conference*, Copenhagen, Denmark.
  - Richardson M. & Schwarz B. (2003). Modal Parameter Estimation from Operation Data, *Sound and Vibration*, January 2003.
  - Rosenow S.-E., Uhlenbrock S. & Schlottmann G. (2007). Parameter extraction of ship structures in presence of stochastic and harmonic excitations, *Proceedings of the 2nd International Operational Modal Analysis Conference*, Copenhagen, Denmark.
  - Ruzzene M., Fasana A., Garibaldi L. & Piombo B. (1997). Natural frequencies and dampings identification using wavelet transform:

## REFERENCES

---

- application to real data, *Mechanical Systems and Signal Processing*, 11(2), pp. 207-218.
- Schmidt T. (2007). Dynamic behaviour of twin bell towers, *Proceedings of the 2nd International Operational Modal Analysis Conference*, Copenhagen, Denmark.
  - Seim C. & Giacomini M.G. (2000). Instrumenting the Golden Gate Bridge to Record Seismic Behaviour and to Deploy Rapid Inspection Response, *Proceedings of the 12-th World Conference on Earthquake Engineering*, Auckland, New Zealand.
  - Shoukens J. & Pintelon R. (1991). *Identification of Linear Systems: a Practical Guideline to Accurate Modelling*, Pergamon Press, London, UK.
  - Silkorsky C. (1999). Development of a Health Monitoring System for Civil Structures using a Level IV Non-Destructive Damage Evaluation Method, *Proceedings of the 2<sup>nd</sup> International Workshop on Structural Health Monitoring*, Stanford, CA, USA.
  - Soderstrom T. (1975). On model structure testing in system identification, *Automatica*, 11, pp. 537-541.
  - Söderström T. & Stoica P. (1989). *System Identification*, Prentice Hall, Englewood Cliffs, New Jersey, USA.



## REFERENCES

---

- Sohn H., Farrar C.R., Hemez F.M., Shunk D.D., Stinemates D.W. & Nadler B.R. (2003). A Review of Structural Health Monitoring Literature. *Technical Report LA-13976-MS*. Los Alamos National Laboratory, Los Alamos, New Mexico, USA.
- Song J. & Zhou T. (2007). Working state monitoring of a pile-supported 18-storey frame-shearwall structure, *Proceedings of the 3<sup>rd</sup> International Conference on Structural Health Monitoring of Intelligent Infrastructure*, Vancouver, Canada.
- Sørensen B.F., Lading L., Sendrup P., McGugan M., Debel C.P., Kristensen O.J.D., Larsen G.C., Hansen A.M., Rheinländer J., Rusborg J. & Vestergaard J.D. (2002). Fundamentals for remote structural health monitoring of wind turbine blades - a preproject, *Risø-R-1336(EN)*, Risø National Laboratory, Risø, Denmark.
- Staszewski W.J. (1997). Identification of damping in MDOF systems using time-scale decomposition, *Journal of Sound and Vibration*, 203(2), pp. 283-305.
- Swamidas A.S.J. & Chen Y. (1995). Monitoring crack growth through the change of modal parameters, *Journal of Sound and Vibration*, 186(2), pp. 325-343.
- Szyniszewski S., Hamilton III H.R. & Chih-Tsai Y. (2008). Wireless Sensors in Prestressed Concrete Piles - Combining Driving Control

- with Long Term Monitoring, *Proceedings of IABSE Conference on Information and Communication Technology (ICT) for Bridges, Buildings and Construction Practice*, Helsinki, Finland.
- Täljsten B., Hejll A. & James G. (2007). Carbon Fiber-Reinforced Polymer Strengthening and monitoring of the Gröndal Bridge in Sweden, *ASCE Journal of Composites for Construction*, Vol. 11, pp. 227-235.
  - Tamura Y., Yoshida A., Zhang L., Ito T., Nakata S. & Sato K. (2005). Examples of modal identification of structures in Japan by FDD and MRD techniques, *Proceedings of the 1st International Operational Modal Analysis Conference*, Copenhagen, Denmark.
  - Thibert K., Ventura C.E., Turek M. & Guerrero S. (2007). Dynamic soil-structure interaction study of a reinforced concrete high-rise building, *Proceedings of the 2<sup>nd</sup> International Operational Modal Analysis Conference*, Copenhagen, Denmark.
  - Turek M. & Ventura C.E. (2007). A method for implementation of damage detection algorithms for civil SHM systems, *Proceedings of the 2<sup>nd</sup> International Operational Modal Analysis Conference*, Copenhagen, Denmark.

## REFERENCES

---

- Van Overschee P. & De Moor B. (1991). Subspace algorithm for the stochastic identification problem, *Proceedings of the 30th IEEE Conference on Decision and Control*, Brighton, UK.
- Van Overschee P. & De Moor B. (1993). Subspace algorithm for the stochastic identification problem, *Automatica*, 29(3), pp. 649-660.
- Van Overschee P. & De Moor B. (1994). N4SID: Subspace algorithms for the identification of combined deterministic-stochastic systems', *Automatica*, Special Issue on Statistical Signal Processing and Control, vol. 30, no. 1, Jan. 1994, pp. 75-93.
- Van Overschee P. & De Moor B. (1996). *Subspace Identification for Linear Systems: Theory – Implementation – Applications*. Dordrecht, the Netherlands: Kluwer Academic Publishers.
- Ventura C.E. & Turek M. (2005). Fifteen years of ambient vibration testing in Western Canada, *Proceedings of the 1st International Operational Modal Analysis Conference*, Copenhagen, Denmark.
- Verboven P., Parloo E., Guillaume P. & Van Overmeire M. (2002). Autonomous structural health monitoring – Part I: modal parameter estimation and tracking, *Mechanical Systems and Signal Processing*, 16(4), pp. 637-657.

## REFERENCES

---

- Verboven P., Parloo E., Guillaume P. & Van Overmeire M. (2003). An automatic frequency domain modal parameter estimation algorithm, *Journal of Sound and Vibration*, 265, pp. 647-661.
- Vold H., Kundrat J. & Rocklin G.A. (1982). Multi-Input Modal Estimation Algorithm for Mini-Computers, *SAE Technical Paper Series* No. 820194.
- Waters T.P. (1995). *Finite element model updating using measured frequency response functions*, PhD Thesis, Department of Aerospace Engineering, University of Bristol, Bristol, UK.
- Weber E., Iannaccone G., Zollo A., Bobbio A., Cantore L., Corciulo M., Convertito V., Di Crosta M., Elia L., Emolo A., Martino C., Romeo A. & Satriano C. (2006). Development and testing of an advanced monitoring infrastructure (ISNet) for seismic early-warning applications in the Campania Region of Southern Italy, in P. Gasparini et al. editors, *Seismic Early Warning*, Springer-Werlag.
- Woodhouse J. (1998). Linear damping models for structural vibration, *Journal of Sound and Vibration*, 215(3), pp. 547-569.
- Zhang L. (2004). An Overview of Major Developments and Issues in Modal Identification, *Proceedings of the 22nd International Modal Analysis Conference (IMAC)*, Detroit, Michigan, USA.

## REFERENCES

---

- Zhang L., Wang T. & Tamura Y. (2005a). A Frequency-Spatial Domain Decomposition (FSDD) Technique for Operational Modal Analysis, *Proceedings of the 1st International Operational Modal Analysis Conference*, Copenhagen, Denmark.
- Zhang L., Brincker R & Andersen P (2005b). An Overview of Operational Modal Analysis: Major Development and Issues, *Proceedings of the 1st International Operational Modal Analysis Conference*, Copenhagen, Denmark.

## PUBLICATIONS

- Fabbrocino G., Rainieri C., Manfredi G. & Cosenza E. (2006). Structural Monitoring of Critical Buildings in Seismic Areas: the School of Engineering Tower in Naples, *Proceedings of the 1st IOMAC Workshop*, Aalborg, Denmark.
- Rainieri C., Fabbrocino G., Manfredi G. & Cosenza E. (2006). Integrated Technologies for Seismic Protection: an Italian Experience, *Proceedings of the 9th International Workshop on Smart Materials and Structures*, Toronto, Ontario, Canada.
- Rainieri C., Fabbrocino G., Manfredi G. & Cosenza E. (2006). L'analisi modale operativa per il monitoraggio strutturale in zona sismica, *Sperimentazione su materiali e strutture*, Convegno Nazionale, Venezia, Italia (in Italian).
- Rainieri C., Fabbrocino G., Cosenza E. & Manfredi G. (2007). Implementation of OMA procedures using LabView: Theory and Application, *Proceedings of the 2nd International Operational Modal Analysis Conference*, Copenhagen, Denmark.

## PUBLICATIONS

---

- Rainieri C., Fabbrocino G., Cosenza E. & Manfredi G. (2007). The Operational Modal Analysis for the identification of historical structures: the Tower of the Nations in Naples, *Proceedings of the 2nd International Operational Modal Analysis Conference*, Copenhagen, Denmark.
- Catalano P., Rainieri C., Giametta F. & Fabbrocino G. (2007). The Operational Modal Analysis for the identification of fruit tree structures, *Proceedings of the 2nd International Operational Modal Analysis Conference*, Copenhagen, Denmark.
- Rainieri C. & Fabbrocino G. (2007). Soluzioni software NI per il Monitoraggio Strutturale in Zona Sismica, *NIDays 2007 - Soluzioni e Applicazioni*, National Instruments Italy, pp. 176-177 (in Italian).
- Rainieri C., Verderame G.M., Fabbrocino G., Cosenza E. & Manfredi G. (2007). La valutazione della risposta dinamica nel progetto di rinforzo sismico della Torre delle Nazioni, *Mostra d'Oltremare, XII Convegno ANIDIS "L'ingegneria sismica in Italia"*, Pisa, Italia (in Italian).
- Rainieri C., Fabbrocino G., Manfredi G. & Cosenza E. (2007). Protezione sismica di edifici strategici e monitoraggio strutturale: applicazione all'Edificio centrale della Facoltà di Ingegneria di Napoli, *XII Convegno ANIDIS "L'ingegneria sismica in Italia"*, Pisa, Italia (in Italian).

- Fabbrocino G., Rainieri C. & Verderame G.M. (2007). L'analisi dinamica sperimentale e il monitoraggio delle strutture esistenti, *Workshop su "Controllo e monitoraggio di edifici in c.a.: il caso-studio di Punta Perotti"*, Bari, Italia (in Italian).
- Rainieri C., Fabbrocino G. & Cosenza E. (2007). Automated Operational Modal Analysis as structural health monitoring tool: theoretical and applicative aspects, *Key Engineering Materials*, Vol. 347 pp. 479-484.
- Rainieri C., Fabbrocino G. & Cosenza E. (2007). Continuous monitoring for performance evaluation of the dynamic response of the School of Engineering Main Building at University of Naples Federico II, *Proceedings of the 6th International Workshop on Structural Health Monitoring*, Stanford, USA.
- Rainieri C., Fabbrocino G. & Cosenza E. (2007). Automated modal parameters extraction via OMA procedures, *Proceedings of the 10th International Workshop on Smart Materials and Structures*, Montreal, Canada.
- Rainieri C., Fabbrocino G., Manfredi G. & Cosenza E. (2007). Structural monitoring and assessment of the School of Engineering Main Building at University of Naples Federico II, *Proceedings of SHMII-3*, Vancouver, Canada.



## PUBLICATIONS

---

- Rainieri C., Fabbrocino G. & Cosenza E. (2007). Automated Operational Modal Analysis solutions for seismic monitoring, *Proceedings of IASS 2007*, Venice, Italy.
- Rainieri C., Fabbrocino G., Cosenza E. & Manfredi G. (2007). Structural monitoring and earthquake protection of the School of Engineering at Federico II University in Naples, *Proceedings of ISEC-04*, Melbourne, Australia (peer reviewed).
- Rainieri C., Fabbrocino G. & Cosenza E. (2008). L'identificazione automatica dei parametri modali delle strutture in condizioni operative: uno strumento per il monitoraggio strutturale, *Terzo Workshop su Problemi di vibrazioni nelle strutture civili e nelle costruzioni meccaniche*, Perugia, Italia (in Italian).
- Rainieri C. & Fabbrocino G. (2008). Soluzioni Hardware/Software per il Monitoraggio Strutturale in Zona Sismica, *NIDays 2008 - Soluzioni e Applicazioni*, National Instruments Italy, pp. 2-3.
- Rainieri C., Fabbrocino G. & Cosenza E. (2008). Hardware and software solutions for continuous near real-time monitoring of the School of Engineering Main Building in Naples, *Proceedings of the IABSE Conference "Information and Communication Technology (ICT) for Bridges, Buildings and Construction Practice"*, Helsinki, Finland.

- Rainieri C., Fabbrocino G. & Cosenza E. (2008). Integrated systems for Structural Health Monitoring, *Proceedings of the Fourth European Workshop on Structural Health Monitoring*, Cracow, Poland.
- Rainieri C. & Fabbrocino G. (2008). Operational Modal Analysis: overview and applications, INTERREG MEETING Final Conference, in *Strategies for reduction of the seismic risk*, ISBN 978-88-88102-15-3, Termoli, Italy.
- Rainieri C., Fabbrocino G. & Cosenza E. (2008). An approach to automated modal parameters identification for structural health monitoring applications, *Proceedings of the Ninth International Conference on Computational Structures Technology*, Athens, Greece.
- Rainieri C., Fabbrocino G., Verderame G.M. & Cosenza E. (2008). Modal analysis of the Tower of the Nations in Naples, *Proceedings of the XIV World Conference on Earthquake Engineering*, Beijing, China.
- Rainieri C., Fabbrocino G. & Cosenza E. (2008). Structural Health monitoring systems as a tool for seismic protection, *Proceedings of the XIV World Conference on Earthquake Engineering*, Beijing, China.
- Rainieri C., Fabbrocino G., Verderame G.M., Cosenza E. & Manfredi G. (2008). Structural and dynamic assessment and model updating of heritage building, *Proceedings of ISMA Conference on Noise and Vibration Engineering*, Leuven, Belgium.

## PUBLICATIONS

---

- Rainieri C., Fabbrocino G. & Cosenza E. (2008). Fully automated modal parameter identification for smart SHM systems, *Proceedings of the 11th International Workshop on Smart Materials and Structures*, Montreal, Canada.
- Fabbrocino G., Laorenza C., Rainieri C. & Santucci De Magistris F. (2008). Structural and geotechnical seismic monitoring by smart systems, *Proceedings of the 11th International Workshop on Smart Materials and Structures*, Montreal, Canada.
- Fabbrocino G., Laorenza C., Rainieri C., Santucci De Magistris F. & Visone C. (2008). Structural and geotechnical seismic monitoring of the new Student House in Campobasso, Italy, *International Conference on Performance-Based Design in Earthquake Geotechnical Engineering - from case history to practice* (submitted), Tsukuba, Japan.
- Rainieri C., Fabbrocino G. & Cosenza E. (2008). An automated procedure for modal parameter identification of structures under operational conditions, *Proceedings of the 2nd Asia Pacific Workshop on Structural Health Monitoring*, Melbourne, Australia (peer reviewed).
- Fabbrocino G., Laorenza C., Rainieri C. & Santucci De Magistris F. (2008). Seismic monitoring of structural and geotechnical integrated systems, *Proceedings of the 2nd Asia Pacific Workshop on Structural Health Monitoring*, Melbourne, Australia (peer reviewed).

- Conte C., Rainieri C., Aiello M.A. & Fabbrocino G. (2008). On-site assessment of masonry vaults: dynamic tests and numerical investigation, *Rudarsko-Geološko-Naftni Zbornik (The Mining-Geological Petroleum Engineering Bulletin)*, 2008, Vol. 20 n. 1.
- Rainieri C. & Fabbrocino G. (2008). Dynamic identification of historical constructions, *Rudarsko-Geološko-Naftni Zbornik (The Mining-Geological Petroleum Engineering Bulletin)*, 2008, Vol. 20 n. 1.
- Rainieri C., Fabbrocino G. & Cosenza E. (2008). Fully automated OMA: an opportunity for smart SHM systems, *XXVII International Modal Analysis Conference*, Orlando, Florida, USA (submitted).